R.I. KHOLODOV
O.P. NOVAK
M.M. DIACHENKO

RESONANT AND POLARIZATION EFFECTS IN THE PROCESSES OF QUANTUM ELECTRODYNAMICS IN A STRONG MAGNETIC FIELD

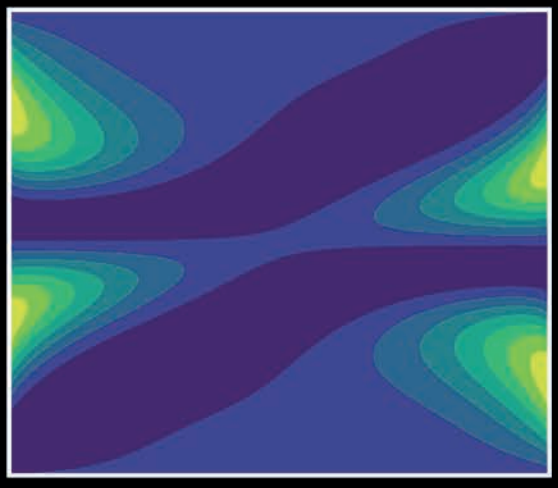

THE NATIONAL ACADEMY
OF SCIENCES OF UKRAINE
INSTITUTE OF APPLIED PHYSICS
OF THE NAS OF UKRAINE

НАЦІОНАЛЬНА
АКАДЕМІЯ НАУК УКРАЇНИ
ІНСТИТУТ ПРИКЛАДНОЇ ФІЗИКИ
НАН УКРАЇНИ

Р.І. ХОЛОДОВ
О.П. НОВАК
М.М. ДЯЧЕНКО

РЕЗОНАНСНІ І ПОЛЯРИЗАЦІЙНІ ЕФЕКТИ В ПРОЦЕСАХ КВАНТОВОЇ ЕЛЕКТРОДИНАМІКИ В СИЛЬНОМУ МАГНІТНОМУ ПОЛІ

ПРОЄКТ
«УКРАЇНСЬКА НАУКОВА КНИГА
ІНОЗЕМНОЮ МОВОЮ»

КИЇВ
АКАДЕМПЕРІОДИКА
2022

R.I. KHOLODOV
O.P. NOVAK
M.M. DIACHENKO

RESONANT AND POLARIZATION EFFECTS IN THE PROCESSES OF QUANTUM ELECTRODYNAMICS IN A STRONG MAGNETIC FIELD

PROJECT
«UKRAINIAN SCIENTIFIC BOOK
IN A FOREIGN LANGUAGE»

KYIV
AKADEMPERIODYKA
2022

UDC 530.145:537.533:539.9
K42
httsp://doi.org/10.15407/akademperiodyka.472.222

Reviewers:

V.P. GUSYNIN,
Corresponding Member of the NAS of Ukraine,
Doctor of Physical and Mathematical Sciences, Professor,
Bogolyubov Institute for Theoretical Physics
of the National Academy of Sciences of Ukraine

O.Yu. KORCHIN,
Corresponding Member of the NAS of Ukraine,

Doctor of Physical and Mathematical Sciences, Professor,
National Science Center «Kharkiv Institute of Physics and Technology»

O.A. LEBED,
Doctor of Physical and Mathematical Sciences, Senior Research,
Institute of Applied Physics of the NAS of Ukraine

Approved for publication by Scientific Councils
of the Institute of Applied Physics
of the National Academy of Sciences of Ukraine
(August 11, 2021, Protocol No. 10)

The publication was funded within the framework of the Targeted Complex Program of the NAS of Ukraine «Scientific Bases of Functioning and Providing for Conditions for the Development of the Scientific and Publishing Complex of the NAS of Ukraine»

Kholodov R.I.

K42 Resonant and polarization effects in the processes of quantum electrodynamics in a strong magnetic field / R.I. Kholodov, O.P. Novak, M.M. Diachenko; Institute of Applied Physics of the NAS of Ukraine. — Kyiv: Akademperiodyka, 2022. — 222 p.

ISBN 978-966-360-472-5

The monograph considers resonance and polarization effects in quantum electrodynamics processes that take place in a strong external magnetic field. A method for analyzing spin-polarization effects has been developed. The factorization of process cross-sections in resonant conditions and the representation of these cross-sections in the form of Breit-Wigner are considered. The possibility of testing these effects in modern international projects to test quantum electrodynamics in strong fields is shown.

For researchers, teachers, graduate students, and students of physical and physical-technical specialties.

UDC 530.145:537.533:539.9

ISBN 978-966-360-472-5

FOREWORD

Quantum ElectroDynamics (QED) is a theory of electromagnetic interaction that studies processes involving photons, electrons, and positrons (leptons), it is the most developed part of **Quantum Field Theory** (QFT) and is tested experimentally with high accuracy, in particular by measuring the anomalous magnetic moment of an electron (muon) and the Lamb shift of atomic levels. QED processes with external electromagnetic fields, in particular, the magnetic field, play an important role in the following phenomena: the formation of synchrotron radiation, the use of which has increased significantly in scientific and applied research; radiation of pulsars associated with strongly magnetized neutron stars; the collision of heavy ions. The question of experimental verification of quantum electrodynamics in strong electromagnetic fields comparable to the critical Schwinger value ($m^2/e = 4.41 \cdot 10^{17}\ V/m$) is still open. The FAIR mega-construction project (Facility for Antiproton and Ion Research), which is currently under construction, includes in its research program the verification of quantum electrodynamics in extremely strong electromagnetic fields. A characteristic feature of QED processes in a strong electromagnetic field is the strong influence of particle polarization on the process and the presence of resonant peculiarities.

Quantum electrodynamics in an external magnetic field as an independent direction of theoretical research begins in the middle of the last century, which is due to the need to create a theory of synchrotron radiation. Synchrotron radiation is widely used today. Sources of X-ray synchrotron radiation are used in radioscopy with elemental analysis, in micromechanics, in microelectronics, and X-ray

diffraction analysis of biomolecules. Synchrotron radiation is used to obtain polarized beams of electrons (positrons), for radiation cooling of electrons and positrons, in particular, to create B-factories. Therefore, finding new properties of the synchrotron radiation is, of course, an urgent task of theoretical physics, despite the in-depth study of this issue.

Another object of research using methods of QED in a magnetic field is a magnetosphere of neutron stars, where the magnetic field reaches a value of 10^{12}—10^{13} *Gs* and above. To date, more than 2.500 pulsars, about two hundred X-ray, and gamma pulsars of our galaxy have been detected. The magnetosphere of a neutron star is a unique laboratory to study QED processes in a strong near-critical magnetic field. Both the first-order processes (synchrotron radiation, e^+e^- pair production by a photon (annihilation)) and second-order processes (a photon scattering by an electron, two-photon synchrotron radiation, two-photon production (annihilation) of e^+e^- pair, vacuum birefringence, etc.) of quantized field perturbation theory play a key role in the formation of the electron-positron plasma of the magnetosphere, the presence of which explains synchrotron radiation of X-ray pulsars. Cyclotron lines, as well as annihilation lines in the emission spectra of pulsars, comptonization processes, cascades, and electromagnetic showers, are quite fully studied. However, the subject of studying X-ray pulsars, which includes both astronomical observations and theoretical calculations, remains relevant to this day, as there is no single theory of X-ray pulsar radiation. In particular, the questions of a spin population of the e^+e^- plasma and its effect on synchrotron radiation of X-ray pulsar, as well as on the influence of a field of cyclotron photons on the process of resonant formation of the e^+e^- plasma have not been resolved. The process of photon propagation in a strong magnetic field, when there is a cascade production of the e^+e^- pair with subsequent annihilation, has not been studied.

The SPARC collaboration (Stored Particles Atomic Physics Research Collaboration) is one of the key collaborations of the FAIR megaproject under construction. It plans to study the QED phenomena in extremely strong electromagnetic fields. In particular, studies involving photons, electrons, and atoms in the presence of strong fast-changing electromagnetic fields, structural studies of heavy ions, as well as studies of the dynamics of collisions of heavy ions in strong fields, including the process of e^+e^- pair production, will be conducted.

It should be noted that when heavy ions collide with target parameters that are larger than the size of the nucleus $\rho \geq R_{nuc}$, quantum-electrodynamic processes in the region between the nuclei in the strong magnetic field of the nuclei are possible. Between the nuclei, the magnetic fields of the moving nuclei add up, and the electric ones compensate. For impact parameters of order 10^{-10} *cm*, heavy nuclei with a charge $Z = 90$, that collide and move with speed $\sim c/10$, create a magnetic field of order 10^{12} *Gs*. In this area, it is quite possible that QED

processes with the participation of a strong magnetic field can take place. It makes their study relevant to the SPARC research of the FAIR project.

The first experiments where first- and second-order quantum-electrodynamic processes in the external field of an intense laser wave were studied were the 1996—1997 SLAC experiments. In these experiments, a beam of electrons with energies ~50 *GeV* was directed toward the laser beam with an intensity of $10^{18}\ W/cm^2$. As a result, gamma quanta with energy $> 2mc^2$ (m is electron mas) were detected, as well as positrons. There is no complete theory of positron production in these experiments. It should be noted that the external electromagnetic field of any configuration in the ultrarelativistic motion of an electron in its rest frame looks like a constant crossed electromagnetic field. In this regard, it is important to solve the problem of the generation of e^+e^- pairs by an ultrarelativistic electron in a magnetic field with subsequent application to SLAC experiments.

The above QED processes that occur in the magnetosphere of X-ray pulsars, processes in the SLAC experiment, and processes that are planned to be investigated in the tasks of testing QED in strong electromagnetic fields in the FAIR project are a single class of QED processes in a magnetic field. It is important to construct a unified approach to the analysis of these processes, taking into account the polarization of particles and resonant phenomena.

The paper is devoted to theoretical research of elementary processes of quantum electrodynamics in a strong magnetic field with polarized particles and photons. Spin-polarization and resonance effects in the processes under study are analyzed in detail in the approximation of the lowest Landau levels in a subcritical magnetic field.

The authors are grateful to V.Yu. Storizhko, N.F. Shulga, V.P. Gusynin, A.Yu. Korchyn, V.V. Skalozub, N.P. Merenkov, A.V. Lysenko as well as employees of the theoretical department of the Institute of Applied Physics of the National Academy of Sciences of Ukraine for numerous useful tips and fruitful discussions of the content of the monograph.

Chapter 1

PROCESSES OF QUANTUM ELECTRODYNAMICS IN A STRONG MAGNETIC FIELD

1.1. Introduction

A review of papers on the study of quantum electrodynamics processes in a strong magnetic field is carried out. Papers on synchrotron radiation and photon e^+e^- pair production, QED processes on pulsars, resonant effects of QED processes of the second order, as well as papers related to the international FAIR project and SLAC experiments are analyzed.

1.2. Synchrotron radiation. Electron-positron pair production by a photon

Synchrotron radiation. The emergence of science which is called «quantum electrodynamics in an external magnetic field», is associated with the discovery of **Synchrotron Radiation** (SR). In 1946, Blewett measured an electron radiation loss in the induction accelerator [1]. A year later, Floyd Haber (Pollock's assistant) experimentally discovered a glow on the synchrotron [2]. This glow is called synchrotron radiation. SR is the electromagnetic radiation of a relativistic charged particle when moving in a uniform constant magnetic field. It is also called magneto-bremsstrahlung radiation. In the case of nonrelativistic motion, the radiation is called cyclotron radiation. A few years later, a complete relativistic theory of this phenomenon was written by Sokolov, Ternov (1953), and others [3—6]. The radiation intensity is inversely proportional to the fourth power of the mass of the moving particle:

$$I_{SR} = \frac{2e^4 H^2 E^2}{3m^4 c^7} \sim \frac{1}{m^4}. \qquad (1.1)$$

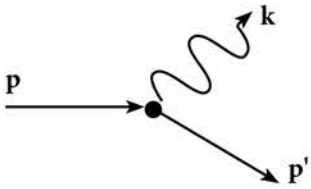

Fig. 1.1. Feynman diagram of photon emission by an electron

As a result, the synchrotron radiation is significant for the lightest charged particles (electrons and positrons). For example, a proton emits 10^{13} times less energy than an electron moving with the same energy. SR for protons is essential if their energy is $E > 10\ TeV$.

Synchrotron radiation is widely used today: sources of X-ray SR (radioscopy with elemental analysis, micromechanics, microelectronics, X-ray diffraction analysis of biomolecules); radiation cooling of electrons and positrons, in particular, to create B-factories; obtaining polarized beams of electrons (positrons). It should be noted the negative side of SR: it is a significant obstacle to the acceleration of high-energy particles.

The process of electron emission of a photon in a magnetic field in the framework of quantum electrodynamics, which corresponds to the Feynman diagram in Fig. 1.1 was calculated by M. Demeur (1953) [7] and Klepikov (1954) [8].

In Fig. 1.1. the initial electron with a 4-momentum **p** emits the photon with a momentum **k** and goes to the final state with a momentum **p'**.

Solid lines are wave functions of the electrons in the initial and the final states in an external magnetic field. Obtained expressions of radiation intensity correspond to a quasiclassical motion of electrons at high energy levels in ultrarelativistic approximation.

The **Lowest Landau Level** approach (LLL approach) is the opposite of the ultrarelativistic case. Implement the LLL approximation requires a strong magnetic field, which is comparable in magnitude to the critical Schwinger value $H_0 = m^2 / e = 4.4 \cdot 10^{13} Gs$.

In the textbook [9], such an approximation in supercritical fields is called the ultraquantum approximation to emphasize that in this case both a process of photon emission and a motion of an electron are purely quantum processes. The process of photon emission by an electron in the LLL approximation was considered in papers [10—12]. In the case of magnetic fields $\sim 10^{12} Gs$, which are characteristic of the magnetosphere of neutron stars, the SR process was studied in [13—16], and in [17] an absorption of radiation was considered.

Polarization effects in SR. In the SR process, polarization phenomena are significant. It is important to consider both the polarization of radiation and the polarization of particles [18]. The SR polarization was calculated in [19] and tested experimentally in [20]. The spin of electrons was taken into account in [21—24]. Analysis of the evolution of the spin of the electron (positron) in the SR process was done in [6, 25, 26]. The phenomenon of radiation self-polarization of particles moving in storage rings has been discovered by A.O. Sokolov

and I.M. Ternov. As a result of the SR process in the storage rings, 92% of the electrons have a spin oriented against the direction of a magnetic field.

One-photon electron-positron Pair Production (OPP). OPP is the process of electron-positron pair production by a single photon. This process is a cross-channel to the process of photon emission by an electron. For the first time it was considered in [8] in the ultrarelativistic approximation. In a strong magnetic field of pulsars, the process was studied in [13, 27—32]. In [27], the OPP theory was developed and a photon attenuation coefficient was found taking into account an additional electric field directed along the magnetic field to model the field configuration in the region of the pulsar poles. In [28, 29], the OPP process was studied near the threshold $\omega \approx 2m$ and it was shown that the attenuation coefficient as a function of the photon frequency has a sawtooth dependence. In [30], the OPP process was studied taking into account the polarization of both the photon and the electron (positron). In [31], the probability of this process in a strong magnetic field that changes over time was calculated, taking into account an additional constant gravitational field.

Modified propagation function and vacuum polarization. After the appearance of Schwinger's paper on gauge invariance and vacuum polarization [33], a series of papers was published, where the propagation function of a charged particle in an external magnetic field was found based on Schwinger's proper time method [34—38]. In [34, 35], the problem was performed for a charged particle with spin 1/2 and 0, respectively. Real and imaginary parts of the found mass operator give a radiation correction to the particle energy and a total probability of the SR, respectively. In [36, 37] a polarization operator was calculated and the photon absorption coefficient due to the OPP process was found using the imaginary part of the polarization operator.

Operator method. In [39—47], an operator method was used to study quantum effects in the motion of a charged high-energy particle in an external magnetic field. For ultrarelativistic energies, the motion of a particle is quasiclassical. The noncommutativeness of dynamic variables associated with the quantization of particle motion has an order of magnitude of the ratio of the cyclotron frequency to the energy of the particle ω_H/ε, which is a small value. The advantage of the method is its application for external fields of any configuration and charged particles with any spin value. The obvious disadvantage is its unsuitability for non-relativistic particles in a strong magnetic field, as, for example, in the case of electron-positron gas particles at the lowest Landau levels in a magnetosphere of neutron stars. In [39, 40] the processes of SR and OPP, as well as the process of annihilation of e^+e^- pair in one photon were considered. In [41, 43, 44] a mass operator was found, and in [42] lepton loops with n-photon lines were calculated, in particular, in the case $n = 2$ a polarization operator was found. Relatively recently, a paper was published [46], where the operator

method considered the OPP process in a strong magnetic field. It was shown that both in the case of weak fields $H << H_0$ and the case of superstrong fields $H \geq H_0$ «the results of quasiclassical calculations are very close to the average probabilities of the exact theory in a wide range of photon energies». It is also worth mentioning [48, 49], where the intrinsic energy of an electron in a strong magnetic field was calculated and the effect of spin on the total probability of SR was studied. In the monograph [50], a wide range of QED issues in a strong external electromagnetic field was considered, and all QED processes of the first order were analyzed in detail.

Even though the general theory of synchrotron radiation was built more than half a century ago, and still in this process, in the process described by the simplest Feynman diagram in Fig. 1, there are unsolved problems. In particular, the spin-polarization effects, i.e. the effect of spin of particles on the polarization of a finite photon, when the particles are at the lowest Landau levels in both nonrelativistic and ultrarelativistic cases in strong magnetic fields, have not been studied.

The polarization of SR in the ultraquantum ultrarelativistic approximation has not been studied. Also relevant is the problem of studying the effect of polarization of an initial photon on spin directions of electron and positron in the process of single-photon production of an electron-positron pair in these cases.

1.3. Physics in a strong magnetic field of neutron stars

The discovery of pulsars. The next burst of scientific activity in the direction of QED in a magnetic field after the discovery of SR occurred in the 70s of the last century, after 1971 the first orbital X-ray observatory Uhuru discovered powerful radiation with a well-defined periodicity, the so-called X-ray pulsar [51]. Shortly before that, the first pulsar (radio pulsar) was discovered on the radio telescope of the Mullard Radio Astronomical Observatory of Cambridge University [52]. X-ray pulsar emission comes from rotating neutron stars, which are located in binary systems in which the accretion process takes place (see Fig. 1.2). Dust and charged particles flow from an ordinary star to a compact, neutron star, causing radiation. All this happens in a strong magnetic field created by a neutron star. The magnetic field of the magnetosphere of neutron stars reaches a value of 10^{12}—10^{13} *Gs*. Also, a distinctive feature of the pulsar is the high speed of rotation of a neutron star. High speed of rotation, as well as a strong magnetic field, are the consequences of the laws of conservation of momentum and conservation of magnetic flux during compression of supernova nucleus during its explosion to the size of a neutron star.

So far, more than 2,500 pulsars, about two hundred X-rays and gamma pulsars of our galaxy have been discovered, and the first information about

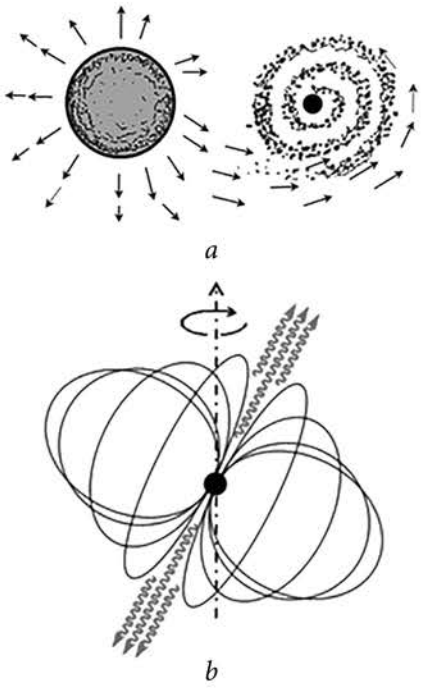

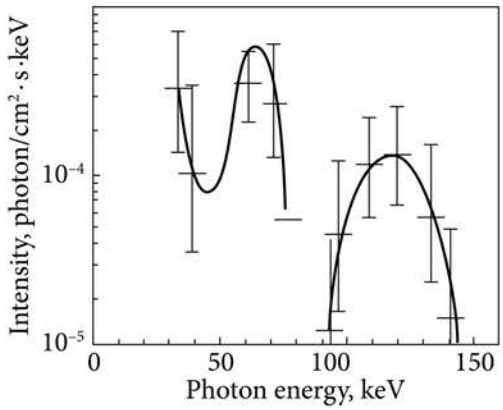

Fig. 1.3. Cyclotron X-ray pulsar Hercules X-1 [54]

◄ ***Fig. 1.2.*** X-ray pulsar in a dual system, *a* — accretion disk, *b* — pulsar radiation (pencil-type)

pulsars of other galaxies appears. Catalogs of pulsars have been created, for example [53—54].

Thus, the magnetosphere of a neutron star is a unique laboratory for the course of QED processes in strong magnetic fields of the order of the critical Schwinger field.

Cyclotron lines. Comptonization. In 1973 Gnedin Yu.N. and Sunyaev R.A. pointed to the possibility of direct measurement of the magnitude of a magnetic field of the pulsar magnetosphere. They predicted gyro lines (cyclotron lines) in the emission (absorption) spectrum of an electron-positron gas of a neutron star's magnetosphere [55], which were discovered by Trümper and colleagues in 1978 [56] (see Fig. 1.3).

From this moment began the study of QED processes in the magnetic field associated with cyclotron lines of X-ray pulsars and processes more complex than SR and OPP, with higher-order processes of perturbation theory. In particular, the issue of comptonization, i.e. the change in the photon frequency due to a series of successive Compton scattering by electrons and positrons, has been studied [57—62]. Comptonization in thermal plasma can lead to characteristic power-law spectra of X-ray emission. It is also responsible for changing the intensity of radiation of a relic background of a radio range of hot electrons of interstellar and intergalactic gas (the Sunyaev-Zeldovich effect).

In [59], the polarization of an optical and X-ray compact thermal source in a magnetic field was calculated. In [60], the calculation of the typical spectrum of radiation from plasma cloud by a mechanism of comptonization showed the effect of comptonization on the profile of spectral lines of iron. In [61], the creation of cyclotron lines in the X-ray spectrum of the Hercules X-1 pulsar was evaluated taking into account the effect of photons passing through hot plasma. In [62], the spectrum and shape of cyclotron lines of the X-ray pulsar atmosphere were calculated taking into account the combination of the effects of comptonization and anisotropy.

Orbital observatories systematically collect data on cyclotron lines, which are registered in most X-ray pulsars. In [63—66], the data are presented from the international orbital X-ray station RXTE (Rossi X-ray Timing Explorer), and in [67—73] the data on cyclotron lines were obtained at the station BeppoSAX (Satellite per Astronomia a raggi X).

Annihilation lines. Annihilation lines were detected in the spectrum of pulsars, in addition to cyclotron lines and spectral lines of atoms and ions in the gamma range. These lines are associated with the process of annihilation of an electron-positron pair in one photon (1γ process) and two photons (2γ process) in the pulsar magnetosphere. Papers [74—81] are devoted to the study of these processes. In [74—75] it was assumed that the particles are initially in the ground energy states $l = 0$. It was shown that the1γ process dominates over the 2γ process for the 10^{13} *Gs* magnetic field. In [76], the excited energy levels of the electron and positron $l > 0$ were taken into account in this process. Asymptotics for the reaction rate in the case of large quantum enumbers of the e^+e^- pair was also obtained. In [77—78], the process of e^+e^- pair annihilation into one photon was considered taking into account spins of particles and arbitrary polarization of radiation. It was shown that the ground spin states (the electron spin is directed against the field and the positron spin is directed along the field) make the main contribution to the probability of the process. In [79], the polarization of radiation in the process of e^+e^- pair annihilation into two photons (2γ process) was studied. In magnetic field $H \sim 0.1\ H_0$, the radiation is linearly polarized, the degree of polarization reaches several tens of percent and depends on the frequency, direction, and magnitude of the field. The 2γ processin supercritical fields in a moderate relativistic mode was considered in [80—81]. Note the paper [82], which studied the process of e^+e^- pair annihilation with the formation of neutrinos and antineutrinos.

The disadvantages of these papers include the lack of analysis of resonances in the 2γ process.

Cascades and electromagnetic showers. If in a magnetosphere of a neutron star in the pole region the electron is accelerated to energies $\sim 10^{12}\ eV$ due to the presence of an electric field parallel to the magnetic one, then the mo-

tion of this electron along curved magnetic field lines will lead to the emission of a hard photon (curvature radiation). This photon, in turn, generates a high-energy electron-positron pair in a magnetic field. The result is a cascade of processes: curvature radiation → electron-positron pair production. Many theoretical studies are devoted to the analysis of the cascade process scenario. In particular, the papers [83—92] are devoted to calculations of cascades. In most of these works, numerical simulations were performed. In [83], a radio emission of a system, where an electron-positron cascade self-supporting process that was realized in parallel magnetic H and electric E fields in case $E << H$, was analyzed. In [84—87], the calculation of up to two dozen steps of a cascade was performed by a Monte Carlo method, and the effect of cascades on the spectra of e^+e^- pairs and gamma rays was analyzed. In [88], the theory of cascade mechanisms of electromagnetic showers was constructed, which was based on kinetic equations for the distribution functions of particles and photons. Simulation of electromagnetic showers in the hard ultrarelativistic case $(\varepsilon/m)\cdot(H/H_0) >> 1$ was carried out in [89]. Simulation of cascades in fast-rotating pulsars was performed in [90]. The cascade included the curvature radiation by a primary electron, a conversion of photons emitted by the primary and secondary particles into e^+e^- pairs, a quantization of the SR, and inverse Compton scattering by secondary pairs. In [91], a self-consistent kinetic simulation of e^+e^- cascades was performed taking into account the shielding of the electric field by particles. In [92], simulation of e^+e^- cascades taking into account the polarization of photons, as well as simulation of resonant Compton scattering in strongly magnetized neutron stars was performed.

Electron-positron plasma of the magnetosphere of pulsars. As a result of repeated cascades together with the processes of pair annihilation and Compton scattering, e^+e^- gas (e^+e^- plasma) of the pulsar magnetosphere is formed. The papers [93—97] are devoted to modeling the process of e^+e^- plasma formation. One of the features of radiation from pulsars is coherent radiation in radio domains. In [96], it was shown that the source of coherence is the instability of the plasma arising in the magnetosphere. In [97], the simulation of e^+e^- plasma in supercritical fields of magnetars $H \sim 10^{14}$—$10^{15} Gs$ was performed. Note also the papers [98, 99], where the thermodynamic properties of e^+e^- gas in a magnetic field are studied.

Quantum-electrodynamic processes near neutron stars in strong magnetic fields were considered in reviews [100—103] and monographs [104—105].

The parameters of the pulsar radiation, which are measured during observations (pulsar brightness curves, its period and pulse profile, energy spectrum and its variability at different time scales, polarization, etc.) certainly depend on the elementary QED processes occurring in the electron-positron plasma in the neutron star magnetosphere. The subject of studying X-ray pulsars, which

includes both astronomical observations and theoretical calculations, remains relevant to this day, as there is no single theory of X-ray pulsar radiation. In particular, the determination of a spin population of a magnetized e^+e^- gas and its effect on the SR of an X-ray pulsar is an unsolved problem in the framework of quantum electrodynamics.

1.4. Second-order QED processes near resonances

Second-order quantum electrodynamic processes, such as **Compton Scattering** (CS), which is the scattering of a photon by an electron or positron, **Double Synchrotron Radiation** (DSR), that is the emission of two photons by an electron, **Two photons e^+e^- Pair Production** (TPP), that is the production of electron-positron pair by two photons, **One-photon e^+e^- Pair Production with a photon Emission** (OPPE), pass through the intermediate electron (positron) state. These processes are cross-channel to each other. An external electromagnetic field allows bringing the intermediate state to the mass surface, which corresponds to resonant conditions of the processes [106—112]. The cross-section of the QED process in resonant conditions can exceed the cross-section in non-resonant cases by several orders of magnitude, which is of great physical interest. The resonant divergence is eliminated by the Breit-Wigner rule [113]. Papers [114—116] are devoted to the elimination of resonant divergences in the case of a stable intermediate state.

Compton scattering. The change in the frequency of a photon during its scattering by a free electron is known to have been discovered by Arthur Compton in 1923 (Compton effect). The complete quantum relativistic theory of the CS process was built by O. Klein and Y. Nishina in 1929 and independently by I. Tamm in 1930. An external magnetic field modifies the CS process. As mentioned above, initially the study of the influence of a field on the CS process was associated with the processes of comptonization that take place in the magnetosphere of neutron stars.

The CS process in a strong magnetic field was studied in [109, 117—128]. In [117], the total cross-section of the CS was found by the Schwinger method when a photon propagates along a field. In [118], the differential cross-section of the CS was obtained if initial and final electrons are in the ground energy states $l = l' = 0$. The CS process was considered in [119] with the study of cyclotron resonances when the initial electron is in the ground energy state $l = 0$. The general case in the LLL approximation was considered in [120] taking into account the process of two-photon Compton scattering. In particular, it was shown that the probability of the latter in cyclotron resonance is comparable to nonresonant single-photon scattering. In [121], the scattering of soft photons by rela-

tivistic electrons was considered when electrons move along the direction of a strong magnetic field. In [122], a comparison of two relativistic processes was performed taking into account particle spins: photon absorption by an electron and CS. It was shown that at the point of cyclotron resonance these cross-sections are equal. In [124], the CS process is resonant and nonresonant modes were considered, taking into account the polarization of radiation when a relativistic electron moves along a supercritical field. In [125—126], resonant and interresonant Compton scattering were considered, taking into account the electron spin. Under resonant conditions, the differential cross-section was represented in the form of Breit-Wigner. In the magnetic field $H \sim 10^{12}\,Gs$, the resonant cross-section is several orders of magnitude larger than the interresonant cross-section, the interresonant cross-section is of the order of the Thomson cross-section, and the resonance width is tens of electron volts. In relatively recently published papers [127], the differential cross-section of this process was obtained in the case of both subcritical $H < H_0$ and supercritical $H > H_0$ magnetic fields, taking into account the electron spin, when the initial photon propagates along the field. In [128], the scattering of a photon by an electron was considered through the study of an intermediate process of photon emission by an electron in a magnetic field and an electromagnetic wave directed along the field (Redmond configuration).

The disadvantages of this paper include the lack of analysis of the effect of polarization of the initial photon, both on the polarization of the radiation and the spin states of the final electron for different spin states of the initial electron under resonant conditions.

An actual problem is to find the mechanism of polarization of electron beams (positrons) by a linearly polarized electromagnetic wave based on the process of resonant CS in a magnetic field.

Two photons electron-positron pair production. The TPP process in a magnetic field was studied in [129—133]. In [129], a probability amplitude of the fourth-order process (the scattering of a photon by a photon) was found, and the total probability of TPP was found by using the optical theorem in the case when both initial photons are directed along the field. In [130—132], expressions were obtained for the probability of the OPP process in the Redmond configuration field with subsequent selection of one initial photon from the electromagnetic wave field. In [132], the total probability of the OPP process was obtained through optical theorem from the polarization operator and it was shown that a magnetic field causes oscillations in the cross-section that have an amplitude that significantly exceeds corrections obtained by perturbation theory. In the end consistently as a process of the second order, the process of TPP was considered in [133]. The case when the energy of each of the photons does not exceed $2m$ was considered to remove the OPP process. The resonant behavior of the OPP cross-section and the dependence of the cross-section on the polarization of pho-

tons were analyzed. A comparison of the processes of electron-positron pair production by one and two photons (OPP and TPP) was performed in [134—138] concerning X-ray pulsars and soft gamma-ray bursts. In particular, in [134] it was shown that the OPP process dominates for most pulsars when the magnetic field is of the order of $H \sim 10^{12}$ *Gs*, the photon density of a magnetosphere does not exceed $n_\gamma < 10^{25}\ cm^{-3}$, the e^+e^- plasma temperature exceeds $kT > m$. The disadvantage of these papers is the use of formulas for the probability of TPP without an external magnetic field. That is, the estimates did not take into account the resonant course of the TPP process and therefore should be revised. In [139], the process of electron-positron pair production by a photon during its propagation in a thermal bath in a superstrong magnetic field $H >> H_0$ was studied.

It should be emphasized that there are two types of divergences (resonances) in the TPP process in the external magnetic field.

The first divergence is related to the case when an intermediate electron (positron) is on the mass shell. In this case, the second-order process splits into two independent first-order processes. The second type of divergence is associated with the discrete motion of an electron (positron) in the plane transverse to the direction of a magnetic field. It takes place at the reaction threshold when particles are produced with zero longitudinal momenta. The OPP process contains a similar divergence. The second type of resonances was studied in [133]. The resonant course of the TPP process in the first scenario was not studied.

The unsolved problems in the study of the TPP process are as follows:

- Investigation of the resonant TPP process when an intermediate particle comes to its mass shell.
- Analysis of the effect of initial photon polarization on the degree of polarization of final particle beams in the resonant TPP process.
- Comparison of the processes of OPP and TPP in the conditions of an e^+e^- plasma of a magnetosphere of X-ray pulsars taking into account the resonant behavior of the process of two-photon production of e^+e^- pair in a magnetic field. Searching for parameters when the last process can compete with the first-order process (production of e^+e^- pair by one photon).

Double synchrotron radiation. Relatively few works were devoted to the process of emission of two photons by an electron (the DSR process) when the electron moves in a magnetic field [140—142]. In [140], the process of radiation of one photon by an electron in the Redmond configuration field with the emission of one photon from an electromagnetic wave was considered. In [141], the DSR process was studied in the second Born approximation in the quasiclassical case with ultrarelativistic particles. Finally, second-order calculations of the perturbation theory were performed in [142] for the process of emission of two photons by an electron in a strong magnetic field. The calculations were applied to the fields of magnetars $H \sim H_0$ and dependences of the process probability

on both the electron spin direction and the photons polarization were found. The conditions for the occurrence of resonances were analyzed and numerical estimates of probabilities were performed.

The disadvantages of these works include the lack of analysis of comparisons of SR processes and resonant DSR process in the LLL approximation (in a strong magnetic field). The conditions of probability factorization in resonant cases and the influence of a spin-flip process in resonant DSR on radiation polarization have not been studied.

One-photon production of e^+e^- pairs with photon emission (OPPE). This process in a strong magnetic field should be characterized by the same basic properties as its cross-channel CS, TPP, and DSR, namely: the presence of resonances, the strong dependence of the process rate on the spin direction of the particles, and the polarization of photons, the achievement of the process rate in resonance to the magnitude of the first-order processes. Therefore, the study of the OPPE process is an urgent task. However, there is no mention of this process in the literature.

1.5. QED test in the FAIR project

An international convention was signed in 2010 to establish a new scientific mega-project — the FAIR accelerator complex (Facility for Antiproton and Ion Research) with a total budget of over one billion euros which is being built in Germany (near Darmstadt) based on the GSI Helmholtz Centre for Heavy Ion Research. The FAIR project includes the study of QED phenomena in extremely strong electromagnetic fields, in addition to the program of studying the hadronic matter, the study of fundamental symmetries and interactions, as well as the study of the dynamics of multiparticle systems taking into account collective effects [143, 144]. This direction is performed by the SPARC collaboration (Stored Particles Atomic Physics Research Collaboration). In particular, studies involving photons, electrons, and atoms in the presence of strong rapidly changing electromagnetic fields, as well as structural studies of heavy ions will be performed. It is planned to perform experiments on the interaction of hydrogen and helium ions with an intense pulsed laser field of the PHELIX laser when an electron in the inner orbit of heavy ion experiences a field of the order of the critical one $E_0 = m^2/e$. Verification of quantum electrodynamics in strong fields within the FAIR project involves consideration of the following tasks: Lamb shift, the fine structure of heavy ion levels, anomalous magnetic moment of bound electrons, ions, and electrons in the intense field of laser. Adjustment of the laser to transitions between electron energy levels is possible in experiments with counter beams (intense laser beam and beam of hydrogen-like heavy ions) due to Doppler shift. The study of the dynamics of collisions in strong fields in the FAIR program includes the following tasks: radiation cap-

ture of an electron in ion-atomic collisions, formation of quasi-molecules in ion-ion collisions, production of e^+e^- pairs in the collision of heavy ions.

Supercritical charge of the nucleus. The solution of the Dirac equation has a singularity for the bound states of an electron in the field of a point nucleus with charge Z [145]. According to Sommerfeld's formula for the fine structure of an atom, the energy of the lower electronic level $1S_{1/2}$ has the form [146]:

$$\varepsilon_0 = m\sqrt{1-(Ze^2)^2}. \tag{1.2}$$

The energy (1.2) approaches zero at $Z = Z_c$, where $Z_c = 137$. When $Z > Z_c$, it becomes an imaginary value, which indicates the incorrectness of the problem without taking into account the boundary conditions for the wave function at zero. Note that the imaginary additive to energy is known to describe a nonstationary process, decay, i.e. the state with $Z > Z_c$ must be unstable. A more realistic model with a finite nucleus size allows it to go beyond $Z > 137$ [147—148]. In [147], the notion of the critical charge of the nucleus Z_c (charge at which the energy of the $1S_{1/2}$ level of electron reaches the value of the energy of the lower continuum) was introduced and this value was estimated $Z_c = 200$. Later in [149—151] a more accurate analysis of the Dirac equation with $Z \sim Z_c$ was performed, whence follows $Z_c \approx 170$. In these papers, it was noted that in the case $Z > Z_c$ for a bare nucleus and with a vacancy on the K-shell there is a spontaneous process of capture of electrons from the negative continuum (Dirac basement) to the K-shell and the formation of a hole in the continuum, which manifests itself as spontaneous positron production. The effect of spontaneous quasi-static positron production at $Z > 170$ can be observed in the collision of two nuclei with a total charge of $Z_1 + Z_2 > Z_c$, for example, in the collision of two bare uranium nuclei [149]. The calculation of the cross-section of the process of spontaneous positrons production in the heavy ion collision by the above mechanism was carried out in [152—153].

Darmstadt peaks. In the late 1970s, the GSI Helmholtz Centre for Heavy Ion Research launched a program for the UNILAC accelerator to study the processes of heavy ions collisions accompanied by the spontaneous production of positrons. As part of this program, two groups EPOS [154—157] and ORANGE [158—161] carried out experiments on the collision of fast with energy near the Coulomb barrier (~6 *MeV/nucl*) heavy ($Z \sim 90$) ions with the formation for a short time $\sim 10^{-21}$ s of a heavy composite nucleus with a supercritical charge. During experiments in both groups, the spectra of positrons formed as a result of nuclear collisions were measured. The main mechanisms of positron production in ion collisions are as follows: 1) internal pair conversion when removing the excitation of the nuclei with a radiation time of $\sim 10^{-15}$ s (conversion positrons), 2) extraction of electrons from the negative continuum under the action of rapidly changing in time and space deep (~ 20 *MeV*) Coulomb potential with a radiation

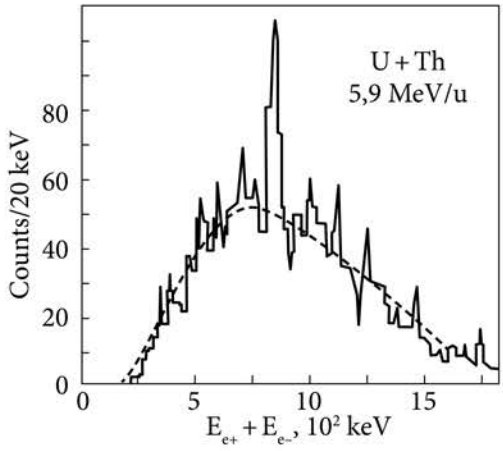

Fig. 1.4. The anomalous peak in the energy spectrum of e^+e^- pair production, which was observed in Darmstadt experiments on the collision of heavy ions [164]

time of ~ 10^{-21} s (dynamic positrons) and, finally, 3) the process of spontaneous production by supercritical charge with a radiation time of ~ 10^{-19} s (spontaneous positrons). The first two processes are the background to the sought process of spontaneous positrons production. The experimentally measured background was in good agreement with theoretical calculations. The time of spontaneous transition of an electron from a negative continuum is two orders of magnitude greater than the time of ion collision, i.e. the time of existence of a supercritical charge. And this was probably the main difficulty in trying to detect spontaneous positrons. However, in the positron spectrum of both groups, abnormal narrow peaks (several tens of kiloelectronvolts wide) were detected in the region of kinetic energies of positrons of 200—400 *keV*. To study electron-positron matches, EPOS and ORANGE spectrometers were further modified with the addition of electron spectrometers [162—164]. In the spectra of electron-positron pairs, narrow lines corresponding to the lines in the positron spectra, but with a smaller width, were also detected (see Fig. 1.4). The location of the lines did not depend on the magnitude of the total charge of the composite nucleus, while the cross-section was proportional ~ $(Z_1 + Z_2)^{20}$.

In [165], an overview of the experiments of both groups is given. Experiments of the APEX group with improved electron and positron spectrometers did not reveal any abnormal features [166] and later experiments in this direction were stopped. A fairly complete review of both the Darmshadst experiments and related issues was conducted in [167].

The strong magnetic field of colliding heavy nuclei. It should be noted that quantum-electrodynamic processes can take place in the region between nuclei in a strong magnetic field of nuclei when heavy ions collide with impact parameters that have an order of magnitude (or more) of the nucleus size $\rho \geq R_{nuc}$ (ultraperipheral collisions). Between the nuclei, the magnetic fields of moving nuclei are added, and the electric ones are compensated (see Fig. 1.5). For impact parameters of the order of 10^{-10} *cm*, colliding heavy nuclei with a charge $Z = 90$, which move at a speed of ~ c / 10, create a magnetic field of the order of 10^{12} *Gs*. In this area, the course of QED processes involving a strong

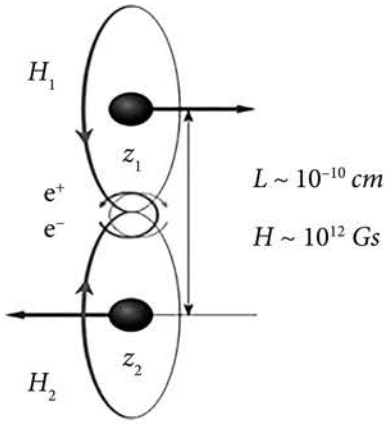

Fig. 1.5. When heavy ions collide in the region between the nuclei, the e^+e^- pair is produced in a strong magnetic field of moving nuclei

magnetic field is quite possible. In the process of production of an electron-positron pair in a collision of nuclei, if the pair is produced between the nuclei, it will be at the Landau levels. The distance between adjacent Landau levels for the field $H = 5 \cdot 10^{12}\ Gs$ is equal to 50 keV, which can be determined experimentally. In the energy spectrum of e^+e^- pairs generated by the collision of nuclei, narrow lines should be observed, located quasi-equidistantly, which correspond to the Landau levels. Cyclotron lines in the X-ray radiation range accompanying electron transitions to neighboring Landau levels should also be observed.

We assume that the series of quasi-equidistant peaks observed in the Darmstadt experiments could exactly correspond to the indicated Landau levels [168]. Note also the work [169], which analyzed the effect of a strong magnetic field of moving nuclei on the generation of positrons in the collision of heavy ions, as well as the possible participation of the magnetic field in the formation of narrow peaks. In this paper, the stationary two-center Dirac equation, which included the magnetic fields of moving charges, was solved and the method of adiabatic phase-correlation diagrams was used. The electron-positron pair production rates obtained in two-center calculations, including the magnetic field, were close to rates calculated in the monopoly approximation without a magnetic field and did not contain a resonant structure.

Thus, it is important to study the QED with magnetic field concerning the SPARC of the FAIR project, including a program to revive the old Darmstadt experiments. This paper studies the process of generating e^+e^- pair at low Landau levels by two photons in a strong magnetic field.

1.6. Photon propagation in a magnetic field

Photon dispersion. The process of photon propagation in a region with an external classical electromagnetic field (in our case, a magnetic field) is similar to the propagation of an electromagnetic wave in an anisotropic optically active medium. Therefore, the study of this process is reduced to the analysis of the optical properties of the active medium using a renormalized polarization tensor (photon polarization operator). The polarization operator

was mentioned above when considering first-order processes, where it was used to obtain the full probability of the OPP process.

Works [170—176] are devoted to the analysis of the analytical properties of the polarization tensor. In [170], the solution of the dispersion equation for eigenmodes was found using the polarization tensor. The solutions near a threshold of e^+e^- pair production (cyclotron resonance) were analyzed in detail. The monograph in FIAN proceedings [171] is devoted to the study of the polarization of vacuum and quantum relativistic gas in a constant external electromagnetic field. The singular behavior of the polarization operator due to the OPP process in a magnetic field was studied in more detail. In [172], the process of photon propagation in a supercritical field $H >> H_0$ was considered. The behavior of a photon in an arbitrary superposition of constant magnetic and electric fields was studied in [173]. The polarization operator in the $2+1$ dimensional QED with nonzero fermion density in a constant uniform magnetic field was calculated in [174]. In [175], the polarization operator of e^+e^- gas in a magnetic field was found using the Matsubar technique for Green's temperature functions. Radiation corrections to the polarization operator were calculated in [176].

Vacuum Birefringence (VB). Birefringence is known to be the effect of splitting a beam of light into two components (ordinary and extraordinary) in anisotropic media (calcite crystals). If we choose the conditions under which the directions of the ordinary and extraordinary rays coincide, then there is an effect of changing the polarization. In addition to crystals, birefringence is observed in isotropic media placed in an external electromagnetic field. So in the electric field, there is a Kerr effect. In the magnetic field, a Cotton-Mouton effect and a Faraday effect are analogs. In the field of a laser wave, this is a Kerr optical effect. Since the external magnetic field, which has a value of an order of the critical field H_0, polarizes the vacuum and the vacuum as a result exhibits properties of an anisotropic medium, it is possible to observe vacuum birefringence of light. This effect was first predicted and theoretically described in [177]. The effect is based on a fourth-order QED process, namely the process of light by light scattering. A cross-section of this process was found in [178, 179].

Further development of methods using the nonlinear Heisenberg-Euler Lagrangian and the study of the VB effect was carried out in [180—188]. The polarization of vacuum and VB in an external electromagnetic field of arbitrary configuration was considered in [180]. In [182], the process of propagation of a linearly polarized laser beam in an external transverse magnetic field was studied. The response of the QED vacuum and its instability in asymptotically large magnetic fields $H >> H_0$ was studied in [183]. Papers [184—185] are devoted to the VB effect in a strong magnetic field, where properties of a photon polarization tensor and a complex refractive index are numerically obtained and analyzed in detail. In [186], polarization effects caused by photon-photon interac-

tion in laser experiments were considered. The laser beam propagates in an area with a magnetic field or it collided with another laser beam. In [187], experiments (astronomical observations) were performed at the Very Large Telescope (Chile), where experimental confirmation of the VB effect in optical-polarimetric measurements of an isolated neutron star was obtained for the first time. Note also the monograph [188], where the process of particles production from a vacuum, as well as the process of polarization and rearrangement of vacuum by an external field, was considered based on Bogolyubov's transformations and the monograph [189], where the theory of perturbations was developed and methods for finding the Green's function have been developed.

Photon Splitting (PS). The photon splitting process is a third-order QED process in the single-loop approximation and cannot occur without an external field according to Farry's theorem [190, 191]. The difference from the polarization operator is the presence of an additional photon in the final state. A strong external magnetic field makes such a process possible and interesting in astrophysics as a mechanism for generating linearly polarized gamma rays. Papers [192—197] are devoted to the study of this process. In [192], a refractive index of photon propagation and an absorption coefficient, as well as the rules for selecting polarization for photon splitting were determined. In [193], the probability per unit time of photon decay into two photons was found. The process of merging two photons into one photon is the reverse process of photon splitting. It was considered in [194]. In [195], numerical results for a probability of photon splitting as a function of photon energy below the energy threshold of the e^+e^- pair for different values of a magnetic field of neutron stars were obtained, and a recalculation of previously obtained results was performed. In [196], the S-matrix approach, which was used in [195] to consider the PS process in a magnetized vacuum, was critically discussed and the problem of amplitude convergence in the case of weak magnetic fields was solved. In [197], the main physical aspects of two processes with the same initial conditions (PS process and OPP process) were presented. Their manifestation in a magnetosphere of neutron stars was discussed.

It should be emphasized that when a photon propagates in a magnetic field under resonant conditions corresponding to the production of a real electron-positron pair, the reverse process to annihilate the pair into one photon is possible. Thus, a cascade of processes of production and annihilation of the e^+e^- pair is formed, which has not been studied before. Relevant issues are:

- the study of the process of photon propagation in a strong magnetic field, when there is a **Cascade of processes of the e^+e^- Pair Production and subsequent the Pair Annihilation** (CPPPA);
- calculation of the change in photon polarization in the CPPPA process in resonant and interresonant regions.

1.7. QED processes in a laser wave field. SLAC experiments

QED processes in a plane electromagnetic wave field. The procedure for calculating the processes of quantum electrodynamics in a plane electromagnetic wave field is methodologically the same as in the external magnetic field, so it is advisable to mention this topic without claiming the completeness of the review. Indeed, in both cases, the Farry picture diagram technique is used [191], when the external classical field is precisely taken into account through the solution of the Dirac equation for the electron (positron). And the interaction of particles with quantum photons is taken into account by perturbation theory. Also note, as will be shown below, under certain conditions, the results of calculations in the laser wave field and the constant magnetic field coincide.

The general solution of the Dirac equation for an electron in a plane electromagnetic wave was found by Volkov in the 1930s [198]. After the advent of lasers, Volkov functions began to be used extensively to study the elementary processes of QED in the laser field.

One of the main parameters of the problem is a relativistically invariant multiphoton parameter, which has the form:

$$\eta = \frac{|e|F}{m\omega}, \tag{1.3}$$

where F, ω are strength (intensity) and frequency of the external electromagnetic field. This parameter has the physical meaning of a work of the field at the wavelength in units of the rest energy of an electron. In this case $\eta << 1$, the QED process involves a small number of virtual photons of the external field, in the extreme case, one photon. If $\eta \sim 1$ or more, multiphoton processes are essential. To reach a value $\eta \sim 1$ in the optical range, the field strength must be of the order of magnitude $F \sim 10^{10}$ *V/cm*. This corresponds to the intensity of the laser $\sim 10^{18}$ W/cm^2. Modern high-power femtosecond lasers are already reaching the required intensity to observe multiphoton nonlinear QED processes. Value $2 \cdot 10^{22}$ W/cm^2 was obtained in [199] as a record value of intensity for 2008 in the optical range $\eta \sim 100$ at a laser with a power of 300 TW. The LFEX (Laser for Fast Ignition Experiments) optical laser with a record power of 2 PW was built in Japan (Osaka University). Two European projects ELI (Extreme Light Infrastructure) [200] and XCELS (Exawatt Center for Extreme Light Studies] [201] are under construction, where it is planned to achieve exavatt power and field strength 10^{24} W/cm^2 and above.

Consideration of first-order QED processes in a laser field (spontaneous photon radiation by an electron, e^+e^- pair production by a photon) is present-

ed, for example, in [44], [202—205]. Recently, such processes have been studied in the field of ultrashort laser pulse with $\eta \geq 1$ [206] and the ultra-strong laser field with $\eta >> 1$ [207]. Scattering of an electron at the Coulomb center in a pulsed field of a laser wave was considered in [208]. Papers [209, 210] were devoted to the cross-channel electron scattering, namely the e^+e^- pair production by a Coulomb field in a laser field in tunnel mode. Resonances in the process of photon scattering by an electron in the field of a plane monochromatic wave were studied in [108] and in the field of a pulsed laser wave in [211—214]. The process of bremsstrahlung of an electron at the Coulomb center in the field of a pulsed laser was studied in [215—217]. The papers [111, 112], [218, 219] are devoted to lepton-lepton scattering. In [220], [221] the process of spontaneous emission of two photons by an electron in an intense laser field was considered. In [222], the total cross-section of high-energy electron-positron pair production by a photon in the combined field of an atom and an intense laser was calculated. A review of studies of the processes of relativistic quantum dynamics, quantum electrodynamics, nuclear physics, and elementary particles in extremely intense laser fields was performed in [223]. In the monographs [224] and [225], the resonant and coherent effects of QED in a light field (field of a plane monochromatic wave) and in a strong pulsed laser field, respectively, were studied.

QED processes in the Redmond configuration field. The Dirac equation for an electron in an external classical field, which is a superposition of the constant magnetic field and the field of a plane electromagnetic wave directed along the magnetic field (Redmond configuration), has an exact solution [226]. The Green's function of an electron in the Redmond configuration field was found in [227]. This allowed me to perform several works on the study of QED processes in this field [109], [128], [130—132], [140], [204], [228—234]. The process of spontaneous emission of a photon by an electron was considered in [204], [228—230]. In [229], the problem was solved when an electron was at the lowest Landau levels. The process of e^+e^- pair production by one photon was studied in [231].

The obtained results of research of QEDs on first-order processes can be used as an auxiliary for studying QEDs of higher-order processes in a purely magnetic field. To do this, you need to select a finite number of photons from the field of the plane electromagnetic wave. The problem of photon scattering by an electron in a magnetic field was performed in this way in [128], [140], [232—233]. In [233], the scattering cross-sections found were further used to obtain a cross-section of bremsstrahlung of an ultrarelativistic electron on a nucleus using the equivalent photon method. The problem of e^+e^- pair production by two photons in a magnetic field was solved in [130, 131]. In [234], the problem of e^+e^- pair production by a single photon on a nucleus in a magnetic

field was considered. The study of cyclotron resonances and the process of scattering in a magnetic field was carried out in [109], analyzing the mass operator of the electron in the Redmond field and using the optical theorem. By a similar method, investigating the polarization operator in the Redmond configuration field, the probabilities of electron pair production by two photons were found in [132].

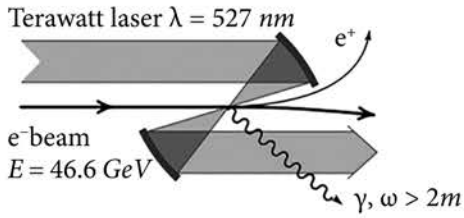

Fig. 1.6. Scheme of collision of the electron beam with the laser beam in the SLAC experiment on the production of e^+e^- pairs [236]

It should be noted that papers with direct calculations of the second-order QED processes in the Redmond field with the analysis of resonant and polarization properties in the literature are absent. To perform them, as a first step, it is necessary to find the expression for Green's electron function in the Redmond configuration field in a form convenient for calculations of resonant processes.

SLAC experiments. The first experiments to study first- and second-order quantum electrodynamic processes in the external field of an intense laser wave were the SLAC experiments of 1996—1997 [235—237].

In these experiments, a beam of electrons with energies of ~ 50 GeV was directed toward a laser beam with an intensity of 10^{18} W/cm^2 (see Fig. 1.6). As a result, hard photons with energies > $2mc^2$ were detected [235], as well as positrons [236]. High-energy electrons moving in an external field, in this case, a laser wave field, inevitably spontaneously emit photons, in the spectrum of which there is a hard component. In turn, a hard photon with an energy > $2mc^2$, moving in the same external laser field, can generate an electron-positron pair, which was experimentally observed.

The authors of SLAC experiments identify two possible channels for electron-positron pair production. The first channel is the Breit Wheeler process, [191] the process of e^+e^- pair production by two photons. One photon is a hard photon formed by inverse Compton scattering of wave photons by an electron. The role of the second photon is performed by n photons of the laser wave. The second channel is the **trident process** (TP), where the initial electron generates an electron-positron pair through an intermediate virtual photon.

Calculations of the multiphoton trident process, which occurs when an intense laser beam interacts with an electron beam, in the Vazzecker-Williams approximation [191] were performed in [238]. A complete theory of the multiphoton trident process of e^+e^- pair production in a strong laser field in the second Born approximation was presented in [239]. The numerically obtained probability per unit time of e^+e^- pair production $R = 4 \cdot 10^{-4}$ s^{-1} was four times higher than the experimental value [236]. In [240], a review of QED processes

in the intense field of a laser beam was presented, where nonlinear collective effects in photon-photon and photon-plasma interactions were analyzed.

The trident process of e^+e^- pair generation in a strong external magnetic field in the Vazzecker-Williams approximation of equivalent photons with ultrarelativistic particles was studied in [13]. The excitation of Landau levels of an electron due to collisions in a strong magnetic field was considered in [241]. Note that in the papers of A.I. Nikishov, and V.I. Ritus [202, 203] it was shown that the expression for the probability of spontaneous emission of a photon by an electron in a laser wave field coincides with the expression for the probability of SR process (photon emission by an electron in a magnetic field) in the case of ultrarelativistic electron motion. The fact is that an external electromagnetic field of any configuration in ultrarelativistic motion of an electron in its rest frame of reference looks like a constant crossed electromagnetic field.

In this regard, it is important solve the following problems:

- To find the probability of e^+e^- pair production by an ultrarelativistic electron in a magnetic field.
- To estimate the yield of positrons in the SLAC experiment [236] using the Nikishov and Ritus theorem (on the equivalence of external fields for ultrarelativistic processes) [202, 203].

1.8. The record values of magnetic field strength and the processes in superstrong magnetic fields

The record magnetic fields. Strong constant magnetic fields, up to $4.5 \cdot 10^5$ *Gs*, are achieved in laboratory conditions in the Bitter electromagnets installed inside superconducting magnets. Pulsed magnetic systems with a magnetic field of $8.9 \cdot 10^5$ *Gs* were developed at the National High Magnetic Field Laboratory (Los Alamos) [242]. In the middle of the last century A.D. Sakharov proposed the idea of magnetic cumulation and the basic design of explosive magnetic generators [243, 244]. As a result of rapid deformation by an explosion of conductive circuits, the seed's initial magnetic field of ~ 100 *kGs* was compressed to a value of 25 *MGs*. The advent of powerful pulsed petawatt lasers has led to the fixation of a new record value of the magnetic field in the experiment. A laser beam with an intensity of $10^{21} W/cm^2$ using pulse compression technology to intervals below picoseconds when interacting with laser materials forms a clot of dense plasma ~ $10^{21} cm^{-3}$ and above (laser-plasma), which creates a dynamic electric field of 100 MV/micron with corresponding magnetic field ~ 1 *GGs* [245—247]. The method of generating a strong magnetic field using magnetic coils with a laser driver is quite promising. The magnetic field of ~ 10 *MGs* was achieved at the Gekko XII laser facility (Osaka Univer-

sity's Institute for Laser Engineering, Japan) with a capacitor-coil target [248]. This approach has been adopted in many laboratories with different targets and the magnetic field strength in such experiments ranges from 10 *kGs* to 10 *MGs*. The differences are determined by the geometry of the target and the parameters of the incident laser. A similar experiment was conducted to study the generation of a magnetic field by a laser when irradiating a snail-type target at the PHELIX (Petawatt High Energy Laser for Heavy Ion Research, GSI, Germany) at a wavelength of 1056 *nm*, the duration of 0.5 *ps* and the intensity of $2 \cdot 10^{19}$ W/cm^2 [249]. The maximum value of the magnetic field in this experiment was 8 *MGs*. The work [250] is devoted to a review of the results of recent experimental studies of magnetic field generation. It should be noted that for the first time the magnetic field of wake waves with a laser driver at a wavelength of 800 *nm*, the duration of 85 *fs*, and the intensity of $3 \cdot 10^{18}$ W/cm^2 was experimentally studied at the JETI (Jena TItanium laser, Helmholtz Institute Jena, Germany). The Faraday rotation was used to measure the values of the magnetic field. According to the results obtained at this facility, the magnetic field was about 10 *MGs* [251]. Similar experiments were also performed in LOA (Laboratoire d'Optique Appliquee, France) [252] and at the European XFEL (European X-ray Free-Electron Lasers, Germany) [253]. Characteristic magnetic fields of the magnetosphere of neutron stars, as noted earlier, are fields of $\sim 10^{12}$ *Gs*. The record surface magnetic fields of $\sim 10^{15}$ *Gs* are characteristic fields for magnetars, which include anomalous X-ray pulsars and soft gamma-ray repeaters [254—258]. The maximum magnetic field in which standard quantum electrodynamics operates, $\sim 10^{42}$ *Gs*, is associated with the effect of positron collapse. The magnetic field significantly increases the Coulomb attraction between electron and positron. This happens until the electron and positron fall on each other, which corresponds to the collapse [259, 260].

Processes in supercritical magnetic fields. In the previously mentioned papers [80], [81], [97], [172], [183] the processes of QED (annihilation of e^+e^- pair, photon propagation) were considered in magnetic fields above the critical Schwinger value H_0. The calculation of ionization energy of atoms in such fields was performed in [261]. Photon emission and relativistic shift of energy levels for a hydrogen-like atom in a supercritical magnetic field were considered in [262]. The process of photon capture by a strong magnetic field and suppression of the e^+e^- pair production process was studied in [263, 264]. The properties of relativistic positronium in a superstrong magnetic field were considered in [265]. The problem of matter and radiation in very strong magnetic fields was devoted to reviewing works [266, 267], as well as a monograph [268].

The papers [269—274] were devoted to the problem of dynamic breaking of symmetries (symmetry of flavors in dimension 2 + 1, chiral symmetry in QED) and generation of mass of fermions in a constant magnetic field. The role of the

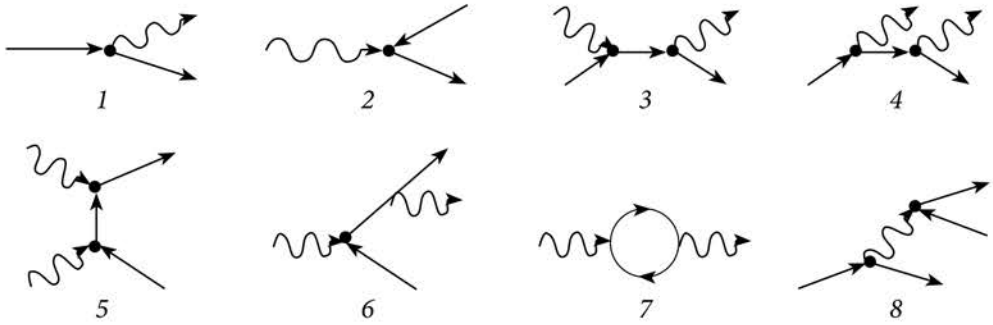

Fig. 1.7. Feynman diagrams of the first and the second-order quantum electrodynamics processes in an external magnetic field

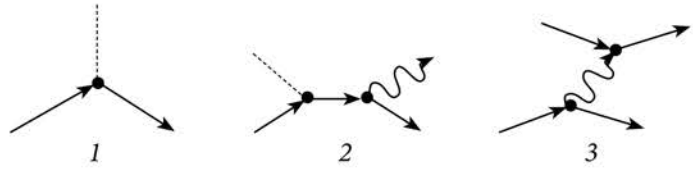

Fig. 1.8. Feynman diagrams of processes: *1* — scattering of an electron on a nucleus, *2* — bremsstrahlung of an electron on a nucleus, *3* — scattering of an electron on an electron

magnetic field in (2 + 1) dimensional models is similar to the role of the Fermi surface in the Bardin-Cooper-Schrieffer theory of superconductivity. This phenomenon is based on the spatial reduction D → D-2 in the dynamics of fermion pairing in a magnetic field, since the motion of a charged particle in a plane perpendicular to the field is limited. It should be noted that the nonperturbative QED dynamics is significant here. In the Farry picture, when the quantized interaction is taken into account perturbatively, a dynamic violation of symmetries in QED processes is not observed. Analysis of the static potential between a particle and an antiparticle in a strong magnetic field in the LLL approximation was performed in [275]. It was been shown that Coulomb's standard law is modified due to the appearance of vacuum polarization in a magnetic field. The problem of spontaneous magnetization of a vacuum of non-Abelian calibration fields at high temperatures was considered in [276]. In 2018—2020, a series of works [277—279] was published, in which QED processes in supercritical magnetic fields were studied. In particular, the process of an electron-positron pair annihilation into two photons was studied in detail. Based on the obtained cross-sections, the radiation of magnetars was simulated by the Monte Carlo method and it was shown that the radiation spectrum has a long low-frequency tail and it coincides with the spectrum of magnetars.

1.9. Conclusions

The above QED processes, namely that run in the magnetosphere of X-ray pulsars, processes in the SLAC experiment [235, 236], and processes that are planned to be studied in the field of quantum electrodynamics in strong electromagnetic fields in the FAIR project are a single class of QED processes of Furry picture. They are described by Feynman diagrams of the first and the second orders, where solid lines are wave and Green's functions of an electron in a homogeneous external magnetic field, and wavy lines are wave functions of a photon (see Fig. 1.7). The figure shows diagrams of the following processes: *1* — the synchrotron radiation (the SR process), *2* — the electron-positron pair production by one photon (the OPP process), *3* — the Compton scattering (the CS process), *4* — the double synchrotron radiation (the DSR process), *5* — the electron-positron pair production by two photons (the TPP process), *6* — the electron-positron pair production by one photon with photon emission (the OPPE process) *7* — the photon propagation in a magnetic field *8* — the trident process.

These processes will be studied in this paper. Note that in addition to those shown in Fig. 1.7 in principle, such processes are also possible, the Feynman diagrams of which are presented in Fig. 1.8. These are *1* — scattering of an electron on a nucleus, *2* — bremsstrahlung of an electron on a nucleus, *3* — scattering of an electron on an electron. The processes shown in Fig. 1.8 are characterized by a cross-section and require the introduction of the value of a flow of initial electrons. The addition of a strong magnetic field, which quantizes the transverse motion of particles, significantly changes the concept of the flow of initial electrons.

Chapter 2

SPIN AND POLARIZATION EFFECTS IN PROCESSES OF SYNCHROTRON RADIATION (SR) AND ONE PHOTON e^+e^- PAIR PRODUCTION (OPP)

2.1. Introduction

Research methods of quantum electrodynamics elementary processes are the standard rules of QED for finding probabilities of processes. To perform calculations of QED processes in an external magnetic field, a diagram technique within the framework of the Farry picture is used, when the interaction of charged particles with a classical magnetic field is taken into account accurately, and interaction with photons is treated within the perturbation theory. The external magnetic field measured in the units of the critical (Schwinger) field is a small parameter of the problem in the ultraquantum approximation, which makes it possible to obtain simple analytical expressions for the probabilities of QED processes.

The relativistic unit system is used hereafter, $\hbar = c = 1$.

In the study of QED processes, the direction of electron (positron) spins and photon polarization are taken into account. In a magnetic field, the motion of an electron is characterized by a specific value of the spin projection in the direction of the field, +1/2, or −1/2. The probability of a process involving an electron with a spin projection plus 1/2 (minus 1/2) will be denoted as W^+ (W^-). The polarization of photons is described by the Stokes parameters ξ_1, ξ_2, ξ_3, which determine the degree of polarization P by the relation

$$P = \sqrt{\xi_1^2 + \xi_2^2 + \xi_3^2}. \tag{2.1}$$

In processes with an external magnetic field, important cases of photon polarization are (i) normal linear polarization, when the photon polarization plane is perpendicular

to the plane of the wave vector and the direction of the magnetic field, in this case, $\xi_3 = -1$; (ii) anomalous linear polarization, when the field plane the photon coincides with the plane of the wave vector and the direction of the magnetic field, with $\xi_3 = +1$.

The spin-polarization effect is the effect of coupling the polarization of the initial photons to the spins of the final particles, and vice versa, coupling the spins of the initial particles to the polarization of the final photons.

Fig. 2.1 shows a schematic view of processes with polarized particles considered within quantum scattering theory. Here, a and b are the particles in the initial and final states respectively; P_a and P_b are the parameters describing the polarization of the particles a and b respectively; f_c is an analyzer filter that selects particles with given polarization P_c.

Thus, as a result of the scattering of the particles of set a, they pass into the set of particles b. After application of the filter f_c, the final particles are characterized by the parameters P_c. In this formulation of the problem, the scattering theory gives an expression for the probability of transition from the initial state with fixed polarization parameters P_a to the final state with fixed polarization parameters P_c. It is not correct to obtain the probabilities of transition to the final state b, P_b without an additional filter, because the final polarization parameters are not set, but are the result of the process. However, the parameters P_b can be found by determining the values of P_c at which the degree of polarization is maximum,

$$P_b = \max\{P_c\}. \tag{2.2}$$

As an example, consider a process with a photon in the final set of particles and let us determine the polarization and the degree of polarization of this photon. In general, the probability resulting from the quantum theory can be written in the form

$$W_\xi = A(1 + b_1\xi_1 + b_2\xi_2 + b_3\xi_3) = A(1 + \vec{b}\vec{\xi}), \tag{2.3}$$

where ξ_i are the Stokes parameters defined by the polarization vector of the wave function of the final photon (see sec. 2.2). These are the polarization parameters of the filter f_c (see Fig. 2.1). Further, A is a factor that does not contain ξ_i, b_i — are the coefficients at the parameters ξ_i. The explicit form of A and b_i is

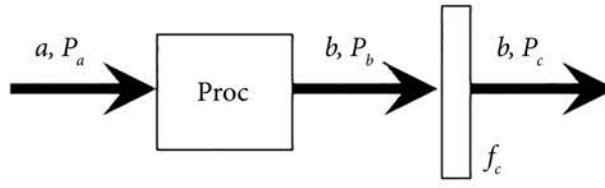

Fig. 2.1. Schematic view of a QED process with polarized particles

determined by the process. The degree of polarization is

$$P = (W_{\xi} - W_{-\xi}) / (W_{\xi} + W_{-\xi}) = \vec{b}\vec{\xi}. \tag{2.4}$$

This expression is maximum when the vectors $\vec{b}$ are $\vec{\xi}$ collinear, and the filter f_c transmits purely polarized states only, e.g. $|\vec{\xi}| = 1$. The obtained quantity is the sought polarization degree of the final photon,

$$P_{\max} = |\vec{b}| = \sqrt{b_1^2 + b_2^2 + b_3^2}, \tag{2.5}$$

It follows from the definition (2.1) that coefficients b_i are the sought Stokes parameters of a final photon.

Wave functions and parameters of particle polarization. Let us set the wave functions of an electron and a photon with defined polarization parameters. For the electron wave function, we will use the following expression [125],

$$\Psi^{-} = \frac{A_l}{\sqrt{S}} e^{-i(\varepsilon_l t - p_y y - p_z z)} [i\sqrt{m_l - \mu m} U_l(\zeta) + \mu\sqrt{m_l + \mu m} U_{l-1}(\zeta)\gamma^1] u_l^{-}, \tag{2.6}$$

where $\varepsilon_l = (m^2 + 2lhm^2 + p_z^2)^{1/2}$ is the electron energy in the magnetic field; p_y, p_z are the projections of the generalized electron momentum to the axes x and y, respectively; S is a normalizing area in the xy plane; $A_l = (h^{1/2}m/4m_l\varepsilon_l)^{1/2}$ is the normalizing constant;

$$m_l = m\sqrt{1 + 2lh}; \tag{2.7}$$

$h = H/H_0 = eH/m^2$ is the magnetic field strength in the units of the critical one; μ is the sign of the spin projection on the field direction; l is the Landau level number;

$$U_l(\zeta) = \frac{1}{\sqrt{\pi^{1/2} 2^l l!}} \exp(-\zeta^2 / 2) H_l(\zeta) \tag{2.8}$$

is the Hermite function and $H_l(\zeta)$ is the Hermite polynomial;

$$\zeta = \sqrt{hm^2}\,(x + \frac{p_y}{hm^2}) \tag{2.9}$$

is the offset dimensionless coordinate along the quantized direction x; γ^1 is the Dirac matrix in the standard representation; u_l^{-} is a constant bispinor of the form

$$u_l^{-} = \frac{1}{\sqrt{\varepsilon_l - \mu m_l}} \begin{pmatrix} 0 \\ \mu m_l - \varepsilon_l \\ 0 \\ p_z \end{pmatrix}. \tag{2.10}$$

Let the constant magnetic field H be directed along the z-axis. In this case, the electron wave function of the form (2.6) corresponds to the following gauge of the external electromagnetic potential (Landau gauge),

$$A^0_{ext} = 0, \quad \vec{A}_{ext} = (0, xH, 0). \tag{2.11}$$

We use the usual expression for the wave function of a photon [191],

$$A^i = \sqrt{\frac{2\pi}{\omega V}} e^i \exp(-i\mathbf{kx}), \tag{2.12}$$

where V is the normalization volume; ω, $\mathbf{k}$ are the frequency and 4-momentum of a photon; e^i is the polarization vector.

In the case when the photon propagates along the z-axis, the photon polarization vector e^i has the form

$$e^i = (0, \vec{e}), \vec{e} = (\cos\alpha, \sin\alpha \cdot e^{i\beta}, 0), \tag{2.13}$$

where α and β are the photon polarization parameters. Vector e^i_{ort} corresponding to the orthogonal polarization can be obtained from (2.13) by the substitution

$$\alpha \to \alpha + \pi/2. \tag{2.14}$$

The following relation is true,

$$e^i e^*_{i,\text{ort}} = 0. \tag{2.15}$$

In the general case of elliptical polarization, the rotation direction of the polarization plane is given by the sign of

$$direct = \text{sgn}(tg(\alpha)\sin(\beta)), \tag{2.16}$$

and the angle between the semi-major axis of the ellipse and x-axis is given by the expression

$$tg(2 \cdot angle) = tg(2\alpha)\cos(\beta). \tag{2.17}$$

For example, the polarization vector is $\vec{e} = (1,0,0)$ when $\alpha = 0$ and $\beta = 0$, which corresponds to the linear polarization along the x-axis. Similarly, if $\alpha = \pi/4$ and $\beta = \pi/2$, the polarization vector is $\vec{e} = (1, i, 0)/\sqrt{2}$, which corresponds to right circular polarization. Photon polarization matrix is defined via x and y components of the polarization vector e^μ according to

$$\rho_{ik} = e_i e^*_k = \begin{pmatrix} \cos^2\alpha & \sin 2\alpha \cdot e^{-i\beta}/2 \\ \sin 2\alpha \cdot e^{i\beta}/2 & \sin^2\alpha \end{pmatrix}. \tag{2.18}$$

Note that summation over two orthogonal polarizations yields the unitary matrix,

$$\rho_{ik} = (\rho_{ik})_{\text{ort}} = \delta_{ik}. \tag{2.19}$$

The most known set of the polarization parameters are the Stokes parameters $\vec{\xi} = (\xi_1, \xi_2, \xi_3)$, which are defined as

$$\vec{\xi} = \text{Sp}\rho\vec{\sigma}, \tag{2.20}$$

where $\vec{\sigma} = (\sigma_1, \sigma_2, \sigma_3)$ are the Pauli matrices. Inserting into this definition the explicit expression of the density matrix (2.18), we obtain the relationship between the Stokes parameters and the parameters α and β:

$$\xi_1 = \sin 2\alpha \cdot \cos\beta, \quad \xi_2 = \sin 2\alpha \cdot \sin\beta, \quad \xi_2 = \cos 2\alpha. \tag{2.21}$$

The transition to the orthogonal polarization vector according to rule (2.14) results in the Stokes parameters with the opposite sign:

$$\xi_i \to -\xi_i, \quad i = 1,2,3. \tag{2.22}$$

Note that the polarization degree (2.1), determined by these parameters, is equal to one corresponding to the pure state:

$$P = \sqrt{\xi_1^2 + \xi_2^2 + \xi_3^2} = 1. \tag{2.23}$$

In the case of an arbitrarily directed photon, with a wave vector

$$\vec{k} = k(\sin\theta\cos\varphi, \sin\theta\sin\varphi, \cos\theta), \tag{2.24}$$

the spatial components of the photon polarization vector can be obtained by rotating the coordinate system, if the z-axis is oriented along the wave vector,

$$\vec{e} = \begin{pmatrix} \cos\theta\cos\varphi & -\sin\varphi & \sin\theta\cos\varphi \\ \cos\theta\sin\varphi & \cos\varphi & \sin\theta\sin\varphi \\ -\sin\theta, & 0 & \cos\theta \end{pmatrix} \begin{pmatrix} \cos\alpha \\ \sin\alpha \cdot e^{i\beta} \\ 0 \end{pmatrix},$$

or

$$\vec{e} = \begin{pmatrix} \cos\theta\cos\varphi\cos\alpha - \sin\varphi\sin\alpha \cdot e^{i\beta} \\ \cos\theta\sin\varphi\cos\alpha + \cos\varphi\sin\alpha \cdot e^{i\beta} \\ -\sin\theta\cos\alpha \end{pmatrix}. \tag{2.25}$$

2.2. Spin-polarization effects in synchrotron radiation

Probability amplitude of SR. To construct the probability amplitude of the process of photon radiation by an electron A_{if} we use the standard QED rules according to the Feynman diagram shown in Fig. 2.2,

$$A_{if} = -ie\int d^4x\overline{\Psi}'(\xi)\gamma^i A_i^*\Psi(\zeta), \tag{2.26}$$

where γ_μ are the Dirac matrices; $\overline{\Psi}'(\xi)$ are the Dirac conjugated wave function of the final electron of the form

$$\overline{\Psi}' = \frac{A_{l'}}{\sqrt{S}} e^{i(\varepsilon_{l'}t - p'_y y - p'_z z)}\overline{u}'_{l'}[-i\sqrt{m_{l'} - \mu' m}U_{l'}(\xi) + \mu'\sqrt{m_{l'} + \mu' m}U_{l'-1}(\xi)\gamma^1]. \tag{2.27}$$

Here, μ' is the sign of the spin projection of the final electron on the magnetic field,

$$m_{l'} = m(1+2l'h)^{1/2}, \quad \xi = \sqrt{hm^2}(x + p'_y/hm^2). \tag{2.28}$$

Integrals in Eq. (2.26) over the variables *t, z, y* yields three Dirac delta functions that correspond to three conservation laws,

$$\varepsilon_l = \varepsilon'_{l'} + \omega, \quad p_z = p'_z + k_z, \quad p_y = p'_y + k_y. \tag{2.29}$$

As follows from Eqs. (2.9) and (2.28), *y* components of the generalized momentum of the initial and final electrons have the meaning of *x* coordinates of the rotation center of the classical particle orbits. The later equation in (2.29) determines the relationship of these coordinates with the *y* component of the photon momentum. The former two equations in (2.29) are the conservation laws for the energy and the longitudinal momentum particles. From these relations, we can obtain the expression for the photon frequency in the form

$$\omega = \frac{1}{1-u^2}(\varepsilon_l - p_z u - \sqrt{(\varepsilon_l - p_z u)^2 - 2hm^2(l-l')(1-u^2)}), \tag{2.30}$$

where

$$u = \cos\theta \tag{2.31}$$

is the cosine of the polar escape angle of the photon.

In the ultraquantum approximation, when the electron occupies the lowest Landau levels as well as in the case of a small angle θ, the frequency ω can be

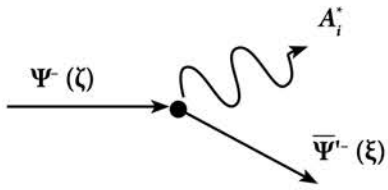

Fig. 2.2. Feynman diagram of the SR process

reduced to the form

$$\omega = \frac{hm^2(l-l')}{\varepsilon_l - p_z u}, \text{ якщо } \theta << 1 \text{ або } h(l-l') << 1. \tag{2.32}$$

It should be noted that the frequency vanishes if one inserts the condition $l = l'$ into Eq. (2.30). This means that the SR process is possible only when the electron transits to a lower Landau level.

Integrating the amplitude (2.26) in the x variable result in the appearance of the special functions

$$I(l',l;\vec{k},p_y) \equiv I(l',l),$$

that occur in the description of all QED processes in an external magnetic field. They are defined as follows:

$$I(l',l) = \sqrt{hm^2}\int_{-\infty}^{+\infty} dx e^{-ik_x x} U_{l'}(\xi) U_l(\zeta). \tag{2.33}$$

The variables ξ *and* ζ are related to each other as

$$\xi = \zeta - k_y / \sqrt{hm^2}. \tag{2.34}$$

The complex function $I(l',l)$ can be expressed via its absolute value and phase as

$$I(l',l) = J(l',l)e^{i\Phi}, \tag{2.35}$$

where the phase Φ is

$$\Phi = \frac{k_x(2p_y - k_y)}{2hm^2} + (l-l')(\varphi - \frac{\pi}{2}). \tag{2.36}$$

Here, ϕ — is the azimuth angle of the final photon, and $J(l',l)$ is a real-valued function of the variable η, defined as

$$J(l',l) = e^{-\frac{\eta}{2}} \eta^{\frac{|l-l'|}{2}} \begin{cases} \sqrt{\frac{l!}{l'!}} \frac{1}{(l-l')!} F(-l', l-l'+1, \eta), & l > l' \\ (-)^{l+l'} \sqrt{\frac{l'!}{l!}} \frac{1}{(l'-l)!} F(-l, l'-l+1, \eta), & l' > l \end{cases}, \tag{2.37}$$

where F is the confluent hypergeometric function, and

$$\eta = \frac{k_x^2 + k_y^2}{2hm^2} = \frac{\omega^2(1-u^2)}{2hm^2}. \tag{2.38}$$

Given the wave functions (2.6), (2.12), and (2.27), the amplitude of the SR process can be reduced to the general form

$$A_{if} = \frac{-ie2\pi^3\sqrt{2\pi}\delta^3(p-p'-k)}{S\sqrt{V}\sqrt{\omega\varepsilon_l\varepsilon'_{l'}m_l m_{l'}}} e^{i\Phi}\sum_{a=1}^{4} Q_a, \tag{2.39}$$

where $Q_1 = -J(l,l')M_m M_m' De_z$, $Q_2 = -J(l'-1,\ l-1)\mu M_p \mu' M_p' De_z$, $Q_3 = -J(l',l-1)\mu M_p M_m' CH_m^*$, $Q_4 = -J(l'-1,l)M_m \mu' M_m' CH_p^*$.
In the above expressions, we denote

$$M_m = \sqrt{m_l - \mu m}, \quad M_p = \sqrt{m_l + \mu m}, \tag{2.40}$$

$$C = -E_m E_m' + \mathrm{sgn}(p_z)\mathrm{sgn}(p_z')E_p E_p',$$

$$D = \mathrm{sgn}(p_z')E_m E_p' + \mathrm{sgn}(p_z)E_p E_m', \tag{2.41}$$

$$E_m = \sqrt{\varepsilon_l - \mu m_l}, \quad E_p = \sqrt{\varepsilon_l + \mu m_l}, \tag{2.42}$$

$$e_z = -\sin\theta\cos\alpha, \quad H_m = \cos\theta\cos\alpha - i\sin\alpha\cdot e^{i\beta}, \quad H_p = \cos\theta\cos\alpha + i\sin\alpha\cdot e^{i\beta}. \tag{2.43}$$

Here, primed quantities M_m, M_p, E_m, E_p corresponds to the final electron. An asterisk near H_m and H_p denotes complex conjugation. Note that the expression for the amplitude (2.39) is a scalar complex value, i.e. calculations of all spinor expressions have already been performed in the amplitude.

Probability of the SR process. The SR probability equals the squared amplitude multiplied by the number of final states. In the general case, the expression of the process rate for SR with arbitrary spins and photon polarization and fixed values of the Landau levels takes the form

$$\frac{dW_{ll';\xi_2,\xi_3}^{\mu\mu'}}{du} = \frac{\alpha\omega}{16 m_l m'_{l'} \varepsilon_l(\varepsilon'_{l'} + \omega u^2 - p_z u)} \left|\sum Q\right|^2. \tag{2.44}$$

Below we analyze these expressions in two cases: the ultraquantum, or LLL (Lowest Landau Level), approximation [9], and the ultrarelativistic approximation.

SR process in the ultraquantum approximation. The probabilities of QED processes significantly depend on the spin projection of particles, so it is

necessary to analyze individual probabilities with fixed values of μ and μ'. Transition to another inertial frame of reference moving along the direction of the magnetic field does not change the field itself, thus, without losing generality we can set the longitudinal momentum of the initial electron p_z to zero.

In the ultraquantum approximation, the quantity lh is a small parameter. Hence, the hypergeometric function F in Eq. (2.37) equals unity, and the square of the transverse frequency of the photon has the form

$$\eta = \frac{1}{2}(l-l')^2 h(1-u^2). \tag{2.45}$$

We write here the expression for the process rate in four cases of particle spin projection,

$$\frac{dW}{du} = \alpha m h^2 \frac{l(l-l')}{4l'} R_{ll'}^2 [1+u^2-(1-u^2)\xi_3 + 2u\xi_2], \tag{2.46}$$

$$\frac{dW^{++}}{du} = \alpha m h^2 \frac{(l-l')}{4} R_{ll'}^2 [1+u^2-(1-u^2)\xi_3 + 2u\xi_2], \tag{2.47}$$

$$\frac{dW^{+-}}{du} = \alpha m h^3 \frac{(l-l')^3}{8l'} R_{ll'}^2 [1+u^2+(1-u^2)\xi_3 + 2u\xi_2], \tag{2.48}$$

$$\frac{dW^{+-}}{du} = \frac{\alpha m}{32} h^5 l(l-l')^3 R_{ll'}^2 \left[(1-\frac{l-l'}{l-l'+1}(1-u^2))^2 (1+\xi_3) + \right.$$

$$\left. +(1+\frac{l-l'}{l-l'+1}(1-u^2))^2 u^2 (1-\xi_3) + 2(1-\frac{(l-l')^2}{(l-l'+1)^2}(1-u^2)^2) u\xi_2 \right] \tag{2.49}$$

In the above expressions, the factor R^2 is

$$R_{ll'}^2 = e^{-\eta} \eta^{l-l'-1} \frac{(l-1)!}{(l'-1)!} \frac{1}{(l-l'-1)!^2}. \tag{2.50}$$

The differential radiation intensity is defined as the product of the differential rate and the frequency:

$$\frac{dI}{du} = \omega \frac{dW}{du}. \tag{2.51}$$

The form of the angular dependence significantly depends on the value of the photon polarization and the particle spin projections.

Fig. 2.3 shows the angular distribution of radiation intensity in the case of linear photon polarization and electron transition from the level $l = 2$ to $l' = 1$.

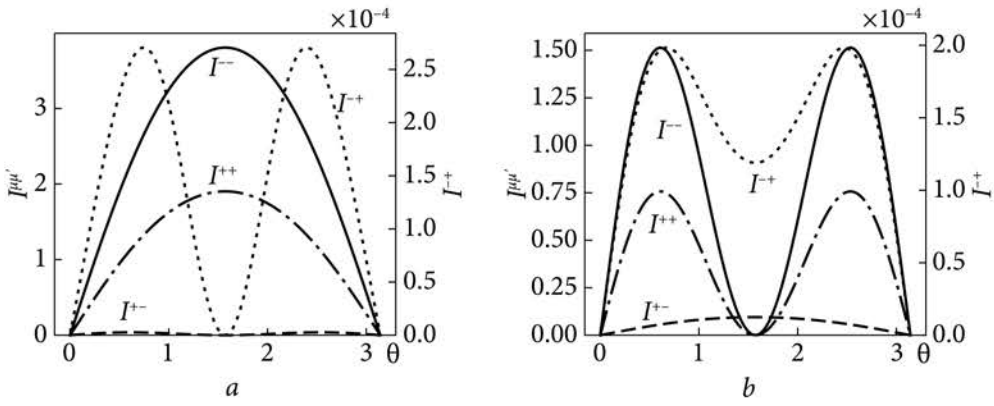

Fig. 2.3. Angular dependence of the SR intensity for the electron transition $l = 2 \to l' = 1$ and the field magnitude $h = 0.1$: *a* — normal photon polarization ($\xi_3 = -1$); *b* — anomalous photon polarization ($\xi_3 = +1$)

Magnetic field strength is $h = 0.1$ ($H = 4 \cdot 10^{12}$ G). Note that the intensity is shown in the units of I_0,

$$I_0 = \alpha h^3 m^2 / 4 \sim 10^{21}\, eB / pa\partial \cdot \mathrm{c}. \tag{2.52}$$

In the case of no-spin-flip processes, the intensity has maxima in the direction perpendicular to the magnetic field, by the previous results [3, 4]. In spin-flip processes, the radiation has a maximum at angles ±45° to the field direction.

After summation over the particle polarizations in Eqs. (2.46) — (2.49), we get the previously found expressions [19, 20]. Note that to obtain expression (2.49) for the probability of the electron transition from the ground state to the state with inversed spin W^{-+}, development in the parameter lh to the second-order is required. In particular, the approximate expression for the hypergeometric function is

$$F(a,c,\eta) = 1 + \frac{a}{c}\eta \tag{2.53}$$

In this case, the photon frequency is

$$\omega = (l-l')hm - \frac{1}{2}h^2 m(l-l')(l+l'+(l-l')u^2). \tag{2.54}$$

Let's analyze the obtained relations (2.46) — (2.49). The transition to the closest Landau level is the most probable one in the SR process. Transition to subsequent levels increases the power of small parameter h. Note that the Stokes polarization parameter ξ_1 is absent in these expressions. This result is predictable, because the ξ_1 parameter describes the linear polarization at angle $\pm 45^0$ relative to the plane of the vectors $\{k, H\}$, and these are the equivalent orientations. T

he most probable are the processes without electron spin inversion. Their probabilities W^{--}, W^{++} have identical dependence on the photon polarization.

To find the polarization of the radiation, it is necessary to find the maximum of the polarization degree P_ξ, as pointed out at the beginning of Section 1. We write separately the multiplier with the photon Stokes parameters entering the expressions (2.46)—(2.47)

$$U_\xi = 1 + u^2 - (1 - u^2)\xi_3 + 2u\xi_2. \tag{2.55}$$

The degree of polarization is

$$P_\xi = \frac{U_\xi - U_{-\xi}}{U_\xi + U_{-\xi}} = \frac{2u}{1+u^2}\xi_2 - \frac{1-u^2}{1+u^2}\xi_3. \tag{2.56}$$

The radiation Stokes parameters are the coefficients of ξ_1, ξ_2, ξ_3 in Eq. (2.56)

$$\xi_{1SR} = 0, \quad \xi_{2SR} = \frac{2u}{1+u^2}, \quad \xi_{3SR} = -\frac{1-u^2}{1+u^2}. \tag{2.57}$$

The degree of polarization P_ξ with the polarization parameters (2.57) is equal to one. The polarization of synchrotron radiation at the lowest Landau levels is determined by Eqs. (2.57) coincides with the previously obtained results [3, 4]. For example, radiation along the direction of the magnetic field ($u = 1$) has the right circular polarization ($\xi_2 = 1, \xi_3 = 0$) and the perpendicular to the field radiation ($u = 0$) has normal polarization ($\xi_2 = 0, \xi_3 = -1$). Inserting the Stokes parameters (2.57) into the expressions for the rates W^{--}, W^{++} (2.46), (2.47), we get the same expression as in the case of summation over the photon polarization,

$$W_{\xi=\xi_{SR}} = \sum_\xi W_\xi. \tag{2.58}$$

Thus, the polarization in the SR process without inversion of the electron spin is the same as in classical electrodynamics. On the other hand, if the electron changes the spin projection (a spin-flip process), then we need to analyze Eq (2.48) to obtain the polarization of radiation,

$$P_\xi^{+-} = \frac{W_\xi^{+-} - W_{-\xi}^{+-}}{W_\xi^{+-} + W_{-\xi}^{+-}} = \frac{2u}{1+u^2}\xi_2 + \frac{1-u^2}{1+u^2}\xi_3, \tag{2.59}$$

and, consequently,

$$\xi_{2SR}^{+-} = \frac{2u}{1+u^2}, \quad \xi_{3SR}^{+-} = \frac{1-u^2}{1+u^2}. \tag{2.60}$$

In this case, the perpendicular to the field component of linear polarization has the opposite sign compared to the no-spin-flip process with photon polarization parameters given by (2.57), i.e. spin inversion changes the linear polarization of the radiation to the opposite one.

Let us consider the resulting radiation polarization for both the main and the spin-flip processes in the case of electron transition to the nearest Landau level. Now the polarization degree looks like

$$P_\xi = \frac{(W^{--} + W^{++} + W^{+-})_\xi - (W^{--} + W^{++} + W^{+-})_{-\xi}}{(W^{--} + W^{++} + W^{+-})_\xi + (W^{--} + W^{++} + W^{+-})_{-\xi}}. \tag{2.61}$$

which results in

$$P_\xi = \frac{2u}{1+u^2}\xi_2 - \frac{1-u^2}{1+u^2}\left(1 - \frac{2h}{2l+1}\right)\xi_3. \tag{2.62}$$

The maximum polarization degree corresponds to the Stokes parameters values

$$\xi_{2SR} = -\frac{2u}{1+u^2}, \quad \xi_{3SR} = -\frac{1-u^2}{1+u^2}\left(1 - \frac{2h}{2l+1}\right). \tag{2.63}$$

and equals to

$$P_{\xi\,\max} = 1 - \frac{4h}{2l+1}\left(\frac{1-u^2}{1+u^2}\right)^2 < 1. \tag{2.64}$$

Thus, after taking into account the spin-flip process, the linear polarization of the radiation reduces by a value proportional to the small parameter h. The radiation is partially polarized. The difference from the pure state is most noticeable at the lowest Landau levels.

Radiation in the case of nonzero longitudinal electron momentum. Fig. 2.4 shows the dependence of the final photon frequency on the longitudinal component of the electron momentum and the photon escape angle (2.30).

If $u = 1$ (emission along the field) the frequency increases monotonically with increasing p_z, while for a fixed $u < 1$ the frequency has a maximum as a function of p_z, as shown in Fig. 2.4. The energy, the longitudinal momentum of the electron, and the photon frequency at the maximum point are

$$\varepsilon_m = \frac{m_l}{\sqrt{1-u^2}}, \quad p_m = \frac{m_l u}{\sqrt{1-u^2}}, \quad \omega_m = \frac{m_l - m_{l'}}{\sqrt{1-u^2}}. \tag{2.65}$$

In this case, the differential rates of the SR process with fixed spin projections are

$$\left.\frac{dW^{--}}{du}\right|_{\omega=\omega_m} = \frac{\alpha}{4} h\omega_m R^2_{ll'} \frac{l}{l'}(1-\xi_3), \tag{2.66}$$

$$\left.\frac{dW^{++}}{du}\right|_{\omega=\omega_m} = \frac{\alpha}{4} h\omega_m R^2_{ll'}(1-\xi_3), \tag{2.67}$$

$$\left.\frac{dW^{+-}}{du}\right|_{\omega=\omega_m} = \frac{\alpha}{8} h^2\omega_m R^2_{ll'} \frac{(l-l')^2}{l'}(1+\xi_3), \tag{2.68}$$

$$\left.\frac{dW^{-+}}{du}\right|_{\omega=\omega_m} = \frac{\alpha}{32} h^4\omega_m R^2_{ll'} \frac{l(l-l')^2}{(l-l'+1)^2}(1+\xi_3). \tag{2.69}$$

Thus, we conclude that at the point of maximum photon frequency for any photon escape angle except emission along the field, the radiation polarization is normal linear for no-spin-flip processes and anomalous linear for spin-flip processes. Note that expressions (2.66) — (2.69) coincide with (2.46) — (2.49) if we set $u = 0$ in the latter.

Consider the case of an ultrarelativistic electron moving in the direction close to the direction of the magnetic field. Consequently, the electron occupies the lowest Landau levels and has a large longitudinal momentum $p_z >> m$. Then, the photon frequency is

$$\omega = \frac{2hm^2(l-l')p_z}{m^2 + (p_z\theta)^2}, \tag{2.70}$$

where θ is the polar escape angle of the photon. Hence, the critical angle is defined as

$$\theta_c = \frac{m}{p_z}. \tag{2.71}$$

distinguishes two cases. If $1 >> \theta >> \theta_c$ (relatively large angle), then the radiation frequency is less than synchrotron frequency and the process rate is negligibly small. On the other hand, in the case $\theta << \theta_c$ the radiation frequency $\omega = 2(l - l')hp_z$ is much greater than synchrotron frequency. If $\theta = 0$ (forward radiation), the η parameter (2.38) vanishes, and the probability amplitude (2.39) is not zero for the nearest Landau levels only. In this case, the radiation rates for the fixed spin projections are

$$\left.\frac{dW^{--}}{du}\right|_{u=1} = \alpha hl\omega(1+\xi_2), \qquad \left.\frac{dW^{++}}{du}\right|_{u=1} = \alpha h(l-1)\omega(1+\xi_2), \tag{2.72}$$

$$\left.\frac{dW^{+-}}{du}\right|_{u=1} = \alpha h^2\omega(1+\xi_2)/2, \qquad \left.\frac{dW^{-+}}{du}\right|_{u=1} = \alpha h^4 l(l-1)\omega(1+\xi_2)/8. \tag{2.73}$$

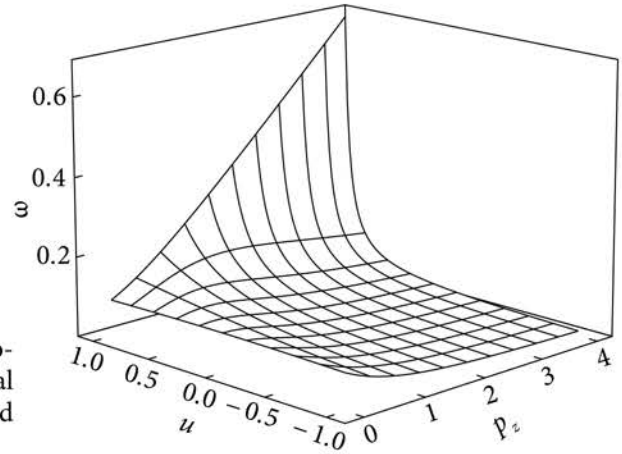

Fig. 2.4. Dependence of the photon frequency on the longitudinal momentum of the electron and the photon escape angle

The radiation is fully polarized with circular polarization for all spin states of the electron.

The SR process in the ultrarelativistic approximation. Now consider the case $l >> 1$, $l' >> 1$ and $p_z = 0$. In this case, the radiation is mostly emitted perpendicular to the direction of the field, so it is convenient to introduce a new angle of photon radiation,

$$\theta = \frac{\pi}{2} - \psi. \tag{2.74}$$

In the general expression for the process amplitude (2.39), we can express the special functions $J'(l,l')$ with different values of l and l' in terms of $J(l,l')$ and its derivative $J'(l,l')$ according to the recurrent relations

$$\sqrt{ll'}J(l'-1,\ l-1) = 0.5(l+l'-\eta)J - \eta J', \tag{2.75}$$

$$\sqrt{l\eta}J(l',\ l-1) = 0.5(l-l'+\eta)J + \eta J', \tag{2.76}$$

$$\sqrt{l'\eta}J(l'-1,\ l) = 0.5(l-l'-\eta)J - \eta J'. \tag{2.77}$$

In the linear approximation, the photon frequency is expressed by the square of a small angle ψ as

$$\omega = m\sqrt{2h}(\sqrt{l}-\sqrt{l'})\left(1-\frac{1}{4h\sqrt{ll'}}-\frac{1}{2\sqrt{l'}}(\sqrt{l}-\sqrt{l'})\psi^2\right). \tag{2.78}$$

Further, the argument of special functions J (l, l') takes on the form

$$\eta = (\sqrt{l}-\sqrt{l'})^2\left(1-\frac{1}{2h\sqrt{ll'}}(1+2hl\psi^2)\right). \tag{2.79}$$

In the ultrarelativistic approximation, the function $J(l,l')$ oscillates rapidly. However, its argument η has a large magnitude. It would be impossible to separate different Landau levels experimentally. Therefore, a fixed value of electron energy (fixed l) implies averaging over the interval of Landau levels $\Delta l >> 1$. In this case, the rapidly oscillating function $J(l,l')$ and its derivative can be replaced by smoothed MacDonald functions according to the prescription given in Ref. [8]:

$$J(l',l;\eta)=\frac{\sqrt{(\sqrt{l}-\sqrt{l'})^2-\eta}}{\pi\sqrt{3}(\sqrt{l}-\sqrt{l'})}K_{1/3}\left(\frac{2}{3}\frac{\sqrt[4]{ll'}((\sqrt{l}-\sqrt{l'})^2-\eta)^{3/2}}{(\sqrt{l}-\sqrt{l'})^2}\right), \tag{2.80}$$

$$\frac{\partial J(l',l;\eta)}{\partial\eta}=\frac{\sqrt[4]{ll'}((\sqrt{l}-\sqrt{l'})^2-\eta)}{\pi\sqrt{3}(\sqrt{l}-\sqrt{l'})^3}K_{2/3}\left(\frac{2}{3}\frac{\sqrt[4]{ll'}((\sqrt{l}-\sqrt{l'})^2-\eta)^{3/2}}{(\sqrt{l}-\sqrt{l'})^2}\right). \tag{2.81}$$

Given the relation (2.79), these functions are equal to

$$J=\frac{F}{\pi\sqrt{6h}\sqrt[4]{ll'}}K_{1/3}(\kappa),\quad J'=\frac{F}{\pi\sqrt{6h}\sqrt[4]{ll'}(\sqrt{l}-\sqrt{l'})}K_{2/3}(\kappa), \tag{2.82}$$

where

$$F=\sqrt{1+2lh\psi^2}=\sqrt{1+\Psi^2}=\sqrt{1+\psi^2/\psi_c^2}, \tag{2.83}$$

$\psi_c=1/\sqrt{2lh}$ is a typical emission angle, and the argument of the MacDonald functions is

$$\kappa=\frac{2}{3}\frac{(\sqrt{l}-\sqrt{l'})}{\sqrt{ll'}\sqrt{2h}^3}F^3. \tag{2.84}$$

Since the individual Landau levels are not separable in the ultrarelativistic case, the Landau level numbers are inconvenient parameters for the description of the process. Instead, we will use the photon frequency and the energy of the initial electron. In the argument of the MacDonald function, the small parameter ψ already enters F, so with given accuracy

$$\frac{(\sqrt{l}-\sqrt{l'})}{\sqrt{l'}}=\frac{\varepsilon_l-\varepsilon'_{l'}}{\varepsilon'_{l'}}=\frac{\omega}{\varepsilon_l-\omega}.$$

Hence, the argument κ can be transformed into the form

$$\kappa=\frac{\omega}{(\varepsilon_l-\omega)z}F^3,\quad z=\frac{3h\varepsilon_l}{m}. \tag{2.85}$$

Here, z is the dimensionless energy of the initial electron. In addition, we define dimensionless photon frequency y as

$$y=\frac{\omega}{\omega_c},\quad \omega_c=\frac{z\varepsilon_l}{2+z}. \tag{2.86}$$

Its maximum value of $y_m = 1+2/z$ corresponds to the radiation frequency equal to ε_l. If $z << 1$ we have $\omega_c = z\varepsilon_l/2$, i.e. $z/2$ is the fraction of the energy that is converted to the radiation. The argument of the MacDonald function can be expressed in terms of the quantities y and z in the form

$$\kappa = yF^3/(2+z-yz), \tag{2.87}$$

and the parameter η equals to

$$\eta = y^2z^2(1-\psi^2)/(18h^3(2+z)^2). \tag{2.88}$$

With the above definitions, the initial and the final Landau level numbers of the electron are

$$l' = \frac{l}{(2+z)^2}((2+z-yz)^2 - y^2z^2\psi^2), \quad l = \frac{z^2}{18h^3}. \tag{2.89}$$

Finally, in the ultrarelativistic case, the differential intensity of the SR can be written as

$$\frac{dI^{\mu\mu'}}{dyd\Psi} = \frac{9I_0y^2F^2}{8\pi^2(2+z)^3(2+z-yz)^2}D^{\mu\mu'}, \tag{2.90}$$

$$I_0 = \alpha h^2\varepsilon^2. \tag{2.91}$$

In Eq. (2.90), the factors $D^{\mu\mu'}$ corresponding to the no-spin-flip processes ($\mu = \mu'$) look like

$$D^{\mu\mu} = [(a\Psi^2 + b)K_{1/3}^2 + aF^2K_{2/3}^2 - 2\mu cFK_{1/3}K_{2/3}] +$$
$$+ 2\xi_2\Psi[aFK_{1/3}K_{2/3} - \mu cK_{1/3}^2] + \xi_3[(a\Psi^2 - b)K_{1/3}^2 - aF^2K_{2/3}^2 + 2\mu cFK_{1/3}K_{2/3}], \tag{2.92}$$

where $a = (4+2z-yz)^2$, $b = y^2z^2$, $c = \sqrt{ab}$.
For the spin-flip processes ($\mu = -\mu'$), the factors $D^{\mu,-\mu}$ have the form

$$D^{\mu,-\mu} = y^2z^2\{[F^2(K_{1/3}^2 + K_{2/3}^2) + 2\mu FK_{1/3}K_{2/3}] +$$
$$2\xi_2\Psi[FK_{1/3}K_{2/3} + \mu K_{1/3}^2] + \xi_3[(1-\Psi^2)K_{1/3}^2 + F^2K_{2/3}^2 + 2\mu FK_{1/3}^2K_{2/3}^2]\}. \tag{2.93}$$

The dependence of the differential intensity of SR on the photon frequency and its escape angle is shown in Fig. 2.5. Intensity is measured in units $I_0 = \alpha m^2 = 3\cdot10^{24}$ *eV/rad·s*. The parameter z is set to $z = 3$, which corresponds to the equality $h\varepsilon = m$. In the ultrarelativistic case ($\varepsilon >> 1$) this means that the magnetic field is much smaller than the critical one ($h << 1$). Fig. 2.5, *a* shows the intensity in the case of normal linear polarization ($\xi_3 = 1$, $\xi_2 = 0$), and Fig. 2.5, *b* shows the case of anomalous polarization ($\xi_3 = 1$, ξ_2 0).

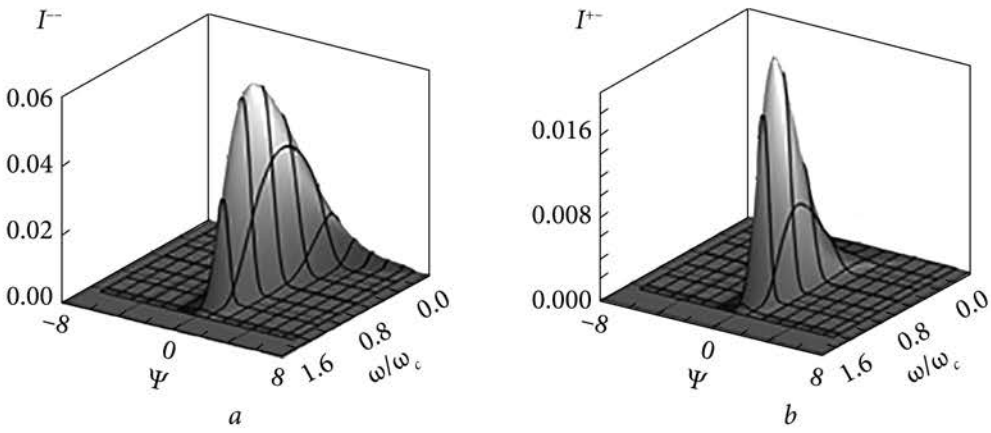

Fig. 2.5. The differential intensity of the SR process as a function of the photon frequency and its escape angle in the ultrarelativistic case: *a* — the process without spin inversion ($\mu = \mu' = -1$), *b* — spin-flip process ($\mu = -\mu' = 1$)

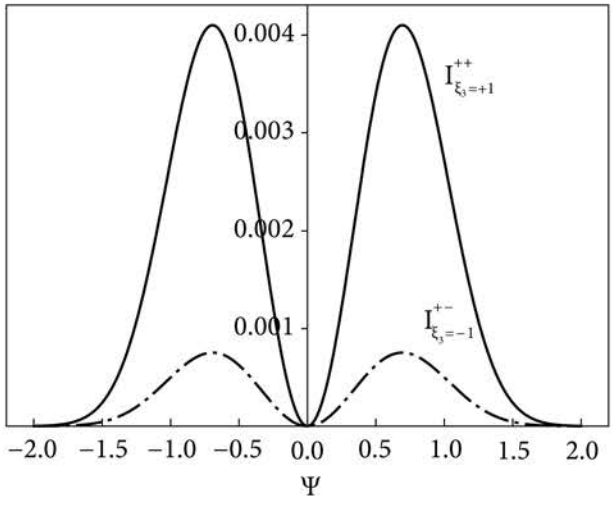

Fig. 2.6. The dependence of SR intensity on the photon escape angle for cases of anomalous photon polarization without electron spin inversion and normal photon polarization with spin inversion

It is clear from Eqs. (2.92), (2.93) that both of these cases have the maximum probability.

The intensity is maximum when $y = 0.8$ which corresponds to the frequency $\omega_{max} = 0.5\varepsilon$ (half the energy of the electron). Note that the known expression for the radiation frequency at the point of maximum intensity [4] gives the incorrect value of 1.5ε,

$$\omega_{\max} = \frac{z\varepsilon}{2} = \frac{3h\varepsilon^2}{2m} = 1.5\varepsilon$$

The above expression has been obtained in the approximation z << 1 and is not applicable in the considered case.

Now let us consider the remaining cases of anomalous photon polarization $\xi_3 = 1$ without electron spin inversion and normal photon polarization $\xi_3 = -1$ with spin inversion. In these cases, the factors $D^{\mu\mu'}$ entering the intensity (2.90) can be transformed to

$$D^{++}_{\xi_3=1} = D^{--}_{\xi_3=1} = 2a\Psi^2 K^2_{1/3}, \quad D^{+-}_{\xi_3=-1} = D^{+-}_{\xi_3=-1} = 2b\Psi^2 K^2_{1/3}. \tag{2.94}$$

Fig. 2.6. shows the dependence of the radiation intensity on the escape angle corresponding to Eqs. (2.94) with $z = 3$ and $y = 1$. It is clear from the figure that the considered processes differ significantly from the main channel shown in Fig 2.5 by the absence of radiation in the direction perpendicular to the magnetic field ($\Psi = 0$).

Thus, we reproduced a result of [19] obtained in classical approximation: an ultrarelativistic electron rotating on a circular orbit emits photons of normal polarization (σ polarization) in a narrow cone with the maximum intensity at the angle $\Psi = 0$, and photons of anomalous polarization (π polarization) in the same narrow cone, but with the total absence of radiation in the direction $\Psi = 0$. Note that a similar effect was observed in the ultraquantum case (see Fig. 2.3).

In Fig. 2.7, the theoretical predictions about angular dependence of σ and π polarized radiation are compared to experimental data for the emission of 250 *MeV* electrons in the visible part of the spectrum [20]. Such value of electron energy and magnetic field strength of several thousand Gauss correspond to a very small value of the parameter $z \sim 10^{-6}$. In this case, the spin-flip processes are small, but at $\Psi = 0$ they contribute to the π component of linear polarization. Let us compare the radiation intensities without spin inversion $I^{\mu\mu}$ and with a flip of spin, $I^{\mu-\mu}$, at $\Psi = 0$. In this case, the factors (2.92) and (2.93) are, respectively,

$$D^{\mu\mu} = (bK^2_{1/3} + aK^2_{2/3} - 2\mu cK_{1/3}K_{2/3})(1-\xi_3),$$

$$D^{\mu,-\mu} = b(K^2_{1/3} + K^2_{2/3} + 2\mu K_{1/3}K_{2/3})(1+\xi_3).$$

Note that in this case always $I^{--} > I^{++}$ and $I^{+-} > I^{-+}$. In these expressions, the coefficients near parameter ξ_3 are equal to –1 and +1, which indicates that SR with σ polarization takes place in the process without spin inversion and SR with π polarization results from the spin-flip process. In the case $z << 1$ the following condition is true,

$$\frac{I^{\mu,-\mu}\Big|_{\xi_3=+1}}{I^{\mu\mu}\Big|_{\xi_3=-1}} = I_\pi / I_\sigma \approx \frac{(yz)^2}{8}.$$

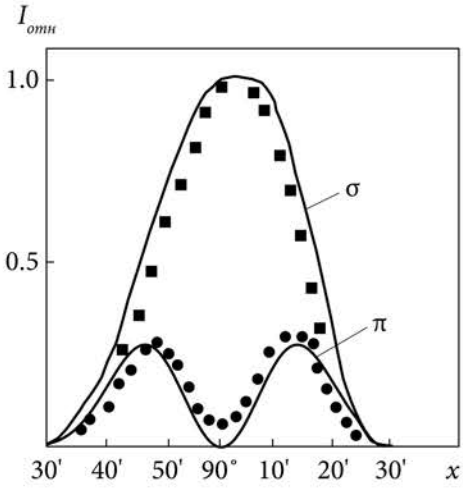

Fig. 2.7. Comparison of theoretical predictions and experimental data for angular dependence of σ and π polarized SR [20]

In the visible part of the spectrum ($y = 0.01$), the obtained ratio is negligibly small ($\sim 10^{-17}$) if $z \sim 10^{-6}$. It can be concluded that the experimental presence of the nonzero π component of the linear polarization at $\Psi = 0$ in Fig. 2.7 is connected with the finite size of the electron beam. It should be stressed, that π polarization of the SR associated with the spin-flip process can be observed experimentally in the frequency range $\omega \sim \varepsilon$ ($y \sim 1/z$), or by increasing z.

Now we proceed to a general analysis of polarization of synchrotron radiation for arbitrary direction and frequency and with arbitrary electron spin projections. We start with a process without electron spin inversion ($\mu = \mu'$), the intensity of which is proportional to expressions (2.92). The degree of polarization of the emitted photon is defined as the maximum value of the expression

$$P^{\mu\mu}_{\xi_{SR}} = \max \frac{D^{\mu\mu}_{\xi} - D^{\mu\mu}_{-\xi}}{D^{\mu\mu}_{\xi} + D^{\mu\mu}_{-\xi}}. \tag{2.95}$$

This allows us to find the Stokes parameters of the emitted photon,

$$\xi_{2SR} = \frac{2\Psi[aFK_{1/3}K_{2/3} - \mu cK^2_{1/3}]}{(a\Psi^2 + b)K^2_{1/3} + aF^2K^2_{2/3} - 2\mu cFK_{1/3}K_{2/3}}, \tag{2.96}$$

$$\xi_{3SR} = \frac{(a\Psi^2 - b)K^2_{1/3} - aF^2K^2_{2/3} + 2\mu cFK_{1/3}K_{2/3}}{(a\Psi^2 + b)K^2_{1/3} + aF^2K^2_{2/3} - 2\mu cFK_{1/3}K_{2/3}}. \tag{2.97}$$

Expectedly, the Stokes parameter ξ_{1SR} vanishes. It can be easily checked that the polarization degree determined by the above expressions equals unity,

$$P^{--}_{\xi_{SR}} = P^{++}_{\xi_{SR}} = 1. \tag{2.98}$$

Consequently, radiation is fully polarized if the electron spin does not change its direction.

Fig. 2.8 shows the dependence of the Stokes parameters of the final photon on the escape angle; *a* — initial energy is 1) $z = 0.03$, 2) $z = 3$. 3) $z = 300$ while

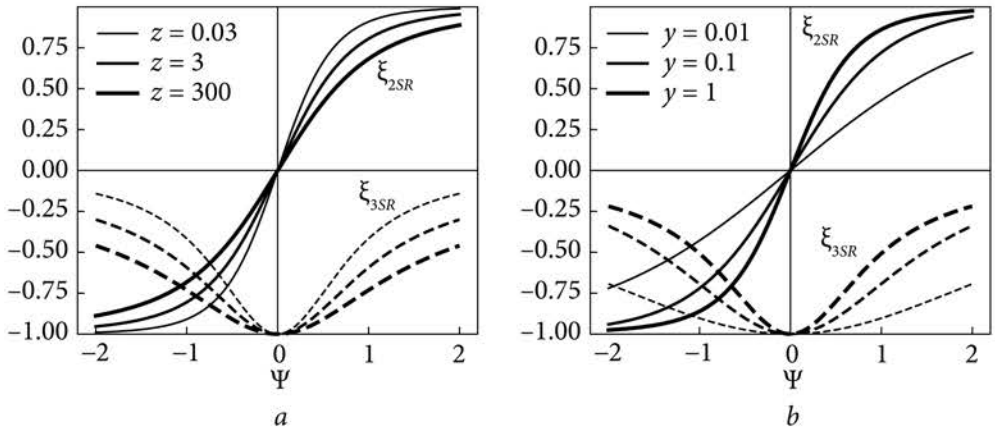

Fig. 2.8. The dependence of the Stokes parameters on the escape angle

$y = 1$; *b* — photon frequency is 1) $y = 0.01$, 2) $y = 0.1$, 3) $y = 1.0$ and the electron spin projection is $\mu = -1$.

It is clear from Fig. 2.8 that the polarization changes from normal linear at $\Psi = 0$ (emission perpendicular to the field) to right circular at $\Psi = +2$ (periphery of the narrow radiation cone).

Note that in the nonrelativistic ultraquantum approximation, the radiation perpendicular to the field is linearly polarized and radiation along the field is circularly polarized. The ultrarelativistic motion of the electron preserves this picture qualitatively, but «compresses» it into a narrow cone of radiation. The typical radiation angle $\psi_c = m/\varepsilon$ ($\Psi = 1$) is determined only by the energy of the initial electron.

Note that for estimation purposes we can set

$$K_{2/3} \approx 1.2K_{1/3}. \tag{2.99}$$

when $y = 1$ and $|\Psi| < 1$.

In the case of moderate relativistic energy $z << 1$, we set approximately $a = 16$ and $b = c = 0$. Then, the Stokes parameters take the simple form

$$\xi_{2SR} = \frac{2\Psi F K_{1/3} K_{2/3}}{\Psi^2 K_{1/3}^2 + F^2 K_{2/3}^2}, \quad \xi_{3SR} = \frac{\Psi^2 K_{1/3}^2 - F^2 K_{2/3}^2}{\Psi^2 K_{1/3}^2 + F^2 K_{2/3}^2} \tag{2.100}$$

and depends on the emission angle only,

$$\xi_{2SR} \approx \frac{2.4\Psi F}{1.4 + 2.4\Psi^2}, \quad \xi_{3SR} \approx -\frac{1.4 + 0.4\Psi^2}{1.4 + 2.4\Psi^2}. \tag{2.101}$$

This well-known result has been obtained theoretically and verified experimentally for unpolarized electron beams [19, 20]. The reason for such agree-

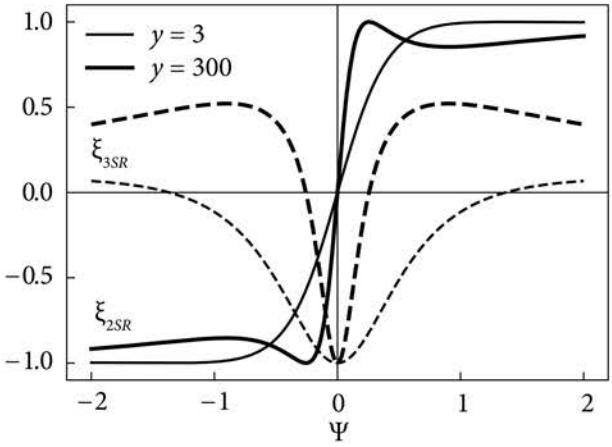

Fig. 2.9. Dependence of the Stokes parameters on the emission angle in the case of inverted electron spin

ment lies in the fact that radiation polarization does not depend on electron spin states in the considered approximation, and the main contribution comes from the no-spin-flip processes.

In the case of hard ultrarelativistic energy $z, >> 1$, the quantities a, b, and c are approximately equal to $a = b = c = z^2$ and the Stokes parameters are

$$\xi_{2SR} = \frac{2\Psi(1.2F - \mu)}{2.4F(F - \mu)}, \quad \xi_{3SR} = -\frac{2.4(1 - \mu F) + 0.4\Psi^2}{2.4F(F - \mu)}. \tag{2.102}$$

The obtained approximate equations are in good agreement with the general expressions (2.96) and (2.97) if the electron occupies the ground spin state ($\mu = -1$). In contrast, the agreement is rather poor when $\mu = +1$.

Fig. 2.9 shows the dependence of the Stokes parameters on the emission angle for the case of inverse electron spin population ($\mu = +1$), with $y = 1$. The emission angle interval with normal linear polarization of SR contracts into a small vicinity of zero angles ($\Psi = 0$) when z reaches hard ultrarelativistic values ($z >> 1$). In the rest of the narrow cone, the radiation has also the anomalous component of linear polarization in addition to a circular one.

If electrons do not change the spin projection and are allowed to be in both spin up ($\mu = +1$) and spin down ($\mu = -1$) states, the polarization degree of SR has the form

$$P_{\xi_{SR}} = \max \frac{D_{\xi}^{--} + D_{\xi}^{++} - D_{-\xi}^{--} - D_{-\xi}^{++}}{D_{\xi}^{--} + D_{\xi}^{++} + D_{-\xi}^{--} + D_{-\xi}^{++}}. \tag{2.103}$$

The corresponding Stokes parameters of the emitted photon can be found by inserting $\mu = 0$ in Eqs (2.96) and (2.97),

$$\xi_{2SR} = \frac{2\Psi aFK_{1/3}K_{2/3}}{(a\Psi^2 + b)K_{1/3}^2 + aF^2K_{2/3}^2}, \quad \xi_{3SR} = \frac{(a\Psi^2 - b)K_{1/3}^2 - aF^2K_{2/3}^2}{(a\Psi^2 + b)K_{1/3}^2 + aF^2K_{2/3}^2}. \tag{2.104}$$

The polarization degree of the final photon is determined by the Stokes parameters (2.104),

$$P_{\xi_{SR}} = \sqrt{\xi_{2SR}^2 + \xi_{3SR}^2},$$

is shown in Fig. 2.10 as a function of the emission angle for $y = 1$. As can be seen, the polarization degree reaches the minimum value of $P = 0.88$ when $z >> 1$ and approximately $\Psi = 1$.

In the moderate relativistic energy range, $z << 1$, the approximate Stokes parameters are given by Eq. (2.100). In this case, $P = 1$. In the case of hard ultra-relativistic energy, $z >> 1$, the Stokes parameters are approximated by

$$\xi_{2SR} = \frac{\Psi}{F}, \quad \xi_{3SR} = -\frac{1}{F^2}, \tag{2.105}$$

and the polarization degree is

$$P = \sqrt{\frac{\Psi^4 + \Psi^2 + 1}{\Psi^2 + 1}}. \tag{2.106}$$

Now consider the spin-flip process ($\mu' = -\mu$). In this case, the general expressions for the Stokes parameters follow from Eq. (2.93),

$$\xi_{2SR} = \frac{2\Psi[FK_{1/3}K_{2/3} + \mu K_{1/3}^2]}{F^2(K_{1/3}^2 + K_{2/3}^2) + 2\mu FK_{1/3}K_{2/3}}, \tag{2.107}$$

$$\xi_{3SR} = \frac{(1-\Psi^2)K_{1/3}^2 + F^2K_{2/3}^2 + 2\mu FK_{1/3}K_{2/3}}{F^2(K_{1/3}^2 + K_{2/3}^2) + 2\mu FK_{1/3}K_{2/3}}. \tag{2.108}$$

The resulting polarization degree equals unity. In the center of the narrow radiation cone ($\Psi = 0$), the parameter ξ_{3SR} has the opposite sign compared to the case without spin inversion ($\mu' = \mu$). Note that in the case of $y = 1$, the obtained expressions practically do not depend on the electron energy (or z parameter).

In the case of $\mu = +1$, $\mu' = -1$, and taking into account the relation (2.99), the Stokes parameters take a simple form in the region of maximum radiation ($y = 1$),

$$\xi_{2SR} = \frac{\Psi}{F}, \quad \xi_{3SR} = \frac{1}{F}. \tag{2.109}$$

In the opposite case of μ=-1 and μ'= +1, the dependence of the Stokes parameters on the emission angle is similar to that shown in Fig. 2.9 (2) but with the opposite sign of ξ_{3SR}.

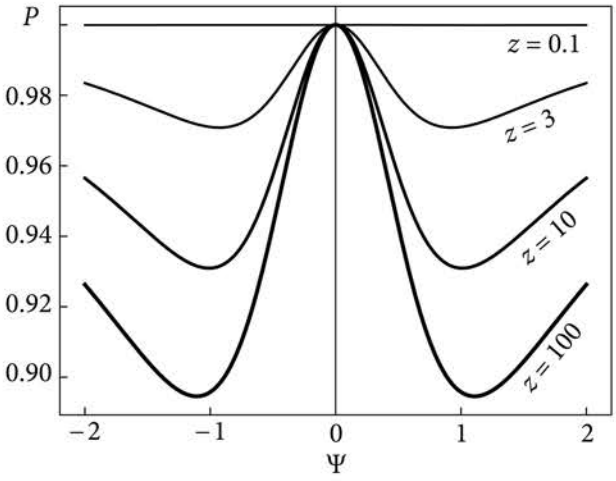

Fig 2.10. Dependence of the polarization degree of SR on the emission angle. An electron occupies both the ground and inverse spin states

If electrons are allowed to occupy both the ground ($\mu = -1$) and inverted ($\mu = +1$) spin states, the SR polarization in the spin-flip process is

$$\xi_{2SR} = \frac{2\Psi K_{1/3}K_{2/3}}{F(K_{1/3}^2 + K_{2/3}^2)} \approx \frac{\Psi}{F}, \tag{2.110}$$

$$\xi_{3SR} = \frac{(1-\Psi^2)K_{1/3}^2 + F^2K_{2/3}^2}{F^2(K_{1/3}^2 + K_{2/3}^2)} \approx \frac{1}{F^2}. \tag{2.111}$$

The radiation is partially polarized and the degree of polarization is determined by expression (2.106), similarly to the no-spin-flip process with hard ultrarelativistic electron energy.

Consider the SR process in which the electron has a fixed spin projection in the initial state, and take the sum of the contributions from all final spin states. In other words, we aim to find the total polarization of all radiation from the initially polarized electron. In this case, the degree of polarization is defined as

$$P_{\xi_{SR}}^{\mu} = \max \frac{D_{\xi}^{\mu\mu} + D_{\xi}^{\mu,-\mu} - D_{-\xi}^{\mu\mu} - D_{-\xi}^{\mu,-\mu}}{D_{\xi}^{\mu\mu} + D_{\xi}^{\mu,-\mu} + D_{-\xi}^{\mu\mu} + D_{-\xi}^{\mu,-\mu}}. \tag{2.112}$$

The Stokes parameters are

$$\xi_{2SR} = \frac{2\Psi[(a+b)FK_{1/3}K_{2/3} + \mu(b-c)K_{1/3}^2]}{K_{1/3}^2(a\Psi^2 + b + bF^2) + K_{2/3}^2(a+b)F^2 + 2\mu(b-c)FK_{1/3}K_{2/3}}, \tag{2.113}$$

$$\xi_{3SR} = \frac{(a-b)\Psi^2K_{1/3}^2 - (a-b)F^2K_{2/3}^2 + 2\mu(c+b)FK_{1/3}K_{2/3}}{K_{1/3}^2(a\Psi^2 + b + bF^2) + K_{2/3}^2(a+b)F^2 + 2\mu(b-c)FK_{1/3}K_{2/3}}. \tag{2.114}$$

In the limit of moderate relativistic electron energy ($z << 1$), the polarization of radiation at characteristic frequency $y = 1$ does not depend on spin projection and is given by Eq. (2.100). The radiation is fully polarized in this case, $P = 1$.

If $z > 1$, the radiation is partially polarized and the degree of polarization strongly correlates with the radiation frequency y electron spin μ. Fig. 2.11 shows the degree of polarization as a function of electron energy z at $\Psi = 0$, $y = 0.8$ (*a*), and as a function of electron energy z and photon frequency y at $\Psi = 0$ (*b*). As can be seen from Fig. 2.11, *a*, if electrons are polarized opposite to the field direction ($\mu = -1$), the SR polarization degree decreases monotonically with increasing electron energy z and reaches the minimum value of $P_m = 0.4$. In contrast, if electrons are polarized along the field ($\mu = +1$), z dependence of P is essentially non-monotonic, and the polarization degree vanishes twice at the points $z_1 = 5.06$ and $z_2 = 877$ while approaching the same value $P_m = 0.4$ in the limit case $z \to \infty$.

It is obvious from Fig. 2.11, *b* that completely unpolarized radiation $P = 0$ corresponds to some «canyon» on the graph of $f = P(y, z)$. On the y, z plane, this line has a maximum and intersects with the line $y = y_0$ at two points, which explains the presence of two minima in Fig. 2.11, *a*. Note that the value of P_m depends on y and vanishes if $y \to 1$.

Fig. 2.12 shows the dependence of the Stokes parameters of the final photon on the emission angle for various values of the electron energy and the frequency of $y = 0.8$. Panels (*a*) and (*b*) depict graphs for the cases $\mu = +1$ and $\mu = -1$ respectively. We can see that in the case $\mu = -1$, $\mu = +1$ in the considered energy range from $z = 1$ to $z = 30$ the parameter ξ_{2SR} weakly depends on the emission angle, as well as ξ_{3SR} in the case $\mu = -1$. At the same time, in the case of $\mu = +1$, linear polarization ξ_{3SR} strongly depends on the angle and changes its sign.

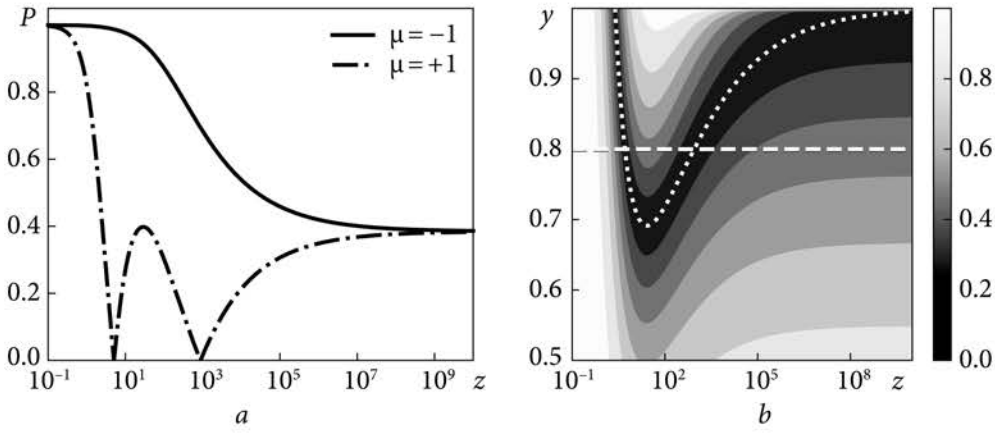

Fig. 2.11. The degree of polarization: *a* — as a function of electron energy z at $\Psi = 0$, $y = 0.8$; *b* — as a function of electron energy z and photon frequency y at $\Psi = 0$

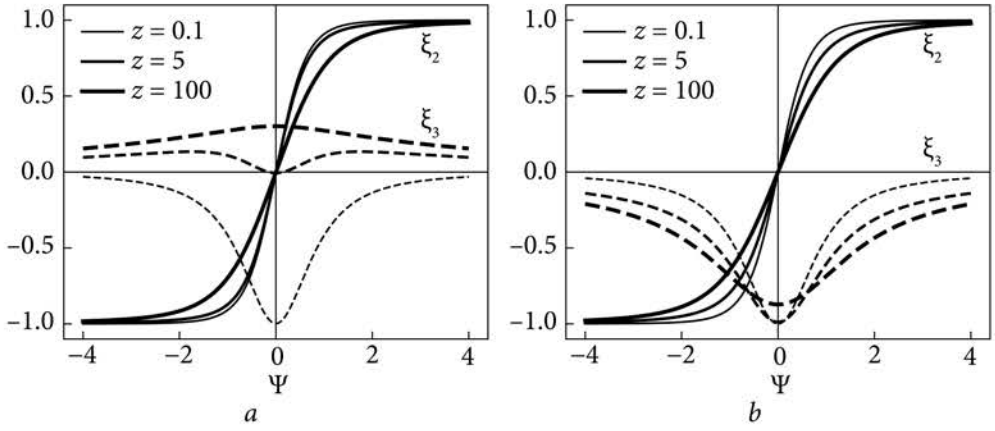

Fig. 2.12. The Stokes parameters as a function of the emission angle, *a* — μ = +1 and *b* — μ = −1. The frequency is *y* = 0.8

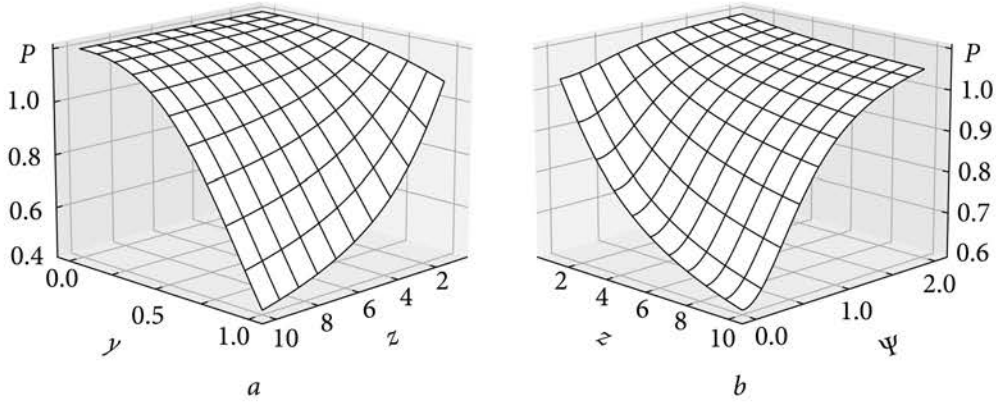

Fig. 2.13. The dependence of the polarization degree: *a* — on electron energy *z* and photon frequency *y* at Ψ = 0; *b* — on electron energy *z* and emission angle Ψ at *y* = 0.8

Let us consider the question of the polarization of SR from an unpolarized electron. To find the Stokes parameters, we set μ = 0 in expressions (2.112) and (2.113):

$$\xi_{2SR} = \frac{2\Psi(a+b)FK_{1/3}K_{2/3}}{K_{1/3}^2(a\Psi^2+b+bF^2)+K_{2/3}^2(a+b)F^2}, \tag{2.115}$$

$$\xi_{3SR} = \frac{(a-b)(\Psi^2K_{1/3}^2-F^2K_{2/3}^2)}{K_{1/3}^2(a\Psi^2+b+bF^2)+K_{2/3}^2(a+b)F^2}. \tag{2.116}$$

In the limit of moderate relativistic energy $z << 1$, the polarization degree equals unity, and the Stokes parameters are approximated by Eq. (2.100), in agreement with the known result [19]. In the hard relativistic limit $z << 1$, the radiation is polarized partially. Fig. 2.13 shows the dependence of the polarization degree (*a*) on electron energy z and photon frequency y at $\Psi = 0$ and (*b*) on electron energy z and emission angle Ψ at $y = 0.8$.

The polarization degree reaches its minimum for radiation in the orbit plane ($\Psi = 0$) near the intensity maximum ($y = 1$) and approximately equals to

$$P = \frac{11.2(z+2)}{4.8z^2 + 11.2(z+2)} \approx \frac{2.3}{z}, \tag{2.117}$$

hence, the radiation is completely unpolarized in the limit case of large electron energy, $z \to \infty$.

Note that in laboratory conditions the typical value of electron energy is of the order of several GeV and magnetic strength is of the order of $H \sim 10^4$ G. This corresponds to $z = 10^{-5}$, i.e. energy lies in the moderate relativistic range. However, magnetic fields up to hundreds of Tesla and electron energies up to several TeV are achievable, which results in a value of $z \sim 1$ and higher. Hence, observation of the considered interplay between electron spin and SR polarization in a highly ultrarelativistic domain becomes experimentally feasible.

2.3. Spin and polarization effects in the process of one photon e^+e^- pair production

The probability amplitude of one photon e^+e^- pair production (OPP). We construct the probability amplitude of the considered process according to the Feynman diagram in Fig. 2.14.

$$A_{if} = -ie\int d^4x \bar{\Psi}^-(\zeta)\gamma^i A_i \Psi^+(\xi), \tag{2.118}$$

where $\bar{\Psi}^-(\zeta)$ is the wave function of a final electron (we replace prime with «–» sign in Eq. (2.27)), $\zeta = \sqrt{hm^2}\,(x + p_y^- / hm^2)$ and $\Psi^+(\xi)$ is the wave function of a

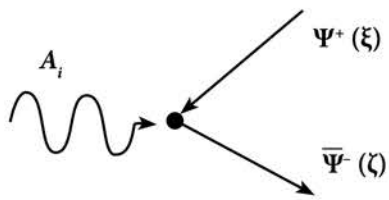

Fig. 2.14. Feynman diagram of the OPP process

positron of the form

$$\Psi^+(\xi)=\frac{A_{l^+}}{\sqrt{S}}e^{i(\varepsilon^+_{l^+}t-p^+_y y-p^+_z z)}[i\sqrt{m^+ +\mu^+ m}U_{l^+}(\xi)- \\ -\mu^+\sqrt{m^+ -\mu^+ m}U_{l^+-1}(\xi)\gamma^1]u^+_{l^+}, \qquad (2.119)$$

where $\xi=\sqrt{hm^2}\,(x-p^+_y/hm^2)$, $m^\pm=m(1+2l^\pm h)^{1/2}$.

The process of kinematics is determined by the conservation laws of energy and longitudinal momentum,

$$\omega=\varepsilon^-_{l^-}+\varepsilon^+_{l^+}, \quad k_z=\omega u=p^-_z+p^+_z, \qquad (2.120)$$

where u=cosθ is the cosine of a polar angle of the incident photon. To find the threshold energy and momentum of the final particles we search for a maximum of the function

$$f(p^-_z)=\omega-\sqrt{(m^-)^2+(p^-_z)^2}-\sqrt{(m^+)^2+(\omega u-p^-_z)^2}. \qquad (2.121)$$

Fig. 2.15 shows the dependence of the function $f(p^-_z)$ on the electron momentum, (*a*) in the case of u = 0 and (*b*) in the case of u = 1, the magnetic field is h = 0.1 in both cases.

According to the conservation laws (2.120), the process is possible when $f(p^-_z)$ = 0, and the process threshold is reached when the maximum value of $f(p_m)$ equals zero. Equating the derivative of $f(p^-_z)$ to zero yields

$$f(p_m)=\frac{\omega(p_m-u\varepsilon_m)}{p_m}. \qquad (2.122)$$

Further, Eq. (2.122) equals zero at the limiting threshold values of the photon frequency and energies and longitudinal momenta of the electron and the positron,

$$\omega_m=(m^-+m^+)/\sqrt{1-u^2}, \quad \varepsilon^\pm_m=m^\pm/\sqrt{1-u^2}, \quad p^\pm_m=u\varepsilon^\pm_m. \qquad (2.123)$$

As follows from these relations, if the photon is directed perpendicular to the field (u = 0), then the threshold values of longitudinal momenta vanish and $\omega_m=m^++m^-$, i.e. the particles are «at rest» at the Landau levels. If the photon is directed along the field (u = 1), then expression (2.122) is always negative and never vanishes, hence the OPP process is impossible in this case. It is useful to express the particle energies and momenta in terms of the photon frequency. For a fixed frequency, the threshold polar angle is given by the ratio

$$u_m=\pm\sqrt{\omega^2-(m^++m^-)^2}\,/\,\omega. \qquad (2.124)$$

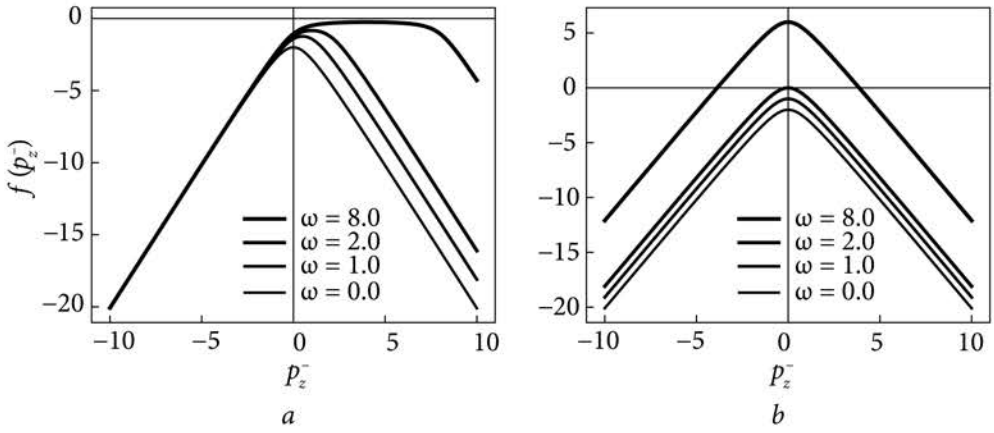

Fig. 2.15. Plot of the function $f(p_z^-)$ for various values of frequency; a — $u = 1$, b — $u = 0$; magnetic field is $h = 0.1$ in both cases

Let the Landau level numbers of the particles be fixed and the photon frequency satisfies the condition $u_m < 1$. Then, the process is impossible if the photon angle meets the condition $u > u_m$. The threshold energies and momenta are

$$\varepsilon_m^{\pm} = \frac{m^{\pm}}{m^+ + m^-}\omega, \quad p_m^- = \pm\frac{m^-}{m^+ + m^-}\sqrt{\omega^2 - (m^+ + m^-)^2},$$
$$p_m^+ = \pm\frac{m^+}{m^+ + m^-}\sqrt{\omega^2 - (m^+ + m^-)^2}. \qquad (2.125)$$

Taking into account the relation $k_m = \omega u_m$ we obtain

$$\omega^2 = (m^+ + m^-)^2 + k_m^2.$$

Hence, at the process threshold, the relation between the photon energy and its longitudinal momentum is of the same form as that of an electron in a magnetic field, provided that we ascribe transversal energy $m_\omega = m^+ + m^-$ to the photon.

To clarify the physical meaning of the obtained expressions (2.123), it is convenient to pass to a new (primed) reference frame moving along the magnetic field, such that the longitudinal photon momentum vanishes, $(p_m^-)' = 0$. The Lorentz transformations of the energy and momentum have the form

$$(\varepsilon_m^-)' = \gamma(\varepsilon_m^- - Vp_m^-), \quad (p_m^-)' = \gamma(p_m^- - V\varepsilon_m^-), \quad \gamma = 1/\sqrt{1-V^2}. \qquad (2.126)$$

The velocity and gamma factor are defined by equating $(p_m^-)'$ to zero,

$$V = u, \quad \gamma = \omega_m/(m^+ + m^-). \qquad (2.127)$$

As a result, in the new reference frame, the energies and momenta are

$$(\varepsilon_m^{\pm})' = m^{\pm}, \quad (p_m^{\pm})' = 0. \tag{2.128}$$

From the conservation laws (2.120) we obtain

$$(\omega_m)' = m^+ + m^-, \quad u' = 0. \tag{2.129}$$

Thus, if the photon frequency equals the limit value, then the longitudinal momenta vanish and the photon frequency equals the sum of the effective masses of the electron and the positron in the reference frame where the photon propagates perpendicular to the field.

When the photon frequency exceeds the threshold value, $\omega > \omega_m$, the conservation laws (2.120) result in the following expressions for the energy and momenta of an electron and a positron,

$$\varepsilon_{1,2}^- = \frac{a^- \pm b^- u}{2\omega(1-u^2)}, \; p_{1\,2,}^- = \frac{a^- u \pm b^-}{2\omega(1-u^2)}, \; \varepsilon_{1,2}^+ = \frac{a^+ \mp b^+ u}{2\omega(1-u^2)}, \; p_{1,2}^+ = \frac{a^+ u \mp b^+}{2\omega(1-u^2)}, \tag{2.130}$$

where $a^{\pm} = \omega^2(1-u^2) \pm (m^+)^2 \mp (m^-)^2$, $b^{\pm} = \sqrt{(a^{\pm})^2 - 4(m^{\pm})^2\omega^2(1-u^2)}$, and the condition $b^+ = b^-$ is true.

Note that two values of the energy and momentum of the particles are possible for each value of the polar angle of the initial photon. In the particular case of pair production to equal Landau levels, the expressions (2.130) take the form

$$\varepsilon_{1,2}^- = \frac{\omega}{2}[1 \pm u\sqrt{1-(\frac{\omega_m}{\omega})^2}], \; p_{1,2}^- = \frac{\omega}{2}[1 \pm u\sqrt{1-(\frac{\omega_m}{\omega})^2}],$$

$$\varepsilon_{1,2}^+ = \varepsilon_{2,1}^-, \; p_{1,2}^+ = p_{2,1}^-, \tag{2.131}$$

Suppose the photon propagates perpendicular to the field, $u = 0$. Then Eq. (2.139) transforms to

$$\varepsilon^- = \frac{1}{2\omega}(\omega^2 + (m^-)^2 - (m^+)^2),$$

$$p^- = \frac{\pm 1}{2\omega}\sqrt{\omega^2 - (m^+ + m^-)^2}\sqrt{\omega^2 - (m^+ - m^-)^2}, \tag{2.132}$$

$$\varepsilon^+ = \frac{1}{2\omega}(\omega^2 + (m^+)^2 - (m^-)^2), \quad p^+ = -p^-. \tag{2.133}$$

Let the photon frequency be a sum of the limit value and a small term,

$$\omega = \omega_m + \delta\omega, \quad \omega_m = m^+ + m^-, \quad \delta\omega << \omega_m, \tag{2.134}$$

then the energies and momenta take the simple form

$$\varepsilon^- = m^- + \frac{m^+\delta\omega}{\omega_m},\ \varepsilon^+ = m^+ + \frac{m^-\delta\omega}{\omega_m},\ p^- = -p^+ = \pm\sqrt{\frac{2m^+m^-\delta\omega}{\omega_m}}. \quad (2.135)$$

If the particles occupy the lowest Landau levels we need to analyze three separate cases of the additional term magnitude. In the first case, let

$$\omega = \omega_m + \delta\omega,\quad \delta\omega = \alpha_1 h^2 m,\quad \alpha_1 \sim 1, \quad (2.136)$$

$$\varepsilon^- = m(1 + l^- h),\ \varepsilon^+ = m(1 + l^+ h),\quad p^- = -p^+ = \pm\sqrt{\alpha_1} hm, \quad (2.137)$$

i.e. particles momenta are comparable with the cyclotron frequency and they can be neglected in the expressions for particle energies. In the second case,

$$\omega = \omega_m + \delta\omega,\quad \delta\omega = \alpha_1 hm,\quad \alpha_1 \sim 1, \quad (2.138)$$

$$\varepsilon^- = m(1 + l^- h + \alpha_1 h/2),\ \varepsilon^+ = m(1 + l^+ h + \alpha_1 h/2),\ p^- = -p^+ = \pm\sqrt{\alpha_1 h} m. \quad (2.139)$$

Hence, the corresponding term in the particle energies is comparable with the distance between Landau levels. In the third case,

$$\omega = \omega_m + \delta\omega,\quad \delta\omega = \alpha_1 m \sim \omega_m, \quad (2.140)$$

$$\varepsilon^- = \varepsilon^+ = m(1 + \alpha_1/2),\quad p^- = -p^+ = \pm m\sqrt{4\alpha_1 + \alpha_1^2}/2. \quad (2.141)$$

As was mentioned before, we can let the photon be directed perpendicular to the field ($u = 0$) without loss of generality. Below we analyze OPP with the assumption that this condition is true. Performing integration in (2.118) with wave functions (2.12), (2.27), (2.119) we obtain the general probability amplitude of OPP in the form

$$A_{if} = \frac{M_{if}\delta^3(k - p^+ - p^-)}{S\sqrt{V}},\quad M_{if} = \frac{-ie2\pi^3\sqrt{2\pi}e^{if}}{\sqrt{\omega\varepsilon^+\varepsilon^- m^+ m^-}}\sum_{a=1}^{4} Q_a, \quad (2.142)$$

where

$$Q_1 = J(l^+, l^-) M_m^- M_p^+ D\sin\theta\cos\alpha,$$

$$Q_2 = -J(l^+ - 1, l^- - 1)\mu^- M_p^- \mu^+ M_m^+ D\sin\theta\cos\alpha,$$

$$Q_3 = -J(l^+, l^- - 1)\mu^- M_p^- M_p^+ C H_m,$$

$$Q_4 = J(l^+ - 1, l^-) M_m^- \mu^+ M_m^+ C H_p.$$

Here, we denote

$$M_m^{\pm} = \sqrt{m^{\pm} - \mu^{\pm} m}, \; M_p^{\pm} = \sqrt{m^{\pm} + \mu^{\pm} m}, \tag{2.143}$$

$$C = -E_m^- E_m^+ + \mathrm{sgn}(p^-)\mathrm{sgn}(p^+) E_p^- E_p^+, \; D = \mathrm{sgn}(p^+) E_m^- E_p^+ + \mathrm{sgn}(p^-) E_p^- E_m^+, \tag{2.144}$$

$$E_m^{\pm} = \sqrt{\varepsilon^{\pm} - \mu^{\pm} m^{\pm}}, \; E_p^{\pm} = \sqrt{\varepsilon^{\pm} + \mu^{\pm} m^{\pm}}. \tag{2.145}$$

The quantities H_m and H_p are defined by Eq. (2.43). The phase Φ is

$$\Phi = \frac{-k_x(2p_y^- - k_y)}{2hm^2} + (l^+ - l^-)(\varphi - \frac{\pi}{2}). \tag{2.146}$$

The special function $J(l^+,l^-)$ is defined by the expression (2.37) and depends on the quantity η given by (2.38) with $u = 0$.

Rate of the OPP process. Let us now consider the normalizing constants S, and V in the amplitude (2.142). We write the amplitude in the form

$$A_{if} = \frac{M_{if}}{S\sqrt{V}} \delta(\omega - \varepsilon^+ - \varepsilon^-)\delta(k_z - p_z^+ - p_z^-)\delta(k_y - p_y^+ - p_y^-). \tag{2.147}$$

The differential rate is the product of the squared absolute value of (2.147) and the number of final states,

$$dN = dN^+ dN^- = \frac{dp_y^+ dp_z^+ S}{(2\pi)^2} \cdot \frac{dp_y^- dp_z^- S}{(2\pi)^2}. \tag{2.148}$$

After transformations, we have

$$dW = \frac{STp_y^-}{V} \cdot \frac{|M_{if}|^2}{(2\pi)^7} \delta(\omega - \varepsilon^+ - \varepsilon^-) dp_z^-. \tag{2.149}$$

To obtain the above formula we used

$$\left(\delta(\omega - \varepsilon^+ - \varepsilon^-)\right)^2 = \frac{T}{2\pi} \delta(\omega - \varepsilon^+ - \varepsilon^-),$$

$$\left(\delta(k_z - p_z^+ - p_z^-)\delta(k_y - p_y^+ - p_y^-)\right)^2 = \frac{S}{(2\pi)^2} \delta(k_z - p_z^+ - p_z^-)\delta(k_y - p_y^+ - p_y^-),$$

and calculated integrals in dp_y^+ and dp_z^+. As was mentioned before, in the Landau gauge the «quantized» x coordinate enters the electron wave function in the form of the quantity (2.9),

$$\zeta = (hm^2)^{1/2}(x - x_0),$$

where the parameter $x_0 = -p_y/hm^2$ defines the center of an electron orbit in the classical approximation. Identifying this quantity as the normalizing length L_p, we can write

$$p_y^- / L_x = Sp_y^- / V = hm^2. \tag{2.150}$$

The resulting differential rate is

$$dW^{\mu^-\mu^+} = hm^2 \cdot \frac{|M_{if}|^2}{(2\pi)^7} \delta(\omega - \varepsilon^+ - \varepsilon^-) dp_z^-. \tag{2.151}$$

The resulting expression contains a single Dirac delta function and a single differential. In the LLL approximation, the individual Landau levels can be resolved, so it is sensible to perform the integration in p_z using the delta function. In this case, the OPP process rates $W^{\mu-\mu+}(\xi_i)$ are the functions of Landau level numbers of the particles, their spin projections, and the Stokes parameters of the photon.

On the other hand, in the ultrarelativistic approximation, we need to average the rate throughout levels. The number of final states is defined by Eq. (2.148) multiplied by $dl^+ \cdot \mathrm{dl}^-$, so the delta function can be used to perform the integration in dl^+. In this case, the OPP process is described by the differential rate of production into the interval of Landau level numbers and the interval of the z-component of the momentum of the electron, $dW^{\mu-\mu+}/dl^- dp_z^-$. It is convenient to pass from $dl^- dp_z^-$ to $d\varepsilon d\Psi$, where

$$\varepsilon = h\varepsilon^- / m, \quad \Psi = p_z^- / \varepsilon^-. \tag{2.152}$$

The OPP process in the LLL approximation. To find the integrals in Eq. (2.151) we use the known property of the Dirac delta function,

$$\delta(\omega - \varepsilon^- - \varepsilon^+) = \sum_{i=1}^{2} \frac{\varepsilon^+ \varepsilon^-}{|\varepsilon^+ p_z^- - \varepsilon^- p_z^+|} \delta(p_z^- - p_i^-), \tag{2.153}$$

where p_i^- are two possible values of the longitudinal momentum of the electron (2.130).

Note that the denominator of (2.153) goes to zero if $p_z^- = p_z^+ = 0$, i.e. at the threshold of e^+e^- pair production by a photon propagating perpendicular to the field. The appearance of singularities in the process rate is explained by the emission of soft photons, which always accompany QED processes but which are neglected in our consideration. This phenomenon is similar to the so-called «infrared catastrophe» considered in the theory of electron scattering by a Coulomb center [190] (see Fig. 2.16). The infrared divergence appears because the perturbation theory cannot describe soft photon emission. The bremsstrahlung

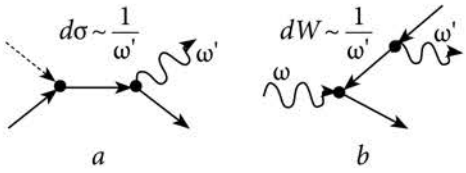

Fig. 2.16. Feynman diagrams of processes: *a* — bremsstrahlung in electron scattering by the Coulomb center, *b* — single-photon e^+e^- pair production with photon emission

cross-section is proportional to the inverse frequency of the emitted photon, $\sigma \sim 1/\omega'$, and it goes to infinity when $\omega' \to 0$. Similarly, if we take into account the emission of an additional photon, the e^+e^- pair production rate has the same dependency on the final photon frequency, $W \sim 1/\omega'$. Note that in this case, the divergence at the process threshold ($p_z^- = p_z^+ = 0$) disappears.

In the LLL approximation, the special function $J(l^+,l^-)$ entering the process amplitude (2.142) reduces to

$$J(l^+,l^-) \equiv J_0 = (-1)^{l^+} \frac{e^{-\eta/2}}{\sqrt{l^+!l^-!}} \eta^{(l^+ + l^-)/2}, \tag{2.154}$$

where $\eta = \omega^2/2hm^2 = 2/h$ in zero-order approximation.

Similarly, the other special function in (2.142) are

$$J(l^+ - 1, l^- - 1) = -\frac{\sqrt{l^+ l^-}}{\eta} J_0, \; J(l^+, l^- - 1) = \sqrt{\frac{l^-}{\eta}} J_0,$$
$$J(l^+ - 1, l^-) = -\sqrt{\frac{l^+}{\eta}} J_0. \tag{2.155}$$

Let us now write the OPP rates for fixed spin projections of the electron and the positron. The analysis of three kinematical cases (2.136) — (2.141) shows that the rates W^{--}, W^{++}, and W^{-+} have the same dependence on the longitudinal electron momentum p^-. They are, respectively,

$$W^{-+} = \frac{\alpha m^4 h}{2\omega\varepsilon^- |p^-|} J_0^2 (1 + \xi_3), \tag{2.156}$$

$$W^{--} = \frac{\alpha m^4 h^2 l^+}{4\omega\varepsilon^- |p^-|} J_0^2 (1 - \xi_3), \tag{2.157}$$

$$W^{++} = \frac{\alpha m^4 h^2 l^-}{4\omega\varepsilon^- |p^-|} J_0^2 (1 - \xi_3). \tag{2.158}$$

In contrast, the rate of pair production to the inverted spin states ($\mu^- = +1$ $\mu^+ = -1$) substantially depends on the difference $\delta\omega = \omega - \omega_m$. In the case of $\delta\omega =$

$= \alpha_1 mh^2$, particle energies and momenta are given by Eq. (2.137), and the corresponding rate is

$$W^{+-} = \frac{\alpha m^3 h^5 l^- l^+}{32\omega\varepsilon^- |p^-|} J_0^2 (1 + \frac{16(p^-)^2}{m^2 h^2} + \xi_3 (1 - \frac{16(p^-)^2}{m^2 h^2})). \qquad (2.159)$$

In the case of $\delta\omega = \alpha_1 mh$, particle energies and momenta are given by Eq. (2.139), and the rate is

$$W^{+-} = \alpha m h^3 |p^-| l^- l^+ J_0^2 (1 - \xi_3)/2\omega. \qquad (2.160)$$

In the case of $\delta\omega = \alpha_1 m$, particle energies and momenta are given by Eq. (2.141), and the rate has the form

$$W^{+-} = \frac{\alpha m^4 h^3 |p^-| l^- l^+}{4\omega(\varepsilon^-)^3} J_0^2 (2 + \frac{(p^-)^2}{2(\varepsilon^-)^2} - \xi_3 (2 - \frac{(p^-)^2}{2(\varepsilon^-)^2})). \qquad (2.161)$$

Note that the most probable process channel is pair production to the ground spin state with $\mu^- = -1$ and $\mu^+ = +1$. In this case, the corresponding rate contains the least power of the small parameter h. In all process channels, the rate depends on the polarization parameter ξ_3 only. The absence of ξ_1 and ξ_2 is obvious from the consideration of the problem symmetries because in the considered frame of reference the photon propagates perpendicular to the magnetic field. In this reference frame, the cases of linear polarization at an angle of ±45° and right and left circular polarization are equivalent.

The total OPP process rate summed over the final particles states and averaged over the photon polarization equals to

$$<W> = \alpha m^4 h J_0^2 / 2\omega\varepsilon^- |p^-|, \qquad (2.162)$$

that coincides with the results of [46]. The dependence of the total rate of the OPP process on the square of the photon frequency is shown in Fig. 2.17 for the case of $h = 0.1$. The dotted line shows the data taken from Ref. [46]. As the Landau level numbers and the photon frequency increase, the curve determined by the formula (2.162) deviates from the results of Ref. [46], which is due to the violation of the applicability of the LLL approximation.

As mentioned above, the most probable channel is the pair production to the ground spin states. However, the rate W^{-+} (2.156) contains a factor $(1 + \xi_3)$ and vanishes for normal linear polarization of the photon, $\xi_3 = -1$. At the same time, the rates W^{--}, W^{++} are proportional to the factor $(1 - \xi_3)$ and they are the main channels in the case of $\xi_3 = -1$.

To correctly compare the rates W^{-+}, W^{--}, W^{++} in the case of $\xi_3 = -1$, let us write the expression for W^{-+} with the account of additional power in h,

$$W^{-+} = \frac{\alpha m^4 h}{2\omega\varepsilon^- g |p^-|} J_0^2 (1 + \xi_3)(1 + \frac{h}{2}(3(l^+ + l^-) - \frac{2l^+ l^-}{g^2})), \qquad (2.163)$$

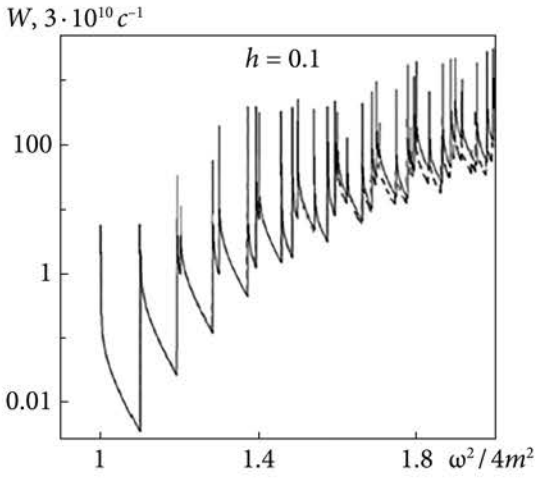

Fig. 2.17. Dependence of the total rate of OPP process on the square of the photon frequency

where $g = 1+(p^-/m)^2$. Note that the refined expression (2.163) has the same dependence on the photon polarization as (2.156). The analysis shows that this is also true for expressions that take into account a higher degree of h.

Thus, e^+e^- pair are produced in the ground spin state except for the small vicinity of photon polarization $\delta\xi$ near the value $\xi_3 = -1$. Therefore, the created particle beams are practically purely polarized. Let us consider a relationship between the magnitude of this polarization interval $\delta\xi$ and the mutual orientation of the external magnetic field $\vec{H}$ and the electric field of the photon $\vec{E}_{ph}$ (see Fig. 2.18). We assume that the angle between these vectors is close to $\pi/2$, and the angle ϑ is correspondingly small. The Stokes parameter can be defined in the terms of the projections of the photon electric field on the x and z axes as follows (see Fig. 2.18):

$$\xi_3 = \frac{E_1^2 - E_2^2}{E_1^2 + E_2^2}. \tag{2.164}$$

For small values of ϑ we can write $E_1 = E_{ph}\vartheta$ and $E_2 = E_{ph}$. Then,

$$\xi_3 = -1 + \delta\xi = -1 + 2\vartheta^2. \tag{2.165}$$

Consequently, the sought interval $\delta\xi$ equals $2\vartheta^2$ and it should be of the order of magnitude of the small parameter h so that the rate of the main channel W^{-+} be of the same order of magnitude with W^{--} and W^{++},

$$\delta\xi_c = 2\vartheta_c^2 = \alpha_c h, \quad \alpha_c \sim 1. \tag{2.166}$$

Let us now find the degree of polarization of the final particles. The degree of polarization of electrons (positrons) is the degree of orientation of their spin and it is defined as

$$P_{e^-} = \frac{(W^{++} + W^{+-}) - (W^{-+} + W^{--})}{(W^{++} + W^{+-}) + (W^{-+} + W^{--})}, \tag{2.167}$$

$$P_{e^+} = \frac{(W^{++} + W^{-+}) - (W^{+-} + W^{--})}{(W^{++} + W^{-+}) + (W^{+-} + W^{--})}. \tag{2.168}$$

If the angle between $\vec{E}_{ph}$ and $\vec{H}$ (see Fig. 2.18) is greater than ϑ_c, then $(1 + \xi_3) > \delta\xi_c$. Taking into account Eqs. (2.157), (2.158), and (2.163), the polarization degree (2.167), (2.168) to the first order in h are

$$P_{e^-} = -1 + hl^- \frac{1-\xi_3}{1+\xi_3},$$

$$P_{e^+} = +1 - hl^+ \frac{1-\xi_3}{1+\xi_3}. \qquad (2.169)$$

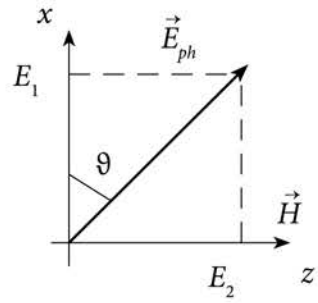

Fig. 2.18. The mutual arrangement of $\vec{E}_{ph}$, $\vec{H}$ vectors

For an anomalous photon polarization ($\xi_3 = 1$), as well as at the zero Landau level (obviously), both electrons and positrons are created purely polarized to the ground spin state, where electron spins are directed against the field and positron spins are directed along the field. In other cases except for the narrow cone $\vartheta < \vartheta_c$, the pure polarization is slightly disturbed by an order of magnitude h. The magnitude of depolarization of electrons (positrons) is proportional to the Landau level number of the electrons (positrons). If the angle between $\vec{E}_{ph}$ and $\vec{H}$ is much less than the critical ϑ_c, then the polarization degree with the account of (2.165) is

$$P_{e^-} = \frac{l^- - l^+ - 2\vartheta/h}{l^- + l^+ + 2\vartheta/h} = \frac{l^- - l^+}{l^- + l^+} - \vartheta \frac{4l^-}{h(l^- + l^+)^2}, \qquad (2.170)$$

$$P_{e^+} = \frac{l^- - l^+ + 2\vartheta/h}{l^- + l^+ - 2\vartheta/h} = \frac{l^- - l^+}{l^- + l^+} + \vartheta \frac{4l^+}{h(l^- + l^+)^2}. \qquad (2.171)$$

It follows from expressions (2.170) and (2.171) that the polarization degree depends only on the Landau level numbers within a small angle ϑ. For $l^- < l^+$ electrons are created mostly to the ground spin state, opposite to the case of $l^- > l^+$ when they are created in the inverse state. The same is true for positrons, i.e. a particle with a higher energy level is born to the inverse spin state, and a particle with a lower level is born to the ground state. If particles are produced to the same level, the polarization is absent within the accuracy ϑ. When the angle ϑ increases, it results in the decrease of P_{e-} and increase of P_{e+}, which means approaching the ground spin state for both electrons and positrons.

Suppose the photon frequency (2.134) is fixed, and the limit value equals to

$$\omega_m = m^- + m^+ = 2m + hm(l^- + l^+). \qquad (2.172)$$

A photon of this frequency can produce e^+e^- pairs to Landau levels with the following conditions,

$$\begin{cases} 1)\ l^+ = l^-: \ l^+ = l, \ l^- = l, \\ 2)\ l^+ > l^-: \ l^+ = l + \Delta l, \ l^- = l - \Delta l, \\ 3)\ l^+ < l^-: \ l^+ = l - \Delta l, \ l^- = l + \Delta l. \end{cases} \tag{2.173}$$

Let us compare the rates W^{-+}, W^{--}, and W^{++} in these cases. Landau level numbers enter the rate of the main channel W^{-+} (2.156) only in the quantity J_0^2 (2.154). The rate can be written as

$$W^{-+} = A\frac{1}{(l^-)!(l^+)!}. \tag{2.174}$$

Denoting the quantity (2.174) for the case of equal level numbers as W_0, we obtain the following expression of the rate for the cases (2) and (3) in (2.173),

$$W^{-+} = \frac{l(l-1)...(l-\Delta l+1)}{(l+1)...(l+\Delta l)} W_0 < W_0. \tag{2.175}$$

Thus, the most probable is symmetrical pair production with an equal level number of the electron and the positron.

To do a similar analysis of the rates W^{--} and W^{++} we write them in the form

$$W^{--} = B\frac{l^+}{(l^-)!(l^+)!}, \quad W^{++} = B\frac{l^-}{(l^-)!(l^+)!}. \tag{2.176}$$

In the case of equal level numbers, let us denote the quantities (2.176) as W_1. If the condition (2) of (2.173) is true, the rates reduce to

$$W^{--} = \frac{(l-1)...(l-\Delta l+1)}{(l+1)...(l+\Delta l-1)} W_1, \quad W^{++} = \frac{(l-1)...(l-\Delta l)}{(l+1)...(l+\Delta l)} W_1. \tag{2.177}$$

Particularly, if $\Delta l = 1$ the rates equal to

$$W^{--} = W_1, \quad W^{++} = \frac{(l-1)}{(l+1)} W_1. \tag{2.178}$$

Thus, the efficiency of pair production is the same in the case of equal levels and the case of the electron being produced to the next lower level in the ground spin state. Other configurations have lesser process rates. In case (3) of (2.173), the expressions for the rates W^{--} and W^{++} in Eq. (2.177) swap places.

The OPP process in the ultrarelativistic approximation. The differential rate is given by Eq. (2.151) multiplied by $dl^+ \cdot dl^-$. The integration in dl^+ can be done using the Dirac delta-function and the relation

$$dl^+ = \frac{\varepsilon^+}{hm^2} d\varepsilon^+. \tag{2.179}$$

We change variables from l^-, p^- to ε,Ψ (2.152), with

$$dl^- dp^- = \frac{1}{mh^2} d\varepsilon d\Psi. \tag{2.180}$$

The resulting differential process rate takes the form

$$dW^{\mu^-\mu^+} = \frac{|M_{if}|^2 m^2 (\Omega - \varepsilon)\varepsilon}{(2\pi)^7 h^5} d\varepsilon d\Psi, \tag{2.181}$$

where $\Omega = h\omega/m$ is the dimensionless photon frequency.

In the amplitude M_{if} (2.142), the asymptotic expressions of the special functions $J(l^+,l^-)$, $J'(l^+,l^-)$ are expressed via the Macdonald functions similarly to Eqs. (2.80) and (2.81),

$$J(l^+,l^-;\eta) = \frac{\sqrt{\eta - (\sqrt{l^+} + \sqrt{l^-})^2}}{\pi\sqrt{3}(\sqrt{l^+} + \sqrt{l^-})} K_{1/3}\left(\frac{2}{3}\frac{\sqrt[4]{l^+l^-}(\eta - (\sqrt{l^+} + \sqrt{l^-})^2)^{3/2}}{(\sqrt{l^+} + \sqrt{l^-})^2}\right), \tag{2.182}$$

$$\frac{\partial J(l^+,l^-;\eta)}{\partial \eta} = \frac{\sqrt[4]{l^+l^-}(\eta - (\sqrt{l^+} + \sqrt{l^-})^2)}{\pi\sqrt{3}(\sqrt{l^+} + \sqrt{l^-})^3} \times$$
$$\times K_{2/3}\left(\frac{2}{3}\frac{\sqrt[4]{l^+l^-}(\eta - (\sqrt{l^+} + \sqrt{l^-})^2)^{3/2}}{(\sqrt{l^+} + \sqrt{l^-})^2}\right). \tag{2.183}$$

After transformation to the variables ε and Ψ, the argument of Macdonald functions takes the form

$$\kappa = \frac{\Omega}{3\varepsilon(\Omega - \varepsilon)} F^3, \quad F^2 = 1 + \Psi^2. \tag{2.184}$$

The differential rate of the pair production to the interval $d\varepsilon d\Psi$ with fixed spins by a photon with defined polarization looks like

$$\frac{dW^{\mu^-\mu^+}}{d\varepsilon d\Psi} = \frac{\alpha m h F^2}{24\pi^2\varepsilon^2\Omega(\Omega - \varepsilon)^2} D^{\mu^-\mu^+}, \tag{2.185}$$

If the particles have the opposite spin projections ($\mu^+ = -\mu^-$), the factors $D^{\mu^-\mu^+}$ in Eq. (2.185) take the form

$$D^{\mu,-\mu} = \Omega^2\{[F^2(K_{1/3}^2 + K_{2/3}^2) + 2\mu FK_{1/3}K_{2/3}] - 2\xi_2\Psi[FK_{1/3}K_{2/3} + \mu K_{1/3}^2] + \\ + \xi_3[(1-\Psi^2)K_{1/3}^2 + F^2K_{2/3}^2 + 2\mu FK_{1/3}K_{2/3}]\}. \quad (2.186)$$

The minus sign of μ, $\mu = -1$, corresponds to the ground spin state, and $\mu = +1$ corresponds to the inverse state. In the case of equal spin projections, $\mu^+ = \mu^-$, the factors $D^{\mu^-\mu^+}$ are

$$D^{\mu\mu} = [(a\Psi^2 + b)K_{1/3}^2 + aF^2K_{2/3}^2 - 2\mu cFK_{1/3}K_{2/3}] - 2\xi_2\Psi[aFK_{1/3}K_{2/3} - \mu cK_{1/3}^2] + \\ + \xi_3[(a\Psi^2 - b)K_{1/3}^2 - aF^2K_{2/3}^2 + 2\mu cFK_{1/3}K_{2/3}], \quad (2.187)$$

where $a = (2\varepsilon - \Omega)^2$, $b = \Omega^2$, $c = (2\varepsilon - \Omega)\Omega$. Note that obtained Eqs. (2.186) and (2.187) coincide with similar expressions (2.93) and (2.92) for the SR process with the opposite sign of the ξ_2 parameter. Fig. 2.19 shows the dependence of the OPP rate on the dimensionless electron energy ε and its longitudinal momentum Ψ in the cases: (*a*) $\xi_3 = -1$, (*b*) $\xi_3 = +1$; the photon frequency is set to $\Omega = 1$.

The main channels (*a*) pair production to the state with equal spin projections by a photon with normal polarization, and (*b*) pair production to the inverse spin state by a photon with anomalous polarization. In both cases, the process rate has a maximum perpendicular to the field plane ($\Psi = 0$) with equal energies of the particles ($\varepsilon = 0.5$).

After inserting $\Psi = 0$ into the factors $D^{\mu^-\mu^+}$ they take the form

$$D^{\mu,-\mu} = b[K_{1/3}^2 + K_{2/3}^2 + 2\mu K_{1/3}K_{2/3}](1+\xi_3), \quad (2.188)$$

$$D^{\mu,\mu} = [bK_{1/3}^2 + aK_{2/3}^2 - 2\mu cK_{1/3}K_{2/3}](1-\xi_3). \quad (2.189)$$

The obtained expressions have the same dependence on the Stokes parameter ξ_3 of the initial photon as in the LLL case (2.156) — (2.158). As before, a photon with normal polarization ($\xi_3 = -1$) creates an e^+e^- pair with the same spin projections, and a photon with anomalous polarization ($\xi_3 = -1$) produces a pair with opposite spin projections. If an electron and a positron have equal energies ($a = c = 0$) the condition $D^{--} = D^{++}$ is true. The same conclusion is true in the LLL approximation. If particles are created with different energies, then the inverted spin state of the less energetic particle is more probable. For example, if $\varepsilon^- > \varepsilon^+$, then $c > 0$ and $D^{++} < D^{--}$. It follows from Eq. (2.188) that always $D^{+-} > D^{-+}$, hence the particles tend to be produced in the inverse spin state. Note that these results are opposite to those obtained in the LLL approximation.

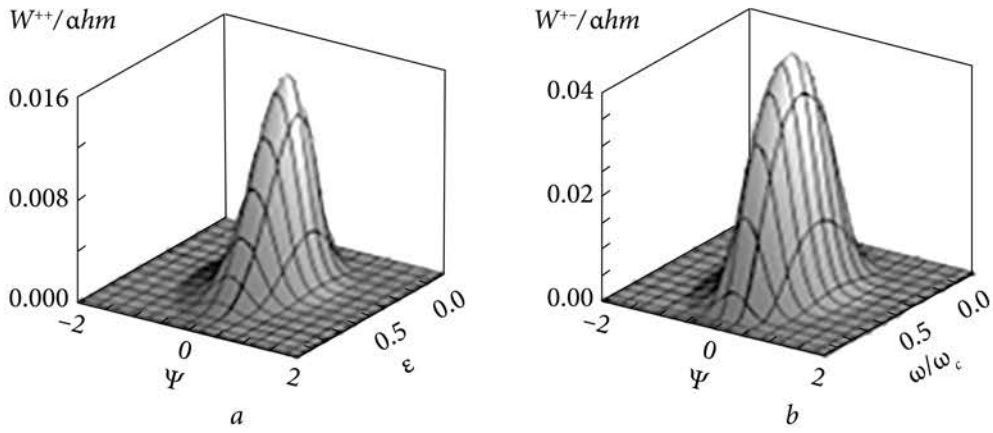

Fig. 2.19. The dependence of the OPP rate on the electron energy and its escape angle: *a* — $\xi_3 = -1$, *b* — $\xi_3 = +1$; the photon frequency is $\Omega = 1$

Let us now find the polarization degree in the case of $\Psi = 0$. Inserting Eqs (2.188) and (2.189) into Eqs. (1.167) and (2.168) we obtain

$$P_{e^\mp} = \frac{2[-c(1-\xi_3) \pm b(1+\xi_3)]K_{1/3}K_{2/3}}{(bK_{1/3}^2 + aK_{2/3}^2)(1-\xi_3) + b(K_{1/3}^2 + K_{2/3}^2)(1+\xi_3)}, \qquad (2.190)$$

where the upper sign corresponds to the electron and the lower sign corresponds to the positron.

If the photon has normal polarization ($\xi_3 = -1$), the polarization degree of the electron (positron) is

$$P_{e^-} = P_{e^+} = \frac{-2cK_{1/3}K_{2/3}}{(bK_{1/3}^2 + aK_{2/3}^2)} \approx \frac{-2c}{b+a}. \qquad (2.191)$$

If particle energies are equal then $c = 0$ and their polarization vanishes. If the energy difference goes to its maximum value, $\varepsilon^- = \omega$, $\varepsilon^+ = 0$, then $a = b = c$ and polarization degrees of electrons and positrons are equal, $P_{e^-} = P_{e^+} = -1$. And vice versa, if $\varepsilon^- = 0$, $\varepsilon^+ = \omega$ then $P_{e^-} = P_{e^+} = 1$.

In the case of anomalous photon polarization ($\xi_3 = +1$), the electron (positron) polarization degree is

$$P_{e^\mp} = \frac{\pm 2K_{1/3}K_{2/3}}{(K_{1/3}^2 + K_{2/3}^2)} \approx \pm 1. \qquad (2.192)$$

Thus, regardless of the particle energies, they are created in the inverted spin state with a 100% polarization degree.

If the photon is polarized at the angle of ± 45° relative to the magnetic field ($\xi_1 = \pm 1$, $\xi_3 = 0$), the electron (positron) polarization degree is

$$P_{e^{\mp}} = \frac{2(-c \pm b)K_{1/3}K_{2/3}}{2bK_{1/3}^2 + (a+b)K_{2/3}^2} \approx \frac{2(-c \pm b)}{3b+a}. \qquad (2.193)$$

When the particles have equal energies it reduces to $P_{e^{\pm}} = \pm 2/3$. In the case of maximum energy difference, $\varepsilon^- = \omega$ and $\varepsilon^+ = 0$, we obtain $P_{e^-} = 0$ and $P_{e^+} = -1$. In the opposite case of $\varepsilon^- = 0$ and $\varepsilon^+ = \omega$, the polarization degrees are $P_{e^-} = 1$ and $P_{e^+} = 0$.

Thus, by selecting various linear polarization of the incident photon, it is possible to obtain particle beams with controlled polarization ranging from the purely polarized to the fully depolarized state. Photon polarization can be changed by rotating the photon beam around its axis at a fixed angle. According to Fig. 2.18, zero $\vartheta = 0$ angles correspond to normal photon polarization, $\xi_3 = -1$. Increasing this angle by +45° gives the case of $\xi_1 = +1$, and, finally, further increase by +45° results in anomalous linear polarization, $\xi_3 = +1$.

The polarization degree of electrons with an arbitrary escape angle Ψ is given by Eqs. (2.186) and (2.187). For circular photon ($\xi_1 = 0$, $\xi_3 = 0$) polarization it equals to

$$P_{e^-} = \frac{2(b-c)K_{1/3}(FK_{2/3} - \xi_2\Psi K_{1/3})}{K_{1/3}^2(2b+(a+b)\Psi^2) + K_{2/3}^2F^2(a+b) - 2\xi_2\Psi(a+b)FK_{1/3}K_{2/3}}. \qquad (2.194)$$

For positron polarization degree the b quantity in the nominator of (2.194) should be replaced according to $b \to -b$. It is clear from (2.194) that electron polarization does not change after the change of right circular polarization to the left one and simultaneously alters the sign of Ψ.

Fig. 2.20 shows the dependence of the electron polarization degree on the escape angle Ψ in the OPP by a circularly polarized photon ($\xi_2 = 1$). Left (a) and right (b) panels correspond to $\Omega = 1$ and $\Omega = 100$ respectively. The electron energy varies from 0.1Ω to 0.9Ω. The maximum electron polarization is reached at small electron energy. In the most likely case when particles have equal energy of $\varepsilon = 0.5\Omega$ the polarization degree is $P_{e^-} = 0.7$. Electrons having energy approaching the energy of the incident photon are practically unpolarized.

The total rate of the OPP process with fixed spin projections can be found by integrating the differential rate (2.185) over the electron energy ε and its escape angle Ψ,

$$W^{\mu^-\mu^+} = \int_0^{\Omega} d\varepsilon \int_{-1}^{1} d\Psi \frac{dW^{\mu^-\mu^+}}{d\varepsilon d\Psi}. \qquad (2.195)$$

After summation of the final particles spin projections and averaging over the photon polarization this expression coincides with the known results [8].

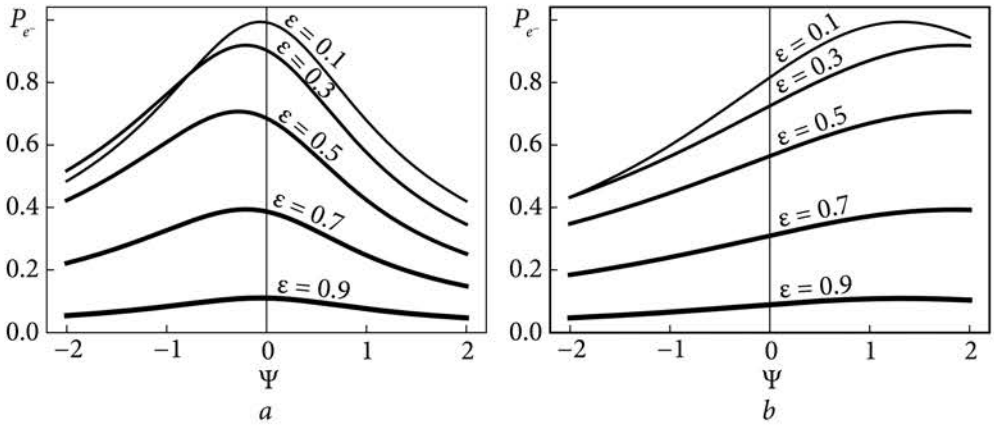

Fig. 2.20. Dependence of the electron polarization degree on the electron escape angle, $\xi_2 = 1$: *a* — $\Omega = 1$; *b* — $\Omega = 100$

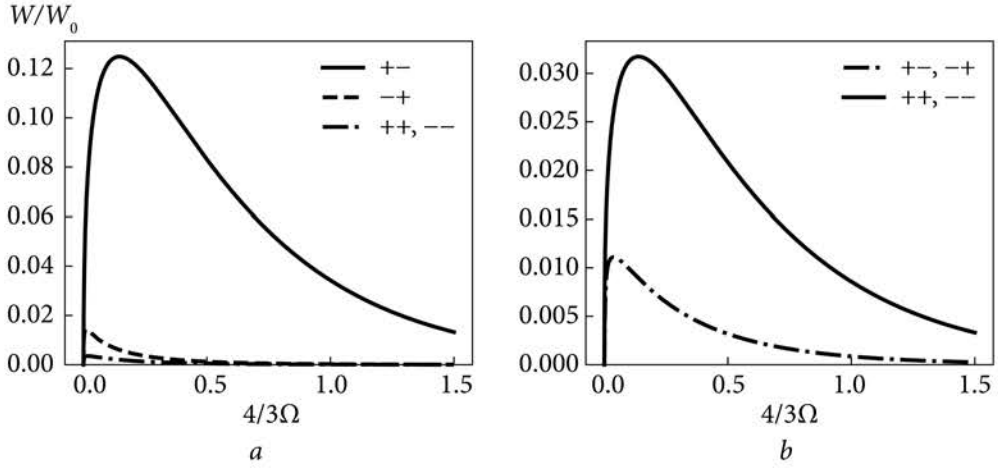

Fig. 2.21. Dependence of the total rate on the parameter $4/3\Omega$: *a* — $\xi_3 = +1$, *b* — $\xi_3 = -1$

The dependence of the total process rate on the inverse of the photon energy is shown in Fig. 2.21. Left and right panels show the cases $\xi_3 = +1$ and $\xi_3 = -1$ respectively. Here we denote $W_0 = \alpha hm$, and W_0 is of the order of $W_0 \sim 10^{18}\,s^{-1}$ for the field strength of $h = 0.1$. The rate has maximum values when the dimensionless frequency is about $\Omega_{max} \approx 10$, which corresponds to photon energy about $\omega_{max} \approx 50$ MeB for the field strength of $h = 0.1$. The rate decreases when photon frequency exceeds ω_{max}.

As shown in Fig. 2.21, the main channel is pair creation with opposite spin projections. Note that for anomalous photon polarization, the rate of the channel with inverse spin state of particles is by an order of magnitude higher than

the rate of the channel process with the ground spin state, $W^{+-} >> W^{-+}$. At the same time, these channels have equal rates, $W^{+-} = W^{-+}$ in the case of normal photon polarization.

Thus, by changing the linear polarization of the initial photon (e. g. rotating the beam around its axis), it is possible to obtain electrons and positrons in a controlled spin state, ranging from fully unpolarized to inversely polarized state.

In laboratory conditions the maximum magnetic field is 10^6 G. In this field, the photon energy of 100 GeV corresponds to the value $\Omega \sim 4.10^{-3}$, which is a small parameter. On the contrary, the Ω can reach very large values in a pulsar magnetosphere.

2.4. Conclusions

In this chapter, we considered spin-polarization effects in SR and OPP process, i.e. the effects arising due to interaction between spin of particles polarization of photons. Let us now formulate some conclusions.

1. SR process in the LLL approximation.

1) The radiation polarization is the same as predicted by classical electrodynamics if an electron does not change its spin orientation. The rates of the corresponding channels satisfy the condition $W^{--} > W^{++}$.

2) The spin-flip radiative transition to the ground spin state ($\mu = -1$) changes the linear polarization of radiation from the normal ($\xi_3 = -1$) to anomalous ($\xi_3 = +1$) one. Its rate is less than the rate of the main channels by a factor of h, where h is a magnetic field strength in the units of the QED critical value, $h = H/H_0 = e\hbar H/m^2c^3$. The other spin-flip channel with a transition to the inverted spin state is small and its fraction is of the order of h^3. The account of the contribution of the spin-flip channels decreases by the amount of $\sim h$.

3) The emission of an electron with finite longitudinal momentum is fully linearly polarized when the frequency approaches the maximum value.

4) An ultrarelativistic electron moving along the magnetic field and occupying a low Landau level emits photons of right circular polarization.

2. SR process in the ultrarelativistic approximation.

1) The angular dependence of the radiation polarization qualitatively resembles the results of the LLL approximation, but «contracts» into a narrow radiation cone of the width of $\sim m/\varepsilon$.

In the channels without spin inversion, the radiation in the orbit plane has pure normal linear polarization (σ polarization). In the spin-flip processes, the linear polarization changes its sign (π polarization).

2) The spin-flip process has a small probability in a moderate relativistic energy range, $z << 1$ ($z = H\varepsilon / H_0 m$). Its contribution is of the order of $\sim z^2/8$

compared to the main channel near the spectral maximum. If $z > 1$, the spin-flip channel is comparable with the channel without spin inversion.

3) In the case of ultrarelativistic electron energy $z > 1$, the polarization of radiation of an initially polarized electron beam depends essentially on energy and its spin projection of electrons, as well as on the radiation frequency. If initially electron spins are oriented opposite to the field, the polarization degree of the radiation decreases monotonically with an increase of z. For electrons in the inverted spin state, the polarization degree of radiation is a nonmonotonic function of z. Radiation in the orbit plane changes the polarization from normal to anomalous and back when the electron energy and the parameter z increase.

4) In the case of $z > 1$, the radiation of an initially unpolarized electron beam is partially polarized with the polarization degree of $2.3/z$.

3. OPP process in the LLL approximation.

1) The most probable channel is pair production to the ground spin states. The rate is maximum for the production of electrons and positrons with equal energies.

2) In the case of anomalous linear photon polarization ($\xi_3 = +1$), the created e^+e^- pairs are fully polarized to the ground spin state. Except for the small interval of $\sim h$ near $\xi_3 = -1$, the particle polarization degree deviates from unity by the small value of the order of h. Within a small vicinity of photon polarization near the value of $\xi_3 = -1$, the polarization of the produced particles depends on the difference in their energies. The particles are unpolarized if their energies are equal. The less energetic particles tend to be created in the ground spin state.

4. OPP process in the ultrarelativistic approximation.

1) If the photon propagates perpendicular to the field, the main channels are (1) creation of a pair with the same spin projections by a photon of normal polarization, and (2) creation of a pair with opposite spin projections by a photon of anomalous polarization.

2) The total process rates satisfy the conditions $W^{+-} >> W^{-+}$ for a photon of anomalous polarization and $W^{+-} = W^{-+}$ for a photon of normal linear polarization.

Thus, by changing the linear polarization of the initial photon (e.g. rotating the beam around its axis), it is possible to obtain electron and positron beams in a controlled spin state, ranging from unpolarized to inversely polarized state.

The main scientific results of this chapter are published in [280—283].

Chapter 3

RESONANT AND SPIN-POLARIZATION EFFECTS IN THE PROCESS OF PHOTON SCATTERING ON AN ELECTRON

3.1. Introduction

In the chapter on the process of photon scattering by an electron, i.e. in Compton scattering (CS) in a magnetic field, spin-polarization effects under resonant conditions are studied, i.e., the effect of initial photon polarization on both radiation polarization and spin states of final electron for different spin states of the initial electron. The process of emission of two photons by an electron, i.e. the process of double synchrotron radiation (DSR) in a magnetic field under resonant conditions with polarized photons and certain values of particle spin projections, has been studied.

Adding a single photon in the initial or final states to the SR process, which was discussed in Chapter 2, gives the CS and DSR processes, which are the object of study in this section. The problems of the chapter consider QED processes, where in addition to particles in the initial and final states, particles in intermediate states also participate. Such particles are described by a Green's function.

Green's function of an electron in a magnetic field. For the Green's function of an electron in an external magnetic field, we use the expression obtained in [284]:

$$G_H(\mathbf{x}_1,\mathbf{x}_2)=\frac{1}{(2\pi)^3}\int d^3\mathbf{g}e^{-i\mathbf{g}(\mathbf{x}_1-\mathbf{x}_2)}G_H(\tilde{g};\rho_1,\rho_2), \qquad (3.1)$$

where $\mathbf{x}=(t,x,y,z)$ is 4-dimensional coordinate, $\mathbf{g}=(g_0,0,g_y,g_z)$, $\tilde{g}=(g_0,0,0,g_z)$, $\rho=\sqrt{h}m(x+g_y/hm^2)$, $G_H(\tilde{g};\rho_1,\rho_2)=\sum_{n=0}^{\infty}\frac{G_H(\rho_1,\rho_2)}{(\tilde{g}^2-m_g^2)}$,

$$G_H(\rho_1,\rho_2)=\sqrt{h}m[U_n(\rho_1)U_n(\rho_2)(\gamma\tilde{g}+m)\alpha_{12}+U_{n-1}(\rho_1)U_{n-1}(\rho_2)(\gamma\tilde{g}+m)\alpha_{21}+$$
$$+i\sqrt{2nh}m(U_{n-1}(\rho_1)U_n(\rho_2)\gamma^1\alpha_{12}-U_n(\rho_1)U_{n-1}(\rho_2)\gamma^1\alpha_{21})], \quad (3.2)$$

$m_g^2=m^2(1+2nh)$, $\alpha_{12}=\frac{1}{2}(1-i\gamma^1\gamma^2)$, $\alpha_{21}=\frac{1}{2}(1-i\gamma^2\gamma^1)$, γ^μ are the Dirac gamma matrices, $U_n(\rho)$ is Hermite function (2.8).

Green's function of an electron in a Redmond configuration field. The study of QED processes in an external magnetic field, along which a plane electromagnetic wave is directed (Redmond field), allows, leaving a fixed number of photons of the wave, to study the QED processes of higher-order perturbation theory in a purely magnetic field. The expression for the Green's function of the electron in the field of this configuration was found in [285] and has the form:

$$G_R(\mathbf{x}_1,\mathbf{x}_2)=\frac{-1}{(2\pi)^3}\int dg_0dg_ydg_z\sum_{n=0}^{\infty}B_g(\varphi_1)\frac{G_H(\tilde{\rho}_1,\tilde{\rho}_2)}{g_0^2-\varepsilon^2}\bar{B}_g(\varphi_2)e^{-i(\Phi(\mathbf{x}_1)-\Phi(\mathbf{x}_2))}, \quad (3.3)$$

where $B_g(\varphi)=1-\frac{1}{2\kappa}e(\gamma^0-\gamma^3)(\gamma\tilde{A})$, $\varphi=t-z$, $\kappa=g^0-g_z$, $e\tilde{A}=(0,eA_x^{ext}-hm^2K_y,eA_y^{ext}+$
$+hm^2K_x,0)$, $\tilde{\rho}=\sqrt{h}m^2(x+\frac{g_y}{hm^2}-K_x)$, $\Phi(\mathbf{x})=\mathbf{gx}+hm^2K_xK_y+\sqrt{h}mK_y\tilde{\rho}+\int\frac{J(\varphi)d\varphi}{2\kappa}$,
$J(\varphi)=h\kappa m^2(\dot{K}_xK_y-K_x\dot{K}_y)-e^2\tilde{A}^2$, $\varepsilon^2=m_g^2+g_z^2$. Functions $K_x(\phi)$, and $K_y(\phi)$ are defined by the following equations:

$$\kappa\dot{K}_x=e\tilde{A}_y,\ \kappa\dot{K}_y=e\tilde{A}_x.$$

The vector potential $\vec{A}^{ext}=(A_x^{ext}(\varphi),A_y^{ext}(\varphi))$ of the external field of a plane wave is perpendicular to the magnetic field, which is directed along the z-axis.

3.2. Spin-polarization effects in the process of photon scattering by an electron

The amplitude of probability of the process of photon scattering by an electron. The expression for the amplitude of the process corresponds to Feynman diagrams shown in Fig. 3.1, and has the form:

$$A_{if}=ie^2\int d^4\mathbf{x}_1d^4\mathbf{x}_2\bar{\Psi}'(\mathbf{x}_1)[\gamma^iA_i(\mathbf{x}_1)G_{H1}(\mathbf{x}_1,\mathbf{x}_2)\gamma^jA'^*_j(\mathbf{x}_2)+$$
$$+\gamma^jA'^*_j(\mathbf{x}_1)G_{H2}(\mathbf{x}_1,\mathbf{x}_2)\gamma^iA_i(\mathbf{x}_2)]\Psi(\mathbf{x}_2), \quad (3.4)$$

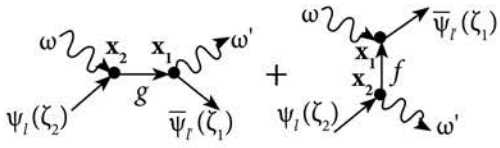

Fig. 3.1. Feynman diagrams the process of photon scattering by an electron

where $\Psi(\mathbf{x}_2) = S^{-1/2} e^{-ir_2p}\psi_l(\zeta_2)$, $\overline{\Psi}(\mathbf{x}_1) = S^{-1/2} e^{-ir_1p'}\psi_{l'}(\zeta_1)$ are wave functions of the initial and final electrons, the explicit form of which is given by expressions (2.6) and (2.27); $\mathbf{r}_{1,2}=(t_{1,2},0,y_{1,2}, z_{1,2})$; $A_i(\mathbf{x})$, $A'^*_j(\mathbf{x})$ are wave functions of the initial and final photons (2.12); $G_{H1}(\mathbf{x}_1,\mathbf{x}_2)$, $G_{H2}(\mathbf{x}_1,\mathbf{x}_2)$ are the Green's functions of the electron in the intermediate state, which correspond to the diagrams *g* and *f* (see Fig. 3.1), and are given by expression (3.1).

The external magnetic field H, which is directed along the z-axis, is given similar to the previous chapter with the field potential (2.11). In a constant magnetic field, the laws of conservation of energy and longitudinal component of momentum are fulfilled, which have the form:

$$\varepsilon + \omega = \varepsilon' + \omega', \quad p + \omega\nu = p' + \omega' u, \tag{3.5}$$

where ω, $\nu = \cos\theta$ and ω', $\nu = \cos\theta'$ are frequencies and cosines of polar angles of the initial and final photons; $\varepsilon \equiv \varepsilon_l$, $p \equiv p_z$ i $\varepsilon' \equiv \varepsilon'_{l'}$, $p' \equiv p'_z$ are energies and longitudinal momenta of the initial and final electrons, respectively, which are related by the laws of dispersion as in the expression (2.6).

For the fixed Landau levels of particles l, l' and the fixed angle of the final photon u, the conservation laws (3.5) specify the frequency of the final photon similar to the expression (2.30)

$$\omega' = \frac{1}{1-u^2}\left(\mathcal{E} - \mathcal{P}u - \sqrt{(\mathcal{E} - \mathcal{P}u)^2 - (\mathcal{E}^2 - \mathcal{P}^2 - m^2 - 2l'hm^2)(1-u^2)}\right), \tag{3.6}$$

where $\mathcal{E} = \varepsilon + \omega$, $\mathcal{P} = p + \omega\nu$. In the case of low frequencies $\omega << m$ or emission along the direction of the field $u \to 1$, the expression (3.6) takes the form:

$$\omega' = \frac{\mathcal{E}^2 - \mathcal{P}^2 - m^2 - 2l'hm^2}{2(\mathcal{E} - \mathcal{P}u)} \overset{h<<1}{=} \omega + (l - l')hm. \tag{3.7}$$

In the ultraquantum approximation, the difference between the frequencies of the initial and final photons is equal to the distance between the Landau levels of the initial and final electrons. In particular, the Landau level of the electron does not change during Thomson scattering ($\omega = \omega'$).

In the ultrarelativistic case, it is convenient to analyze the dependence of the process probability on the frequency and the polar angle of the final photon ω', u. The Landau level of the final photon in this case has the form:

$$l' = \frac{1}{2hm^2}\left[(\varepsilon + \omega - \omega')^2 - (\omega\nu - \omega' u)^2\right]. \tag{3.8}$$

After taking the integrals over 4-dimensional coordinates in (3.4) and introducing special functions defined by expression (2.37), the amplitude of the CS process with polarized initial and final photons, as well as initial and final electrons with given spins in the general case can be reduced to:

$$A_{if} = (2\pi)^4 \frac{M_{if}}{SV} \delta^3(p + k - p' - k'), \tag{3.9}$$

$$M_{if} = \frac{-ie^2 e^{i\Phi}}{4\sqrt{\omega\omega'\varepsilon\varepsilon' m_l m_{l'}}} \left[e^{i\Delta\Phi} \sum_{n_g=0}^{\infty} \frac{e^{-i\Phi_g} \sum_{a=1}^{10} Q_{ga}}{g_0^2 - \varepsilon_g^2} + \sum_{n_f=0}^{\infty} \frac{e^{i\Phi_f} \sum_{a=1}^{10} Q_{fa}}{f_0^2 - \varepsilon_f^2} \right]. \tag{3.10}$$

Two terms in expression (3.10) correspond to the two Feynman diagrams in Fig. 3.1. Zero and longitudinal to field components of the 4-pulses **g** and **f** of the intermediate particle in these diagrams, respectively, are equal to:

$$g_0 = \varepsilon + \omega, \quad g = p + \omega\nu, \quad f_0 = \varepsilon - \omega', \quad f = p - \omega' u. \tag{3.11}$$

The energies ε_g and ε_f of intermediate states at fixed Landau levels n_g and n_f are equal to:

$$\varepsilon_g = \sqrt{m^2 + 2n_g hm^2 + g^2}, \ \varepsilon_f = \sqrt{m^2 + 2n_f hm^2 + f^2}. \tag{3.12}$$

The general phase Φ, phase difference $\Delta\Phi$, and phases Φ_g and Φ_f have the form:

$$\Phi = \frac{1}{2hm^2}(k_x k_y - k'_x k'_y - 2p_y(k_x - k'_x)) + \frac{\pi}{2}(l' - l) + l\varphi' - l'\varphi, \tag{3.13}$$

$$\Delta\Phi = \frac{k_y(k_x - k'_x)}{hm^2} + (l + l')(\varphi - \varphi'), \ \Phi_g = n_g(\varphi - \varphi'), \ \Phi_f = n_f(\varphi - \varphi'), \tag{3.14}$$

where k_x, k_y, k'_x, and k'_y are transverse components of momenta of the initial and final photons, φ,φ' are azimuthal angles of photons. The values Q_{ga} in the first term (3.10) have the form:

$$\begin{aligned}
Q_{g1} &= J_{g1}^{++} J_{g2}^{++} [m\tilde{C} + g_0 C + gD], \quad Q_{g2} = J_{g1}^{+-} J_{g2}^{+-} [mC + g_0\tilde{C} - gD], \\
Q_{g3} &= J_{g1}^{-+} J_{g2}^{-+} [-mC + g_0\tilde{C} - gD], \quad Q_{g4} = J_{g1}^{--} J_{g2}^{--} [-mC + g_0\tilde{C} + gD], \\
Q_{g5} &= J_{g1}^{-+} J_{g2}^{++} [-mD - g_0\tilde{D} + gC], \quad Q_{g6} = J_{g1}^{++} J_{g2}^{-+} [-mD + g_0\tilde{D} + gC], \\
Q_{g7} &= J_{g1}^{--} J_{g2}^{+-} [mD + g_0\tilde{D} + gC], \quad Q_{g8} = J_{g1}^{+-} J_{g2}^{--} [mD - g_0\tilde{D} + gC], \\
Q_{g9} &= [J_{g1}^{++} J_{g2}^{+-} + J_{g1}^{+-} J_{g2}^{++} + J_{g1}^{-+} J_{g2}^{--} + J_{g1}^{--} J_{g2}^{-+}] D_h, \\
Q_{g10} &= [J_{g1}^{-+} J_{g2}^{+-} + J_{g1}^{+-} J_{g2}^{-+} - J_{g1}^{--} J_{g2}^{++} - J_{g1}^{++} J_{g2}^{--}] C_h,
\end{aligned} \tag{3.15}$$

where the notations are entered

$$J_{g1}^{++} = J_1(l,n_g)M_m e_z,\quad J_{g1}^{--} = J_1(l-1,n_g-1)\mu M_p e_z,$$
$$J_{g1}^{+-} = J_1(l,n_g-1)M_m H_m,\quad J_{g1}^{-+} = J_1(l-1,n_g)\mu M_p H_p. \tag{3.16}$$

The values M_m, M_p, C, D, H_m, and H_p are defined by expressions (2.40) — (2.43), and the values $\tilde{C}$, $\tilde{D}$, C_h, D_h, e_z are equal, respectively:

$$\tilde{C} = E_m E_m' + \mathrm{sgn}(p_z)\mathrm{sgn}(p_z')\, E_p E_p',\quad \tilde{D} = \mathrm{sgn}(p_z')\, E_m E_p' - \mathrm{sgn}(p_z) E_p E_m', \tag{3.17}$$

$$C_h = \sqrt{2n_g hm}C,\quad D_h = \sqrt{2n_g hm}D, e_z = -\sin\theta\cos\alpha. \tag{3.18}$$

The functions J_{g2}^{++}, J_{g2}^{--}, J_{g2}^{+-}, J_{g2}^{-+} are defined by expressions (3.16), where you want to replace $1 \to 2$. The values l, M_m, M_p, and μ related to the initial electron should be replaced by the corresponding primed ones describing the final electron. The values e_z, H_m, and H_p describing the initial photon should be replaced by primed complex conjugate analogs related to the final photon. $J_1(l,n_g)$, $J_2(l',n_g)$ are special functions (2.37), whose arguments η, η' are:

$$\eta = \frac{\omega^2(1-v^2)}{2hm^2},\quad \eta' = \frac{\omega'^2(1-u^2)}{2hm^2}. \tag{3.19}$$

The values of Q_{fa} in the second term of the amplitude (3.9) have the form (3.15), where you want to replace $g \to f$, as well as $J^{+-} \leftrightarrow J^{-+}$, with

$$J_{f1}^{++} = J_1(n_f,l')M_m' e_z,\quad J_{f1}^{--} = J_1(n_f-1,l'-1)\mu' M_p' e_z,$$
$$J_{f1}^{+-} = J_1(n_f,l'-1)\mu' M_p' H_m,\quad J_{f1}^{-+} = J_1(n_f-1,l')M_m' H_p. \tag{3.20}$$

The expressions for J_2 are similar (3.20) and depend on the parameters of the initial electron and the final photon.

Cross-section of the CS process. The number of final states of the CS process coincides with that similar to the SR process (2.148). The product of the squared modulus of the amplitude (3.9) by the number of final states and divided by the time T and the flux of the initial photons $j = 1 / V$ gives the expression for the differential cross-section CS

$$d\sigma \equiv d\sigma_{l'} = |M_{if}|^2 \delta(\varepsilon + \omega - \varepsilon' - \omega')\omega'^2\, d\omega'\, du d\varphi', \tag{3.21}$$

where $du d\varphi'$ is a solid angle element of the final photon. The index l' in $d\sigma_{l'}$ shows that expression (3.21) is a partial scattering cross-section of the CS process, as a result of which the electron passes to a fixed Landau level l'. In a gen-

eral case, the total scattering cross-section is equal to:

$$\sigma_{tot} = \int d\omega' du d\varphi' \sum_{l'=0}^{l'\max} \frac{d\sigma_{l'}}{d\omega' du d\varphi'}, \tag{3.22}$$

where $l'_{\max}$ is the maximum possible Landau level of the finite electron, which is determined by the law of conservation of energy with the condition $\omega' = 0$. Only one term in the sum over the parameter l' in the total cross-section (3.22), which corresponds to the transition of an electron to the neighboring Landau level, plays the main role in ultraquantum approximation. In expression (3.21), which contains the Dirac delta function, integration over frequency ω' is easily carried out

$$d\sigma = \frac{|M_{if}|^2 \varepsilon' \omega'^2 du d\varphi'}{|\varepsilon' - u(p + \omega v - \omega' u)|}. \tag{3.23}$$

Assuming that only one term in the sum of the Landau levels n_g in the expression (3.10) gives the main contribution to the cross-section (resonance in the diagram g Fig. 3.1), the amplitude (3.10) can be represented as

$$M_{if} = \frac{N_{if}}{g_0^2 - \varepsilon_g^2} = \frac{e^2}{4\sqrt{\omega\omega' \varepsilon\varepsilon' m_l m_{l'}}} \frac{Q_g}{g_0^2 - \varepsilon_g^2}, \tag{3.24}$$

where the insignificant phase is rejected. In the case of resonance

$$g_0^2 - \varepsilon_g^2 = 2\varepsilon_g (g_0 - \varepsilon_g).$$

Breit's phenomenological rule is used to eliminate divergence at the resonance point [113]

$$\varepsilon_g \to \varepsilon_g - i\Gamma/2, \tag{3.25}$$

where Γ is a resonance width, which is defined as the total probability of decay of an intermediate state. Then the differential cross-section (3.22) can be represented as:

$$\frac{d\sigma}{du} = \frac{\pi\omega'^2 |N_{if}|^2}{2m^2[(g_0 - \varepsilon_g)^2 + \Gamma^2/4]}. \tag{3.26}$$

If resonance takes place in the f diagram, the denominator of the cross-section (3.26) must be replaced by $g_0 - \varepsilon_g \to f_0 - \varepsilon_f$.

In ultrarelativistic approximation, the factor dl' is added to the number of final states, and integration by this value removes the Dirac delta function, as a result, the differential cross-section has the form:

$$d\sigma = \frac{1}{hm^2} |M_{if}|^2 \varepsilon' \omega'^2 d\omega' du d\varphi'. \tag{3.27}$$

The sum in the first term of the amplitude (3.10) over the Landau levels of the intermediate particle n_g is replaced by an integral, which is easy to take because it contains a pole $(g_0 - \varepsilon_g + i\Gamma/2)$:

$$\sum_{n_g} \frac{Q_g}{g_0^2 - \varepsilon_g^2} = -\int \frac{dn_g Q_g}{2\varepsilon_g(\varepsilon_g - g_0 - i\Gamma/2)} = \frac{-\pi i}{2hm^2} Q_g \Big|_{n_{g0}}$$

and similarly in the second term of the amplitude (3.10). Q_g is the sum of terms (3.15). Landau level numbers n_g, n_f in the obtained amplitude should be replaced by the expressions:

$$n_{g0} = \frac{(\varepsilon + \omega)^2 - \omega^2 v^2}{2hm^2}, \quad n_{f0} = \frac{(\varepsilon - \omega')^2 - \omega'^2 u^2}{2hm^2}. \tag{3.28}$$

Neglecting the interference term of two amplitudes g and f (see Fig. 3.1), the differential scattering cross section in ultrarelativistic approximation can be reduced to the form:

$$\frac{d\sigma}{d\omega' du} = \frac{\pi^3 e^4 \varepsilon' [\,|Q_g|^2 + |Q_f|^2]}{32h^3 m^6 \omega \varepsilon \sqrt{\varepsilon'^2 - p'^2}}, \tag{3.29}$$

where the energy and momentum of the final electron are determined by the conservation laws (3.5).

Resonance conditions in the CS process. Resonance in the process of photon scattering by an electron corresponds to the transition of the intermediate state on the mass shell. The resonance in the g diagram (see Fig. 3.1) corresponds to hitting the pole point in the first term of the amplitude (3.10), that is, fulfillment of the equality

$$\varepsilon_g - \varepsilon - \omega = 0. \tag{3.30}$$

In general, you can put the longitudinal momentum of the initial electron to zero:

$$p = 0. \tag{3.31}$$

Condition (3.30) specifies the value of the frequency of the initial photon to enter the resonance at a fixed Landau level n_g:

$$\omega_g = \frac{1}{1 - v^2}[\sqrt{\varepsilon^2 + 2(n_g - l)hm^2(1 - v^2)} - \varepsilon]. \tag{3.32}$$

It can be seen that the resonant conditions do not depend on the parameters of the final particles and are determined only by the initial particles, while the polarization of the initial particles does not affect the resonant conditions.

In the ultraquantum approximation, the frequency of the initial photon in resonant conditions is equal to (up to h^2):

$$\omega_g = (n_g - l)hm - h^2 m(n_g - l)(n_g + l - (n_g - l)v^2)/2. \quad (3.33)$$

Under such conditions, the final photon is emitted with frequency

$$\omega'_g = (n_g - l')hm - h^2 m(n_g - l')[n_g + l' + (n_g - l')u^2 - 2(n_g - l)vu]/2. \quad (3.34)$$

Thus, up to the first degree of magnetic field h, the resonant frequencies of the initial and final photons are multiples of the cyclotron frequency hm. They are equal to the distances between the Landau levels of the initial and intermediate electrons, and the intermediate and final electrons, respectively.

The resonance in the f diagram (see Fig. 3.1) corresponds to hitting the pole point in the second term of the amplitude (3.10), that is, fulfillment of one of the two equalities

$$\varepsilon_f - \varepsilon + \omega' = 0, \quad \varepsilon_f + \varepsilon - \omega' = 0. \quad (3.35)$$

The first condition (3.35) is satisfied if the initial electron emits a final photon with a frequency

$$\omega'_f = \frac{1}{1-u^2}[\varepsilon - \sqrt{\varepsilon^2 - 2(l - n_f)hm^2(1-u^2)}]. \quad (3.36)$$

Since the frequency of the final photon, in any case, must be equal to (3.6), equation (3.36) determines the frequency of the initial photon under resonant conditions, which in this case is equal to

$$\omega_f = \frac{1}{a}[-b + \sqrt{b^2 + ac}], \quad (3.37)$$

where $a = (1 - v^2)(1 - u^2)$, $b = k(1 - vu) + \varepsilon(vu - u^2)$, $c = 2(l' - n_f)hm^2(1 - u^2)$, $k = (\varepsilon^2 - 2(l - n_f)hm^2(1 - u^2))^{1/2}$.

In ultraquantum approximation, the resonant frequencies (3.36), and (3.37) have the form:

$$\omega'_f = (l - n_f)hm - h^2 m(l - n_f)[l + n_f + (l - n_f)u^2]/2, \quad (3.38)$$

$$\omega_f = (l' - n_f)hm - h^2 m(l' - n_f)[l' + n_f - (l' - n_f)v^2 + 2(l - n_f)vu]/2. \quad (3.39)$$

Note, up to h^2, the frequency of the initial photon resonant in diagram f, in addition to the Landau level numbers of particles l, l', n_f and the polar angle of the initial photon v, also depends on the outlet angle of the final photon u, except the case v = 0. To realize this resonance, one can choose a fixed value of the frequency of the initial photon, a multiple of the cyclotron frequency with a

given detuning $-\delta h^2 m(l' - n_f)/2$, and enter the resonance by choosing the angle of emission of the final photon u_f:

$$\omega_f = hm(l' - n_f)(1 - h\delta/2), \quad u_f = \frac{\delta + (l' - n_f)v^2 - l' - n_f}{2(l - n_f)v}. \tag{3.40}$$

The second condition (3.35) for the appearance of resonance in the f diagram determines the frequency of the final photon, which has the form

$$\omega'_f = \frac{1}{1-u^2}[\varepsilon + \sqrt{\varepsilon^2 - 2(l - n_f)hm^2(1-u^2)}]. \tag{3.41}$$

Upon entering such a resonance, the initial photon generates an electron-positron pair, and the intermediate positron subsequently annihilates with the initial electron into the final photon. The frequency of the initial photon is determined by expression (3.37), where you want to replace the value $b \to -b$ that is equal to $b = k(1 - vu) - \varepsilon(vu - u^2)$.

In the ultraquantum case, the frequencies of photons in the zero approximation (up to h^0) have the form:

$$\omega_f = \omega'_f \frac{1 + u^2 - 2vu}{(1 - v^2)}, \quad \omega'_f = \frac{2m}{1 - u^2}. \tag{3.42}$$

In particular, for the case $v = u = 0$ the frequencies of photons up to h are equal to:

$$\omega_f = 2m + (l' + n_f)hm, \quad \omega'_f = 2m + (l + n_f)hm, \tag{3.43}$$

that is, the frequency of the photon, both initial and final, is equal to the sum of the energies of particles produced at fixed Landau levels with zero longitudinal pulses.

Interference of resonances in two diagrams can take place when thecondition (3.30) and the first condition (3.35) are simultaneously satisfied, which leads to the expression

$$\varepsilon_g + \varepsilon_f = \varepsilon + \varepsilon', \tag{3.44}$$

which in ultraquantum approximation leads to the following conditions:

$$n_g + n_f = l + l', \quad vu = 1. \tag{3.45}$$

that is, the initial and final photons move along the field.

The CS process in ultraquantum approximation. First, we analyze spin-polarization effects in the process of photon scattering by an electron under resonant conditions (3.33) (resonance in the g diagram of Fig. 3.1). Differential cross-sections of the process with certain values of spins projections of the ini-

tial and final electrons $\sigma^{\mu\mu'}$ can be reduced to the form:

$$\frac{d\sigma_{\xi\xi'}^{--}}{du} = \frac{2\pi}{\omega^2} \frac{\frac{dW_{\xi}^{--}}{dv} \cdot \frac{dW_{\xi'}^{--}}{du}}{[(\omega - \omega_g)^2 + \Gamma^2/4]}, \quad \frac{d\sigma_{\xi\xi'}^{++}}{du} = \frac{2\pi}{\omega^2} \frac{\frac{dW_{\xi}^{++}}{dv} \cdot \frac{dW_{\xi'}^{++}}{du}}{[(\omega - \omega_g)^2 + \Gamma^2/4]}, \tag{3.46}$$

$$\frac{d\sigma_{\xi\xi'}^{+-}}{du} = \frac{2\pi}{\omega^2} \frac{\frac{dW_{\xi}^{++}}{dv} \cdot \frac{dW_{\xi'}^{+-}}{du}}{[(\omega - \omega_g)^2 + \Gamma^2/4]}, \quad \frac{d\sigma_{\xi\xi'}^{-+}}{du} = \frac{2\pi}{\omega^2} \frac{\frac{dW_{\xi}^{+-}}{dv} \cdot \frac{dW_{\xi'}^{++}}{du}}{[(\omega - \omega_g)^2 + \Gamma^2/4]}, \tag{3.47}$$

where differential probabilities dW_{ξ}^{++}/dv, dW_{ξ}^{--}/dv, dW_{ξ}^{+-}/dv can be written as (2.46) — (2.48), in which replacements are made

$$u \to v, l \to n_g, l' \to l. \tag{3.48}$$

Such probabilities can be interpreted as differential probabilities of radiation of the initial photon with polarization ξ (ie with Stokes parameters ξ_1, ξ_2, ξ_3) by the intermediate electron at the certain Landau level n_g and in certain spin state μ_g (the first sign in the probability W), with the transition of the electron to initial state at the Landau level l. Differential probabilities $dW_{\xi'}^{++}/du$, $dW_{\xi'}^{--}/du$, $dW_{\xi'}^{+-}/du$ in the cross-sections (3.46), and (3.47) are described by the same expressions (2.46) — (2.48), in which replacements are made

$$l \to n_g, \eta \to \eta', \tag{3.49}$$

that is, it is the probability of emission of the final photon with polarization ξ' by the intermediate electron, which is also at the Landau level n_g and in the certain spin state, with transition of the electron to the final state at the Landau level l'.

From the obtained cross-sections σ^{+-}, σ^{-+}, which correspond to spin-flip processes, it follows that the intermediate electron is in the inverse spin state ($\mu_n = +1$). This is due to the lack of probability W^{-+}, described by expression (2.49), which has a higher degree of small parameter h. All cross-sections are factorized, which means that in resonance the polarization of the final photon does not depend on the polarization of the initial one.

Differential cross-sections (3.46), (3.47), averaged over the polarization of the initial photon and summed over the polarization of the final photon (for this, all Stokes parameters must be zeroed in them and the result must be doubled), correspond to the process of scattering of an unpolarized photon by an electron and coincide with the results [125].

The analysis and the obtained results of the influence of electron spin states on the polarization of the final photon in processes with fixed values of particle

spins coincide with those in the process of photon emission by an electron. In the CS process without spin-flip (σ^{++}, σ^{--}), the polarization of radiation is determined by the Stokes parameters (2.57). In the spin-flip process to the ground spin state (σ^{+-}), the polarization of the final photon is determined by expressions (2.60), in which the sign of the linear polarization is changed in comparison with (2.57). In the spin-flip process to the inverse spin state (σ^{-+}), the polarization of the final photon is the same as in the process without spin-flip (2.57). A significant difference between the spin-flip of the CS process from the SR process is that the cross-sections (3.47) have the same degree h, that is, the probabilities of the spin-flip in the CS to the ground and inverse states are close in magnitude, while in the SR process, the flip to the inverse spin state is suppressed.

The degree of polarization of the spin-flip of the SR process by electrons, which are both in the ground ($\mu = -1$) and in the inverse ($\mu = +1$) spin states, has the form:

$$P_{\xi'} = \max \frac{\sigma^{+-}_{\xi,\xi'} + \sigma^{-+}_{\xi,\xi'} - (\sigma^{+-}_{\xi,-\xi'} + \sigma^{-+}_{\xi,-\xi'})}{\sigma^{+-}_{\xi,\xi'} + \sigma^{-+}_{\xi,\xi'} + \sigma^{+-}_{\xi,-\xi'} + \sigma^{-+}_{\xi,-\xi'}}, \tag{3.50}$$

whence the expressions for the Stokes parameters of the emitted photon follow:

$$\xi'_{1CS} = 0, \quad \xi'_{2CS} = \frac{2u}{1+u^2}, \quad \xi'_{3CS} = \frac{1-u^2}{1+u^2} \cdot \frac{l(n_g - l')^2 \Pi - l'(n_g - l)^2 \tilde{\Pi}}{l(n_g - l')^2 \Pi + l'(n_g - l)^2 \tilde{\Pi}}, \tag{3.51}$$

$$\Pi = 1 - \frac{1-v^2}{1+v^2}\xi_3 + \frac{2v}{1+v^2}\xi_2, \quad \tilde{\Pi} = 1 + \frac{1-v^2}{1+v^2}\xi_3 + \frac{2v}{1+v^2}\xi_2. \tag{3.52}$$

In such a process, the circular polarization of the final photon has the same form as in the process without spin-flip. The linear polarization of the final photon substantially depends both on the Landau levels of the electron and on the polar angle and polarization of the initial photon. In particular, the elastic channel (Thomson scattering $l = l'$) ξ'_{3CS} has the form:

$$\xi'_{3CS} = -\frac{1-u^2}{1+u^2} \cdot \frac{1-v^2}{1+v^2+2v\xi_2}\xi_3, \tag{3.53}$$

that is, the parameter ξ'_{3CS} is proportional to the degree of linear polarization of the initial photon and is opposite in sign. Fig. 3.2 shows the dependence of the degree of polarization on a) the angle of the final photon, and b) the angle of the initial photon. Wherein $l = 2$, $n_g = 4$, $\xi_2 = 0.3$, $\xi_3 = 0.5$; $v = 0.1$ in Fig. 3.2, *a*; $u = 0.1$ in Fig. 3.2, *b*. The three curves in Fig. 3.2 correspond to the cases: 1. $l' = 1$ is inverse Compton scattering $\omega < \omega'$, 2. $l' = 2$ is Thomson scattering $\omega = \omega'$, 3. $l' = 3$ is direct Compton scattering $\omega > \omega'$. From Fig. 3.2 it follows that the small-

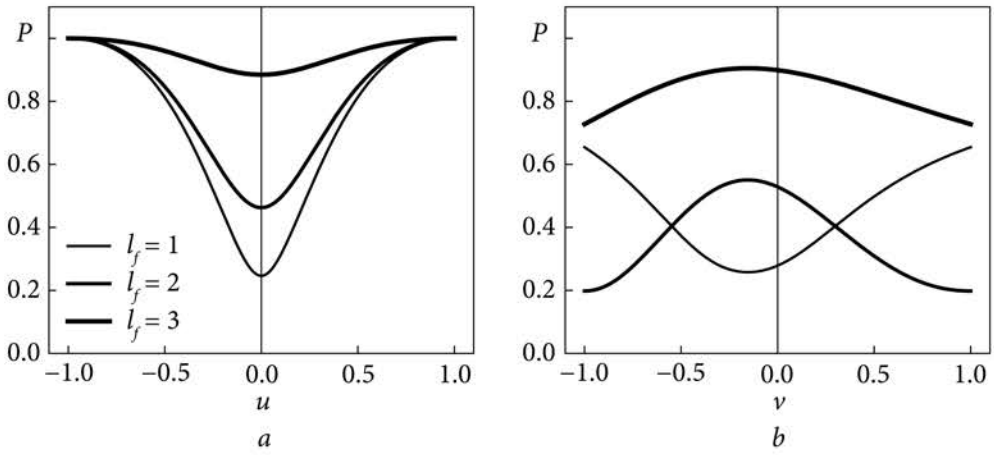

Fig. 3.2. The degree of polarization of the radiation in the spin-flip process of CS from the ground and inverse spin states as a function of *a* — the angle of the final photon, *b* — the angle of the initial photon; 1. $l' = 1$, 2. $l' = 2$, 3. $l' = 3$

est degree of polarization of the final photon corresponds to inverse Compton scattering in the direction perpendicular to the magnetic field.

Suppose that in the initial state the spin of the electron has a certain orientation, and the final states are summed over the spins. Let us analyze the influence of the spin-flip process on the degree of radiation polarization. The cross-sections of the CS process are proportional to the values:

$$\sigma^{-}_{\xi\xi'} \sim W^{--}_{\xi} \cdot W^{--}_{\xi'} + W^{+-}_{\xi} \cdot W^{++}_{\xi'}, \quad \sigma^{+}_{\xi\xi'} \sim W^{++}_{\xi} \cdot W^{++}_{\xi'} + W^{++}_{\xi} \cdot W^{+-}_{\xi'}, \qquad (3.54)$$

where σ^{-} corresponds to the process with the electron with spin initially oriented against the field, σ^{+} — corresponds to the process with the electron with spin along the field. The degree of polarization of the final photon in these cases is equal to:

$$P^{-}_{\xi'} = \max \frac{\sigma^{-}_{\xi,\xi'} - \sigma^{-}_{\xi,-\xi'}}{\sigma^{-}_{\xi,\xi'} + \sigma^{-}_{\xi,-\xi'}} = 1, \qquad (3.55)$$

$$P^{+}_{\xi'} = \max \frac{\sigma^{+}_{\xi,\xi'} - \sigma^{+}_{\xi,-\xi'}}{\sigma^{+}_{\xi,\xi'} + \sigma^{+}_{\xi,-\xi'}}, \; P^{+}_{\xi'}\big|_{l'\neq 0} = 1 - \frac{2h(n_g - l')^2(1-u^2)^2}{l'(1+u^2)^2}, \; P^{+}_{\xi'}\big|_{l'=0} = 1. \quad (3.56)$$

Thus, in the CS process, electrons with spins initially oriented against the field emit fully polarized photons with radiation polarization as in the JI process (2.64). Photons scattered by electrons, initially oriented along the field, are partially polarized. The linear polarization of the final photons is partially violated by $\sim h$ and depends on the Landau level of the final electron.

The polarization of the final photon in the process with electrons, unpolarized in both the initial and final states, is determined by analyzing the sum $\sigma^- + \sigma^+$ of expressions (3.54). In this case, the Stokes parameters of the final photon are

$$\xi'_{2CS} = \frac{2u}{1+u^2}, \quad \xi'_{3CS} = -\frac{1-u^2}{1+u^2}\left(1 - h\frac{(n_g - l')^2 l}{n^2 + ll'}\right). \tag{3.57}$$

The linear polarization of radiation in the CS process differs from the linear polarization of the SR process (2.64) by ~ h, which depends on the Landau levels of both the initial and final electrons. The polarization of the final photon does not depend on the polarization of the initial one.

Now let us consider the question of the orientation of the electron spins as a result of the CS process, or vice versa, the depolarization of the initially oriented spins, and the influence of the polarization of the initial photon on the spin states of the final electron. Let the spin of the initial electron be directed against the field (ground spin state), i.e, a beam of the initial electrons is completely polarized against the field P = –1. The degree of polarization of the electron beam due to the spin-flip process in CS differs from -1 and is determined by the expression:

$$P_{e^-}^- = \frac{d\sigma_{\xi\xi'}^{-+}/du - d\sigma_{\xi\xi'}^{--}/du}{d\sigma_{\xi\xi'}^{-+}/du + d\sigma_{\xi\xi'}^{--}/du}, \tag{3.58}$$

which, taking into account the explicit form of the cross-sections (3.46), (3.47), is equal to

$$P_{e^-}^- = \frac{-\Pi + hl'(n_g - l)^2 \tilde{\Pi}/2n_g^2}{\Pi + hl'(n_g - l)^2 \tilde{\Pi}/2n_g^2}, \tag{3.59}$$

where the values Π, $\tilde{\Pi}$ are determined by expressions (3.52). If $\Pi \neq 1$, then to the first-degree h:

$$P_{e^-}^- = -1 + hl'\frac{(n_g - l)^2 \tilde{\Pi}}{n_g^2 \Pi}. \tag{3.60}$$

In the case when the initial photon is directed perpendicular to the field ($\nu = 0$), the values Π, $\tilde{\Pi}$ are equal to:

$$\Pi = 1 - \xi_3, \quad \tilde{\Pi} = 1 + \xi_3. \tag{3.61}$$

The expression for the degree of polarization of the final electrons (3.60) is similar to the degree of polarization of an electron in the process of one-photon e^+e^- pair production (2.169). Except for a narrow cone $\vartheta < \vartheta_c$, where $\xi_3 = 1 - 2\vartheta$ (see Fig. 2.18), the degree of polarization is $P \approx -1$ and less than one by an amount of the order of h. The magnitude of non-polarization (depolarization)

of electrons is proportional to the Landau level number of the final electron. In a narrow cone $\vartheta < h$, the spins of the final electrons are oriented along the field.

If the initial photon is directed along the field ($\nu = 1$), the values Π, $\tilde{\Pi}$ have the form:

$$\Pi = \tilde{\Pi} = 1 + \xi_2, \tag{3.62}$$

that is, the polarization of the initial photon does not affect the orientation of the electron spins. Note that if the initial photon has a left-hand circular polarization, then $\Pi = \tilde{\Pi} = 0$. the CS process does not take place.

Now let the spin of the initial electron be directed along the field (inverse spin state), i.e $P = +1$. The degree of polarization of the electron beam due to the spin-flip process in CS is less than one and is equal to:

$$P_{e^-}^{+} = \frac{d\sigma_{\xi\xi'}^{++}/du - d\sigma_{\xi\xi'}^{+-}/du}{d\sigma_{\xi\xi'}^{++}/du + d\sigma_{\xi\xi'}^{+-}/du} = \frac{\Pi' - h(n_g - l')^2 \tilde{\Pi}'/2l'}{\Pi' + h(n_g - l')^2 \tilde{\Pi}'/2l'}, \tag{3.63}$$

$$\Pi' = 1 - \frac{1-u^2}{1+u^2}\xi'_3 + \frac{2u}{1+u^2}\xi'_2, \quad \tilde{\Pi}' = 1 + \frac{1-u^2}{1+u^2}\xi'_3 + \frac{2u}{1+u^2}\xi'_2. \tag{3.64}$$

If we do not fix the polarization of the final photon, that is, we put the value $\xi'_i = 0$, then $\Pi' = \tilde{\Pi}' = 1$. As a result, the degree of polarization of the final electron depends only on the Landau level numbers and up to h is equal to:

$$P_{e^-}^{+} = 1 - h\frac{(n_g - l')^2}{l'}. \tag{3.65}$$

The spins of the electrons in the initially unpolarized beam due to the self-polarization effect acquire a predominant direction. The effect of self-polarization was first discovered by A.A. Sokolov, and I.M. Ternov in the JI process [4], where the spins of electrons are oriented mainly in the ground spin state. This effect in the CS process leads to the orientation of the electron spins both along and against the field, which is also affected by the polarization of the initial photon. The degree of self-polarization of the electron is equal to:

$$P_{e^-} = \frac{d\sigma_{\xi\xi'}^{+-}/du - d\sigma_{\xi\xi'}^{-+}/du}{d\sigma_{\xi\xi'}^{+-}/du + d\sigma_{\xi\xi'}^{-+}/du} = \frac{\delta - 1}{\delta + 1}, \quad \delta = \frac{d\sigma_{\xi\xi'}^{+-}/du}{d\sigma_{\xi\xi'}^{-+}/du} = \frac{(n_g - l')^2 l \Pi\tilde{\Pi}'}{(n_g - l)^2 l' \tilde{\Pi}\Pi'}. \tag{3.66}$$

If the initial photon is unpolarized and the polarization of the final photon is not fixed, then the degree of self-polarization depends only on the Landau levels

$$\delta = \frac{(n_g - l')^2 l}{(n_g - l)^2 l'}. \tag{3.67}$$

In the «elastic» channel $l = l'$ (Thomson scattering) $\delta = 1$ and $P = 0$, i.e. self-polarization is absent. In direct Compton scattering $l < l'$, $\delta < 1$, $P < 0$, i.e. the spins of the electrons are mainly oriented against the field. In the inverse Compton scattering $l > l'$, $\delta > 1$, $P > 0$, i.e. the spins of the electrons are mainly oriented along the field.

Let $l = l'$ (Thomson scattering) and the initial photon is polarized, then the degree of polarization of the final electron is equal to:

$$P_{e^-} = -\frac{(1-v^2)\xi_3}{1+v^2+2v\xi_2}. \tag{3.68}$$

If the initial photon is directed perpendicular to the field $v = 0$, then $P^- = -\xi_3$. Thus, by rotating the beam of initial photons about its axis, that is, changing the linear polarization of photons from normal to abnormal polarization, it is possible to orient the spins of electrons from the direction against the field in the direction along the field. A significant difference between this effect in the CS process and a similar effect in the OPP process is that in the CS process the change in the degree of polarization of electrons is proportional to the change in the degree of polarization of photons. This makes the CS process more promising for obtaining electron beams with variable polarization.

Now we analyze the spin-polarization effects in the CS process under resonant conditions (3.39) (resonance in the *f* diagram of Fig. 3.1). Differential cross-sections of the process with certain values of the spin projections of the initial and final electrons $\sigma^{\mu\mu'}$ have a form similar to the expressions (3.46), (3.47):

$$\frac{d\sigma^{--}_{\xi\xi'}}{du} = \frac{2\pi}{\omega^2}\frac{\dfrac{dW^{--}_{\xi}}{dv}\cdot\dfrac{dW^{--}_{\xi'}}{du}}{[(\omega-\omega_f)^2+\Gamma^2/4]}, \quad \frac{d\sigma^{++}_{\xi\xi'}}{du} = \frac{2\pi}{\omega^2}\frac{\dfrac{dW^{++}_{\xi}}{dv}\cdot\dfrac{dW^{++}_{\xi'}}{du}}{[(\omega-\omega_f)^2+\Gamma^2/4]}, \tag{3.69}$$

$$\frac{d\sigma^{+-}_{\xi\xi'}}{du} = \frac{2\pi}{\omega^2}\frac{\dfrac{dW^{--}_{\xi}}{dv}\cdot\dfrac{dW^{+-}_{\xi'}}{du}}{[(\omega-\omega_f)^2+\Gamma^2/4]}, \quad \frac{d\sigma^{-+}_{\xi\xi'}}{du} = \frac{2\pi}{\omega^2}\frac{\dfrac{dW^{+-}_{\xi}}{dv}\cdot\dfrac{dW^{--}_{\xi'}}{du}}{[(\omega-\omega_f)^2+\Gamma^2/4]}, \tag{3.70}$$

where the differential probabilities dW^{++}_{ξ}/dv, dW^{--}_{ξ}/dv, dW^{+-}_{ξ}/dv are described by the expressions (2.46) — (2.48), in which substitutions are made:

$$u \to v,\ l \to l',\ l' \to n_f, \tag{3.71}$$

and to obtain differential probabilities $dW^{++}_{\xi'}/du$, $dW^{--}_{\xi'}/du$, $dW^{+-}_{\xi'}/du$ the following substitution is made in the expressions (2.46) — (2.48):

$$l' \to n_f,\ \eta \to \eta'. \tag{3.72}$$

Note that in spin-flip processes, the intermediate electron is in the ground spin state.

The analysis of spin-polarization effects is similar to the analysis performed for the CS process in resonance in the g diagram. The polarization of the final photon for the process without spin-flip and in the spin-flip process to the ground state is determined by formulas (2.57). In the spin-flip process in the inverse spin state, it is determined by the formula (2.60). The Stokes parameters of the final photons in the CS process, where electrons are located both in the ground ($\mu = 1$) and in the inverse ($\mu = +1$) spin states, with a flip of their spins, have the form:

$$\xi'_{1CS} = 0, \quad \xi'_{2CS} = \frac{2u}{1+u^2}, \quad \xi'_{3CS} = \frac{1-u^2}{1+u^2} \cdot \frac{l'(l-n_f)^2 \Pi - l(l'-n_f)^2 \tilde{\Pi}}{l'(l-n_f)^2 \Pi + l(l'-n_f)^2 \tilde{\Pi}}. \quad (3.73)$$

From a comparison of this expression with a similar one (3.51), it follows that the polarization of the final photons coincides in both channels (diagrams *g* and *f*) for elastic scattering $l = l'$.

In the case where the electrons have spins initially oriented against the field, the final photons are completely polarized, as in the CS process (2.64). If the spins of the electrons are initially oriented along the field, the degree of polarization of the final photons is equal to:

$$P_{\xi'}^{+} = 1 - \frac{2h(l-n_f)^2(1-u^2)^2}{n_f(1+u^2)^2}, \quad (3.74)$$

which is analogous to the expression (3.56).

The Stokes parameters describing the polarization of the radiation of final photons in the CS process with unpolarized electrons have a form similar to expressions (3.57):

$$\xi'_{1CS} = 0, \quad \xi'_{2CS} = \frac{2u}{1+u^2}, \quad \xi'_{3CS} = -\frac{1-u^2}{1+u^2}\left(1 - h\frac{(l-n_f)^2 n_f}{n_f^2 + ll'}\right). \quad (3.75)$$

We now turn to the question of the influence of polarization of the initial photon on the spin states of the final electron in the CS process at resonance in diagram f (see Fig. 3.1). The initially oriented spins against the field are depolarized due to the spin-flip process and the degree of polarization of the final electron is equal to:

$$P_{e^-}^{-} = \frac{d\sigma_{\xi\xi'}^{-+}/du - d\sigma_{\xi\xi'}^{--}/du}{d\sigma_{\xi\xi'}^{-+}/du + d\sigma_{\xi\xi'}^{--}/du} = -\frac{2l'\Pi - h(l'-n_f)^2\tilde{\Pi}}{2l'\Pi + h(l'-n_f)^2\tilde{\Pi}}. \quad (3.76)$$

If the initial photon moves perpendicular to the field ($\nu = 0$) and $l'\,\Pi \neq 0$, the degree of polarization has a simple form similar to (3.60)

$$P_{e^-}^{-} = -1 + h\frac{(l'-n_f)^2(1+\xi_3)}{l'(1-\xi_3)}. \tag{3.77}$$

If the electrons in the initial state have spins oriented along the field, then the degree of polarization of the final electrons is determined similarly to (3.63) and is equal to:

$$P_{e^-}^{+} = +1 - h\frac{l'(l-n_f)^2}{n_f^2}. \tag{3.78}$$

The degree of self-polarization of the electron as a result of CS is determined by the first expression in (3.66) and in the resonance in diagram f is equal to:

$$P_{e^-} = \frac{\delta-1}{\delta+1}, \quad \delta = \frac{l'(l-n_f)^2\Pi}{l(l'-n_f)^2\tilde{\Pi}}. \tag{3.79}$$

For an elastic channel ($l = l'$) the degree of self-polarization P_{e^-} is determined by expression (3.68). Thus, the two diagrams *f* and *g* make the same contribution to the self-polarization process in the elastic channel, which is the most probable. In direct ($l < l'$) Compton scattering the electrons are oriented against the field, in reverse ($l > l'$) Compton scattering they are oriented towards the field.

Let us consider the RFE process when the resonance conditions are realized in both diagrams (see Fig. 3.1). Since the cross-sections of the process in resonances in the diagrams *f* and *g* are proportional to the product of the probabilities of the SR process, that is, they are proportional, respectively, to the factors

$$(1-v^2)^{n_g-l-1}(1-u^2)^{n_g-l'-1},\ (1-v^2)^{l'-n_f-1}(1-u^2)^{l-n_f-1}, \tag{3.80}$$

then, taking into account conditions (3.45), for the cross-sections to be non-zero, it is necessary to zero the degrees in expressions (3.80). It means that interference of the resonances of the two diagrams takes place for the elastic channel ($l = l'$), if the electron in the process goes over to the neighboring Landau level, with the initial photon directed parallel to the magnetic field:

$$l' = l, \quad n_g = l+1, \quad n_f = l-1, \quad vu = 1. \tag{3.81}$$

The differential cross-section of the process without spin-flip in these conditions is equal to:

$$\frac{d\sigma_{\text{int}}^{\mu\mu}}{du} = \frac{\pi}{2}\alpha^2 h^2 \Pi\Pi' \left| \frac{l+1/2-\mu/2}{\omega-\omega_g+i\Gamma_g/2} + \frac{l-1/2-\mu/2}{\omega_f-\omega+i\Gamma_f/2} \right|^2, \tag{3.82}$$

where ω_g, and ω_f are the resonant frequencies of the initial photon under resonant conditions (3.33) and (3.39), respectively; Γ_g and Γ_f are resonance widths in diagrams g and f, respectively. Under condition (3.81) the frequencies ω_g and ω_f coincide and are equal to the cyclotron frequency accurate to h:

$$\omega_g = \omega_f \approx hm. \tag{3.83}$$

The widths of the resonances are defined as the total probabilities of the SR process at the corresponding Landau levels, averaged over the polarization of the initial particles and summed over the polarization of the final particles. In resonance in the diagram g, the width is equal to the sum of the probabilities of emission of the initial and final photons by the intermediate electron. In resonance in diagram f, the width is equal to the sum of the probabilities of emitting the final photon by the initial electron and emitting the initial photon by the final electron. As a result, the same width for both diagrams is equal to:

$$\Gamma_g = \Gamma_f = \frac{4}{3}\alpha h^2 m(2l+1). \tag{3.84}$$

Differential cross-sections of spin-flip processes in the ground and inverse spin states at the interference of the resonances coincide and have the form:

$$\frac{d\sigma_{\text{int}}^{+-}}{du} = \frac{d\sigma_{\text{int}}^{-+}}{du} = \frac{\pi}{4}\alpha^2 h^3 \Pi\Pi' \left| \frac{1}{\omega - \omega_g + i\Gamma_g/2} + \frac{1}{\omega_f - \omega + i\Gamma_f/2} \right|^2. \tag{3.85}$$

At the point of resonance, the differential cross-sections are equal to:

$$\frac{d\sigma_{\text{int}}^{--}}{du} = \frac{9\pi\Pi\Pi'}{8h^2m^2}, \quad \frac{d\sigma_{\text{int}}^{++}}{du} = \frac{9\pi\Pi\Pi'}{8h^2m^2}\left(\frac{2l-1}{2l+1}\right)^2, \tag{3.86}$$

$$\frac{d\sigma_{\text{int}}^{+-}}{du} = \frac{d\sigma_{\text{int}}^{-+}}{du} = \frac{9\pi\Pi\Pi'}{16hm^2}\frac{1}{(2l+1)^2}. \tag{3.87}$$

Due to the equality of the cross-sections of the spin-flip processes in the ground and inverse spin states, the effect of electron self-polarization is absent under the considered conditions.

All cross-sections are proportional to the factor $\Pi\Pi'$, which implies that in the interference of two resonances, the polarization of the initial photons does not affect the orientation of the electron spins, i.e., the spin-polarization effects are absent.

When the initial photon propagates along and against the field, the factors ΠΠ' are equal, respectively:

$$\Pi\Pi' = \begin{cases} (1+\xi_2)(1+\xi'_2), & e.\ \nu = u = +1 \\ (1-\xi_2)(1-\xi'_2), & e.\ \nu = u = -1 \end{cases}. \tag{3.88}$$

This means that if the initial photon is directed along the field, then the cross-section is maximum when this photon is right-handed and circularly polarized. The probability of the CS process with the initial photon of the left-handed circular polarization is zero. And vice versa, if the initial photon is directed against the field, then the cross-section is maximum if this photon has left-handed circular polarization and is equal to zero at the right-handed circular polarization of the photon. The final photon is circularly polarized, and the direction of polarization coincides with the initial one.

Electron polarizer. The ultraquantum approximation in the case of small magnetic fields, of the laboratory order, passes into the dipole approximation, and the Landau level numbers take large values of $l >> 1$. Therefore, the results obtained on the orientation of electron spins in the CS process in the ultraquantum approximation can be used to create an electron beam polarizer under laboratory conditions. The scheme of the polarizer is shown in Fig. 3.3.

This setting polarizes the electron beam, and the degree of polarization changes smoothly, in proportion to the change in the polarization of the electromagnetic wave (EMW) over the entire range. According to Fig. 3.3 unpolarized electron beam is introduced into a region with a uniform magnetic field almost perpendicular to the field. A beam of polarized electromagnetic radiation, which irradiates a section of the path of electrons, is also perpendicular to the magnetic field. The design must be able to change the polarization of the EMW beam (rotation relative to its axis by an angle of 90°).

In the dipole approximation, that is, the approximation: $l >> 1$, $hl << 1$, $n_g = l + 1$, $n_f = l - 1$, after integrating the differential cross-sections (3.46), (3.47) and (3.69), (3.70) over the emission angle of the final photon at the resonance point with the width (3.84), the cross-sections of the CS process have the form:

$$\sigma^{--} = \sigma^{++} = \sigma_0(1-\xi_3), \quad \sigma^{+-} = \frac{h}{2l}\sigma_0(1-\xi_3),$$

$$\sigma^{-+} = \frac{h}{2l}\sigma_0(1+\xi_3), \quad \sigma_0 = \frac{3\pi}{2\omega^2}. \tag{3.89}$$

Initial photon flux is determined by the power of the electromagnetic wave W_γ:

$$j = W_\gamma / \omega S, \tag{3.90}$$

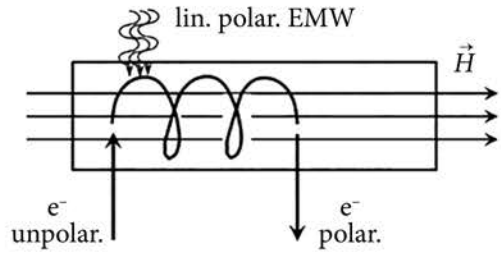

Fig. 3.3. Scheme of electron beam polarization under the action of an electromagnetic wave in a magnetic field

where S is the EMW beam cross-section. The polarization time of the electron beam is equal to the inverse rate of the CS process:

$$\tau = 1 / j\sigma^{+-} = \hbar\omega S / W_\gamma \sigma^{+-}. \tag{3.91}$$

The irradiation power W_γ and the cross-section S must be large enough so that the polarization time is less than the flight time of the irradiation region.

As an example, we will give the following values of physical quantities in the polarizer: irradiation wavelength $\lambda = 2.5\ mm$, which corresponds to the energy of the photon $\hbar\omega = 5 \cdot 10^{-4}\ eV$; to enter the cyclotron resonance, the magnetic field must be equal to $h = 10^{-9}$ ($H = 40\ kGs$); let the Landau level number be equal to $l = 2 \cdot 10^6$ (the condition is fulfilled $lh << 1$), then the kinetic energy of the electron is equal to $\varepsilon = 1\ keV$, the velocity of the electron is equal to $\upsilon = 0.06 \cdot c$; the power of the electromagnetic wave generator is equal to $W_\gamma = 10\ kW$; the cross-section of the beam is equal to $S = 0.04\ cm^2$. The cross-section of the spin-flip process of CS according to expression (3.89) is equal to $\sigma^{+-} = 3.8 \cdot 10^{-18}\ cm^2$. Then the polarization time of the electrons according to (3.91) $\tau = 10^{-10}$ c. During this time, the electron will fly along the direction of the magnetic field, the distance $\upsilon\tau = 1.8\ mm$, which is comparable to the transverse dimensions of the EMW beam. Note that the effect of Sokolov-Ternov self-polarization [6] is very small for given parameters. Time of self-polarization $3 / \alpha m h^3 \approx 5 \cdot 10^8\ c$.

3.3. Spin-polarization effects in the process of two photons emission by an electron

Probability of two-photon synchrotron radiation (Double Synchrotron Radiation, DSR). The process of two-photon radiation in a strong magnetic field in the LLL approximation was considered in [286]. Feynman diagrams of the DSR process are shown in Fig. 3.4. Since the CS and DSR processes are cross-channel, the amplitude of the DSR process can be obtained from expression (3.9) by substituting

$$k(\omega, \vec{k}) \to -k_1(\omega_1, \vec{k}_1), \quad k'(\omega', \vec{k}') \to k_2(\omega_2, \vec{k}_2). \tag{3.92}$$

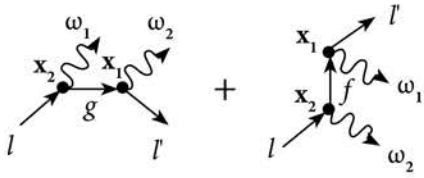

Fig. 3.4. Feynman diagrams of the DSR process

The resonant conditions of the DSR process in the LLL approximation after the replacement (3.92) coincide with the resonant conditions for the CS process. Thus, the resonance in the *g* diagram occurs if the frequency of the first photon ω_{1g} is equal to expression (3.33) with the opposite sign, and the frequency of the second photon ω_{2g} is determined by expression (3.34). The resonance in the *f* diagram occursif the frequency of the first photon ω_{1f} is equal to expression (3.39) with the opposite sign, and the frequency of the second photon ω_{2g} is equal to expression (3.38).

Equating the frequencies $\omega_{1g} = \omega_{2g}$ and similarly, $\omega_{1f} = \omega_{2f}$ leads to the conditions

$$n_g = n_f = l - 1 = l' + 1, \; \nu u = 1. \tag{3.93}$$

This is fulfilled under conditions (3.45) and means the interference of resonances in both diagrams, while the photon frequencies are equal to the cyclotron frequency. Outside the interference conditions (3.93), the resonances in the *g* and *f* diagrams occur separately. On the one hand, photons ω_1 and ω_2 do not differ experimentally. It is impossible to specify which of the two experimental frequencies is ω_1. On the other hand, the probability of the DSR process in the *f* diagram can be obtained from the probability in the *g* diagram by replacing $\omega_1 \longleftrightarrow \omega_2$. This leads to the fact that the resulting probability of the process in one of the resonances must be doubled.

The differential probability of the DSR process dW_D can be obtained from the differential cross-section of the CS process $d\sigma_{CS}$, if we equate the amplitudes and take into account the number of final states in these processes, as a result

$$\frac{dW_D}{\omega_1^2 d\omega_1 d\nu} = 2 \cdot \frac{d\sigma_{CS}}{4\pi^2}. \tag{3.94}$$

The sum of the two differential probabilities, which correspond to the individual resonances in the *g* and *f* diagrams, for the DSR process without electron spin-flip ($\mu' = \mu$) is equal to:

$$\frac{dW_D^{\mu\mu}}{d\omega_1 d\nu du} = \frac{1}{\pi} \frac{\dfrac{dW_{l\to n_g}^{\mu\mu}}{d\nu} \cdot \dfrac{dW_{n_g\to l'}^{\mu\mu}}{du}}{[(\omega_1 - \omega_{1g})^2 + \Gamma_g^2/4]} + \frac{1}{\pi} \frac{\dfrac{dW_{l\to n_f}^{\mu\mu}}{du} \cdot \dfrac{dW_{n_f\to l'}^{\mu\mu}}{d\nu}}{[(\omega_1 - \omega_{1f})^2 + \Gamma_f^2/4]}, \tag{3.95}$$

where the resonance widths Γ_g, and Γ_f are defined as the sum of the two total probabilities of the SR process of the initial and intermediate electrons, respectively, and have the form:

$$\Gamma_g = \frac{4}{3}\alpha h^2 m(l + n_g - 1), \quad \Gamma_f = \frac{4}{3}\alpha h^2 m(l + n_f - 1), \tag{3.96}$$

which become the same at $n_g = n_f$. The differential probabilities of SR of the first and second photons written in the numerator of expression (3.96) are defined by expressions (2.46), and (2.47) with the corresponding notation. The integration of expression (3.95) over the frequency of the first photon and the polar angles of both photons, as well as the averaging over the initial spin states and the summation over the final polarization of the particles, gives the full probability of the process under resonant conditions. The most probable case in the DSR process is the case of an electron transition to neighboring Landau levels $l \to l-1 \to l-2$, for which the total probability has the form:

$$W_D = \frac{2W_{l\to l-1}W_{l-1\to l-2}}{\Gamma} = \alpha h^2 m \frac{2(2l-1)(2l-3)}{6(l-1)}. \tag{3.97}$$

For the lowest possible level of the initial electron $l = 2$, the probability is equal to $W_D = \alpha h^2 m$. The process of emission of one photon by an electron from the level $l = 2$ is equal to $W_{opp} = 2\alpha h^2 m$, i.e. in resonance, the process of the second order becomes comparable to the process of the first order.

Polarization of radiation in the DSR process. Note that in the differential probability DSR (3.95) the dependence on polarization parameters of the photons is the same as in the SR process. Thus, in the process without an electron spin-flip, the emission of two photons has the same polarization as the emission of one photon.

Consider the spin-flip process of DSR in resonance in the g diagram, when an electron passes into the ground spin state. According to (3.47), the differential probability of such a process should be proportional to the value:

$$\frac{dW_D^{+-}}{d\omega_1 dv du} \propto \frac{dW_{l\to n_g}^{++}}{dv} \cdot \frac{dW_{n_g\to l'}^{+-}}{du}.$$

However, there is a second channel for the implementation of such a process, the probability of which has the same degree of h:

$$\frac{dW_D^{+-}}{d\omega_1 dv du} \propto \frac{dW_{l\to n_g}^{+-}}{dv} \cdot \frac{dW_{n_g\to l'}^{--}}{du}.$$

Therefore, you need to take into account both channels and add not the probabilities, but the amplitudes of the probabilities. As a result, taking into ac-

count (2.46) — (2.48) and (2.43), the differential probability finally looks like:

$$\frac{dW_D^{+-}}{d\omega_1 dv du} = \frac{1}{\pi}\frac{A_g D_g}{(\omega_1 - \omega_{1g})^2 + \Gamma_g^2/4}, \tag{3.98}$$

$$A_g = \frac{1}{8l'}\alpha^2 h^3 \omega_1 \omega_2 R_{1g}^2 R_{2g}^2, \tag{3.99}$$

$$D_g = \frac{(1+v^2)(1+u^2)}{4}\left[a_g^2 \tilde{\Pi}_1 \Pi_2 + b_g^2 \Pi_1 \tilde{\Pi}_2\right] + a_g b_g H, \tag{3.100}$$

$$H = 2vu + u(1+v^2)\xi_2 + v(1+u^2)\xi'_2 + (1-v^2)(1-u^2)\xi_1 \xi'_1 + (1+v^2)(1+u^2)\xi_2 \xi'_2, \tag{3.101}$$

$$a_g = \sqrt{l - n_g}, \quad b_g = \sqrt{n_g - l'}, \tag{3.102}$$

where the factors R_{1g}^2, R_{2g}^2 are determined by expression (2.50), while the first factor refers to the first photon and in (2.50) you need to replace $l' \to n_g$, and the second factor refers to the second photon and in (2.50) you need to replace $l \to n_g$; $\Pi_1, \tilde{\Pi}_1$ are polarization functions, which are determined by expression (3.52), and $\Pi_2, \tilde{\Pi}_2$ are determined by expression (3.64); ξ_i are the Stokes parameters, they refer to the first photon, and the primed parameters ξ'_i refer to the second photon.

Note that the found probability (3.98) depends on the Stokes parameters ξ_1, ξ'_1. For a single photon process, the SR process, the presence of the parameter ξ_1 in the probability would mean that the probabilities for the emitted photon to have a plane of polarization oriented at angles +45° and −45° relative to the plane $(\vec{k}, \vec{H})$are the same, which is impossible due to the symmetry of these situations. If two photons directed in different directions are measured at the same time, there is no symmetry concerning these angles, which explains the appearance of Stokes parameters ξ_1, ξ'_1.

Let's analyze the polarization of one of the photons (let for certainty ω_1). If you do not fix the second photon, you need to integrate the probability (3.98) on its polar angle u and sum up the polarizations. As a result, the factor D_g has the form (the most probable case $l' = n_g - 1$ is taken):

$$D_g = \frac{4}{3}(1+v^2)(l - n_g + 1)\left[1 + \frac{l - n_g - 1}{l - n_g + 1}\cdot\frac{1-v^2}{1+v^2}\xi_3 + \frac{2v}{1+v^2}\xi_2\right], \tag{3.103}$$

whence, according to (2.3), the form of the Stokes parameters of the emitted photon follows:

$$\xi_{1\,DSR} = 0, \ \xi_{2\,DSR} = \frac{2v}{1+v^2}, \ \xi_{3\,DSR} = \frac{l - n_g - 1}{l - n_g + 1}\cdot\frac{1-v^2}{1+v^2}. \tag{3.104}$$

From expressions (3.104) it follows that the Stokes parameter ξ_{2DSR}, responsible for the circular polarization of the emitted photon, has the same form as in the process of emission of one photon. The degree of linear polarization of the emitted photon in the spin-flip process depends on the value of $l - n_g$, i.e. on the multiplicity of the cyclotron frequency. For the most probable case of the transition of an electron to the adjacent Landau level $l - n_g = 1$, the final photon has no linear polarization, in particular, the photon emitted perpendicular to the field is completely unpolarized.

The spin-flip process of DSR in resonance in the f diagram, when the electron goes into the ground spin state, is described by the differential probability (3.98), where the index g must be replaced by f with the corresponding replacement of Landau level numbers, the factors a_f, b_f are equal to:

$$a_f = \sqrt{n_f - l'}, \quad b_f = \sqrt{l - n_f}\,. \tag{3.105}$$

If you fix the parameters of only one of the photons, the value of D_f has the form similar to (3.103):

$$D_f = \frac{4}{3}(1+v^2)(n_f - l'+1)\left[1 + \frac{n_f - l' - 1}{n_f - l' + 1}\cdot\frac{1-v^2}{1+v^2}\xi_3 + \frac{2v}{1+v^2}\xi_2\right], \tag{3.106}$$

whence it follows that the polarization of the final photon is the same as for the process in resonance in the diagram g. The linear polarization of the photon in the spin-flip process is absent during the transition of the electron to the neighboring Landau level.

The probability of the spin-flip process of DSR with the transition of the electron to the inverse spin state W_D^{-+} is extremely small.

3.4. Conclusions

The process of photon scattering by an electron (the CS process) is considered under resonant conditions in the LLL approximation in the nonrelativistic case, taking into account the polarization of all particles. In the CS process, the influence of the polarization of the initial photons on the degree of orientation of the electron spins and the polarization of the radiation was studied. In the process of resonant double synchrotron radiation (the DSR process) the influence of the spin-flip process on the polarization of radiation was studied. As a result, it was shown:

1. Resonant conditions in the CS process occur if the photon frequencies are multiples of the cyclotron frequency, the polarization of the photons does not affect these conditions. Interference of two resonances in two Feynman dia-

grams occurs if both photons have the same frequency and are directed along the magnetic field.

2. The differential cross-section of the CS process in resonance outside the interference region is factorized and represented as a Breit-Wigner formula. The electron in the intermediate state has a certain value of the spin direction.

3. For the processes with fixed values of the spins projections of the initial and final electrons, the polarization of the final photon does not depend on the polarization of the initial one. In the process, without spin-flip (with cross-section σ^{--}, σ^{++}) and spin-flip process in the inverse spin state (with cross-section σ^{-+}) the polarization of radiation is the same as in the SR process, and in the spin-flip process in the ground spin state, (with cross-section σ^{+-}) radiation has anomalous linear polarization.

4. For the spin-flip process in the ground and inverse states, the degree of linear polarization of the radiation is proportional to the degree of linear polarization of the initial photon and the opposite sign. The lowest degree of general polarization of the radiation corresponds to the inverse Compton scattering in the direction perpendicular to the field.

5. Electrons with spins initially oriented against the field (in the ground state) emit fully polarized photons with polarization as in the SR process. If the initial photons have a normal linear polarization $\xi_3 = -1$, then the violation of the degree of electron polarization is proportional to h. If the initial photons are abnormally linearly polarized $\xi_3 = +1$, the spins of the electrons are oriented along the field.

6. Electrons with spins oriented along the field (in the inverse state) emit partially polarized photons, the degree of depolarization of the radiation is proportional to h and depends on the Landau level of the final electron. The degree of depolarization of the electron beam is also proportional to h, depending on the values of the Landau levels of the electron in the initial, intermediate, and final states.

7. The degree of self-polarization of the initially unpolarized electron beam depends on the Landau level numbers of the initial and final electrons, for the Thomson process ($\omega = \omega'$) it is equal to the degree of linear polarization of the initial photon with the opposite sign: $P^- = -\xi_3$. The proportionality of a change in the degree of polarization of electrons to a change in the degree of polarization of photons is a significant difference between this effect in the CS process and a similar effect in the OPP process. In the region of resonance interference in both Feynman diagrams, the polarization of the initial photon does not affect the orientation of the electron spins, and the self-polarization effect is absent.

8. A scheme of an electron beam polarizer is proposed, where the directions of the electron spins change during the CS process in a magnetic field in proportion to the change in the polarization of the electromagnetic wave.

8. A linearly polarized electromagnetic wave of the millimeter range ($\lambda = 2.5\ mm$) with a power of 10 kW in a magnetic field of 40 kGs completely polarizes the electron beam in a time $\tau = 10^{-10}\ s$ in a $2mm$ area.

9. The probability of the DSR process without an electron spin-flip is factored in resonance conditions. Each of the two emitted photons has the same polarization as the photon in the SR process.

10. The probability of a spin-flip of the DSW process with the transition of an electron to the ground spin state is not factorized under resonance conditions. The degree of linear polarization of radiation in such a process depends on the parameter, which is a multiple of the cyclotron frequency. For the most probable case of the transition of an electron to the neighboring Landau level in the spin-flip process, the final photons do not have linear polarization, in particular, the radiation perpendicular to the field is completely unpolarized.

The main scientific results of this chapter are published in [125], [126], [284—286].

Chapter 4

e^+e^- PAIR PRODUCTION BY TWO POLARIZED PHOTONS IN RESONANCE CONDITIONS

4.1. Introduction

In this chapter, two-photon e^+e^- pair production (TPP) is studied, taking into account spin particles and photon polarizations in the resonance conditions, when an intermediate particle comes to the mass surface. The influence of polarization of the initial photons on the degree of polarization of the final particles is analyzed. The influence of the field of cyclotron photons on e^+e^- pair creation in the conditions of the magnetosphere of the X-ray pulsars is analyzed and the polarization of electrons and positrons in the generation of pair plasma radiation from the pulsar magnetosphere is taken into account.

4.2. Cross-section of the TPP process

The amplitude of two-photon e^+e^- pair production. The expression for the process amplitude corresponds to the Feynman diagrams shown in Fig. 4.1,
and has the form

$$A_{if} = ie^2 \int d^4\mathbf{x}_1 d^4\mathbf{x}_2 \bar{\Psi}^-(\mathbf{x}_1)[\gamma^i A_{1i}(\mathbf{x}_1) G_{H1}(\mathbf{x}_1,\mathbf{x}_2)\gamma^j A_{2j}(\mathbf{x}_2) + \\ + \gamma^j A_{2j}(\mathbf{x}_1) G_{H2}(\mathbf{x}_1,\mathbf{x}_2)\gamma^i A_{1i}(\mathbf{x}_2)]\Psi^+(\mathbf{x}_2), \qquad (4.1)$$

where $\bar{\Psi}^-(\mathbf{x}_1)$, $\Psi^+(\mathbf{x}_2)$ are the wave functions of electron and positron in the final states; $A_{1i}(\mathbf{x}), A_{2j}(\mathbf{x})$ are the wave functions of photons in the initial states; $G_{H1}(\mathbf{x}_1,\mathbf{x}_2)$, $G_{H2}(\mathbf{x}_1,\mathbf{x}_2)$ are the electron propagator in a magnetic field, according to the diagrams g and f (see Fig. 4.1). The TPP process is a cross-channel to the CS process, which differs from the latter by replacing the final positron with the initial electron and one of the initial photons with the final one.

The laws of conservation of energy and the longitudinal component of momentum are similar to (3.5)

$$\omega_1 + \omega_2 = \varepsilon^- + \varepsilon^+, \quad \omega_1 v + \omega_2 u = p^- + p^+, \tag{4.2}$$

where $v = \cos\theta_1$ and $u = \cos\theta_2$ are the cosines of polar angles of the first and second photons, respectively. If we denote the total energy and total longitudinal momentum of photons as

$$\omega = \omega_1 + \omega_2, \quad k = \omega_1 v + \omega_2 u, \tag{4.3}$$

then the conservation laws (4.2) coincide with the laws (2.120) of the OPP process.

The expressions for threshold values of the total frequency of photons, energies and longitudinal momentum of electron and positron have the form (2.123), where we need to replace

$$u \to U = \frac{\omega_1 v + \omega_2 u}{\omega_1 + \omega_2}. \tag{4.4}$$

The threshold values of energies and momentum of particles with fixed Landau levels can be reduced to the form:

$$\varepsilon^{\pm} = \frac{m^{\pm}\omega}{m^- + m^+}, \quad p^{\pm} = \frac{m^{\pm}k}{m^- + m^+}, \tag{4.5}$$

where $m^{\pm} = m(1 + 2l^{\pm}h)^{1/2}$, hence the threshold condition looks like

$$(\omega_1^{th} + \omega_2^{th})^2 - (k_1^{th} + k_2^{th})^2 = (m^+ + m^-)^2. \tag{4.6}$$

As can be seen, condition (4.6) does not hold, if both photons move parallel to the field in the same direction.

For the photon frequency above the threshold value $\omega > \omega_m$, taking into account (4.3) and (4.4), the expressions for energies and momentum of the electron have the form (2.130). Without loss of generality, we can eliminate the longitudinal momentum of photons by appropriately choosing the reference frame so that

$$k = k_1 + k_2 = 0. \tag{4.7}$$

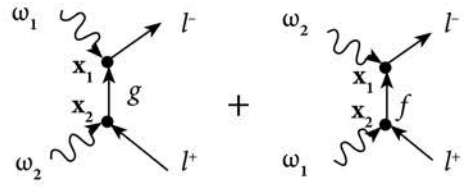

Fig. 4.1. Feynman diagrams of two-photon e^+e^- pair production

In this case, the energies and momentum of particles are determined by expressions (2.132), and (2.133). Also, for an analysis of the process in resonant conditions, it is convenient to choose the reference frame in which the hard photon ($\omega > m^+ + m^-$) is directed perpendicular to a magnetic field.

After integration of the expression (4.1), in the general case, the amplitude of the TPP process can be represented as

$$A_{if} = (2\pi)^4 \frac{M_{if}}{SV} \delta^3(k_1 + k_2 - p^- - p^+), \quad M_{if} = M_{if}^{(g)} + M_{if}^{(f)}, \tag{4.8}$$

where the two terms $M_{if}^{(g)}$ and $M_{if}^{(f)}$ correspond to g and f Feynman diagrams, respectively (see Fig. 4.1). The term $M_{if}^{(g)}$ has the form

$$M_{if}^{(g)} = \frac{-ie^2}{4\sqrt{\omega_1 \omega_2 \varepsilon^- \varepsilon^+ m^- m^+}} \sum_{n_g=0}^{\infty} \frac{e^{-i\Phi_g} Q^{(g)}}{g_0^2 - \varepsilon_g^2}, \quad Q^{(g)} = \sum_{a=1}^{10} Q_a. \tag{4.9}$$

The zero and longitudinal to the field components of the 4-momentum of g and f intermediate particle are equal to

$$g_0 = \varepsilon^- - \omega_1, \quad g = p^- - \omega_1 v, \quad f_0 = \varepsilon^- - \omega_2, \quad f = p^- - \omega_2 u. \tag{4.10}$$

The phase Φ_g is determined

$$\Phi_g = \frac{k_{1x}(2p_y^- - k_{1y})}{2hm^2} + \frac{k_{2x}(2g_y - k_{2y})}{2hm^2} + (l^- - n_g)\varphi_1 + (n_g - l^+)\varphi_2 + \frac{\pi}{2}(l^+ - l^-), \tag{4.11}$$

where k_{1x}, k_{1y}, k_{2x}, and k_{2y} are the transverse components of photon momentum, φ_1, φ_2 are azimuthal angles, l^+, l^-, n_g are the Landau levels of the final positron, final electron, intermediate particle. The phase Φ_f in the amplitude of the Feynman diagram f differs from expression (4.11) by a sign and after re-designation of parameters is equal to

$$\Phi_f = -\frac{k_{1x}(2p_y^+ - k_{1y})}{2hm^2} - \frac{k_{2x}(2p_y^- - k_{2y})}{2hm^2} + (n_f - l^+)\varphi_1 + (n_f - l^-)\varphi_2 + \frac{\pi}{2}(l^- - l^+). \tag{4.12}$$

The terms Q_a in the amplitude $M_{if}^{(g)}$ have the form

$$Q_1 = J_1^{++} J_2^{++}[-m\tilde{C} - g_0 C - gD], \quad Q_2 = J_1^{++} J_2^{-+}[-mD + g_0 \tilde{D} + gC],$$

$$Q_3 = J_1^{-+} J_2^{+-}[-mC - g_0 \tilde{C} + gD], \quad Q_4 = J_1^{-+} J_2^{--}[mD - g_0 \tilde{D} + gC],$$

$$Q_5 = J_1^{+-} J_2^{++}[mD + g_0 \tilde{D} - gC], \quad Q_6 = J_1^{+-} J_2^{-+}[-mC + g_0 \tilde{C} - gD],$$

$$Q_7 = J_1^{--} J_2^{+-}[-mD - g_0\tilde{D} - gC],\ \ Q_8 = J_1^{--} J_2^{--}[-mC + g_0\tilde{C} + gD],$$
$$Q_9 = [-J_1^{-+} J_2^{++} - J_1^{++} J_2^{+-} + J_1^{--} J_2^{-+} + J_1^{+-} J_2^{--}] D\sqrt{2n_g hm},$$
$$Q_{10} = [J_1^{-+} J_2^{-+} - J_1^{++} J_2^{--} + J_1^{--} J_2^{++} - J_1^{+-} J_2^{+-}] C\sqrt{2n_g hm}, \qquad (4.13)$$

where the functions J_1 have the form similar to (3.16)

$$J_1^{++} = J_1(n_g, l^-) M_m^- e_{1z},\quad J_1^{--} = J_1(n_g - 1, l^- - 1)\mu^- M_p^- e_{1z},$$
$$J_1^{+-} = J_1(n_g, l^- - 1)\mu^- M_p^- H_{1m},\quad J_1^{-+} = J_1(n_g - 1, l^-) M_m^- H_{1p}, \qquad (4.14)$$

and similarly the expressions for J_2 can be written

$$J_2^{++} = J_2(l^+, n_g) M_p^+ e_{2z},\quad J_2^{--} = J_2(l^+ - 1, n_g - 1)\mu^+ M_{\mathbf{m}}^+ e_{2z},$$
$$J_2^{+-} = J_2(l^+, n_g - 1) M_p^+ H_{2m},\quad J_2^{-+} = J_2(l^+ - 1, n_g)\mu^+ M_m^+ H_{2p}, \qquad (4.15)$$

where μ^+, μ^- are the signs of spin projections of positron and electron. The indices 1, and 2 correspond to the first and second photons. The amplitude $M_{if}^{(f)}$ is obtained by replacing indices $1 \longleftrightarrow 2$ in the expression $M_{if}^{(g)}$, which corresponds to a replacement of the initial photons. Taking into account (4.10), the energies of intermediate states ε_g, ε_f for the fixed Landau levels n_g, n_f are equal to

$$\varepsilon_g = \sqrt{m^2 + 2n_g hm^2 + (p^- - \omega_1 v)^2},\quad \varepsilon_f = \sqrt{m^2 + 2n_f hm^2 + (p^+ - \omega_1 v)^2}. \qquad (4.16)$$

Conditions of resonances in the TPP process. For the occurrence of resonance in the diagram g (see. Fig. 4.1), it is necessary to satisfy the conditions

$$g_0 = \varepsilon_g \ \text{ that is } \ \varepsilon^- - \omega_1 = \sqrt{m^2 + 2n_g hm^2 + (p^- - \omega_1 v)^2}. \qquad (4.17)$$

First, consider the case of propagation of the initial photons perpendicular to a magnetic field: $v = 0$, $u = 0$. In this case, based on expressions (2.130) and taking into account (4.3), the energy and momentum of the electron are equal to

$$\varepsilon^- = a^- / 2\omega,\quad p^- = b^- / 2\omega, \qquad (4.18)$$

where $a^- = \omega^2 + (m^-)^2 - (m^+)^2$, $b^- = \sqrt{(a^-)^2 - 4(m^-)^2\omega^2}$. Expanding in a series by the small parameter h of the expressions a^-, b^- and leaving only the zero term (essentially, assuming $h = 0$) we obtain

$$a^- = \omega^2,\quad b^- = \omega\sqrt{\omega^2 - 4m^2}, \qquad (4.19)$$

accordingly, the equation (4.17) can be rewritten as

$$\omega_2 - \omega_1 = \omega_2 + \omega_1. \tag{4.20}$$

This equality occurs if in the zero approximation on the field h the frequency is $\omega_1 = 0$, taking into account (4.19) we can show that $\omega_2 \geq 2$. Taking into account the first degree by h, we have $\omega_1 \propto h$. Thus, in the resonance (4.17), two initial photons play a fundamentally different role. The hard photon ω_2 creates an e^+e^- pair and the intermediate state is electronic. The soft photon ω_1 is absorbed by this intermediate electron, which can be represented by the Feynman diagram in Fig. 4.2. Note that for the realization of resonance in addition to conditions (4.17) the following equality may also occur: $g_0 = -\varepsilon_g$. This condition coincides with (4.17) when we mutually replace ω_1 by ω_2.

Choose the frame reference in which the hard photon ω_2 is directed perpendicular to the field, while the soft photon ω_1 is directed arbitrarily

$$u = 0, \ \forall v. \tag{4.21}$$

The frequency of the hard photon ω_2 is chosen arbitrarily, but it is sufficient for the creation of an e^+e^- pair at the levels l^+, l^-. The frequency of the soft photon is written in the form: $\omega_1 = \beta_1 h$. Expanding equation (4.17) in a series by the parameter h with the accuracy of the first degree, we have, the frequency of soft photon in resonance within a given accuracy:

$$\omega_{1g} = \frac{2(l^- - n_g)hm^2}{\omega_2 - vR}, \ R = \sqrt{\omega_2^2 - 4m^2}. \tag{4.22}$$

This frequency corresponds to the energies and momentum of the final particles, which have the form:

$$\varepsilon^- = \frac{\omega_2}{2} + \frac{hm^2}{\omega_2}[(l^- - n_g)\frac{\omega_2 + vR}{\omega_2 - vR} + l^- - l^+], \tag{4.23}$$

$$p^- = \frac{R}{2} + \frac{hm^2}{R}[(l^- - n_g)\frac{\omega_2 + vR}{\omega_2 - vR} - l^- - l^+], \tag{4.24}$$

$$\varepsilon^+ = \frac{\omega_2}{2} + \frac{hm^2}{\omega_2}(l^+ - n_g), \quad p^+ = -\frac{R}{2} + \frac{hm^2}{R}(l^+ + n_g). \tag{4.25}$$

Note that according to the expression (4.22), the frequency of the soft photon ω_1 is proportional to the difference between the Landau level numbers of the intermediate and finale electrons $l^- - n_g$ and it does not depend on the Landau level number of the position.

It should be emphasized that the condition (4.22) determines the resonance only with the accuracy of the first degree by h, and a detuning from resonance has the following order $\Delta \sim h^2 m$. The resonance width is determined mainly by the radiation width (total probability of synchrotron radiation), which is equal in magnitude $\Gamma \sim \alpha h^2 m$, where α is the fine-structure constant. A ratio of the TPP probability in the case (4.22) to the probability at the maximum point, as a result, is equal to $(\Gamma/\Delta)^2 \sim \alpha^2 \sim 10^{-4}$. On the other hand, the ratio of the TPP probability in the case (4.22) to the nonresonant probability has the order $(m/\Delta)^2 \sim h^{-4}$.

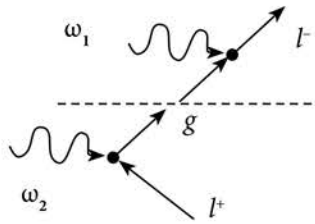

Fig. 4.2. Feynman diagram g of the resonant two-photon e^+e^- pair production

Expanding the equation (4.17) by parameter h up to the second degree, the frequency of soft photon has the form

$$\omega_{1g} = \frac{2(l^- - n_g)hm^2}{\omega_2 - vR} + \beta_g h^2 m, \tag{4.26}$$

where $\beta_g = \dfrac{4(l^- - n_g)m^3[2v\omega_2^2 l^+ + R\omega_2(l^- - l^+ - v^2(l^- + l^+)) + 4vm^2(n_g - l^+)]}{3v\omega_2^2(\omega_2^2 - 4m^2)(\omega_2 - vR) - 8m^2\omega_2 v^3(\omega_2^2 - 2m^2) + \omega_2^4(v^3\omega_2 - R)}$.

The special case of resonance is the case near a threshold. Then, the small parameter is $\sqrt{h}$. Let us represent the frequency of hard photon in the form

$$\omega_2 = 2m + (l^+ + n_g + \alpha_g)hm. \tag{4.27}$$

In this case, the hard photon creates a positron and an intermediate electron at levels l^+ and n_g, respectively. The small additive $\alpha_g hm$ is transmitted to the longitudinal momentum of particles. The resonance condition (4.17) determines the frequency of soft photon that with the accuracy of the second degree by h has the form

$$\omega_{1g} = (l^- - n_g)hm\left\{1 + v\sqrt{\alpha_g h} + \frac{h}{2}\left[v^2(l^- - n_g) - l^- - n_g + \alpha_g(2v^2 - 1)\right]\right\}. \tag{4.28}$$

The selected frequencies (4.27), and (4.28) set the values of energies and momentum of the final particles in the form

$$\varepsilon^- = m + (l^- + \frac{\alpha_g}{2})hm + (l^- - n_g)v\alpha_g^{1/2}h^{3/2}m +$$
$$+\frac{h^2 m}{4}\left[2v^2(l^- - n_g)^2 + l^{+2} + n_g^2 - 2l^{-2} + \alpha_g(l^+ + n_g - 2l^-) + 4\alpha_g v^2(l^- - n_g)\right], \tag{4.29}$$

$$p^- = \alpha_g^{1/2} h^{1/2} + (l^- - n_g) vhm +$$
$$+ \frac{h^{3/2} m}{8} \left[8\alpha_g^{1/2} v^2 (l^- - n_g) + 2\alpha_g^{1/2} (l^+ + n_g) + 2\alpha_g^{-1/2} (l^{+2} + n_g^2) + \alpha_g^{3/2} \right], \quad (4.30)$$

$$\varepsilon^+ = m + (l^+ + \frac{\alpha_g}{2}) hm - \frac{h^2 m}{2} \left[\alpha_g (l^+ - n_g) + l^{+2} - n_g^2 \right], \quad (4.31)$$

$$p^+ = -\alpha_g^{1/2} h^{1/2} m - \frac{h^{3/2} m}{8} \left[2\alpha_g^{1/2} (l^+ + n_g) + 2\alpha_g^{-1/2} (l^{+2} + n_g^2) + \alpha_g^{3/2} \right]. \quad (4.32)$$

In conclusion regarding the question of resonant conditions in the *g* diagram (see Fig. 4.2), we illustrate the exact dependences of the resonant frequency of soft photon ω_1 on its polar angle θ_1 ($v = \cos\theta_1$) and on the detuning from the threshold value of the frequency of hard photon $\delta\omega = \alpha_g hm$, which are shown in Fig. 4.3, *a* and Fig. 4.3, *b*, respectively. At the same time, we have $h = 0.1$ and the numbers of energy levels of particles are equal to $l^- = 1$, $l^+ = 0$. As can be seen from Fig. 4.3, the resonant frequency of soft photon near the process threshold ($\delta\omega = 0$) does not depend on the polar angle, and with increasing the detuning $\delta\omega$ it has a maximum value if the photon is directed along the field $\theta_1 = 0$.

Next, we analyze the conditions of resonance in the *f* diagram (see Fig. 4.1). In this case, the following condition is met

$$f_0 = \varepsilon_f \quad \text{that is} \quad \varepsilon^+ - \omega_1 = \sqrt{m^2 + 2n_f hm^2 + (p^+ - \omega_1 v)^2}. \quad (4.33)$$

f diagram of the resonant process is shown in Fig. 4.4.

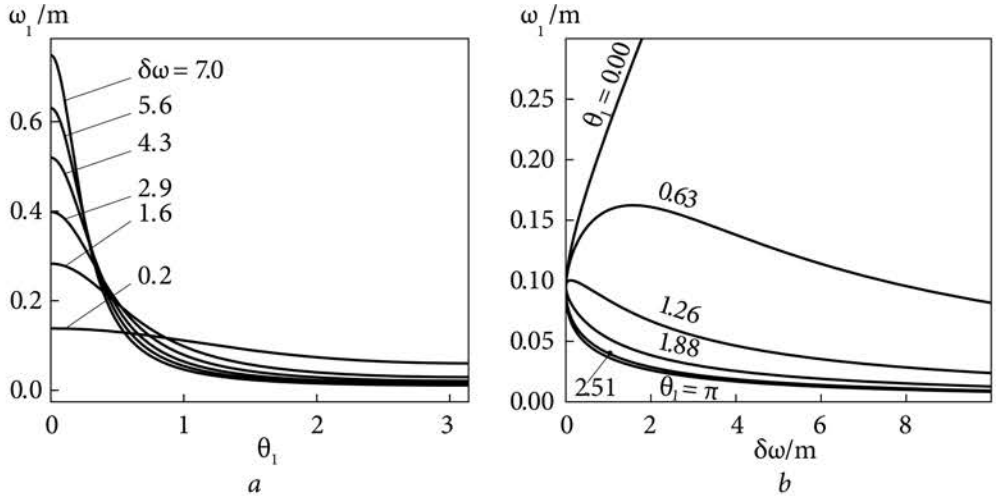

Fig. 4.3. Dependence of the frequency of soft photon ω_1 on its polar angle (*a.*) and the detuning of frequency from the threshold value $\delta\omega$ (*b*)

In resonance, a hard photon ω_2 creates an e^+e^- pair with an electron in the final state, at the same time the intermediate state is a positron and a soft photon ω_1 is absorbed by this intermediate positron.

Performing the expansion of equation (4.33) in a series by the parameter h with an accuracy of the first degree, we have the expression for the frequency of soft photon in resonance

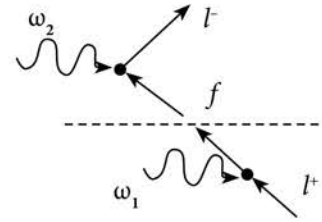

Fig. 4.4. Feynman diagram f of the resonant two-photon e^+e^- pair production

$$\omega_{1f} = \frac{2(l^+ - n_f)hm^2}{\omega_2 + vR}, \quad R = \sqrt{\omega_2^2 - 4m^2}, \qquad (4.34)$$

where ω_2 is the frequency of a hard photon that takes an arbitrary value greater than the threshold value. The energies and momentum of the final particles in resonance have the form

$$\varepsilon^- = \frac{\omega_2}{2} + \frac{hm^2}{\omega_2}(l^- - n_f), \quad p^- = \frac{R}{2} - \frac{hm^2}{R}(l^- + n_f), \qquad (4.35)$$

$$\varepsilon^+ = \frac{\omega_2}{2} + \frac{hm^2}{\omega_2}[(l^+ - n_f)\frac{\omega_2 - vR}{\omega_2 + vR} + l^+ - l^-], \qquad (4.36)$$

$$p^+ = -\frac{R}{2} + \frac{hm^2}{R}[(n_f - l^+)\frac{\omega_2 - vR}{\omega_2 + vR} + l^- + l^+]. \qquad (4.37)$$

As noted earlier, the resonance width $\Gamma \sim \alpha h^2 m$ requires that the resonance condition (4.17) be fulfilled to the second-order of the parameter h and the frequency of soft photon has a form similar to expression (4.26)

$$\omega_{1f} = \frac{2(l^+ - n_f)hm^2}{\omega_2 + vR} + \beta_f h^2 m, \qquad (4.38)$$

where $\beta_f = \dfrac{4(l^+ - n_f)m^3[2v\omega_2^2 l^- + R\omega_2(l^- - l^+ + v^2(l^- + l^+)) + 4vm^2(n_f - l^-)]}{3v\omega_2^2(\omega_2^2 - 4m^2)(\omega_2 + vR) - 8m^2\omega_2 v^3(\omega_2^2 - 2m^2) + \omega_2^4(v^3\omega_2 + R)}$.

Near the threshold, the frequency of the hard photon is represented as

$$\omega_2 = 2m + (l^- + n_f + \alpha_f)hm, \qquad (4.39)$$

which determines the frequency of soft photon in resonance taking into account (4.17) the form

$$\omega_{1f} = (l^+ - n_f)hm\left\{1 - v\sqrt{\alpha_f h} + \frac{h}{2}\left[v^2(l^+ - n_f) - l^+ - n_f + \alpha_f(2v^2 - 1)\right]\right\}. \qquad (4.40)$$

The frequencies (4.39), and (4.40) correspond to the following energies and momentum of the final particles

$$\varepsilon^- = m + (l^- + \frac{\alpha_f}{2})hm - \frac{h^2}{4}\left[\alpha_f(l^- - n_f) + l^{-2} - n_f^2\right], \tag{4.41}$$

$$p^- = \alpha_f^{1/2} h^{1/2} m + \frac{h^{3/2} m}{8}\left[2\alpha_f^{1/2}(l^- + n_f) + 2\alpha_f^{-1/2}(l^{-2} + n_f^2) + \alpha_f^{3/2}\right], \tag{4.42}$$

$$\varepsilon^+ = m + (l^+ + \frac{\alpha_f}{2})hm - (l^+ - n_f)v\alpha_f^{1/2} h^{3/2} m +$$

$$+\frac{h^2 m}{4}\left[2v^2(l^- - n_f)^2 + l^{-2} + n_f^2 - 2l^{+2} + \alpha_f(l^- + n_f - 2l^+) + 4\alpha_f v^2(l^+ - n_f)\right], \tag{4.43}$$

$$p^+ = \alpha_f^{1/2} h^{1/2} m + (l^+ - n_f)vhm -$$

$$-\frac{h^{3/2} m}{8}\left[8\alpha_f^{1/2} v^2(l^+ - n_f) + 2\alpha_f^{1/2}(l^- + n_f) + 2\alpha_f^{-1/2}(l^{-2} + n_f^2) - \alpha_f^{3/2}\right]. \tag{4.44}$$

Resonance interference in both diagrams g and f can occur if the conditions (4.17) and (4.33) are satisfied simultaneously. Far from the threshold, this corresponds to the equality of the frequencies of a soft photon (4.26), (4.38), which sets the resonant value of the frequency of the hard photon. Fig. 4.5 shows the dependence of the resonant frequencies (4.26), and (4.38) on ω_2. At the same time selected $h = 0.1$, $v = 0.6$, $l^+ = 5$, $l^- = 4$. Curves 1, 2, 3, 6 correspond to expression (4.26) with the Landau level numbers $n_g = 0, 1, 2, 3$, respectively, and curves 4, 5, 7, 8, 9 correspond to expression (4.38) with $n_f = 0, 1, 2, 3, 4$, respectively. In Fig. 4.5, the points A1—A8 of the intersection of the curves correspond to the interference of resonances.

In the special case $v = 0$, interference occurs when the Landau levels of final particles are the same and $n_g = n_f$:

$$v = 0,\ l^+ = l^-,\ n_g = n_f, \tag{4.45}$$

in this regard, frequency ω_2 takes any value above the threshold. For $l^+ \neq l^-$, the resonances g and f can only approach each other to the following value

$$\omega_{1f} - \omega_{1g} = 2\beta h^2 m,\quad \beta = \beta_f = -\beta_g = \frac{4(l^- - n_g)(l^- - l^+)m^3}{\omega_2^3}, \tag{4.46}$$

if the condition (4.47) is met

$$l^- - n_g = l^+ - n_f. \tag{4.47}$$

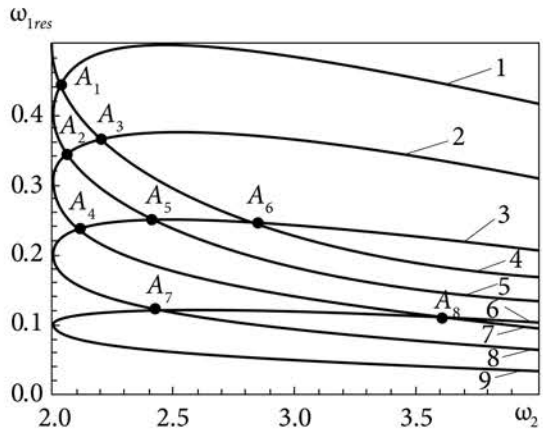

Fig. 4.5. Dependence of the soft photon frequency in the resonant conditions on the hard photon frequency

To realize the interference of resonances of two diagrams near the threshold, it is necessary to fulfill the equality of expressions (4.27) and (4.39), as well as (4.28) and (4.40). There is no interference of diagrams for $\nu \neq 0$. Under condition (4.47) and taking into account equality $\alpha_g = \alpha_f$, the difference in the resonant frequencies of a soft photon is

$$\omega_{1f} - \omega_{1g} = -2(l^- - n_g)\nu h^{3/2} m. \tag{4.48}$$

The interference still occurs if conditions (4.45) are met.

Cross section of the TPP process in the LLL approximation. A number of the final states in the TPP process is the same as in the OPP process (2.148), so in the general case, the process probability per unit time is determined similarly to expression (2.151). The delta function conforms to the law of conservation of energy and removes the last integral over the longitudinal component of momentum using rule (2.153), where p_i^- are two values of longitudinal momentum of an electron, which are determined by expression (2.130) taking into account (4.3) and (4.4). As noted earlier, the role of two initial photons is different: one (hard) photon creates a pair of particles, and the other (soft) is absorbed by one of these particles. In doing so, in the general case, the frequencies of photons are arbitrary, i.e. there is a scattering of the flux of soft photons in the process of e^+e^- pair production by the hard photons. The cross-section of the TPP process is defined as the ratio of the process probability per unit of time to the flux of the initial photons j ($j = (1 - \cos\chi)/V$, where χ is the angle between the directions of motion of the photons) and has the form

$$\sigma = \frac{W}{Tj} = \frac{2\pi h m^2}{(1-\cos\chi)} |M_{if}|^2 \sum_{i=1}^{2} \frac{\varepsilon_i^- \varepsilon_i^+}{\varepsilon_i^+ p_i^- - \varepsilon_i^- p_i^+}. \tag{4.49}$$

Taking into account (4.9), the expression (4.49) in the LLL approximation is written in the form

$$\sigma = \frac{e^4 \pi h}{8m^2 p^- \omega_1 \omega_2 (1-\cos\chi)} \left| \sum_{n_g} \frac{e^{-i\Phi_g} Q^{(g)}}{g_0^2 - \varepsilon_g^2} + \sum_{n_f} \frac{e^{-i\Phi_f} Q^{(f)}}{f_0^2 - \varepsilon_f^2} \right|^2. \tag{4.50}$$

In the resonance of the diagram g, in the sum of the Landau level numbers of the intermediate particle, there is only one term, as a result, we have

$$\sigma = \frac{e^4 \pi h \left| Q^{(g)} \right|^2}{32m^4 p^- \omega_1 \omega_2 (1-\cos\chi)\left[(g_0 - \varepsilon_g)^2 + \Gamma_g^2 / 4 \right]}. \tag{4.51}$$

The cross-section in the resonance of diagram f with amplitude $Q^{(f)}$ looks similar.

Amplitudes $Q^{(g)}$ in the LLL approximation with fixed values of projections of spins of the final particles can be written as

$$Q^{-+} = 4\sqrt{2} \sqrt{\frac{l^- h}{n_g}} m^3 G_1 G_2 H_{1m} e_{2z}, \tag{4.52}$$

$$Q^{--} = -4 \sqrt{\frac{l^- l^+}{n_g}} h m^3 G_1 G_2 H_{1m} H_{2p}, \tag{4.53}$$

$$Q^{++} = \frac{4hm^3}{\sqrt{n_g}} G_1 G_2 (A_g + B_g), \; A_g = (n_g - l^-) \tilde{H}_{1m} e_{2z}, \; B_g = n_g H_{1m} H_{2m}, \tag{4.54}$$

$$Q^{+-} = 2\sqrt{2}(l^- - n_g) \sqrt{\frac{l^+}{n_g}} h^{3/2} m^3 G_1 G_2 \tilde{H}_{1m} H_{2p}, \tag{4.55}$$

where H_m, H_p, and e_z are the quantities defined by expressions (2.43), and (3.18), respectively, while the indices 1, and 2 denote the first and second photons,

$$\tilde{H}_m = \cos\alpha - i\cos\theta \cdot \sin\alpha \cdot e^{i\beta}, \quad \tilde{H}_p = \cos\alpha + i\cos\theta \cdot \sin\alpha \cdot e^{i\beta}, \tag{4.56}$$

$$G_1 = \frac{e^{-\eta_1/2} \eta_1^{\frac{l^- - n_g - 1}{2}}}{(l^- - n_g - 1)!} \sqrt{\frac{(l^- - 1)!}{(n_g - 1)!}}, \quad G_2 = \frac{(-1)^{l^+} e^{-\eta_2/2} \eta_2^{\frac{l^+ + n_g}{2}}}{\sqrt{l^+ ! n_g !}}, \tag{4.57}$$

$$\eta_1 = \frac{\omega_1^2 (1-\nu^2)}{2hm^2}, \quad \eta_2 = \frac{\omega_2^2}{2hm^2}. \tag{4.58}$$

The signs + and – in the quantity Q denote the sign of the projections of spins of the final particles, with the first sign corresponding to the spin of the electron and the second to the spin of the positron.

The amplitude (4.52) contains the smallest degree of the parameter h and it corresponds to the most probable case of particles created in the main spin states when the electron spin is directed opposite to the field direction and the positron spin is co-directed to the field. Taking into account the amplitude (4.52), the cross-section (4.51) has the form

$$\sigma^{-+} = \frac{\pi e^4 h^2 m^3 (l^- / n_g) G_1^2 G_2^2 \, |H_{1m}|^2 \, e_{2z}^2}{p^- \omega_1 \omega_2 (1-\cos\chi)\left[(g_0 - \varepsilon_g)^2 + \Gamma_g / 4\right]}. \tag{4.59}$$

In the cross-section (4.59), the resonance width Γ_g is equal to the total probability of SR of the final electron, in which the main contribution is made by the transition of an electron to the neighboring Landau level

$$\Gamma_g = W_{\text{CB}}(l^- \to l^- - 1) = \frac{2}{3}(2l^- - 1)\alpha h^2 m, \tag{4.60}$$

also similarly to (3.52), and (3.61), we have

$$|H_{1m}|^2 = \frac{1}{2}(1+\nu^2)\Pi_1 = \frac{1}{2}(1+\nu^2)\left(1 - \frac{1-\nu^2}{1+\nu^2}\xi_3^{(1)} + \frac{2\nu}{1+\nu^2}\xi_2^{(1)}\right), \tag{4.61}$$

$$e_{2z}^2 = \frac{1}{2}(1+\xi_3^{(2)}). \tag{4.62}$$

The cross-section (4.59) is factorized, which means independence of the process of e^+e^- pair creation by hard photon and absorption of a soft photon by the electron in the resonant conditions. Taking into account the expressions for probabilities of SR $dW_{SR\,e^-}^{--} / dv$ (2.46) and the OPP process W_{OPP}^{-+} (2.156), the expression (4.59) can be reduced to the Breit-Wigner form

$$\sigma^{-+} = \frac{2\pi}{\omega_1^2 (1-\cos\chi)} \frac{\dfrac{dW_{SR\,e^-}^{--}}{dv} \cdot W_{OPP}^{-+}}{(\omega_1 - \omega_{1g})^2 + \Gamma_g^2 / 4}. \tag{4.63}$$

In the case of pair production at the lowest possible Landau levels ($l^+ = 0$, $l^- = 1$) in the magnetic field $h = 0.1$ by unpolarized photons directed towards each other perpendicular to the field and with frequencies of hard and soft photons

equal to $\omega_2 = 2m + 1{,}25hm$, $\omega_1 = hm$, respectively, an estimation of the cross-section of the TPP process gives

$$\sigma_{10}^{-+} = \frac{\pi e^{-2/h}}{h^3 p^- m} = \frac{2\pi e^{-2/h}}{h^4 m^2} \approx 2 \cdot 10^{-25} cm^2. \tag{4.64}$$

For the TPP process, in which the spins of the final particles are directed opposite to the field, the resonant cross-section σ^{--} has the form

$$\sigma^{--} = \frac{\pi e^4 h^3 m^3 (l^- l^+ / n_g) G_1^2 G_2^2 \, |H_{1m}|^2 |H_{2p}|^2}{2p^- \omega_1 \omega_2 (1 - \cos\chi)\left[(\omega_1 - \omega_{1g})^2 + \Gamma_g / 4\right]}, \tag{4.65}$$

where

$$|H_{2p}|^2 = \frac{1}{2}(1+u^2)\Pi_2 = \frac{1}{2}(1 - \xi_3^{(2)}). \tag{4.66}$$

Similar to expression (4.63) and taking into account the expressions for the probabilities of SR dW_{SR}^{--}/dv (2.46) and OPP W_{OPP}^{--} (2.157), the resonant cross section can be reduced to the Breit-Wigner form

$$\sigma^{--} = \frac{2\pi}{\omega_1^2 (1 - \cos\chi)} \frac{\dfrac{dW_{SR\,e^-}^{--}}{dv} \cdot W_{OPP}^{--}}{(\omega_1 - \omega_{1g})^2 + \Gamma_g^2 / 4}. \tag{4.67}$$

The found cross-section σ^{--} is an order of magnitude h smaller than the cross-section σ^{-+}.

For the TPP process, in which the final particles are in the inverse spin states (the spin of an electron is directed opposite to the field, and the spin of the positron is so-directed to the field), the resonant cross-section σ^{+-} has the form

$$\sigma^{+-} = \frac{\pi e^4 h^4 m^3 (l^- - n_g)^2 (l^+ / n_g) G_1^2 G_2^2 \, |\tilde{H}_{1m}|^2 |H_{2p}|^2}{4p^- \omega_1 \omega_2 (1 - \cos\chi)\left[(\omega_1 - \omega_{1g})^2 + \Gamma_g / 4\right]}, \tag{4.68}$$

where

$$|\tilde{H}_{1m}|^2 = \frac{1}{2}(1+\nu^2)\tilde{\Pi}_1 = \frac{1}{2}(1+\nu^2)\left(1 + \frac{1-\nu^2}{1+\nu^2}\xi_3^{(1)} + \frac{2\nu}{1+\nu^2}\xi_2^{(1)}\right), \tag{4.69}$$

or in the Breit-Wigner form

$$\sigma^{+-} = \frac{2\pi}{\omega_1^2 (1 - \cos\chi)} \frac{\dfrac{dW_{SR\,e^-}^{+-}}{dv} \cdot W_{OPP}^{--}}{(\omega_1 - \omega_{1g})^2 + \Gamma_g^2 / 4}. \tag{4.70}$$

The cross sections (4.63), (4.67), and (4.70) can be written in a single way

$$\sigma^{\mu^-\mu^+} = \frac{2\pi}{\omega_1^2(1-\cos\chi)} \frac{\dfrac{dW^{\mu^-\mu_g}_{SR\,e^-}}{d\nu} \cdot W^{\mu_g\mu^+}_{OPP}}{(\omega_1-\omega_{1g})^2+\Gamma_g^2/4}, \tag{4.71}$$

where $\mu_g = -1$ is the spin of the intermediate electron directed opposite to the field.

Finally, for the TPP process, in which the spins of the final particles are co-directed to the field, the resonant cross-section σ^{++} has the form

$$\sigma^{++} = \frac{\pi e^4 h^3 m^3 (1/n_g) G_1^2 G_2^2 \,|\, A_g + B_g \,|^2}{2p^-\omega_1\omega_2(1-\cos\chi)\left[(\omega_1-\omega_{1g})^2+\Gamma_g/4\right]}. \tag{4.72}$$

The found expression is not factorized, because the components A_g and B_g have the same degree of the parameter h. If only the term A_g is left in the expression (4.72), then the cross-section is factorized and in the Breit-Wigner form looks like

$$\sigma_A^{++} = \frac{2\pi}{\omega_1^2(1-\cos\chi)} \frac{\dfrac{dW^{+-}_{SR\,e^-}}{d\nu} \cdot W^{-+}_{OPP}}{(\omega_1-\omega_{1g})^2+\Gamma_g^2/4}. \tag{4.73}$$

Similarly, if in the expression (4.72) the term B_g is left, then the cross-section is also factorized

$$\sigma_B^{++} = \frac{2\pi}{\omega_1^2(1-\cos\chi)} \frac{\dfrac{dW^{++}_{SR\,e^-}}{d\nu} \cdot W^{++}_{OPP}}{(\omega_1-\omega_{1g})^2+\Gamma_g^2/4}. \tag{4.74}$$

Thus, the intermediate electron in this process of particle production with spins in the direction of the field is in a mixed spin state. Two process channels with cross-section σ^{++} have the same order of magnitude. In channel A, a hard photon creates an e^+e^- pair in the most favorable spin states $\mu^+ = +1$, $\mu_g = -1$, and then the intermediate electron absorbs a soft photon with a change of spin to the opposite value, which adds a degree of the parameter h compared to the absorption process without changing a spin. As a result, the spin of the final electron is co-directed to the field $\mu_g = -1 \rightarrow \mu^- = +1$. In channel B, a hard photon immediately creates an e^+e^- pair with spins in the direction of the field $\mu^+ = +1$, $\mu_g = +1$. Herewith, the probability contains an additional degree of the parameter h in comparison with the previous case, and then the intermediate electron absorbs a soft photon without changing the spin $\mu_g = +1 \rightarrow \mu^- = +1$.

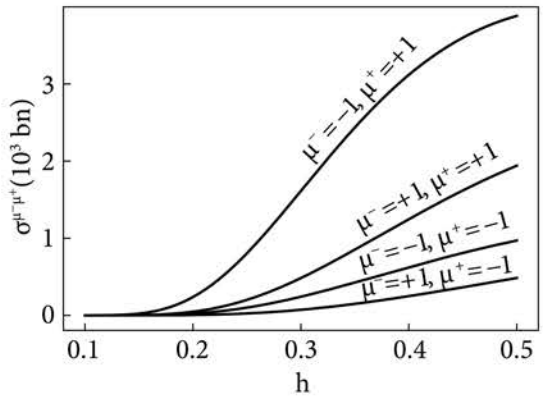

Fig. 4.6. Dependence of the cross-section of pair production by unpolarized photons on the field strength h in $l^- = 2$, $l^+ = 1$, $\omega_1 = \delta\omega = hm$

The cross-section (4.72) can be reduced to the form

$$\sigma^{++} = \sigma_A^{++} + \sigma_B^{++} + \sigma_{\text{int}\,AB}^{++}, \tag{4.75}$$

$$\sigma_{\text{int}\,AB}^{++} = \frac{\pi e^4 h^3 m^3 (l^- - n_g) G_1^2 G_2^2 \Xi_g}{2p^- \omega_1 \omega_2 (1-\cos\chi)\left[(\omega_1 - \omega_{1g})^2 + \Gamma_g / 4\right]}, \tag{4.76}$$

$$\Xi_g = \nu \xi_2^{(2)} - \frac{1}{2}(1-\nu^2)\xi_1^{(1)}\xi_1^{(2)} + \frac{1}{2}(1+\nu^2)\xi_2^{(1)}\xi_2^{(2)}. \tag{4.77}$$

In the case of the unpolarized initial photons, we have $\Xi = 0$ and thus the interference term (4.76) is absent.

Fig. 4.6 shows the dependence of the resonant cross-section of two-photon e^+e^- pair production on a magnetic field for different projections of particle spins. As the magnetic field increases, the ratio of a cross-section of the main process σ^{-+} to the rest decreases.

We proceed to find the cross-section of the TPP process in the resonant conditions in diagram *f*. The cross-section is defined by an expression similar to (4.51)

$$\sigma = \frac{e^4 \pi h \left|Q^{(f)}\right|^2}{32 m^4 p^- \omega_1 \omega_2 (1-\cos\chi)\left[(f_0 - \varepsilon_f)^2 + \Gamma_f / 4\right]}, \tag{4.78}$$

where the resonance width (the probability of the SR process of final positron) is given by the Landau level of positron

$$\Gamma_f = W_{SR}(l^+ \to l^+ - 1) = \frac{2}{3}(2l^+ - 1)\alpha h^2 m. \tag{4.79}$$

The amplitudes $Q^{(f)}$ in the LLL approximation with fixed values of the projections of spins of the final particles $Q^{\mu^-\mu^+}$ have the form

$$Q^{-+} = -4\sqrt{2}\sqrt{\frac{l^+h}{n_f}}m^3F_1F_2H_{1p}e_{2z}, \tag{4.80}$$

$$Q^{++} = -4\sqrt{\frac{l^-l^+}{n_f}}hm^3F_1F_2H_{1p}H_{2m}, \tag{4.81}$$

$$Q^{--} = \frac{4hm^3}{\sqrt{n_f}}F_1F_2(A_f + B_f),\ A_f = (n_f - l^+)\tilde{H}_{1p}e_{2z},\ B_f = n_fH_{1p}H_{2p}, \tag{4.82}$$

$$Q^{+-} = -2\sqrt{2}(l^+ - n_f)\sqrt{\frac{l^-}{n_f}}h^{3/2}m^3F_1F_2\tilde{H}_{1p}H_{2m}, \tag{4.83}$$

where

$$F_1 = \frac{e^{-\eta_1/2}\eta_1^{\frac{l^+-n_f-1}{2}}}{(l^+-n_f-1)!}\sqrt{\frac{(l^+-1)!}{(n_f-1)!}},\quad F_2 = \frac{(-1)^{n_f}e^{-\eta_2/2}\eta_2^{\frac{l^-+n_f}{2}}}{\sqrt{l^-!n_f!}}, \tag{4.84}$$

For the case of fixed spins of the final particles and taking into account the amplitudes (4.80), (4.81), (4.83), the cross section (4.78) can be reduced to the form similar to the expressions (4.63), (4.67), (4.70), respectively

$$\sigma^{-+} = \frac{2\pi}{\omega_1^2(1-\cos\chi)}\frac{\frac{dW^{++}_{SR\,e^+}}{dv}\cdot W^{-+}_{OPP}}{(\omega_1-\omega_{1f})^2+\Gamma_f^2/4}, \tag{4.85}$$

$$\sigma^{++} = \frac{2\pi}{\omega_1^2(1-\cos\chi)}\frac{\frac{dW^{++}_{SR\,e^+}}{dv}\cdot W^{++}_{OPP}}{(\omega_1-\omega_{1f})^2+\Gamma_f^2/4}, \tag{4.86}$$

$$\sigma^{+-} = \frac{2\pi}{\omega_1^2(1-\cos\chi)}\frac{\frac{dW^{-+}_{SR\,e^+}}{dv}\cdot W^{++}_{OPP}}{(\omega_1-\omega_{1f})^2+\Gamma_f^2/4}. \tag{4.87}$$

The cross-sections (4.85) — (4.87) are factorized, the spin states of the intermediate positron are pure, and the spin is co-directed to the field. These cross-sections are combined in one expression, which can be obtained from expression (4.71) if we introduce the replacements $W_{SR\,e^-}^{\mu^-\mu_g} \to W_{SR\,e^+}^{\mu^+\mu_f}$ and $W_{OPP}^{\mu_g\mu^+} \to W_{OPP}^{\mu_f\mu^-}$, with $\mu_f = +1$. Finally, we will write the cross-section of the TPP process with spins directed opposite to the direction of the field σ^{--} in resonance. This cross-section is not factorized because the intermediate positron is in the mixed spin state, similar to the cross-section (4.75) it can be represented as

$$\sigma^{--} = \sigma_A^{--} + \sigma_B^{--} + \sigma_{\text{int}\,AB}^{--}, \tag{4.88}$$

$$\sigma_A^{--} = \frac{2\pi}{\omega_1^2(1-\cos\chi)} \frac{\dfrac{dW_{SR\,e^+}^{-+}}{dv} \cdot W_{OPP}^{-+}}{(\omega_1 - \omega_{1f})^2 + \Gamma_f^2/4},$$

$$\sigma_B^{--} = \frac{2\pi}{\omega_1^2(1-\cos\chi)} \frac{\dfrac{dW_{SR\,e^+}^{--}}{dv} \cdot W_{OPP}^{--}}{(\omega_1 - \omega_{1f})^2 + \Gamma_f^2/4}, \tag{4.89}$$

$$\sigma_{\text{int}\,AB}^{--} = \frac{\pi e^4 h^3 m^3 (l^+ - n_f) F_1^2 F_2^2 \Xi_f}{2p^-\omega_1\omega_2(1-\cos\chi)\left[(\omega_1 - \omega_{1f})^2 + \Gamma_f/4\right]}, \tag{4.90}$$

$$\Xi_f = -v\xi_2^{(2)} - \frac{1}{2}(1-v^2)\xi_1^{(1)}\xi_1^{(2)} + \frac{1}{2}(1+v^2)\xi_2^{(1)}\xi_2^{(2)}. \tag{4.91}$$

The expression (4.91) differs from the similar one (4.77) only by the sign of the first term.

4.3. Spin-polarization effects in the TPP process

In this section we analyze the spin-polarization effects in the TPP process in the resonant conditions, using obtained expressions for the cross-sections (4.63), (4.67), (4.70), (4.75), (4.85) — (4.88). The degree of polarization of the final electrons is determined by the expression

$$P_{e^-} = \frac{\sigma^{++} + \sigma^{+-} - \sigma^{-+} - \sigma^{--}}{\sigma^{++} + \sigma^{+-} + \sigma^{-+} + \sigma^{--}}. \tag{4.92}$$

In the resonance conditions of the diagram g and taking into account (4.63), (4.67), (4.70), and (4.75), the degree of polarization can be reduced to the form

$$P_{e^-} = \frac{-2l^-\Pi_1\tilde{\Pi}_2 - l^-l^+h\Pi_1\Pi_2 + hK_g}{2l^-\Pi_1\tilde{\Pi}_2 + l^-l^+h\Pi_1\Pi_2 + hK_g}, \tag{4.93}$$

$$K_g = (l^- - n_g)^2\tilde{\Pi}_1\tilde{\Pi}_2 + n_g^2\Pi_1\Pi_2 + \frac{4(l^- - n_g)n_g}{1+v^2}\Xi_g. \tag{4.94}$$

For comparison, we write the degree of polarization in the OPP process $P_{\mathrm{OPP}e^-}$ with the final particles in the same states (2.167)

$$P_{OPPe^-} = -\frac{2\tilde{\Pi}_2 + (l^+ - l^-)h\Pi_2}{2\tilde{\Pi}_2 + (l^+ + l^-)h\Pi_2}. \tag{4.95}$$

Let us consider a few individual cases. If a hard photon has abnormal linear polarization $\xi_3^{(2)} = +1$, in this case we have

$$\Pi_2 = 0,\ \tilde{\Pi}_2 = 2,\ \xi_1^{(2)} = 0,\ \xi_2^{(2)} = 0,\ \Xi_g = 0,$$

then the degree of polarization of the final electrons in the TPP process is equal to

$$P_{e^-} = -\frac{2l^-\Pi_1 - h(l^- - n_g)\tilde{\Pi}_1}{2l^-\Pi_1 + h(l^- - n_g)\tilde{\Pi}_1}. \tag{4.96}$$

The degree of polarization of electrons in the OPP process in such conditions is equal to $P_{OPPe^-} = -1$, in other words, the spin of all electrons is directed opposite to the field. From the expression (4.96) it follows that for $\Pi_1 \neq 0$ the degree of polarization P_{e^-} close to the value –1 and only in the narrow interval $\Pi_1 < h$, the degree P_{e^-} significantly depends both on the polarization of a soft photon, its angle of incidence, and the Landau level of the final electron. If the polarization of the soft photon is such that $\tilde{\Pi}_1 = 0$, then the degree of polarization of electrons is equal to $P_{e^-} = -1$, as in the OPP process. For this purpose it is necessary, according to the expression (4.61), that Stokes parameters of polarization of soft photon are equal to

$$\xi_1^{(1)} = 0,\quad \xi_2^{(1)} = -\frac{2v}{1+v^2},\quad \xi_3^{(1)} = -\frac{1-v^2}{1+v^2}. \tag{4.97}$$

In particular, for the case of a soft photon perpendicular to the field $\xi_3^{(1)} = -1$, i.e. its polarization must be completely normal. If we choose the opposite case

$\Pi_1 = 0$, then $P_{e^-} = +1$, in other words, all electrons are in the inverse spin states. In this case, it is necessary to change the sign of linear polarization $\xi_3^{(1)}$

$$\xi_1^{(1)} = 0, \quad \xi_2^{(1)} = -\frac{2\nu}{1+\nu^2}, \quad \xi_3^{(1)} = +\frac{1-\nu^2}{1+\nu^2}. \tag{4.98}$$

Thus, under changing the linear polarization of a soft photon, which is perpendicular to the field, in the entire range from $\xi_3^{(1)} = -1$ to $\xi_3^{(1)} = +1$, the orientation of electron spins can be changed from polarized in the ground spin state to fully polarized in the inverse state.

Now let a hard photon have the normal linear polarization $\xi_3^{(2)} = -1$, in this case we have

$$\Pi_2 = 2, \ \tilde{\Pi}_2 = 0, \ \xi_1^{(2)} = 0, \ \xi_2^{(2)} = 0, \ \Xi_g = 0$$

and the degree of polarization of the final electrons is equal to

$$P_{e^-} = \frac{n_g^2 - l^- l^+}{n_g^2 + l^- l^+}. \tag{4.99}$$

For the OPP process according to the expression (2.170), a similar quantity has the form:

$$P_{OPPe^-} = \frac{l^- - l^+}{l^- + l^+}. \tag{4.100}$$

In the case of the particles production at the same Landau levels $l^- = l^+$, the degree of polarization is $P_{e^-} < 0$, because $n_g < l^-$ is always satisfied, while in the OPP process the degree of polarization is equal to $P_{OPPe^-} = 0$. The most probable is the TPP process when a hard photon creates pairs at the same energy levels, i.e. $n_g = l^+$ and $l^- > l^+$. In this case, we have

$$P_{e^-} = -P_{OPPe^-} < 0,$$

i.e. in the TPP process with normally polarized photons, the electrons are created mainly in normal spin states.

Let us analyze the dependence of the degree of polarization P_{e^-} on the circular polarization of photons. Consider the Stokes parameters of photons in the form

$$\xi_2^{(1,2)} = \pm 1, \ \xi_1^{(1,2)} = 0, \ \xi_3^{(1,2)} = 0,$$

that is, both photons are completely circularly polarized. In this case, the degree of electron polarization is equal to

$$P_{e^-} = -1 + \frac{h}{l^-}(l^- - n_g + n_g \xi_2^{(1)} \xi_2^{(2)})^2, \tag{4.101}$$

in particular, under the transition to the neighboring Landau level $n_g = l^- - 1$

$$P_{e^-} = -1 + \frac{h}{l^-}(1 + n_g \xi_2^{(1)} \xi_2^{(2)})^2,$$

that is, preferably the electrons are in the ground spin state. The violation of the polarization of electrons is proportional to the parameter h and it is greatest if photons have the same direction of circular polarization. It should be noted that the dependence of the degree of orientation of particle spins on the circular polarization of photons distinguishes the TPP process from the OPP process and it is the consequence of a mixed intermediate state of the TPP process with the spins of the final particles, which are co-directed to the field.

Let us analyze the degree of polarization of the final positrons, which is determined by the expression

$$P_{e^+} = \frac{\sigma^{++} + \sigma^{-+} - \sigma^{+-} - \sigma^{--}}{\sigma^{++} + \sigma^{-+} + \sigma^{+-} + \sigma^{--}}. \tag{4.102}$$

Taking into account (4.63), (4.67), (4.70), and (4.75), the degree of polarization can be reduced to the form

$$P_{e^+} = \frac{2l^- \Pi_1 \tilde{\Pi}_2 - l^- l^+ h \Pi_1 \Pi_2 + hK_g}{2l^- \Pi_1 \tilde{\Pi}_2 + l^- l^+ h \Pi_1 \Pi_2 + hK_g}. \tag{4.103}$$

If an initial hard photon is abnormally polarized $\xi_3^{(2)} = +1$ ($\Pi_2 = 0$), then all final positrons have spins in the direction of the field $P_{e^+} = +1$, regardless of the type of polarization of the soft photon. Note that the polarization of soft photons significantly affects the degree of electron polarization, changing it to the opposite in the narrow interval near the polarization (4.98).

In the case of normal polarization of hard photon $\xi_3^{(2)} = -1$ ($\tilde{\Pi}_2 = 0$), the expression for the degree of polarization of positrons coincides with a similar expression for electrons (4.99) $P_{e^+} = P_{e^-}$. As mentioned earlier, this quantity in the TPP process with the most probable values of Landau levels of final particles is negative, i.e. positrons are mainly in the inverse spin state.

If both photons are completely circularly polarized $\xi_2^{(1)} \xi_2^{(2)} = \pm 1$, the degree of polarization of positrons takes the simple form

$$P_{e^+} = 1 - l^+ h, \tag{4.104}$$

that coincides with a similar degree of polarization (2.169) in the OPP process. Thus, the circular polarization of the initial photons does not affect the degree of orientation of the spins of the final positrons.

Consider the spin-polarization effects in the TPP process in the resonance of diagram *f* with resonant conditions (4.39), (4.40). In this case, taking into account the expressions for the cross-sections (4.85) — (4.88), the degree of polarization of the final electrons (4.92) and positrons (4.102) can be reduced to the form

$$P_{e^-} = \frac{-2l^+\Pi_1^+\tilde{\Pi}_2 + l^-l^+h\Pi_1^+\Pi_2 - hK_f}{2l^+\Pi_1^+\tilde{\Pi}_2 + l^-l^+h\Pi_1^+\Pi_2 + hK_f}, \tag{4.105}$$

$$P_{e^+} = \frac{2l^+\Pi_1^+\tilde{\Pi}_2 + l^-l^+h\Pi_1^+\Pi_2 - hK_f}{2l^+\Pi_1^+\tilde{\Pi}_2 + l^-l^+h\Pi_1^+\Pi_2 + hK_f}, \tag{4.106}$$

$$K_f = (l^+ - n_f)^2\tilde{\Pi}_1^+\tilde{\Pi}_2 + n_g^2\Pi_1^+\Pi_2 + \frac{4(l^+ - n_f)n_f}{1+v^2}\Xi_f, \tag{4.107}$$

where the polarization functions of soft photons $\Pi_1^+, \tilde{\Pi}_1^+$ differ from similar ones $\Pi_1, \tilde{\Pi}_1$ (4.61), (4.69) by changing the sign in the term with $\xi_2^{(1)}$, because changing the sign of the charge changes the sign of the circular polarization of the SR process.

If the first terms of the numerators in (4.105), and (4.106) are not equal to zero (more precisely, much larger than the parameter *h*), the degree of polarization in the linear approximation on the parameter *h* takes a simpler form

$$P_{e^-} = -1 + l^-h\frac{\Pi_2}{\tilde{\Pi}_2}, \quad P_{e^+} = 1 - h\frac{K_f}{l^-\Pi_1^+\tilde{\Pi}_2}. \tag{4.108}$$

Note that the degree of electron polarization in the TPP process coincides with a similar expression in the OPP process (2.169). This is understandable because, in the resonance of diagram *f*, a hard photon immediately creates a final electron and an intermediate positron, and the latter absorbs an additional soft photon. In particular, if $\Pi_2 = 0$ (anomalous linear polarization of the hard photon)

$$P_{e^-} = -1, \quad P_{e^+} = 1 - \frac{(l^+ - n_f)^2h}{l^+}\cdot\frac{\tilde{\Pi}_1^+}{\Pi_1^+}, \tag{4.109}$$

the spins of electrons are completely oriented opposite to the field, and the degree of polarization of positron is slightly disturbed (by the value ~ *h*). The spins of

positrons are completely oriented to the field $P_{e^+} = +1$, if $\tilde{\Pi}_1^+ = 0$ that is realized in the conditions

$$\xi_1^{(1)} = 0, \quad \xi_2^{(1)} = \frac{2\nu}{1+\nu^2}, \quad \xi_3^{(1)} = -\frac{1-\nu^2}{1+\nu^2}. \tag{4.110}$$

When choosing the polarization of a soft photon, when $\Pi_1^+ = 0$ that is realized if

$$\xi_1^{(1)} = 0, \quad \xi_2^{(1)} = \frac{2\nu}{1+\nu^2}, \quad \xi_3^{(1)} = \frac{1-\nu^2}{1+\nu^2}, \tag{4.111}$$

the final particles are completely polarized

$$P_{e^-} = -1, \quad P_{e^+} = -1,$$

moreover, all electrons are in the ground spin state and positrons are in the inverse state.

In this case, if $\tilde{\Pi}_2 = 0$ (normal linear polarization of the hard photon), the degrees of polarization of the particles are the same

$$P_{e^-} = P_{e^+} = \frac{l^- l^+ - n_f^2}{l^- l^+ + n_f^2}. \tag{4.112}$$

Because the most probable Landau levels of the final particles are $n_f = l^-$ and $l^- < l^+$, then $P_{e^-} = P_{e^+} > 0$, i.e. in the TPP process with the normally polarized hard photon, the electrons are mainly created in the inverse spin states, and the positrons are in the normal ones.

Finally, when both photons are completely circularly polarized $\xi_2^{(1)}, \xi_2^{(2)} = \pm 1$, the degree of polarization of the final particles is equal to

$$P_{e^-} = -1 + l^- h, \quad P_{e^+} = 1 + \frac{h}{l^+}(l^+ - n_f + n_f \xi_2^{(1)} \xi_2^{(2)})^2. \tag{4.113}$$

The first expression in (4.113) coincides with a similar expression in the OPP process (2.169) when the hard photon is not polarized. The degree of polarization of positron has a form similar to expression (4.101) for the degree of polarization of electron in the resonance TPP process of the diagram *g*.

4.4. Production of e⁺e⁻ pair by a photon in a magnetic field and SR field in a pulsar magnetosphere

It is known that the production of e^+e^- pairs are an important element of the model of X-ray pulsars because the existence of an electron-positron plasma in a magnetized magnetosphere with the magnetic field ~ 10^{12} *Gs* is

necessary for the generation of pulsar radiation. To date, it is considered that the main source of pairs is the process of e^+e^- pair production by one photon [134—137]. e^+e^- pairs are also created as a result of the interaction of two photons with total energy $> 2m$, which appear due to the inverse Compton scattering of thermal X-rays from the surface of a neutron star. Since the attenuation length of γ photons beam for a two-photon process is greater than for a one-photon process, traditionally the process of production of a pair by two photons is considered insignificant in comparison with the one-photon process. The only exceptions are magnetars, where in the supercritical magnetic fields $\sim 10^{15}$ Gs the one-photon generation of a pair is suppressed by the process of photon splitting.

It should be emphasized that this opinion is not correct, because it does not take into account the influence of a strong magnetic field on the process of two-photon pair production. In the TPP process, as shown above, there are resonances in which the cross-section is several orders of magnitude larger than the cross-section of the process without the field, which significantly increases the contribution to plasma generation.

In the first stage of e^+e^- plasma formation, when its density is not high, the one-photon process is indeed the most significant. However, over time, one hard photon will create an e^+e^- pair, not in an empty vacuum, but the field of photons with cyclotron frequency and multiple of it, as electrons and positrons appear, which move in a strong magnetic field accompanied by cyclotron radiation. Thus, e^+e^- pair can be created by one hard photon with the capture of a soft cyclotron photon, i.e. we get a resonance production of a pair by two photons. As follows from the previous section, the resonance conditions of this process near the threshold (4.27), and (4.28) are automatically fulfilled. The hard photon must have the above-threshold frequency (4.27) to create a pair at given Landau levels. This condition is necessary for both second-order and first-order processes. According to (4.28) the frequency of soft photon should be multiple of the cyclotron frequency that takes place.

Let us make an estimated comparison of these processes, when the particles are created at the lowest possible energy levels in the main spin states, provided that the two-photon process takes place in the resonant conditions of the *g* diagram. Herewith, the Landau levels, spin values of particles, and Stokes parameters of photon polarizations are equal to

$$l^- = 1,\ l^+ = n_g = 0,\ \mu^- = -1,\ \mu^+ = 1,\ \xi^{(1)}_{1,2,3} = \xi^{(2)}_{1,2,3} = 0. \qquad (4.114)$$

Taking into account (4.114), the cross section of the two-photon pair production (4.59) is equal to

$$\sigma = \frac{\pi e^4 h e^{-2/h}}{2(1-\cos\chi)\Gamma^2}\sqrt{\frac{m}{\delta\omega}}, \qquad (4.115)$$

where the resonance width is taken as the radiation width $\Gamma = 2e^2mh^2/3$.

The probability of the process per unit time is related to the cross section by the expression

$$W_{2\gamma} = n_{\gamma}\sigma(1-\cos\chi), \tag{4.116}$$

where n_{γ} is the density of cyclotron photons in the pulsar magnetosphere. The rate of the one-photon pair production in the ground energy states (2.156) with momentum $p = \sqrt{\delta\omega m}$ is equal to

$$W_{1\gamma} = \frac{e^2 hme^{-2/h}}{4\sqrt{\delta\omega / m}}. \tag{4.117}$$

Equality of probabilities (4.116) and (4.117) give the expression for the critical density

$$n_{\gamma c} = 2e^2h^4m^3 / 9\pi, \tag{4.118}$$

as we see, it is determined only by the magnetic field. If the density of cyclotron photons exceeds the critical value (4.118), the two-photon process dominates over the one-photon process. When the magnetic field strength is $h = 0.1$ then the critical density is $n_{\gamma c} \sim 10^{24}\ cm^{-3}$, which is an order of magnitude higher than the estimated characteristic density of photons in the magnetosphere of pulsars [134]. Thus, if in the first stages the electron-positron plasma is generated due to the one-photon pair production, then at the final stage of its formation the resonant two-photon process dominates.

4.5. Influence of particle polarization on the intensity of pulsar synchrotron radiation

In the previous section, we considered the formation of e^+e^- plasma in the magnetosphere of an X-ray pulsar. When the e^+e^- pair is formed by a hard photon or by picking up a soft one, the electrons (positrons) at excited energy levels in a magnetic field of the pulsar generate synchrotron radiation, which is the object of observation. In the modern pulsar model, the particles are considered unpolarized. Consider the influence of particle polarization on the intensity of synchrotron radiation. According to expression (2.151), the degree of polarization of particles strongly depends on the polarization of the initial hard photon and as follows from (2.44), itself significantly affects the probability of emission of the final photons.

We introduce the ratio of intensities R:

$$R = < I >_{pol} / < I >_{therm}, \tag{4.119}$$

where $< I >_{pol}$ is the total intensity of radiation by electron, which is averaged with the weight fractions of electrons in the inverse and ground spin states x_+, x_-,

respectively. $< I >_{therm}$ is the total intensity of radiation, averaged over the spins of the initial electron and summed over the spins of the final one. Thus, under using the magnitude of $< I >_{therm}$, it is considered a common view of the thermodynamic preparation of plasma particles, that are not polarized and under using expression $< I >_{pol}$, the polarization of particles formed in the OPP process or resonant TPP is taken into account. These averaged intensities of the SR process are determined as follows

$$< I >_{pol} = I^- x_- + I^+ x_+, \quad < I >_{therm} = (I^- + I^+)/2, \tag{4.120}$$

where I^-, I^+ are the total intensities of the SR process of the polarized initial electron with spin opposite and in the direction of the field, respectively, which are taken from (2.51). The weight fractions x_+, x_- are defined by expressions

$$x_- = (W^{-+} + W^{--})/\sum W^{\mu^-\mu^+}, \; x_+ = (W^{++} + W^{+-})/\sum W^{\mu^-\mu^+}, \tag{4.121}$$

where $W^{\mu^-\mu^+}$ is the total probability of e^+e^- pair production, which is obtained in the general case from expression (2.151) after integration on the longitudinal component of the momentum of the final electron, while the obvious ratio is fulfilled

$$x_- + x_+ = 1. \tag{4.122}$$

The LLL approximation. In this approximation, the relation (4.119) with the fixed value of the parameter x_+ is obtained after averaging the expressions (2.46) — (2.49) and it has the form

$$R = 2(l - x_+(l - l'))/(l + l'). \tag{4.123}$$

In the case of unpolarized particles $x_+ = x_- = 1/2$, the intensity ratio is equal to $R = 1$. If the initial electrons are completely polarized with the spin directed opposite to the field $x_+ = 0$, the ratio is equal to $R = 2l/(l + l')$, in particular, under the transition of electrons to the ground energy state, we have $l' = 0$: $R = 2$ and the intensity of polarized electrons is twice the intensity of unpolarized ones.

The probability of the OPP process with the fixed values of the projections of the spins of particles created at given Landau levels in the LLL approximation is determined by the expressions (2.156) — (2.159). Then part of the electrons with spins co-directed to the field x_+ in the case when e^+e^- pairs are created at the same Landau level $l^+ = l^- = l$ has the form

$$x_+ = lh(1 - \xi_3)/2(1 + \xi_3 + lh(1 - \xi_3)), \tag{4.124}$$

where ξ_3 is the Stokes parameter of the linear polarization of the initial hard photon.

As follows from the obtained expression (4.124), the ratio of intensities R (4.123) significantly depends on the linear polarization of the initial photon. In

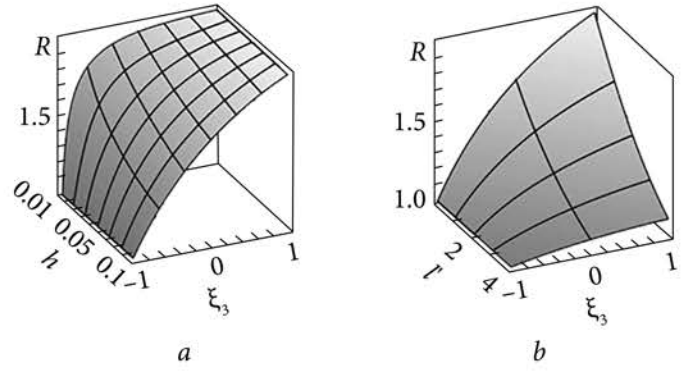

Fig. 4.7. Dependence of the ratio of intensities of synchrotron radiation of polarized and unpolarized electrons: *a* — on the Stokes parameter ξ_3 of the initial photon and the magnetic field *h*, *b* — on the Landau level number of the final electron, and the Stokes parameter ξ_3

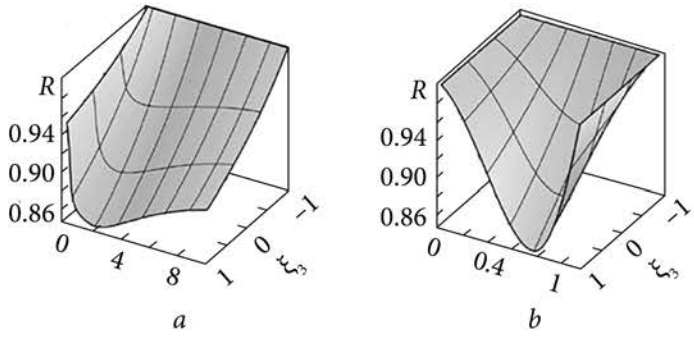

Fig. 4.8. Dependence of the ratio of the SR intensities of polarized and unpolarized electrons: *a* — on the Stokes parameter ξ_3 of the initial photon and the parameter $\Omega = h\omega/m$, *b* — on the Stokes parameter ξ_3, and the frequency of the final photon $y = \omega/\omega_c$

the case of the unpolarized initial photon $\xi_3 = 0$, the fraction $x_+ = lh/2$ is small, and the spins of electrons are preferably directed opposite to the field. The ratio *R* does not depend on the frequency of the initial photon. Fig. 4.7, *a* shows the dependence of the ratio of the intensities *R* on the linear polarization of the initial photon and the magnitude of a magnetic field in the case of the transition of an electron from $l = 5$ to $l' = 0$. Fig. 4.7, *b* shows the dependence of the magnitude *R* on the polarization of the photon and the Landau level number of the final electron, $h = 0.1$. As can be seen from Fig. 4.7, $R > 1$ is always satisfied if $\xi_3 \neq -1$ and $R = 1$ when $\xi_3 = -1$. Thus, taking into account the polarization of the particles of a pulsar magnetosphere leads to higher values of the SR intensity in the LLL approximation.

Ultrarelativistic approximation. In this approximation, the intensity ratio R can be obtained by integrating expressions (2.90), and (2.185). Fig. 4.8, *a* shows the dependence of the ratio R on the linear polarization of the initial photon ξ_3 and the parameter $\Omega = h\omega/m$ (product of the field on the frequency of the initial photon), with $\omega = 100\ m$, and the magnetic field takes values from $h = 0.001$ to $h = 0.1$. Fig. 4.8, *b* shows the dependence of R on the Stokes parameter ξ_3 and the frequency of the finite photon $y = \omega/\omega_c$, where $h = 0.1$.

As can be seen from Fig. 4.8 in the ultrarelativistic case R < 1. The minimum value of $R = 0.86$ corresponds to the anomalous linear polarization of the initial photon and monotonically goes to $R = 1$ when $\xi_3 = -1$.

Thus, taking into account the spin population of e^+e^- plasma leads to a change in the SR spectrum, increases the low-frequency part of the spectrum, and decreases the high-frequency part.

4.6. Conclusions

The process of electron-positron pair production by two polarized photons taking into account the spin of particles in a strong external magnetic field was first studied in resonant conditions if one photon (hard) creates a pair and the other (soft) causes resonance. As a result, it was shown:

1. In the analyzed process of two-photon e^+e^- pair production (TPP), the resonance is possible near the threshold if the frequency of the hard photon exceeds the sum of the energies of the pair, and the frequency of the soft photon is multiple of the cyclotron frequency. Far from the threshold, the frequency of a soft photon depends on its polar angle and it is maximum in the case of movement of this photon along the field. Interference of two resonances near the process threshold occurs if both photons are directed perpendicular to the field and the relation for Landau levels of the final and intermediate particles $l^- - n_g = l^+ - n_f$ is fulfilled.

2. The largest cross-section of the process corresponds to the particles produced in the main spin states σ^{-+}. It has the maximum value if a soft photon is normally polarized and a hard photon is abnormally polarized. In the case when the magnetic field strength is $H = 10^{12}$Гс, the cross-section of the process has the order of the Thomson cross-section, and the width of the resonance is 30 eB. Cross-sections of processes in which the particles have the same spin direction σ^{--}, σ^{++} have an additional degree of small parameter h. The smallest is the cross-section with particles in the inverse spin states σ^{+-}. In resonance, the cross-sections with the electronic intermediate state σ^{-+}, σ^{--}, σ^{+-} are factorized and they can be represented in the Breit-Wigner form. The cross-section σ^{++} is not factorized because the intermediate electron is in the mixed state. For resonance with the positron intermediate state, the cross-section σ^{--} is not factorized.

3. Spin-polarization effects in the resonant TPP process with an intermediate electron are expressed as follows:

a. In the process with abnormally linear polarized of hard photons ($\xi_3 = 1$), the change in the linear polarization of soft photons in the whole range changes the orientation of the electron spins from fully oriented opposite to the field to fully oriented to the field without changing the spin direction of the positron.

b. In the process with normally linearly polarized hard photon ($\xi_3 = -1$), the degree of orientation of the electron spins does not depend on the polarization of soft photon and it is determined only by the Landau levels of the intermediate and final particles. For the process with the lowest possible energy levels, the electrons are completely unpolarized and the first excited levels correspond mainly to the normal spin population.

c. If both photons of the process are circularly polarized, the particles are preferably in the ground spin state. Violation of the polarization of particles ~ h and the maximum if the photons have the same direction of circular polarization.

4. Taking into account the field of cyclotron photons in the process of e^+e^- plasma formation in the magnetosphere of the X-ray pulsar showed the dominant role of resonances in the field $H = 10^{12}$ *Gs* under the characteristic photon concentration, which refutes the generally accepted view of the dominant role of the OPP process in magnetosphere formation.

5. Taking into account the spin population of electrons and positrons in the process of e^+e^- plasma generating in a pulsar magnetosphere leads to a change in the SR spectrum, increases the low-frequency part of the spectrum, and decreases the high-frequency.

The main scientific results of this chapter are published in [283], [287—289].

Chapter 5

ONE-PHOTON PRODUCTION OF AN ELECTRON-POSITRON PAIR WITH EMISSION OF A PHOTON

5.1. Introduction

The process of production of an e^+e^- pair by a photon with subsequent emission of a final photon (OPPE) in a strong magnetic field is studied as a single second-order process. The kinematics of the process and the conditions for the occurrence of resonances are analyzed. The probabilities of the process are calculated in the resonant and nonresonant cases, taking into account the polarization of the particles in the nonrelativistic LLL approximation. Spin-polarization effects are studied. The possibility of the existence of mixed spin states of an intermediate electron (positron) under resonance conditions is analyzed.

5.2. Kinematics of the OPPE process

A feature of the process under study, in contrast to those previously considered, is the presence of three particles in the final state. As a result of the increase in the phase space of the final particles, the kinematics of the process becomes more complicated and requires separate consideration. The CS, TPP, and OPPE processes are cross-channels of one generalized reaction. Therefore, the laws of conservation of energy and longitudinal momentum component are constructed from the same parameters for these processes. Similarly to expressions (3.5), and (4.2) they can be written in the form:

$$\omega = \varepsilon^- + \varepsilon^+ + \omega', \quad \omega v = p^- + p^+ + \omega' u, \tag{5.1}$$

where $\omega, v = \cos\theta$ and $\omega', u = \cos\theta'$ are frequencies and cosines of the polar angles of the initial and final photons; ε^-,

p^- and ε^+, p^+ are energies and longitudinal momenta of the electron and the positron, respectively. As before, the energies and momenta of the particles are related by relations:

$$\varepsilon^{\pm} = ((m^{\pm})^2 + (p^{\pm})^2)^{1/2} = (m^2 + 2l^{\pm}hm^2 + (p^{\pm})^2)^{1/2}. \tag{5.2}$$

For fixed Landau levels of final particles l^+, l^-, longitudinal momentum of the electron p^-, and the angle of emission of the final photon u, conservation laws (5.1) specify the frequency of the final photon as follows:

$$\omega' = \frac{1}{1-u^2}(\omega_\varepsilon - k_p u - \sqrt{(\omega_\varepsilon - k_p u)^2 - (\varepsilon_\varepsilon^2 - k_p^2 - (m^+)^2)(1-u^2)}), \tag{5.3a}$$

where $\omega_\varepsilon = \omega - \varepsilon^-$, $k_p = \omega v - p^-$. The frequency of the final photon is set in the range:

$$0 \le \omega' \le \omega - (m^- + m^+). \tag{5.3b}$$

The upper limit is the threshold value, it corresponds to the next condition $p^- = p^+ = 0$.

To determine the limiting values of the energy and momentum of the electron, it is convenient, similarly to (2.121), to introduce function $f(p)$, which tends to zero for a real process:

$$f(p) = \omega - \omega' - \sqrt{(m^-)^2 + p^2} - \sqrt{(m^+)^2 + (p + \omega' u - \omega v)^2}. \tag{5.4}$$

The dependence of this function on the longitudinal momentum of the electron is presented in Fig. 5.1.

As follows from Fig. 5.1. the limit values ε^- and p correspond to the zero of the maximum of the function $f(p)$, are determined by the system of equations

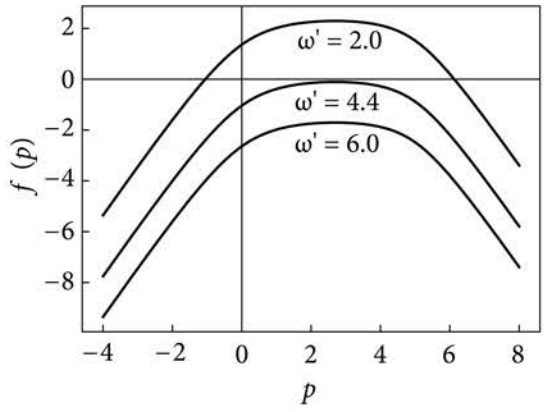

Fig. 5.1. Graph of the function $f(p)$ for various values of the frequency of the final photon, $h = 0.3$, $l^- = 2$, $l^+ = 1$, $\omega = 10$, $v = 0.5$, $u = 0$

$\partial f/\partial p = 0, f = 0$, and are equal to:

$$\varepsilon_m^{\pm} = m^{\pm} W / (m^+ + m^-), \quad p_m^{\pm} = \beta \varepsilon_m^{\pm}, \tag{5.5}$$

where

$$W = \omega - \omega', \quad \beta = (\omega\nu - \omega' u) / (\omega - \omega'). \tag{5.6}$$

Expressions (5.5) follow from (2.123) by replacing:

$$\omega \to W, \quad u \to \beta. \tag{5.7}$$

Note that taking into account the laws of conservation (5.1)

$$\beta = (p^- + p^+) / (\varepsilon^- + \varepsilon^+), \quad |\beta| < 1. \tag{5.8}$$

In the general case, the values of the energies and momenta of the final electron and positron follow from expressions (2.130) by replacing (5.7).

Let us determine the limiting values of the emission angle of the final photon by analyzing the dependence of the electron momentum $p^- = p(u)$ on the cosine of the emission angle u at fixed values of the Landau levels of particles and the frequency of the final photon:

$$p(u) = p_{1,2}^- = (a^-(u) \cdot \beta \pm b^-(u)) / 2(\omega - \omega')(1 - \beta^2), \tag{5.9}$$

where $a^-(u) = W^2(1-\beta^2) + (m^-)^2 - (m^+)^2$, $b^-(u)^2 = a^-(u)^2 - 4(m^-)^2 W^2(1-\beta^2)$. The sought interval of angles is determined by the condition $p_1 = p_2$, which is equivalent to the equation $b(u) = 0$. The dependence $b^2(u)$ is shown in Fig. 5.2.

The following parameters are selected: $h = 0.3$, $l^- = 2$, $l^+ = 1$, $\omega = 10m$, $\nu = 0.5$. The three curves correspond to the frequencies of the final photon ω'/m: 9.0, 7.25, 6.0. In the general case, the $b^2(u)$ curves have four roots (points of

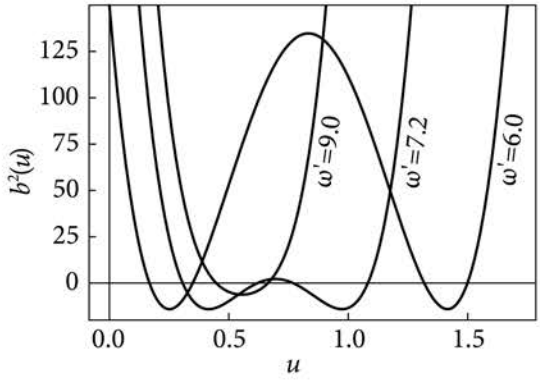

Fig. 5.2. Graph of the function $b^2(u)$ for different values of the final photon frequency, $h = 0.3$, $l^- = 2$, $l^+ = 1$, $\omega = 10m$, $\nu = 0.5$

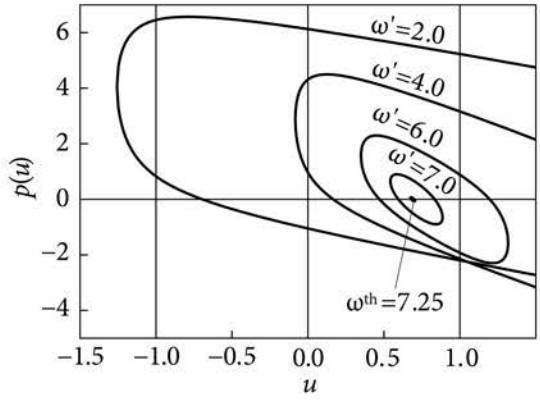

Fig. 5.3. Dependence of the electron momentum on the emission angle of the final photon, $h = 0.3$, $l^- = 2$, $l^+ = 1$, $\omega = 10m$, $v = 0.5$

intersection of the curve with the abscissa), and the interval of the photon emission angles are determined by two internal roots. For example, the curve $\omega'/m = 9.0$ has only two intersections with the abscissa, and radiation is absent in this case. The curve $\omega'/m = 7.25$ corresponds to the threshold of the process, the final photon is emitted in a narrow cone with $u = 0.69$. Finally, for the curve $\omega'/m = 6.0$, the inner roots are equal: $u_{\min} = 0.35$, $u_{\max} = 1.32$, hence $0.35 < u < 1$. In the general case, the boundaries of the interval of polar angles of the final photon are determined by expressions:

$$u_{\min} = \frac{1}{\omega'}(\omega v - \sqrt{W^2 - m_\Sigma^2}), \quad u_{\max} = \frac{1}{\omega'}(\omega v + \sqrt{W^2 - m_\Sigma^2}),$$

$$m_\Sigma = m^- + m^+, \tag{5.10}$$

further, if necessary, you need to redefine

$$u_{\min} = \max\{u_{\min}, -1\}, \; u_{\max} = \min\{u_{\max}, 1\}. \tag{5.11}$$

Fig. 5.3 shows the dependence of the longitudinal momentum of the electron on the cosine of the emission angle of the final photon.

As can be seen from Fig. 5.3, in the case of emission of a low-frequency photon (curve $\omega'/m = 2$ for the chosen parameters $h = 0.3$, $l^- = 2$, $l^+ = 1$, $\omega = 10m$, $v = 0.5$), the final photon can be emitted in any direction, while the electron momentum weakly depends on u. At the threshold of the process, when $\omega'_{th}/m = 7.25$, $u_{th} = 0.69$, the longitudinal momentum of the electron (and the positron) is zero. That is, particles at the threshold are produced motionless at fixed Landau levels. The principal difference between the threshold in the OPPE process and the similar threshold in the OPP process is that it is possible for any frequency and polar angle of the initial photon (sufficient for the production of a pair) and corresponds to the threshold maximum possible fre-

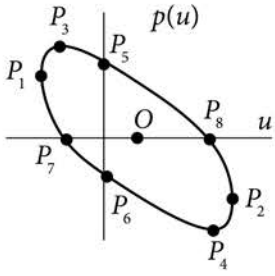

Fig. 5.4. Characteristic limiting values of electron momentum on the $p(u)$ curve

quency of the final photon. The threshold frequency and cosine of the emission angle of the final photon are determined by the expressions:

$$\omega'_{th} = \omega - m_{\Sigma} \qquad u_{th} = \omega v / \omega'_{th}. \tag{5.12}$$

The cosine of the emission angle of the final photon u is proportional to the cosine of the angle v of the initial photon. The condition $u \le 1$ defines constraint $v \le 1 - m_{\Sigma}/\omega$. Inverse to relation (5.9), the dependence $u(p)$ has the form:

$$u(p) = (\omega v - p \pm \sqrt{(W - \sqrt{(m^-)^2 + p^2})^2 - (m^+)^2}\,)/\omega'. \tag{5.13}$$

Let us analyze the properties of the characteristic limiting values of the electron momentum and the corresponding emission angles of the final photon. In the general case, there are eight such quantities, they correspond to the points P_1 — P_8 indicated in Fig. 5.4, where characteristic dependence $p(u)$ is shown.

A similarly closed curve also takes place for the dependence of positron momentum on u. Points P_1 and P_2 corresponds to the limiting value of the cosine of the final photon angle, which are determined by expressions (5.10): $u_1 = u_{\min}$, $u_2 = u_{\max}$. The longitudinal momentum of the electron and positron at these points is equal to:

$$p_1^- = -p_2^- = m^- \sqrt{W^2 - m_{\Sigma}^2}\,/\,m_{\Sigma},\ p_1^+ = -p_2^+ = m^+ \sqrt{W^2 - m_{\Sigma}^2}\,/\,m_{\Sigma}. \tag{5.14}$$

Points P_3 and P_4 correspond to the maximum and minimum values of electron momentum, respectively:

$$p_3^- = -p_4^- = \sqrt{(W - m^+)^2 - (m^-)^2},\ p_{3,4}^+ = 0, \tag{5.15}$$

in this case, the longitudinal momentum of the positron is zero. Thus, the excess of the initial photon energy over the limiting value is completely converted into the electron momentum.

$$u_{3,4} = (\omega v \mp \sqrt{(W - m^+)^2 - (m^-)^2}\,)/\omega'. \tag{5.16}$$

Points P_5 and P_6 correspond to the case when the final photon emits perpendicular to the direction of the magnetic field, that is $u_5 = u_6 = 0$. The longitudinal momentum of the electron is determined from (5.9), where $\beta = \omega v / W$.

Finally, the points P_7, and P_8 corresponds to the zero value of the longitudinal momentum of the electron. They are similar to points P_3, and P_4, only now the electron and positron are swapped. The positron momentum at points P_7 and P_8 is maximum and is expressed by relation (5.15), where it is necessary to replace $m^+ \leftrightarrow m^-$. The angles of emission of the photon are determined by the relation (5.16) with the replacement $m^+ \leftrightarrow m^-$. As seen in Fig. 5.4. the curve $p(u)$ has central symmetry about the point O with coordinates $u_0 = \omega v/\omega'$, $p_0 = 0$.

Let us analyze the range of emission angles of the final photon near the reaction threshold. Let, for definiteness, the initial photon be perpendicular to the field $v = 0$. Let certain meanings have l^-, l^+, ω'. At the threshold $W = W_m = m_\Sigma$, longitudinal momenta of particles are absent $p^- = p^+ = 0$, and the final photon, as well as the initial one, is perpendicular to the magnetic field $u = 0$. We choose the value of the frequency of the initial photon close to the threshold value, so that

$$W = W_m + \delta W = m_\Sigma + \delta W, \quad \delta W << W. \tag{5.17}$$

Under these conditions, the limiting values of the angles $u_{1,2}$ and the corresponding momenta of the electron and positron have the form:

$$u_{1,2} = \frac{\mp 1}{\omega'}\sqrt{2m_\Sigma \delta W}, \; p^-_{1,2} = \pm m^- \sqrt{\frac{2\delta W}{m_\Sigma}}, \; p^+_{1,2} = \pm m^+ \sqrt{\frac{2\delta W}{m_\Sigma}}. \tag{5.18}$$

The range of angles is $\Delta u \equiv u_2 - u_1 = 2\sqrt{2m_\Sigma \delta W}\,/\,\omega'$. For the radiation frequency, which is equal to the cyclotron frequency $\omega' = hm$, and for the lowest Landau levels, $m^- \approx m^+ \approx m$, the interval of radiation angles is $\Delta u = 4\sqrt{\delta W / m}\,/\,h$. In the case of a power-law dependence of the above-threshold addition δW on a small parameter h, that is, when $\delta W \sim h^k m$ (k is a natural number), the angle interval is of the order of magnitude: $\Delta u \sim h^{k/2-1}$. For $k > 2$, we have $\Delta u << 1$, that is, radiation occurs in a narrow cone along the direction perpendicular to the field. If $k = 2$, then $\Delta u \sim 1$, that is, radiation occurs in a wide range of directions. Finally, if $k < 2$, then the estimates give $\Delta u >> 1$, but the physical interval is $\Delta u = 2$, that is, radiation occurs in all directions, while the longitudinal momenta of the particles weakly depend on the angle of emission of the photon.

5.3. Probability amplitude and resonance conditions of the OPPE process

The probability amplitude of OPPE. The expression for the amplitude of the process corresponds to the Feynman diagrams shown in

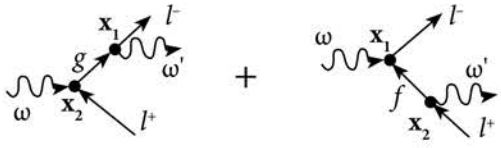

Fig. 5.5. Feynman diagrams of the process of one-photon production of an e^+e^- pair with emission of a photon

Fig. 5.5, and has the form:

$$A_{if} = ie^2 \int d^4\mathbf{x}_1 d^4\mathbf{x}_2 \bar{\Psi}^-(\mathbf{x}_1)[\gamma^i A'_i(\mathbf{x}_1) G_{H1}(\mathbf{x}_1,\mathbf{x}_2)\gamma^j A_j(\mathbf{x}_2) + \\ + \gamma^j A_j(\mathbf{x}_1) G_{H2}(\mathbf{x}_1,\mathbf{x}_2)\gamma^i A'_i(\mathbf{x}_2)]\Psi^+(\mathbf{x}_2), \tag{5.19}$$

where $\bar{\Psi}^-(\mathbf{x}_1)$, $\Psi^+(\mathbf{x}_2)$ are wave functions of the final electron and positron; $A_j(\mathbf{x})$, $A'_i(\mathbf{x})$ are wave functions of the initial and final photons; $G_{H1}(\mathbf{x}_1,\mathbf{x}_2)$, $G_{H2}(\mathbf{x}_1,\mathbf{x}_2)$ are Green's functions of the electron in an intermediate state, corresponding to the *g* and *f* diagrams (see Fig. 5.5). Expression (5.19) is obtained from amplitude (4.1) by replacing $A_{2j}(\mathbf{x}) \to A_j(\mathbf{x})$, $A_{1i}(\mathbf{x}) \to A'_i(\mathbf{x})$.

Similarly to the TPP process, after taking the integrals in (5.19), the amplitude of the OPPE probability in the general case can be represented as:

$$A_{if} = (2\pi)^4 \frac{M_{if}}{SV} \delta^3(k - k' - p^- - p^+), \quad M_{if} = M_{if}^{(g)} + M_{if}^{(f)}. \tag{5.20}$$

The value $M_{if}^{(g)}$ corresponds to the first diagram in Fig. 5.5 and has the form:

$$M_{if}^{(g)} = \frac{-ie^2}{4\sqrt{\omega_1\omega_2\varepsilon^-\varepsilon^+ m^- m^+}} \sum_{n_g=0}^{\infty} \frac{e^{i\Phi_g} Q^g}{g_0^2 - \varepsilon_g^2}, \quad Q^g = \sum_{a=1}^{10} Q_a^g, \tag{5.21}$$

where

$$Q_1^g = -J_1^{++} J_2^{++}[m\tilde{C} + g_0 C + gD], \quad Q_2^g = J_1^{-+} J_2^{++}[-mD + g_0\tilde{D} + gC],$$

$$Q_3^g = J_1^{+-} J_2^{+-}[-mC - g_0\tilde{C} + gD], \quad Q_4^g = J_1^{--} J_2^{+-}[mD - g_0\tilde{D} + gC],$$

$$Q_5^g = J_1^{++} J_2^{-+}[mD + g_0\tilde{D} - gC], \quad Q_6^g = -J_1^{-+} J_2^{-+}[mC - g_0\tilde{C} + gD],$$

$$Q_7^g = -J_1^{+-} J_2^{--}[mD + g_0\tilde{D} + gC], \quad Q_8^g = J_1^{--} J_2^{--}[-mC + g_0\tilde{C} + gD],$$

$$Q_9^g = [-J_1^{++} J_2^{+-} - J_1^{+-} J_2^{++} + J_1^{-+} J_2^{--} + J_1^{--} J_2^{-+}] D\sqrt{2n_g hm},$$

$$Q_{10}^g = [J_1^{-+} J_2^{+-} - J_1^{--} J_2^{++} + J_1^{++} J_2^{--} - J_1^{+-} J_2^{-+}] C\sqrt{2n_g hm}, \tag{5.22}$$

functions J_1 and J_2 have a form similar to (4.14), (4.15):

$$J_1^{++} = J_1(l^+, n_g) M_p^+ e_z, \quad J_2^{++} = J_2(l^-, n_g) M_m^- e'_z,$$

$$J_1^{-+} = J_1(l^+ - 1, n_g) \mu^+ M_m^+ H_p, \quad J_2^{-+} = J_2(l^- - 1, n_g) \mu^- M_p^- H_p^{'*},$$

$$J_1^{+-} = J_1(l^+, n_g - 1) M_p^+ H_m, \quad J_2^{+-} = J_2(l^-, n_g - 1) M_m^- H_m^{'*},$$

$$J_1^{--} = J_1(l^+ - 1, n_g - 1) \mu^+ M_m^+ e_z, \quad J_2^{--} = J_2(l^- - 1, n_g - 1) \mu^- M_p^- e'_z. \qquad (5.23)$$

The definition of the notation in (5.22), and (5.23) is given in the previous chapters. The parameters η, η', which are defined by expression (3.19), are the arguments of the functions $J_1(l^+, n_g)$, $J_2(l^-, n_g)$. The zero g_0 and longitudinal g components of the 4-momentum of the intermediate state in the ***g*** diagram, as well as the energy of the intermediate state ε_g, which is at a fixed Landau level n_g, respectively, are equal to:

$$g_0 = \omega - \varepsilon^+, \; g = \omega v - p^+, \; \varepsilon_g = \sqrt{m^2 + 2n_g hm^2 + g^2}. \qquad (5.24)$$

The phase Φ_g is equal to:

$$\Phi_g = \frac{k_x k_y - k'_x k'_y}{2hm^2} + \frac{g_y (k'_x - k_x)}{hm^2} + \frac{\pi}{2}(l^- - l^+) - .$$

$$-(n_g - l^+)\varphi + (n_g - l^-)\varphi' \qquad (5.25)$$

The amplitude $M_{if}^{(f)}$ corresponding to the second diagram in Fig. 5.5 has the form (5.21) with the replacement $g \to f$, where

$$Q_1^f = -J_1^{++} J_2^{++} [m\tilde{C} - f_0 C - fD], \quad Q_2^f = -J_1^{++} J_2^{+-} [mD + f_0 \tilde{D} + fC],$$

$$Q_3^f = -J_1^{-+} J_2^{-+} [mC - f_0 \tilde{C} + fD], \quad Q_4^f = J_1^{-+} J_2^{--} [mD + f_0 \tilde{D} - fC],$$

$$Q_5^f = J_1^{+-} J_2^{++} [mD - f_0 \tilde{D} + fC], \quad Q_6^f = -J_1^{+-} J_2^{+-} [mC + f_0 \tilde{C} - fD],$$

$$Q_7^f = -J_1^{--} J_2^{-+} [mD - f_0 \tilde{D} - fC], \quad Q_8^f = -J_1^{--} J_2^{--} [mC + f_0 \tilde{C} + fD],$$

$$Q_9^f = [-J_1^{-+} J_2^{++} - J_1^{++} J_2^{-+} + J_1^{--} J_2^{+-} + J_1^{+-} J_2^{--}] D \sqrt{2n_f hm},$$

$$Q_{10}^f = [J_1^{-+} J_2^{+-} - J_1^{++} J_2^{--} + J_1^{--} J_2^{++} - J_1^{+-} J_2^{-+}] C \sqrt{2n_f hm}, \qquad (5.26)$$

functions J_1 and J_2 have the form:

$$J_1^{++} = J_1(n_f, l^-) M_m^- e_z, \quad J_2^{++} = J_2(n_f, l^+) M_p^+ e'_z,$$

$$J_1^{+-} = J_1(n_f, l^- - 1)\,\mu^- M_p^- H_m, \quad J_2^{+-} = J_2(n_f, l^+ - 1)\mu^+ M_m^+ H_m^{'*},$$

$$J_1^{-+} = J_1(n_f - 1, l^-) M_m^- H_p, \quad J_2^{-+} = J_2(n_f - 1, l^+) M_p^+ H_p^{'*},$$

$$J_1^{--} = J_1(n_f - 1, l^- - 1)\,\mu^- M_p^- e_z, \quad J_2^{--} = J_2(n_f - 1, l^+ - 1)\mu^+ M_m^- e'_z. \qquad (5.27)$$

The zero f_0 and longitudinal f components of the 4-momentum of the intermediate state in the ***f*** diagram, as well as the energy of the intermediate state ε_f which is at a fixed Landau level n_f, respectively, are equal to:

$$f_0 = \omega - \varepsilon^-, \quad f = \omega v - p^-, \quad \varepsilon_f = \sqrt{m^2 + 2n_f hm^2 + f^2}. \qquad (5.28)$$

The phase Φ_f is equal to:

$$\Phi_f = \frac{k_x k_y - k'_x k'_y}{2hm^2} - \frac{p_y^- k_x + p_y^+ k'_x}{hm^2} + \frac{\pi}{2}(l^- - l^+) -$$

$$-(l^- - n_f)\varphi + (l^+ - n_f)\varphi'. \qquad (5.29)$$

Resonant conditions of the OPPE process. Let us consider the question of the realization of resonance conditions in the ultraquantum approximation. With accuracy to the first power of h, neglecting the longitudinal momenta of the particles, the energies of the particles can be written in the form:

$$\omega = 2m + \kappa hm, \quad \omega' = \kappa' hm, \quad \varepsilon^{\pm} = m + l^{\pm} hm, \quad \varepsilon_g = m + n_g hm. \qquad (5.30)$$

Energy conservation law (5.1) for expressions (5.30) gives:

$$\kappa - \kappa' = l^+ + l^-. \qquad (5.31)$$

The condition for a resonant process with resonance in the first Feynman diagram ***g*** (see Fig. 5.5) is similar to expression (4.17):

$$g_0 = \varepsilon_g \qquad (5.32)$$

and defines an expression for κ, κ':

$$\kappa = n_g + l^+, \quad \kappa' = n_g - l^-. \qquad (5.33)$$

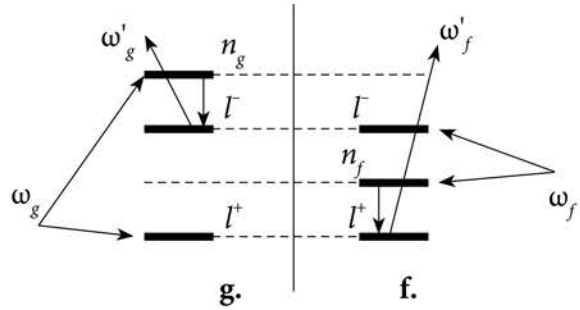

Fig. 5.6. Arrangement of Landau levels of particles with the interference of resonances of the first and second Feynman diagrams

Thus, resonance in the first diagram at the threshold of the process (without longitudinal momenta of particles) occurs if the frequency of the initial photon is equal to the sum of the energies of the intermediate electron at the Landau level n_g and the final positron at the Landau level l^+, and the frequency of the final photon is equal to the distance between the Landau levels intermediate and final electron.

Similarly, the resonance in the second diagram of Fig. 5.5 at the threshold of the process occurs if the next condition is fulfilled

$$f_0 = \varepsilon_f. \tag{5.34}$$

In this case, the frequency of the initial photon is equal to the sum of the energies of the intermediate positron at the Landau level n_f and the final electron at the Landau level l^-, and the frequency of the final photon is equal to the distance between the Landau levels of the intermediate and final positron

$$\kappa = n_f + l^-, \quad \kappa' = n_f - l^+. \tag{5.35}$$

The interference of two resonances is determined by the simultaneous fulfillment of conditions (5.33) and (5.35), which leads to such a relation between the Landau levels

$$n_g - l^- = n_f - l^+. \tag{5.36}$$

This relation is illustrated in Fig. 5.6. Thus, resonance is possible for any above-threshold frequency of the initial photon and, up to h, does not depend on the emission angle of the final photon. In resonance, the frequency of the final photon is a multiple of the cyclotron frequency. Resonance conditions with an accuracy of h in both diagrams are fulfilled simultaneously, that is, at resonance, there is always «interference» between two diagrams.

It should be noted that resonance conditions (5.33) and (5.35) were obtained up to the first power of the small parameter h. However, the resonance

width is of the order of magnitude $\Gamma \sim e^2h^2m$. Therefore, the analysis of conditions (5.32) and (5.34) should be carried out more correctly up to the value of h^2 inclusive. Since the momenta of particles in the ultraquantum approximation are multiples of $h^{1/2}$, then $h^{1/2}$ will be a small parameter.

Let's start by analyzing the resonance condition in the first diagram (5.32) up to h^2 inclusive. Let's represent the frequencies of the initial and final photons in the form:

$$\omega = 2m + (n_g + l^+)hm + \alpha_g hm, \tag{5.37}$$

$$\omega' = (n_g - l^-)hm + \beta_{1g}h^{3/2}m + \beta_{2g}h^2m. \tag{5.38}$$

The case $\alpha_g = 0$, $\beta_{1g} = 0$, $\beta_{2g} = 0$ corresponds to the resonance at the threshold (5.30), (5.33). Note that the two values of the momentum of the particles (5.9) correspond to the fixed values of the photon frequencies and the Landau level numbers of the final particles. Resonance conditions taking into account h^2 differ for these two values of the particle momenta. For definiteness, let us denote by α_{ga}, β_{1ga}, β_{2ga} the coefficients in (5.37), (5.58) corresponding to the upper sign in (5.9), and by α_{gb}, β_{1gb}, β_{2gb} corresponding to the lower sign. After substituting the photon frequencies of the form (5.37), and (5.58) into the expression for the longitudinal momentum of the final electron (5.9) and similarly for the positron, it is easy to find expressions for g_0 and ε_g from (5.24) in the form of an expansion in $h^{1/2}$ up to h^2 inclusive. The requirement that the factors are equal for each degree h in the equation $g_0 = \varepsilon_g$ determines the desired coefficients. For the case a) they are equal:

$$\beta_{1ga} = \sqrt{\alpha_{ga}}(n_g - l^-)u, \tag{5.39}$$

$$\beta_{2ga} = -(n_g - l^-)[u^2(n_g - l^- - 2\alpha_{ga}) + n_g + l^- + \alpha_{ga}]/2. \tag{5.40}$$

Thus, the above-threshold value of the frequency of the initial photon $\alpha_{ga}hm$ does not affect the appearance of resonance, but only changes the parameters (5.39), (5.40). These parameters correspond to the momenta of the electron and positron in the form of expansion:

$$p_a^- = \sqrt{\alpha_{ga}}hm - (n_g - l^-)uh +$$

$$+h^{3/2}[-8\alpha_{ga}u^2(n_g - l^-) + 2\alpha_{ga}(n_g + l^+) + 2(n_g^2 + l^{+2}) + \alpha_{ga}^2]/8\sqrt{\alpha_{ga}}, \tag{5.41}$$

$$p_a^+ = -\sqrt{\alpha_{ga}}hm - h^{3/2}[\alpha_{ga}(n_g + l^+) + (n_g^2 + l^{+2}) + \alpha_{ga}^2/2]/4\sqrt{\alpha_{ga}}, \tag{5.42}$$

as well as the energies of these particles

$$\varepsilon_a^- = m + (l^- + \alpha_{ga}/2)hm - \sqrt{\alpha_{ga}}(n_g - l^-)uh^{3/2}m +$$

$$+\frac{h^2 m}{4}[(n_g^2 + l^{+2} - 2l^{-2}) + \alpha_{ga}(n_g + l^+ - 2l^-) +$$

$$+ u^2(4\alpha_{ga}(l^- - n_g) + 2(l^- - n_g)^2)], \tag{5.43}$$

$$\varepsilon_a^+ = m + (l^+ + \alpha_{ga}/2)hm + h^2 m(n_g - l^+)(n_g + l^+ + \alpha_{ga})/4. \tag{5.44}$$

For the case b), i.e. the lower sign in (5.9) the parameters β_{1gb}, β_{2gb} are equal to the previous value:

$$\beta_{1gb} = \beta_{1ga}, \quad \beta_{2gb} = \beta_{2ga}, \tag{5.45}$$

where you need to replace

$$\alpha_{ga} \to \alpha_{gb}, \; u \to -u. \tag{5.46}$$

To find expressions for the energies and momenta of final particles, one can use relations (5.41) — (5.44), namely

$$p_b^- = -p_a^-, \; p_b^+ = -p_a^+, \; \varepsilon_b^- = \varepsilon_a^-, \; \varepsilon_b^+ = \varepsilon_a^+ \tag{5.47}$$

with replacement (5.46).

When choosing photon frequencies (5.37), (5.38) with coefficients (5.39), (5.40) and selecting electrons and positrons with energies and momenta (5.41) — (5.44) (case a)), the denominator of the Green's function within a given accuracy is equal to zero, and when selecting particles with energies and momenta (5.47), it is proportional to $h^{3/2}$:

$$(g_0 - \varepsilon_g)\big|_a = 0(h^2), \; (g_0 - \varepsilon_g)\big|_b = 2\sqrt{\alpha_g}(n_g - l^-)uh^{3/2}. \tag{5.48}$$

A similar analysis of the resonance conditions takes place for the second Feynman diagram (see Fig.5.5) using equation (5.34). The frequencies of the initial and final photons are given in the form:

$$\omega = 2m + (n_f + l^-)hm + \alpha_f hm, \tag{5.49}$$

$$\omega' = (n_f - l^+)hm + \beta_{1f}h^{3/2}m + \beta_{2f}h^2 m. \tag{5.50}$$

For the case a), that is, the upper sign in (5.9), equation (5.34) is realized up to h^2, inclusive if the coefficients β_{1fa}, β_{2fa} are:

$$\beta_{1fa} = -\sqrt{\alpha_{fa}}(n_f - l^+)u, \tag{5.51}$$

$$\beta_{2fa} = -(n_f - l^+)[u^2(n_f - l^+ - 2\alpha_{fa}) + n_f + l^+ + \alpha_{fa}]/2. \tag{5.52}$$

Note that formulas (5.49) — (5.52) are obtained from similar expressions from the previous analysis of the first Feynman diagram with the following replacement of parameters:

$$\alpha_{ga} \to \alpha_{fa},\ n_g \to n_f,\ l^+ \leftrightarrow l^-,\ u \to -u. \tag{5.53}$$

Longitudinal momenta and energies of the electron and positron are obtained from expressions (5.41) — (5.44) according to the rule

$$p_a^- \to -p_a^+, p_a^+ \to -p_a^-, \varepsilon_a^- \to \varepsilon_a^+,\ \varepsilon_a^+ \to \varepsilon_a^- \tag{5.54}$$

with subsequent replacement (5.53).

When resonance is realized in the case of the lower sign in (5.9) (case b)), the coefficients β_{1fb}, β_{2fb} differ from expressions (5.51), and (5.52) by the sign of the cosine of the angle u, that is, equal

$$\beta_{1fb} = \beta_{1fa},\ \beta_{2fb} = \beta_{2fa}, \tag{5.55}$$

with replacement $\alpha_{ga} \to \alpha_{gb}$, $u \to -u$. The energies and momentum of the particles can be found by rule (5.47) with the same substitution.

The interference of resonances in the first and second Feynman diagrams takes place if the energies and momenta of all the corresponding particles coincide. For the equality of the photon frequencies, which are determined by expressions (5.37), (5.38), and (5.49), (5.50), the equality of the corresponding coefficients is necessary:

$$\alpha_g = \alpha_f,\ \beta_{1ga} = \beta_{1fa},\ \beta_{2ga} = \beta_{2fa}. \tag{5.56}$$

Here, for definiteness, case a) is written, that is, the upper sign in expression (5.9). From equations (5.56) follow the conditions of interference of resonances:

$$l^- = l^+,\ n_g = n_f,\ u = 0, \tag{5.57}$$

which are much more stringent than conditions (5.36), which are necessary for the interference of resonances only up to h.

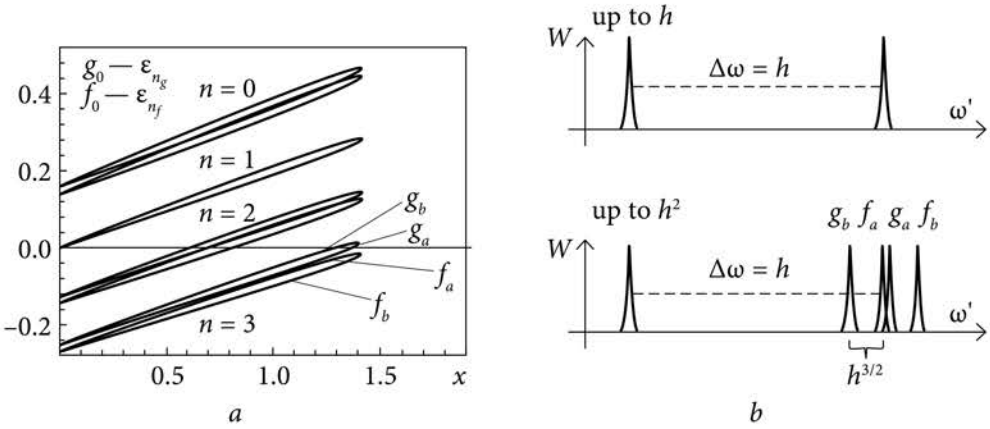

Fig. 5.7. *a* — dependence of the quantities $g_0 - \varepsilon_g$ and $f_0 - \varepsilon_f$ on the radiation frequency ($x = \omega'/hm$); *b* — location of resonances on the graph of the dependence of the probability of the OPPE process on the radiation frequency

Note that the production of a final electron and positron at the same energy levels is not the most probable, since the process in resonance is two-stage. In the first stage, particles are born at equal levels, and in the second stage, one of the particles, emitting a final photon, goes to a lower Landau level.

The case of equality $\omega'_{ga} = \omega'_{fb}$ takes place if the first two equations in (5.57) hold for arbitrary u. In this case, the longitudinal momenta of the electron (positron) in the resonance of the first and second diagrams differ in sign. That is, this is not the interference of two resonances, although the resonances themselves on the graph of the dependence of the process probability on the radiation frequency of the final photon will coincide.

As an illustration, Fig. 5.7. depicts the dependence of the denominators of Green's functions on the frequency of radiation (Fig. 5.7, *a*) and schematic arrangement of resonances (Fig. 5.7, *b*).

To construct the dependences of $g_0 - \varepsilon_g$ and $f_0 - \varepsilon_f$ on the radiation frequency ($x = \omega'/hm$) (see Fig. 5.7, *a*) it was chosen: $l^- = 2$, $l^+ = 1$, $n_f = n$, $n_g = n + 1 (n = 0..4)$, $\omega = 2m + (4 + \alpha)$, $\alpha = 1/20$, $u = 1/20$, $h = 0.2$. In Figure 5.7, *a* 4 groups of curves are presented (cases $n = 0, 1, 2, 3$). In each group, there are four monotonously growing branches (g_a, g_b, f_a, f_b). In the approximation h in the first power, the curves of one group merge into one line. The intersection of zero corresponds to resonance. Therefore, up to h^1, there is only one resonance. With an accuracy of h^2, there are already four resonances (two diagrams for cases *a* and *b*). These zeros correspond to the resonant peaks schematically shown in Fig. 5.7, *b* Two pairs of resonances correspond to two different kinematic regions (cases *a* and *b*). One pair is the outer peaks (case *b*), for which the distance between the peaks is proportional ~ $h^{3/2}$. The

second pair are internal peaks (case *a*), for which the distance between them can be $<< h^{3/2}$.

Thus, taking into account the higher degree of the small parameter h in the analysis of resonance conditions leads to the appearance of pair resonances, the distance between which is much less than the distance between neighboring Landau levels. Pair resonances are clear evidence of the existence of two Feynman diagrams describing the OPPE process. The whole range of possible values of the radiation frequency can be divided into three sections (Fig. 5.7, *b*): 1) a narrow interval of a single resonance, its width $\Gamma \sim e^2h^2m$, 2) a region of pair resonances with the width $\sim h^{3/2}m$, 3) a nonresonant region with a width $\sim hm$.

5.4. Probability of the OPPE process

The amplitudes $Q^{(g)}$ (5.21) of the OPPE process in the ultraquantum approximation with fixed values of the projections of the electron and positron spins and photon frequencies close to the values (5.37), (5.38) are written in the form:

$$Q_{\mathrm{OPPE}}^{-+(g)} = 4\sqrt{2}\sqrt{\frac{n_g h}{l^-}}m^3 G_p G_s e_z H_m^{'*}\,\mathrm{sgn}(p^-), \tag{5.58}$$

$$Q_{\mathrm{OPPE}}^{--(g)} = -4\sqrt{\frac{n_g l^+}{l^-}}hm^3 G_p G_s H_p H_m^{'*}, \tag{5.59}$$

$$Q_{\mathrm{OPPE}}^{++(g)} = 4\sqrt{n_g}hm^3 G_p G_s H_m H_m^{'*}, \tag{5.60}$$

$$Q_{\mathrm{OPPE}}^{+-(g)} \sim h^2, \tag{5.61}$$

where the notation is similar to the expressions (4.52) — (4.55). Functions G_p and G_s are similar (4.57):

$$G_p = \frac{(-1)^{l^+}\eta^{\frac{n_g+l^+}{2}}e^{-\eta/2}}{\sqrt{(l^+)!\cdot(n_g)!}},\quad G_s = e^{-\eta'/2}\eta'^{\frac{n_g-l^--1}{2}}\sqrt{\frac{(n_g-1)!}{(l^--1)!}}\frac{1}{(n_g-l^--1)!} \tag{5.62}$$

and depend on the variables η, η', respectively

$$\eta = \frac{\omega^2}{2hm^2},\quad \eta' = \frac{\omega'^2(1-u^2)}{2hm^2}. \tag{5.63}$$

To establish the relationship between the amplitudes of the processes of OPPE and OPP, SR we write the latter in the ultraquantum approximation. For the SR process with the transition of the electron from the level of n_g to l^-, the values of Q_{SR} in the amplitude (2.39) with the same fixed electron spins are equal to:

$$Q_{SR}^{--} = -2\sqrt{2}\sqrt{\frac{n_g h}{l^-}}m^2 G_s H_m^{'*}, \quad Q_{SR}^{++} = -2\sqrt{2}\sqrt{h}m^2 G_s H_m^{'*}. \tag{5.64}$$

For the OPP process with the electron at the n_g level and the positron at the l^+ level with fixed spins of particles, the value of Q_{OPP} in the amplitude (2.142) is equal to:

$$Q_{OPP}^{-+} = 4m^2 e_z G_p \operatorname{sgn}(p^-), \quad Q_{OPP}^{--} = -2\sqrt{2}m^2\sqrt{l^+ h}G_p H_p,$$

$$Q_{OPP}^{++} = +2\sqrt{2}m^2\sqrt{l^- h}G_p H_m. \tag{5.65}$$

The amplitudes (5.58) — (5.60) are expressed in terms of (5.64), and (5.65) by simple relations:

$$Q_{OPPE}^{-+(g)} = \frac{-1}{2m}Q_{OPP}^{-+}Q_{SR}^{--}, \quad Q_{OPPE}^{--(g)} = \frac{-1}{2m}Q_{OPP}^{--}Q_{SR}^{--},$$

$$Q_{OPPE}^{++(g)} = \frac{-1}{2m}Q_{OPP}^{++}Q_{SR}^{++}. \tag{5.66}$$

The phase (5.25) of the OPPE process is equal to the sum of phases (2.36) and (2.146) of the first-order processes

$$\Phi_{OPPE} = \Phi_{OPP} + \Phi_{SR}. \tag{5.67}$$

As a result, the sought-for relationship between the amplitudes for the first g diagram has the form:

$$A_{OPPE}^{\mu^-\mu^+(g)} = \frac{-i2mS}{(2\pi)^3}\int d^3 g \sum_{n_g}\frac{A_{OPP}^{\mu_{n_g}\mu^+}A_{SR}^{\mu_{n_g}\mu^-}}{g_0^2 - \varepsilon_g^2}, \tag{5.68}$$

in this case, the spin of the intermediate electron is

$$\mu_{n_g} = \mu^-. \tag{5.69}$$

Note that in the OPPE process in the ultraquantum approximation, the intermediate electron emits a final photon without spin-flip (spin-flip occurred in the DPP process).

Similar to expression (5.68) there is a relationship of amplitudes for the second f diagram

$$A_{\text{OPPE}}^{\mu^-\mu^+(f)} = \frac{-i2mS}{(2\pi)^3}\int d^3f \sum_{n_f} \frac{A_{\text{OPP}}^{\mu^-\mu_{n_f}} A_{\text{SR}}^{\mu_{n_f}\mu^+}}{f_0^2 - \varepsilon_f^2}, \tag{5.70}$$

where $\mu_{n_f} = \mu^+$; $A_{\text{OPP}}^{\mu^-\mu_{n_f}}$ is the amplitude of the process of one-photon e^+e^- pair production with the final electron and the intermediate positron at the Landau levels l^- and n_f, respectively. Q_{OPP} values included in the amplitude have the form:

$$Q_{\text{OPP}}^{-+} = 4m^2 e_z F_p \operatorname{sgn}(p^-), \quad Q_{\text{OPP}}^{--} = -2\sqrt{2}m^2\sqrt{n_f h}F_p H_p,$$

$$Q_{\text{OPP}}^{++} = +2\sqrt{2}m^2\sqrt{l^- h}F_p H_m. \tag{5.71}$$

$A_{\text{SR}}^{\mu_{n_f}\mu^+}$ is the amplitude of the process of synchrotron radiation of the positron with Q_{SR} values that have the form

$$Q_{\text{SR}}^{++} = 2\sqrt{2}\sqrt{\frac{n_f h}{l^+}}m^2 F_s H_p^{'*}, \quad Q_{\text{SR}}^{--} = 2\sqrt{2}\sqrt{h}m^2 F_s H_p^{'*}. \tag{5.72}$$

F_p, F_s functions have the form:

$$F_p = \frac{(-1)^{n_f}\eta^{\frac{n_f+l^-}{2}}e^{-\eta/2}}{\sqrt{(l^-)!\cdot(n_f)!}}, \; F_s = e^{-\eta'/2}\eta'^{\frac{n_f-l^+-1}{2}}\sqrt{\frac{(n_f-1)!}{(l^+-1)!}}\frac{1}{(n_f-l^+-1)!}. \tag{5.73}$$

The phases of the amplitudes are related as follows

$$\Phi_{\text{OPPE}} = \Phi_{\text{OPP}} + \Phi_{\text{SR}} + \pi(n_f - l^+). \tag{5.74}$$

Values $Q^{(f)}$ similar to (5.66) can be written as:

$$Q_{\text{OPPE}}^{-+(f)} = \frac{-1}{2m}Q_{\text{OPP}}^{-+}Q_{\text{SR}}^{++}, \quad Q_{\text{OPPE}}^{--(f)} = \frac{-1}{2m}Q_{\text{OPP}}^{--}Q_{\text{SR}}^{--},$$

$$Q_{\text{OPPE}}^{++(f)} = \frac{-1}{2m}Q_{\text{OPP}}^{++}Q_{\text{SR}}^{++}. \tag{5.75}$$

Thus, the general expression for the amplitude of the OPPE process in the ultraquantum approximation is the sum of two quantities (5.68) and (5.70).

The amplitude of the OPPE process near the resonance (5.36) with particles in the main spin states ($\mu^- = -1$, $\mu^+ = +1$) without insignificant total phase has the form

$$A^{-+}_{\text{OPPE}} = N_1 e_z \Upsilon', \quad N_1 = \frac{(2\pi)^4 e^2 h^{1/2} R \cdot \delta^3(k - k' - p^- - p^+)}{2VS\sqrt{m\omega'}}, \tag{5.76}$$

$$\Upsilon' = \left[\frac{H'^{*}_{m} e^{i\kappa'\chi}}{(\omega' - \varepsilon_g + \varepsilon^-) + i\dfrac{n_g \Gamma}{2}} - \frac{H'^{*}_{p} e^{-i\kappa'\chi}}{(\omega' - \varepsilon_f + \varepsilon^+) + i\dfrac{n_f \Gamma}{2}} \right], \tag{5.77}$$

where width $\Gamma = 4e^2h^2m/3$, $R = (n_g / l^-)^{1/2} |G_p| G_s$, the χ value has the form:

$$\chi = (\varphi' - \varphi) - \sin\theta' \cdot \sin(\varphi' - \varphi). \tag{5.78}$$

The expression for the amplitude is simplified in the case of particle production at the same Landau levels ($l^+ = l^- = l, n_g = n_f = n$):

$$\Upsilon' = \frac{2i(u\cos\alpha' \cdot \sin\kappa'\chi + \sin\alpha' \cdot \cos\kappa'\chi \cdot e^{-i\beta'})}{(\omega' - \omega_{res}) + i\dfrac{n\Gamma}{2}}, \tag{5.79}$$

The amplitudes of the process with particles in other spin states have a similar simple form:

$$A^{--}_{\text{OPPE}} = N_1 \sqrt{\frac{l^+ h}{2}} H_p \Upsilon', \quad A^{++}_{\text{OPPE}} = N_1 \sqrt{\frac{l^- h}{2}} H_m \Upsilon'. \tag{5.80}$$

Resonant probability of the OPPE process. Let us write down an expression for the probability of the OPPE process at a point near the resonance of the first *g* diagram with an accuracy of h^2 (a narrow region of the individual resonance), when conditions (5.39), (5.40) are satisfied, and particles are produced in the ground spin states W^{-+}. The probabilities with other spin states W^{--}, W^{++} are not difficult to obtain by replacing the expression for the amplitude (5.76) with (5.80). The second term in (5.77) can be neglected. The differential probability of the OPPE process is equal to the product of the square of the modulus of the amplitude (5.76) by the number of final states *dN*,

$$dN = \frac{VS^2}{(2\pi)^7} d^3k' \cdot d^2p^+ \cdot d^2p, \tag{5.81}$$

and can be reduced to the form:

$$dW_{\text{OPPE}}^{-+(g)} = \frac{e^4}{64(2\pi)^2\,\omega\omega' m^6}\left|\frac{Q_{\text{OPPE}}^{-+(g)}}{g_0 - \varepsilon_g + i\dfrac{n_g\Gamma}{2}}\right|^2 \times$$

$$\times\,\delta(\omega - \omega' - \varepsilon^+ - \varepsilon^-)d^3k'\cdot dp_z\frac{p_y T}{L_x}. \qquad (5.82)$$

The $p_y T/L_y$ multiplier is traditionally interpreted as hm^2. The Dirac delta function of the particle energies removes the integral over the longitudinal momentum of the electron, $p = |p_z| = (\alpha_g h)^{1/2}m$. In this case, the probability does not depend on the azimuthal angles of photons and is equal to:

$$\frac{dW_{\text{OPPE}}^{-+(g)}}{d\omega' du} = \frac{e^4 h\omega' |\,Q_{\text{OPPE}}^{-+(g)}\,|^2}{2^8(2\pi)m^4 p}\left[\frac{1}{(g_0 - \varepsilon_g)_a^2 + \dfrac{n_g^2\Gamma^2}{4}} + \frac{1}{(g_0 - \varepsilon_g)_b^2 + \dfrac{n_g^2\Gamma^2}{4}}\right]. \qquad (5.83)$$

The subscripts *a* and *b* at the brackets in the denominator of the terms in square brackets of expression (5.83) correspond to the kinematics of the process described by expression (5.9) with upper and lower signs, respectively. Note that only one of the two terms remains essential in the square brackets of expression (5.83) at resonance up to h^2. These terms can be considered equal with an accuracy of the order of h^1. Taking into account the relationship between the amplitudes (5.66), as well as expressions for the probabilities SR of an electron $dW_{\text{SR}\,e^-}^{--}/du$ (2.46) and OPP W_{OPP}^{-+} (2.156), the expression for the OPPE probability can be reduced to the Breit-Wigner form (for definiteness, the first term is left (case a)):

$$\left.\frac{dW_{\text{OPPE}}^{-+(g)}}{d\omega' du}\right|_a = \frac{1}{4\pi}\frac{W_{\text{OPP}}^{-+}\cdot\dfrac{dW_{\text{SR}\,e^-}^{--}}{du}}{(\omega' - (\varepsilon_g - \varepsilon^-))_a^2 + \dfrac{n_g^2\Gamma^2}{4}}. \qquad (5.84)$$

Factorization of expression (5.84) means the independence of the processes of the electron-positron pair production by the initial photon and emission of the final photon by the intermediate electron. Similar relations are valid for other spin states of particles:

$$\left.\frac{dW_{\text{OPPE}}^{\mu^-\mu^+(g)}}{d\omega' du}\right|_a = \frac{1}{4\pi}\frac{W_{\text{OPP}}^{\mu_{n_g}\mu^+}\cdot\dfrac{dW_{\text{SR}\,e^-}^{\mu_{n_g}\mu^-}}{du}}{(\omega' - (\varepsilon_g - \varepsilon^-))_a^2 + \dfrac{n_g^2\Gamma^2}{4}}, \qquad (5.85)$$

where μ_{n_g} is determined from (5.69).

Let us estimate the integral probability of the OPPE process in the region of resonances a) and b), where conditions (5.39), and (5.40) are satisfied with accuracy h^2. Taking into account

$$\int_{\Gamma} \frac{A dx}{(x-x_0)^2+\Gamma^2/4} \approx A \int_{-\infty}^{+\infty} \frac{dx}{(x-x_0)^2+\Gamma^2/4} = \frac{2\pi A}{\Gamma} \tag{5.86}$$

the integration of expression (5.83) over the frequency ω' within the width $n_g\Gamma$ and the polar angle of photon emission (over u from –1 to 1) gives

$$\Delta W_{\text{OPPE}}^{-+(g)} = \frac{W_{\text{OPP}}^{-+} \cdot W_{\text{SR}\,e^-}^{--}}{n_g \Gamma}, \tag{5.87}$$

where the total probability of the SR process of an electron in the ground spin state $W_{\text{SR}\,e^-}^{--}$ is determined by the integral of expression (2.46) over the photon emission angle with subsequent summation over the polarization of the final photon. The largest integral probability OPPE (5.87) corresponds to the transition of an electron to the neighboring Landau level $W_{\text{SR}\,e^-}^{--} = 4n_g e^2 h^2 m/3 = n_g\Gamma$, then

$$\Delta W_{\text{OPPE}}^{-+(g)} = W_{\text{OPP}}^{-+}, \tag{5.88}$$

that is, we found that the second-order OPPE process in the resonance region is equiprobable with the first-order OPP process. In the case of the e^+e^- pair production in the ground energy states $l^- = l^+ = 0$ ($n_g = 1$) in a magnetic field of value $h = 0.1$ ($H = 4.4 \cdot 10^{12}\,Gs$), the probabilities of OPP and SR are equal in the order of magnitude, respectively:

$$W_{\text{OPP}}^{-+} \sim 10^{10}[1/s], \quad W_{\text{SR}e^-}^{--} \sim 10^{17}[1/s]. \tag{5.89}$$

Near the resonance of the second Feynman diagram (diagram *f* Fig. 5.5), when the conditions (5.39), and (5.40) are satisfied, the probability of ONPV is equal to expression (5.83) with replacement $g \to f$, $g_0 - \varepsilon_g \to f_0 - \varepsilon_f = \omega' - (\varepsilon_f - \varepsilon^+)$. The analysis performed for the first diagram is also valid in this case. The probability of the process in the resonance is factorized, the integral probability of OPPE is equal to the probability of OPP (5.89), i.e. taking into account both diagrams gives a double result (5.89). The difference is that the intermediate particle for the first diagram is an electron, and for the second diagram is a positron.

Synchrotron radiation of a positron. Since in the second Feynman diagram the intermediate state is the positron, it makes sense to give some expres-

sions for the probability of the SR of the positron. The amplitude of the probability of the SR of the positron is equal to (2.39), where

$$Q_1 = J(l',l)M_p^+ M_p{}' De'_z, \quad Q_2 = J(l'-1,l-1)\mu^+ M_m^+ \mu^+{}' M_m{}' De'_z,$$

$$Q_3 = J(l',l-1)\mu^+ M_m^+ M_p^+{}' CH'^*_p, \quad Q_4 = J(l'-1,l)M_p^+ \mu^+{}' M_m^+{}' CH'^*_m,$$

phase $\Phi^+ = -\dfrac{k_x'(2p_y^+ + k_y')}{2hm^2} - (l-l')(\varphi' + \dfrac{\pi}{2})$. The plus sign at the top left indicates the positron, the dash means that the particle is in the final state.

The differential probability of the process per unit time (rate of the process) is determined by expression (2.44), which in the ultraquantum approximation is equal to

$$\frac{dW}{du} = \frac{\alpha\omega'}{16m^3}\left|\sum Q\right|^2,$$

analogs of expressions (2.46) — (2.48) are

$$\frac{dW_{\mathrm{SR}\,e^+}^{++}}{du} = e^2\omega' h\frac{l}{2l'}R_{ll'}^2 \left|H'_p\right|^2, \quad Q^{++} = -2\sqrt{\frac{2lh}{l'}}m^2 R_{ll'}H'^*_p, \tag{5.90}$$

$$\frac{dW_{\mathrm{SR}\,e^+}^{--}}{du} = e^2\omega' h\frac{1}{2}R_{ll'}^2 \left|H'_p\right|^2, \quad Q^{--} = 2\sqrt{2hm^2}R_{ll'}H'^*_p, \tag{5.91}$$

$$\frac{dW_{\mathrm{SR}\,e^+}^{-+}}{du} = e^2\omega' h^2\frac{(l-l')^2}{4l'}R_{ll'}^2 \left|\tilde{H}'_p\right|^2, Q^{-+} = \frac{2(l-l')h}{\sqrt{l'}}m^2 R_{ll'}\tilde{H}'^*_p. \tag{5.92}$$

Note, taking into account the form of the polarization functions (2.43), (4.56), that the SR of a positron differs from the SR of an electron only by the opposite sign of circular polarization.

Probability of the OPPE process in the region of pair resonances. As shown above, for any above-threshold frequency of the initial photon, the probability of emission of a photon with a frequency that is a multiple of the cyclotron frequency has a resonant character. In this case, conditions (5.36) determine the energy levels of intermediate particles n_g, n_f. Under these conditions, hitting the resonance has an accuracy h, that corresponds to the region of pair resonances (see Fig. 5.7, *b*), excluding the narrow peaks themselves. There is the interference of two Feynman diagrams, that is, it is necessary to take into account the contribution from both diagrams. For definiteness, we will choose the same energy levels of particles ($l^+ = l^- = l, n_g = n_f = n$), which simplifies analyti-

cal expressions but does not detract from the generality of consideration. The square of the module Υ (5.79) is equal to:

$$|\Upsilon'|^2 = \frac{K(\xi', \Omega')}{(\omega - \omega_{res})^2 + n^2\Gamma^2/4}, \tag{5.93}$$

$$K(\xi', \Omega') = 2[u^2 \sin^2 \kappa'\chi + \cos^2 \kappa'\chi + \xi_3' \times$$
$$\times (u^2 \sin^2 \kappa'\chi - \cos^2 \kappa'\chi) + \xi_1' u \sin 2\kappa'\chi]. \tag{5.94}$$

The second term with width Γ in the denominator (5.93), in principle, should be discarded, because in this area it is very small. The differential probability of OPPE has the form:

$$\left.\frac{dW^{-+}}{d\omega' du}\right|_a = \frac{B \cdot K(\xi', \Omega')}{(\omega' - \omega_{res})_a^2 + \frac{n^2\Gamma^2}{4}}, \quad B = \frac{(e^2 Rhme_z)\omega'}{2(4\pi)^2 p}, \tag{5.95}$$

where the lower index a corresponds to the longitudinal momentum of the electron directed along the field (upper sign (5.9)).

The angular dependence of the probability of OPPE is characterized by the function $K(\xi', \Omega')$ shown in Fig. 5.8. The function $K(\xi', \Omega')$ with parameters $l = l'$, $\xi_1' = \xi_3' = 2^{-1/2}$, $\kappa' = 1$ has maxima at $u = 1$ and $\varphi' - \varphi = n\pi/2$. The significant dependence of the process probability on the difference between the azimuthal angles of the initial and final photons in the region of an individual resonance is the difference between the region of pair resonances and the narrow region of an individual resonance.

The differential probability of the OPPE process (5.95), summed over the polarization of the final photon, is proportional to the quantity

$$\sum_{\xi'} K(\xi', \Omega') = 4[u^2 \sin^2 \kappa'\chi + \cos^2 \kappa'\chi]. \tag{5.96}$$

The value (5.96) has a maximum value of $\Sigma K = 4$, when the radiation is directed along the magnetic field, it does not depend on the azimuthal angles of the photons. If the radiation is perpendicular to the field, the value (5.96) is maximum, when the difference in azimuthal angles $\Delta\varphi = \{0, \pi\}$ and is equal to zero, when $\Delta\varphi = 3\pi/4$.

Thus, when photons propagate $\perp \vec{H}$, the radiation in the plane perpendicular to the field in the region of pair resonances is maximum in the direction (parallel and antiparallel) of the initial photons and is absent at an angle $\Delta\varphi = 3\pi/4$. In the region of individual resonance, the radiation does not depend on azimuthal angles.

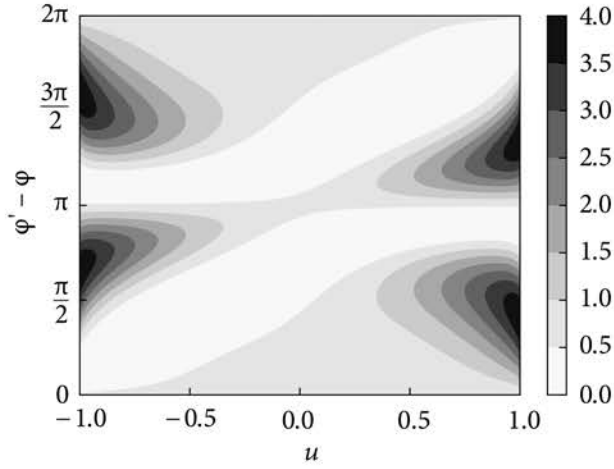

Fig. 5.8. Angular dependence of the probability of OPPE in the region of pair resonances, $l = l'$, $\xi_1' = \xi_3' = 2^{-1/2}$, $\kappa' = 1$

The probability of the OPPE process in the non-resonant region. Consider the process near the threshold, when particles are produced in the ground energy states:

$$\omega = 2m + amh^2, \quad l^+ = l^- = 0, \quad \mu^+ = -\mu^- = 1, \tag{5.97}$$

where $a \sim 1$. In this case, the frequency of the final photon and the momentum of the final electron can be written as:

$$\omega' = \kappa' mh^2, \quad |p^-| = \sqrt{a - \kappa'}hm, \quad 0 < \kappa' < a. \tag{5.98}$$

Only two terms $n_g = 0, 1$ ($n_f = 0, 1$) remain in the amplitude (5.20), and (5.21) in the sums over the energy levels of the intermediate particle. The amplitude can be reduced to the form

$$A_{if} = \frac{-ie^2(2\pi)^4\delta^3(k - k' - p^+ - p^-)}{4VS\sqrt{\omega\omega' m^+ m^- \varepsilon^+ \varepsilon^-}} \sum,$$

$$\sum = 4m\frac{1}{h}e^{-1/h}e_z e^{-i\Lambda/2}\mathrm{Y}, \tag{5.99}$$

$$\mathrm{Y} = \left[\Delta e'_z \frac{\sqrt{a - \kappa'}}{\kappa'} - H_m'^{*} e^{i\Delta\varphi} + H_p'^{*} e^{i\Lambda - i\Delta\varphi}\right], \tag{5.100}$$

$$\Delta\varphi = \varphi' - \varphi, \quad \Lambda = 2\kappa' h \cdot \sin\theta' \cdot \sin\Delta\varphi, \quad \Delta = \mathrm{sgn}(p^-). \tag{5.101}$$

The differential probability of the process per unit of time is equal to the square of the module (5.99) multiplied by the number of final states:

$$dW = \frac{\pi\alpha^2 h^2 e^{-2/h}}{\sqrt{a-\kappa'}}\,\kappa'\,|e_z|^2\cdot|\Upsilon|^2\,d\omega' d'\Omega', \tag{5.102}$$

where

$$|\Upsilon|^2 = \frac{a-\kappa'}{\kappa'^2}\cdot K + \frac{\Delta\sqrt{a-\kappa'}}{\kappa'}\cdot L + M, \tag{5.103}$$

$$K = (1+\xi'_3)(1-u^2)/2, \tag{5.104}$$

$$L = (1+\xi'_3)\sin 2\theta'(\cos\Delta\varphi - \cos(\Delta\varphi-\Lambda))/2 +$$

$$+\xi'_2\sin\theta'(\cos\Delta\varphi-\cos(\Delta\varphi-\Lambda)) - \xi'_1\sin\theta'(\sin\Delta\varphi+\sin(\Delta\varphi-\Lambda)), \tag{5.105}$$

$$M = (1+u^2) - \xi'_3(1-u^2) + ((1-u^2) -$$

$$-\xi'_3(1+u^2))\cos(2\Delta\varphi-\Lambda) + 2\xi'_1\,u\sin(2\Delta\varphi-\Lambda). \tag{5.106}$$

The angular dependence of the differential probability of the OPPE process (the dependence of the value $|\Upsilon|^2$ on the angles θ' and φ') is shown in Fig. 5.9. To get the graphs Fig. 5.9. the following parameters are selected $h = 0.1$, $a = 1$, $\kappa' = 2/3$, $\Delta = 1$.

After integrating expression (5.102) over the polar and azimuthal angles of the final photon, the differential probability takes the form:

$$\frac{dW}{d\omega'} = \frac{2\pi^2}{3}e^4 h^2 e^{-2/h}(1+\xi_3)Z,\ Z =$$

$$= \left\{\frac{\sqrt{a-\kappa'}}{\kappa'}(1+\xi'_3) + \frac{2\kappa'}{\sqrt{a-\kappa'}}(2-\xi'_3)\right\}. \tag{5.107}$$

Fig. 5.10 shows the spectral dependence of the probability of the OPPE process at different values of the Stokes parameter ξ'_3. with $h = 0.1$, $a = 1$. After summation over the polarization of the final photon and averaging over the polarization of the initial photon, the probability of the OPPE process per unit of time has the form:

$$\frac{dW}{d\kappa'} = \frac{4\pi^2}{3}e^4 m h^4 e^{-2/h}\left\{\frac{\sqrt{a-\kappa'}}{\kappa'} + \frac{4\kappa'}{\sqrt{a-\kappa'}}\right\}. \tag{5.108}$$

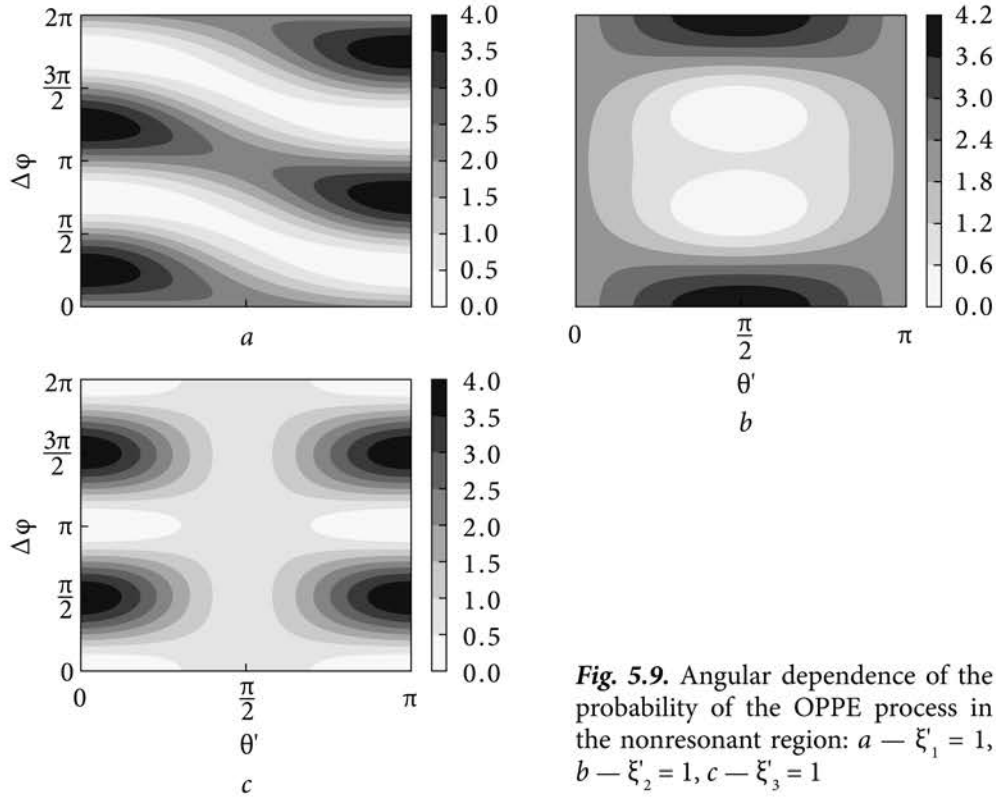

Fig. 5.9. Angular dependence of the probability of the OPPE process in the nonresonant region: *a* — $\xi'_1 = 1$, *b* — $\xi'_2 = 1$, *c* — $\xi'_3 = 1$

Total probability

$$W = \int_0^a \frac{dW}{d\kappa'} d\kappa'$$

logarithmically diverges at the lower bound of integration. The reason for this so-called infrared divergence is that the emission of soft photons is not taken into account in the framework of the perturbation theory of the quantum theory of scattering [190].

The elimination of this divergence is carried out by replacing the lower boundary $0 \to \kappa_{min} = \omega_{min} / h^2 m$, which gives an expression for the total probability per unit time of the OPPE process:

$$W = \frac{4\pi^2}{3} e^4 m h^4 e^{-2/h} \sqrt{a} \left\{ \ln \frac{a}{\kappa_{min}} + \frac{16a}{3} \right\}. \qquad (5.109)$$

Estimation of the probability W in the case when $h = 0.1$, $a = 1$, $\ln = 10$, gives

$$W \approx 10^6 s^{-1}. \qquad (5.110)$$

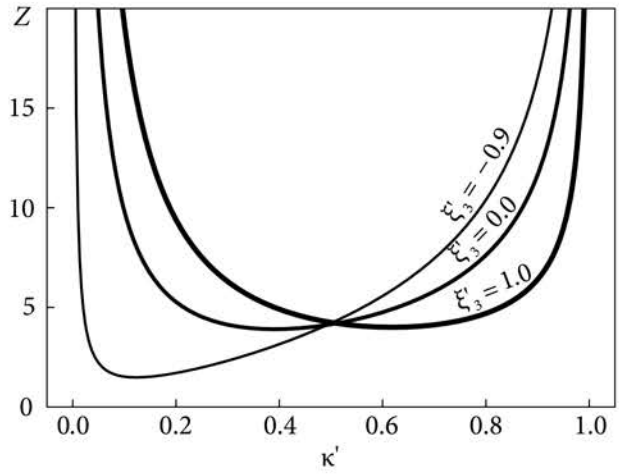

Fig. 5.10. Spectral distribution of the probability of the OPPE at various values of the Stokes parameter ξ'_3

The integral probability of the process within the isolated resonance is equal to the total probability of the OPP (5.88) and for the parameters as in the estimation (5.110) is equal to $10^{10}\,s^{-1}$ (5.89), that is, 4 orders of magnitude greater than the obtained estimation for the nonresonant process (5.109).

5.5. Spin-polarization effects of the OPPE process

To analyze the spin-polarization properties of the particles involved in the OPPE process, it is convenient to write the probabilities of the process with explicitly selected polarization functions. Expressions for the differential probabilities of the OPPE process in the region of individual resonance of the first Feynman diagram g have the form:

$$\frac{dW^{-+(g)}_{\text{OPPE}}}{d\omega' du} = C_g \frac{n_g}{l^-} \tilde{\Pi}\Pi', \quad \frac{dW^{--(g)}_{\text{OPPE}}}{d\omega' du} = C_g \frac{hl^+ n_g}{2l^-} \Pi\Pi',$$

$$\frac{dW^{++(g)}_{\text{OPPE}}}{d\omega' du} = C_g \frac{hn_g}{2} \Pi\Pi', \tag{5.111}$$

where the polarization functions $\Pi, \tilde{\Pi}, \Pi'$ are given by expressions (3.52), (3.64), with u = 0. The factor C_g is a common factor for three expressions (5.111), which does not contain polarization parameters and is determined by the expression for probability (5.85). Similar expressions for the probabilities in the region of

individual resonance of the second Feynman diagram f have the form:

$$\frac{dW_{\text{OPPE}}^{-+(f)}}{d\omega' du} = C_f \frac{n_f}{l^+} \tilde{\Pi}\hat{\Pi}', \quad \frac{dW_{\text{OPPE}}^{++(f)}}{d\omega' du} = C_f \frac{hl^- n_f}{2l^+} \Pi\hat{\Pi}',$$

$$\frac{dW_{\text{OPPE}}^{--(f)}}{d\omega' du} = C_f \frac{hn_f}{2} \Pi\hat{\Pi}', \tag{5.112}$$

where $\hat{\Pi}'$ is defined as the function Π' in which the replacement $\xi'_2 \to -\xi'_2$ is performed. Finally, the expressions for the probabilities of the OPPE process in the interference region and the region of pair resonances in the case $l^- = l^+$ can be reduced to the form:

$$\frac{dW_{\text{OPPE}}^{-+(pair)}}{d\omega' du} = C_p \tilde{\Pi}\text{K}', \quad \frac{dW_{\text{OPPE}}^{--(pair)}}{d\omega' du} = C_p \frac{hl^+}{2} \hat{\Pi}\text{K}',$$

$$\frac{dW_{\text{OPPE}}^{++(pair)}}{d\omega' du} = C_p \frac{hl^-}{2} \Pi\text{K}', \tag{5.113}$$

where K' is defined by expression (5.94) and is more compactly written as:

$$\text{K}' = 2(u^2 S_\chi^2 + C_\chi^2)\left[1 + \frac{u^2 S_\chi^2 - C_\chi^2}{u^2 S_\chi^2 + C_\chi^2} \xi'_3 + \frac{2uS_\chi C_\chi}{u^2 S_\chi^2 + C_\chi^2} \xi'_1\right], \tag{5.114}$$

where $S_\chi = \sin\kappa'\chi$, $C_\chi = \cos\kappa'\chi$.

It should be noted that in all three cases (5.111) — (5.113) the dependence of the probabilities on the Stokes parameters of the final photon is the same for any spin states of the electron and positron. That is, the polarization of the radiation does not depend on the spin states of the particles.

The probabilities summed over the spins of the particles in the three indicated regions, respectively, are equal:

$$\sum_{\mu^-\mu^+} \frac{dW_{\text{OPPE}}^{\mu^-\mu^+(g)}}{d\omega' du} = C_g \frac{n_g}{l^-}\left[\tilde{\Pi} + \frac{h}{2}(l^+ + l^-)\Pi\right]\Pi', \tag{5.115}$$

$$\sum_{\mu^-\mu^+} \frac{dW_{\text{OPPE}}^{\mu^-\mu^+(f)}}{d\omega' du} = C_f \frac{n_f}{l^+}\left[\tilde{\Pi} + \frac{h}{2}(l^+ + l^-)\Pi\right]\hat{\Pi}', \tag{5.116}$$

$$\sum_{\mu^-\mu^+} \frac{dW_{\text{OPPE}}^{\mu^-\mu^+(pair)}}{d\omega' du} = C_p\left[\tilde{\Pi} + \frac{h}{2}(l^+ + l^-)\Pi\right]\text{K}'. \tag{5.117}$$

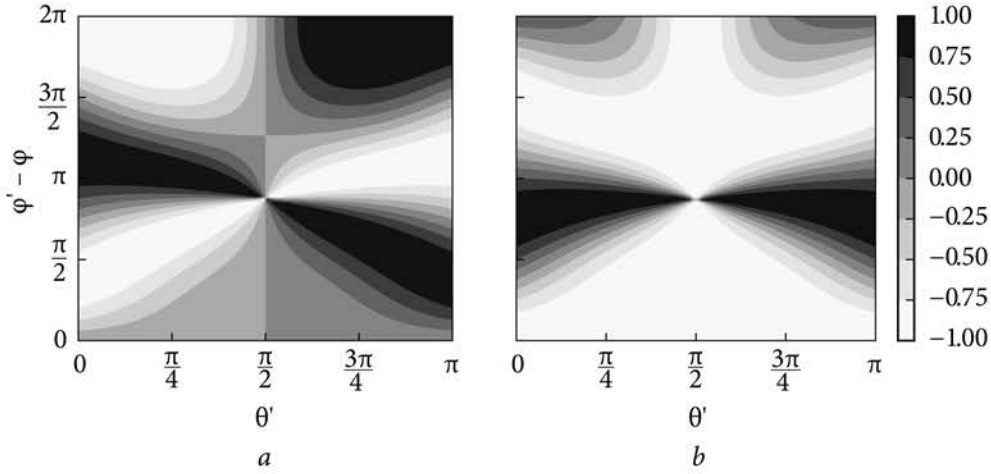

Fig. 5.11. Angular dependence of the Stokes parameters of radiation: *a* — for ξ_1; *b* — for ξ_3

From the written expressions (5.115) — (5.117) it follows that the polarization of the final photon is determined only by the functions Π', $\hat{\Pi}'$, K', respectively, and does not depend on the polarization of the initial photon. In the region of individual resonance of the first Feynman diagram, the polarization of the final photon coincides with the polarization of the classical synchrotron radiation of an electron. And in the region of individual resonance of the second Feynman diagram, the polarization of the final photon coincides with the polarization of the classical synchrotron radiation of a positron. In the region of pair resonances, in the case of $l^- = l^+$, the Stokes parameters of the emitted photon follow from expression (5.114) and are equal to:

$$\xi'_1 = \frac{2uS_\chi C_\chi}{u^2 S_\chi^2 + C_\chi^2}, \quad \xi'_2 = 0, \quad \xi'_3 = \frac{u^2 S_\chi^2 - C_\chi^2}{u^2 S_\chi^2 + C_\chi^2}. \tag{5.118}$$

The angular dependence of the radiation polarization (dependence ξ'_1, ξ'_3 on φ', θ') is shown in Fig. 5.11. As follows from Fig. 5.11, the polarization of radiation in the region of pair resonances substantially depends not only on the polar angle of radiation θ', but also on the difference between the azimuthal angles of the initial and final photons.

The degree of polarization of the radiation, as follows from (5.118), is equal to one

$$P'^2_\xi = \xi'^2_1 = \xi'^2_2 = \xi'^2_3 = 1,$$

that is, the radiation is completely polarized in all directions. In particular, in the interference region ($u = 0$) the radiation is normally linearly polarized:

$\xi'_1 = 0$, $\xi'_2 = 0$, $\xi'_3 = -1$. Note that in the region of pair resonances in all directions there is no circular polarization of radiation. This is because, in the indicated region, two Feynman diagrams make the same contribution, and the circular polarization of radiation differs from these diagrams in sign.

The degree of orientation of the spins of the final particles is determined by relations (2.167), (2.168). For all three cases (the region of individual resonances of the first and second diagrams, the region of pair resonances), for which the probabilities are given by relations (5.111) — (5.113), the degrees of orientation of the spins of electrons (positrons) are given by the same expressions, which have the form:

$$P_{e^-} = -\frac{2\tilde{\Pi} + h(l^+ - l^-)\Pi}{2\tilde{\Pi} + h(l^+ + l^-)\Pi}, \quad P_{e^+} = \frac{2\tilde{\Pi} + h(l^- - l^+)\Pi}{2\tilde{\Pi} + h(l^+ + l^-)\Pi}, \tag{5.119}$$

in this case, as applied to the region of pair resonances in (5.119), one must set $l^+ = l^-$.

Expressions (5.119) coincide with those corresponding to the OPP process (4.95). Thus, the addition of a final photon in the OPP process (that is, the OPPE process) in the resonant kinematics does not affect the degree of orientation of the spins of the final particles and its dependence on the polarization of the initial photon, while the addition of an initial photon in the OPP process (the DPP process) significantly changes spin orientation. This is because the spin states of the intermediate particles are pure in the OPPE process under resonance conditions, while for the DPP process they are mixed.

5.6. Mixed spin states of the intermediate electron (positron) under resonant conditions

Chapter 3—5 considers second-order QED processes, which are cross-channels of one generalized process with the presence of an intermediate electron (positron). Mixed spin states of intermediate particles were found in DSR and DPP processes under resonance conditions with certain values of the spin states of the initial and final particles. In such cases, the resonant probabilities are not factorized.

Let us analyze all possible situations of the appearance of mixed spin states of intermediate particles under the resonance conditions of the process. In total, there are ten second-order QED processes with one intermediate lepton state (intermediate electron or positron). Feynman diagrams of these processes are shown in Fig. 5.12. These diagrams correspond to the following processes: Fig. 5.12, *a* is double synchrotron radiation by an electron (DSR), Fig. 5.12, *b* is absorption of two photons by an electron or double synchrotron absorption (DSA), Fig. 5.12, *c* is scattering of a photon by an electron or Compton scattering (CS),

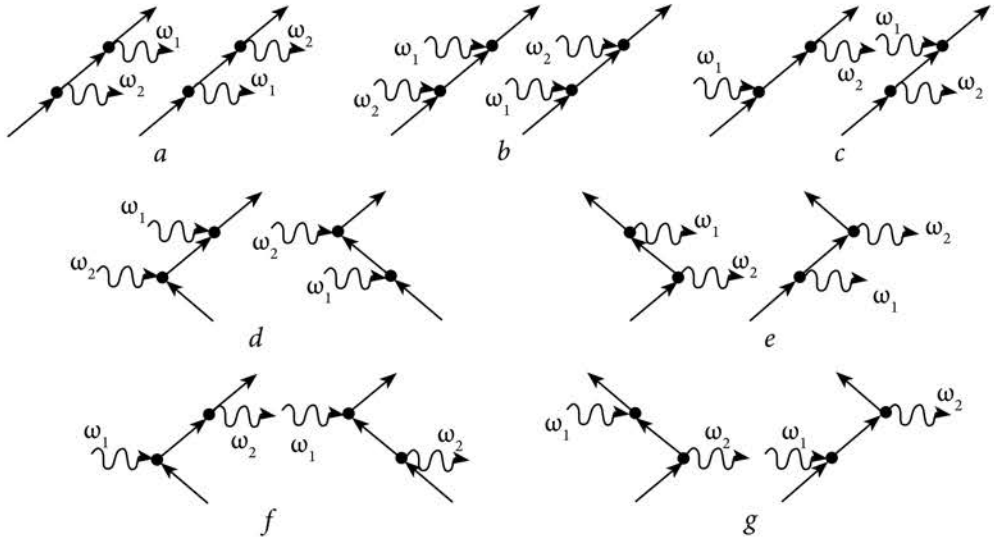

Fig. 5.12. Feynman diagrams of QED processes of the second order with one intermediate lepton state

Fig. 5.12, *d* is two-photon production of an e^+e^- pair (TPP), Fig. 5.12, *e* is the annihilation of an e^+e^- pair into two photons or two photons annihilation of an e^+e^- pair (TPA), Fig. 5.12, *f* is one-photon production of an e^+e^- pair with emission of a photon (OPPE), Fig. 5.12, *g* is the annihilation of an e^+e^- pair into one photon with the absorption of a photon or one photon annihilation with photon absorption (OPAA). Also note that there are three more QED processes with a positron, which are described by Feynman diagrams in Fig. 5.12, *a*, Fig. 5.12, *b*, and Fig. 5.12, *c* with a change in the direction of the arrows of solid lines.

Each QED process, which is depicted in Fig. 5.12, under resonant conditions can be represented as a cascade of two first-order processes, each of which is one of six: emission of a photon by an electron, emission of a photon by a positron, absorption of a photon by an electron, absorption of a photon by a positron, production of e^+e^- pair by a photon, the annihilation of an e^+e^-pair into one photon, with amplitudes $A_{rad\,e^-}, A_{rad\,e^+}, A_{abs\,e^-}, A_{abs\,e^+}, A_{pr}, A_{ann}$, respectively. Cases without a change in direction of a spin of the particles are most probable in the processes of radiation, and absorption of a photon. The particles are in the ground spin states ($\mu^+ = +1$, $\mu^- = -1$) with a greater probability in the processes of production and annihilation of an e^+e^- pair.

Let us write down the degrees of the small parameter *h* of the amplitudes of the process of photon emission by an electron concerning the most probable case ($\mu^- = \mu'^-$) for all spin states of the particles:

$$A^{--}_{rad\,e^-} \sim A^{++}_{rad\,e^-} \sim 1, \quad A^{+-}_{rad\,e^-} \sim \sqrt{h}, \quad A^{-+}_{rad\,e^-} \sim h\sqrt{h}, \qquad (5.120)$$

where the first and second superscript signs (+, –) correspond to the projections of the spins of the initial and final electron, respectively. The powers of parameter h of amplitudes of the process of photon emission by a positron are determined by expressions (5.120) with the replacement of spin states $+ \leftrightarrow -$. The degrees h of amplitudes of the processes of production and annihilation of an e^+e^- pair concerning the most probable case ($\mu^- = -1$, $\mu^+ = +1$) are equal to:

$$A_{pr}^{-+} \sim 1, \quad A_{pr}^{--} \sim A_{pr}^{++} \sim \sqrt{h}, \quad A_{pr}^{+-} \sim h\sqrt{h}, \quad A_{ann}^{\mu^-\mu^+} \sim A_{pr}^{\mu^-\mu^+}. \qquad (5.121)$$

The powers of the parameter h of the amplitudes of absorption of a photon by an electron (positron) are determined from expression (5.120) by mutual replacement of the initial particles with the final ones

$$A_{abs\,e^-}^{\mu^-\mu'^-} \sim A_{rad\,e^-}^{\mu'^-\mu^-}, \quad A_{abs\,e^+}^{\mu^+\mu'^+} \sim A_{rad\,e^+}^{\mu'^+\mu^+}. \qquad (5.122)$$

Note that the intermediate state in the second-order processes under consideration is described by Green's function of the electron, in which the summation over the spin states of the intermediate particle is carried out. Thus, in the general case, the spin states of the intermediate electron (positron) are mixed. The amplitude of the QED process of the second-order under resonance conditions is proportional to the sum (of two terms) of the product of two amplitudes determined by expressions (5.120) — (5.122). The latter, in turn, have different degrees of small parameter h. As a result, cases are possible when only one of the two terms has the smallest degree of h. This corresponds to a pure intermediate state. The probability of the process in such situations is factorized and has the form of the Breit-Wigner formula. If both terms of the above sum have the same degree h, a mixed spin state takes place.

Let's move on to analyzing the amplitudes of the individual processes shown in Fig. 5.12. The amplitudes of the DSR process of an electron $A_{\mathrm{DSR}\,e^-}^{\mu\mu'}$, relative to the most probable cases, taking into account (5.120), have such degrees of the parameter h for the first diagram in Fig. 5.12, *a*

$$A_{\mathrm{DSR}\,e^-}^{--} \sim A_{rad1\,e^-}^{--} A_{rad2\,e^-}^{--} + \cancel{A_{rad1\,e^-}^{+-} A_{rad2\,e^-}^{-+}} \sim 1, (-), \qquad (5.123)$$

$$A_{\mathrm{DSR}\,e^-}^{++} \sim \cancel{A_{rad1\,e^-}^{-+} A_{rad2\,e^-}^{+-}} + A_{rad1\,e^-}^{++} A_{rad2\,e^-}^{++} \sim 1, (+), \qquad (5.124)$$

$$A_{\mathrm{DSR}\,e^-}^{+-} \sim A_{rad1\,e^-}^{+-} A_{rad2\,e^-}^{++} + A_{rad1\,e^-}^{--} A_{rad2\,e^-}^{+-} \sim \sqrt{h}, (\pm), \qquad (5.125)$$

$$A_{\mathrm{DSR}\,e^-}^{-+} \sim A_{rad1\,e^-}^{++} A_{rad2\,e^-}^{-+} + A_{rad1\,e^-}^{-+} A_{rad2\,e^-}^{--} \sim h\sqrt{h}, (\pm), \qquad (5.126)$$

where the subscript numbers 1,2 denote the first and second photons, respectively, the terms with a greater degree of h are crossed out, and the sign of projection of spin of the intermediate electron is indicated at the end of the expressions in parentheses. Thus, in DSW processes without electron spin-flip (5.123), (5.124), the spin intermediate state is pure, and in spin-flip processes, it is a mixed state. This result coincides with the direct calculations of the amplitude of the DSR process performed in Chapter 3. The second Feynman diagram of this process is in Fig. 5.12, *a* is obtained from the first as a result of replacing the photons in places, which does not change the spin states of the particles, that is, the previous result will be true for it as well.

The amplitudes of the process of absorption of two photons by an electron $A^{\mu\mu'}_{\mathrm{DSA}\,e^-}$, relative to the most probable cases, have degrees of the parameter h for the first and second diagrams in Fig. 5.12, *b*, which are determined by expressions (5.123) — (5.126) taking into account rule (5.122). As a result, the pure spin states take place for a process without spin-flip and mixed states for a spin-flip process.

The process of scattering a photon by an electron is described by the first Feynman diagram in Fig. 5.12, *c* (a straight diagram in which the initial particles meet at one point) has relative amplitudes $A^{\mu\mu'}_{\mathrm{CS}}$ (referred to as the magnitude of the amplitude in the most probable spin configuration), which are proportional to such powers of h:

$$A^{--}_{\mathrm{CS}} \sim A^{--}_{rad1\,e^-} A^{--}_{rad2\,e^-} + \cancel{A^{+-}_{rad1\,e^-} A^{+-}_{rad2\,e^-}} \sim 1, (-), \tag{5.127}$$

$$A^{++}_{\mathrm{CS}} \sim \cancel{A^{-+}_{rad1\,e^-} A^{-+}_{rad2\,e^-}} + A^{++}_{rad1\,e^-} A^{++}_{rad2\,e^-} \sim 1, (+), \tag{5.128}$$

$$A^{+-}_{\mathrm{CS}} \sim A^{++}_{rad1\,e^-} A^{+-}_{rad2\,e^-} + \cancel{A^{-+}_{rad1\,e^-} A^{--}_{rad2\,e^-}} \sim \sqrt{h}, (+), \tag{5.129}$$

$$A^{-+}_{\mathrm{CS}} \sim A^{+-}_{rad1\,e^-} A^{++}_{rad2\,e^-} + \cancel{A^{--}_{rad1\,e^-} A^{-+}_{rad2\,e^-}} \sim \sqrt{h}, (+). \tag{5.130}$$

For the second diagram in Fig. 5.12, *c* (exchange diagram), the amplitudes of the process without changing the electron spin are similar to expressions (5.127), (5.128). The relative amplitudes for the spin-flip process are of the following degrees h:

$$A^{+-}_{\mathrm{CS}} \sim A^{+-}_{rad1\,e^-} A^{--}_{rad2\,e^-} + \cancel{A^{++}_{rad1\,e^-} A^{-+}_{rad2\,e^-}} \sim \sqrt{h}, (-), \tag{5.131}$$

$$A^{-+}_{\mathrm{CS}} \sim A^{--}_{rad1\,e^-} A^{+-}_{rad2\,e^-} + \cancel{A^{-+}_{rad1\,e^-} A^{++}_{rad2\,e^-}} \sim \sqrt{h}, (-). \tag{5.132}$$

Thus, for all spin configurations, intermediate spin states in the CS process are pure, which coincides with the direct calculations in Chapter 3. For a spin-flip process, according to the direct Feynman diagram, the spin of the intermediate electron is directed along the field (inverse state), and according to the exchange diagram, the spin of the intermediate electron is directed against the field (ground spin state). It is the presence in the general case of two terms in the amplitudes that explains the same degree of amplitudes for spin-flip processes with spin-flip along and against the field $A^{-+}_{\rm CS} \sim A^{+-}_{\rm CS}$, which differs significantly from the spin-flip process of the SR.

An analysis of the amplitudes of the processes of emission of two photons by a positron, absorption of two photons by a positron, and scattering of a photon by a positron gives the same corresponding expressions (5.127) — (5.132) with mutual replacement of spin states $+ \leftrightarrow -$.

The relative amplitudes of the DPP process, corresponding to the first diagram in Fig. 5.12, *d*, contain the following powers of h:

$$A^{-+}_{\rm DPP} \sim A^{-+}_{pr2} A^{--}_{rad1\,e^-} + \cancel{A^{++}_{pr2} A^{-+}_{rad1\,e^-}} \sim 1, (-), \tag{5.133}$$

$$A^{+-}_{\rm DPP} \sim A^{--}_{pr2} A^{+-}_{rad1\,e^-} + \cancel{A^{+-}_{pr2} A^{++}_{rad1\,e^-}} \sim h, (-), \tag{5.134}$$

$$A^{--}_{\rm DPP} \sim A^{--}_{pr2} A^{--}_{rad1\,e^-} + \cancel{A^{+-}_{pr2} A^{-+}_{rad1\,e^-}} \sim \sqrt{h}, (-), \tag{5.135}$$

$$A^{++}_{\rm DPP} \sim A^{-+}_{pr2} A^{+-}_{rad1\,e^-} + A^{++}_{pr2} A^{++}_{rad1\,e^-} \sim \sqrt{h}, (\pm) \tag{5.136}$$

and similarly to the second diagram of Fig. 5.12, *d*

$$A^{-+}_{\rm DPP} \sim A^{-+}_{pr2} A^{++}_{rad1\,e^+} + \cancel{A^{--}_{pr2} A^{+-}_{rad1\,e^+}} \sim 1, (+), \tag{5.137}$$

$$A^{+-}_{\rm DPP} \sim A^{++}_{pr2} A^{-+}_{rad1\,e^+} + \cancel{A^{+-}_{pr2} A^{--}_{rad1\,e^+}} \sim h, (+), \tag{5.138}$$

$$A^{++}_{\rm DPP} \sim A^{++}_{pr2} A^{++}_{rad1\,e^+} + \cancel{A^{+-}_{pr2} A^{+-}_{rad1\,e^+}} \sim \sqrt{h}, (+), \tag{5.139}$$

$$A^{--}_{\rm DPP} \sim A^{-+}_{pr2} A^{-+}_{rad1\,e^+} + A^{--}_{pr2} A^{--}_{rad1\,e^+} \sim \sqrt{h}, (\pm). \tag{5.140}$$

Here the second photon products a pair, and the first photon is emitted. As a result, in both diagrams, three out of four variants contain pure spin states of intermediate particles, and one variant contains a mixed state. A mixed spin state occurs when particles are produced with identically directed spins, the

spin of an intermediate electron (positron) is directed along the field (against the field), that is, it is in an inverse state. Pure states are ground spin states. The result coincides with the direct calculations of Chapter 4.

For the process of annihilation of an e^+e^- pair into two photons (Fig. 5.12, *e*), the same expressions (5.133) — (5.140), taking into account the property (5.121), will be suitable. That is, the previous conclusions are valid in this case as well.

Finally, we will give estimates of the degrees of h for the relative amplitudes of the OPPE process, which proceeds by the first diagram in Fig. 5.12, *f*. In this case, the first photon products a pair, and the second photon is emitted

$$A^{-+}_{\text{OPPE}} \sim A^{-+}_{pr1}A^{--}_{rad2\,e^-} + \cancel{A^{++}_{pr1}A^{+-}_{rad2\,e^-}} \sim 1,(-), \tag{5.141}$$

$$A^{+-}_{\text{OPPE}} \sim A^{+-}_{pr1}A^{++}_{rad2\,e^-} + \cancel{A^{--}_{pr1}A^{-+}_{rad2\,e^-}} \sim h\sqrt{h},(+), \tag{5.142}$$

$$A^{--}_{\text{OPPE}} \sim A^{--}_{pr1}A^{--}_{rad2\,e^-} + \cancel{A^{+-}_{pr1}A^{+-}_{rad2\,e^-}} \sim \sqrt{h},(-), \tag{5.143}$$

$$A^{++}_{\text{OPPE}} \sim A^{++}_{pr1}A^{++}_{rad2\,e^-} + \cancel{A^{-+}_{pr1}A^{-+}_{rad2\,e^-}} \sim \sqrt{h},(+) \tag{5.144}$$

and for the second Feynman diagram of Fig. 5.12, *f*

$$A^{-+}_{\text{OPPE}} \sim A^{-+}_{pr1}A^{++}_{rad2\,e^+} + \cancel{A^{--}_{pr1}A^{-+}_{rad2\,e^+}} \sim 1,(+), \tag{5.145}$$

$$A^{+-}_{\text{OPPE}} \sim A^{+-}_{pr1}A^{--}_{rad2\,e^+} + \cancel{A^{++}_{pr1}A^{+-}_{rad2\,e^+}} \sim h\sqrt{h},(-), \tag{5.146}$$

$$A^{--}_{\text{OPPE}} \sim A^{--}_{pr1}A^{--}_{rad2\,e^+} + \cancel{A^{-+}_{pr1}A^{+-}_{rad2\,e^+}} \sim \sqrt{h},(-), \tag{5.147}$$

$$A^{++}_{\text{OPPE}} \sim A^{++}_{pr1}A^{++}_{rad2\,e^+} + \cancel{A^{+-}_{pr1}A^{-+}_{rad2\,e^+}} \sim \sqrt{h},(+). \tag{5.148}$$

Thus, in all variants, the spin states of the intermediate particles are pure. The spin-flip process when the second photon is emitted is suppressed; as a result, the direction of the spin of the intermediate particle coincides with the direction of the electron spin for the first diagram and the positron for the second one. The result is the same as the direct calculation done in Section 5.4.

For the process of annihilation of an e^+e^- pair into one photon with the absorption of a photon (Fig. 5.12, *g*), the same conclusions are valid as for the OPPE process.

Thus, the analysis of the spin states of an intermediate particle in ten QED processes under resonance conditions showed that mixed spin states take place

in processes where two photons are involved in the initial or final state, that is, in the processes: emission of two photons by an electron (positron), absorption of two photons by an electron (positron), production of an e^+e^- pair by two photons, the annihilation of an e^+e^- pair into two photons.

5.7. Conclusions

A theory of the process of one-photon production of an electron-positron pair with photon emission (OPPE) is constructed by taking into account the spin of particles in a strong external magnetic field under resonant and nonresonant conditions. As a result, it was shown:

1. The principal difference between the threshold in the OPPE process and the analogous one in the OPP process is that it is possible for any frequency and polar angle of the initial photon (sufficient for the production of a pair) in the first case and corresponds to the threshold maximum possible frequency of the final photon.

2. In the OPPE process, there are pair resonances (a consequence of the presence of two Feynman diagrams), the distance between which is much less than the distance between neighboring Landau levels. Resonance is realized for any above-threshold frequency of the initial photon. In the region of pair resonances, the frequency of the final photon is equal to the distance between the Landau levels of the intermediate and final electron (positron), and there is an «interference» between the two diagrams. To get into the region of individual resonance, it is necessary to select the frequency of the final photon with an accuracy of h^2 inclusive. Pair resonances merge into one when particles are produced at the same energy levels and when a photon is emitted perpendicular to the field.

3. The differential probability of the OPPE process per unit time with a fixed value of the frequency and angle of photon emission at resonance is factorized and reduced to the Breit-Wigner form for any values of the projections of the particle spin. The integral probability of the OPPE process (second-order process) in the region of resonances coincides with the probability of the e^+e^- pair production by one photon (first-order process). In the case of the production of an e^+e^- pair in the ground energy states $l^- = l^+ = 0$ in a magnetic field of $h = 0.1$ ($H = 4.4 \cdot 10^{12}\,Gs$), the OPP and SR probabilities are, respectively, in order of magnitude

$$W^{-+}_{\mathrm{OPP}} \sim 10^{10}[1/s], \quad W^{--}_{\mathrm{SR}e^-} \sim 10^{17}[1/s].$$

4. The difference between the region of pair resonances and the narrow region of an individual resonance is significant dependence on the probability of the process in the first case on the difference between the azimuthal angles $\Delta\varphi$ of the initial and final photons. When the initial photon propagates $\perp \vec{H}$

in the region of pair resonances, the radiation is maximum in the plane, that is perpendicular to the field, in the direction (parallel and antiparallel) of the initial photons, and is absent at an angle $\Delta\varphi = 3\pi/4$. Estimation of the probability W in the nonresonant region near the threshold, when particles are produced in the ground energy states, for $h = 0.1$ gives a value $W \approx 10^6 s^{-1}$ that is four orders of magnitude less than the probability of the process in a region of the individual resonance.

5. In the region of individual resonance of the first Feynman diagram (see Fig. 5.5), the polarization of the final photon coincides with the polarization of the classical synchrotron radiation of an electron. In the region of individual resonance of the second Feynman diagram, the polarization of the final photon coincides with the polarization of the classical synchrotron radiation of a positron. In the region of pair resonances, if the e^+e^- pair is born at the same Landau levels ($l^- = l^+$), the polarization of the radiation depends on both the polar angle and the azimuthal angle and is purely linear in any direction. The polarization of the initial photon does not affect the polarization of the final one. The degree of orientation of the electron and positron spins is the same as in the OPP process, that is, the addition of a final photon to the OPP process in resonant kinematics does not affect the spins of the final particles.

6. An analysis of the appearance of pure and mixed spin states of an intermediate particle under resonance conditions in all second-order QED processes with one intermediate lepton state (intermediate electron or positron) showed the following:

— mixed spin states take place in processes where two photons participate in the initial or final states, that is, in the processes: emission of two photons by an electron (positron), absorption of two photons by an electron (positron), production of an e^+e^- pair by two photons, annihilation e^+e^- pairs into two photons;

— in the DSR process without an electron spin-flip, the spin intermediate state is pure, and in the spin-flip process it is mixed;

— a mixed spin state in the DPP process occurs when particles are produced with identically directed spins, while the spin of an intermediate electron (positron) is directed along the field (against the field), that is, it is in an inverse spin state. Pure states are ground spin states.

The main scientific results of this chapter are published in [290—292].

Chapter 6

CASCADE OF e^+e^- PAIR PRODUCTION BY A PHOTON WITH SUBSEQUENT ANNIHILATION TO A SINGLE PHOTON

6.1. Introduction

In this chapter, the cascade of processes of e^+e^- pair production and subsequent pair annihilation (CPPPA) in a strong magnetic field is considered. The polarization operator of a photon in a magnetic field is found by the direct method of scattering theory. The resonant conditions of the CPPPA process are analyzed. A comparison of the amplitude of the CPPPA process with the probability of the OPP process (optical theorem) is performed, as well as an estimate of the ratio of the CPPPA probabilities in non-resonant and resonant cases in the LLL approximation in a subcritical field is found. The influence of the polarization of the initial photon on the polarization of the final one is studied. The effect of vacuum birefringence in a strong magnetic field is analyzed.

6.2. Probability amplitude and resonant conditions of the CPPPA process

Probability amplitude of the CPPPA process. The expression for the amplitude of the process corresponds to the Feynman diagram shown in Fig. 6.1 and it has the form

$$A_{if} = -e^2 Tr \int d^4\mathbf{x}_1 d^4\mathbf{x}_2 (A'(\mathbf{x}_2)^* \gamma) \times$$

$$\times G_{Hg}(\mathbf{x}_2, \mathbf{x}_1)(A(\mathbf{x}_1)\gamma) G_{Hf}(\mathbf{x}_1, \mathbf{x}_2), \qquad (6.1)$$

where $A(\mathbf{x}_1)$, $A'(\mathbf{x}_2)^*$ are the wave functions of the initial and final photons, $G_{Hg}(\mathbf{x}_2, \mathbf{x}_1)$, $G_{Hf}(\mathbf{x}_1, \mathbf{x}_2)$ are the Green's function of the electron in an external magnetic field, γ are

the Dirac gamma matrices, and the symbol *Tr* means a trace of spinor indices. In the general case, the amplitude of the CPPPA process after taking the integrals in (6.1) can be represented as

$$A_{if} = \frac{-8\pi^2 e^2 hm^2}{\omega V}\delta^4(k-k')\sum_{n_g=0}^{\infty}\sum_{n_f=0}^{\infty}\int dg_0 dg_z \frac{\sum_{j=1}^{5} Q_j}{(g_0^2-\varepsilon_g^2)(f_0^2-\varepsilon_f^2)}, \qquad (6.2)$$

where $f_0 = \omega - g_0$, $f_z = k_z - g_z$. The energies of the intermediate states ε_g, ε_f, at fixed Landau levels n_g, n_f are equal to

$$\varepsilon_g = \sqrt{m^2 + 2n_g hm^2 + g_z^2}, \quad \varepsilon_f = \sqrt{m^2 + 2n_f hm^2 + f_z^2}. \qquad (6.3)$$

Note that the amplitude (6.2) contains the factor $\delta^4(k - k')$, which means that in this process, both the law of conservation of energy and the law of conservation of momentum are fulfilled, despite the presence of an external magnetic field. For all the processes discussed earlier in this paper, the amplitude contained only three Dirac delta functions ($\delta(k_x - k_x'$)which is absent in the process amplitudes for the external field potential selected in the Landau calibration). However, given that the laws of dispersion $k^2 = 0$, $k'^2 = 0$ are satisfied for the initial and final photons, and considering that the amplitude always contains $\delta^3(k - k')$ the QED processes in the external field, it is easy to obtain $k_x' = \pm k_x$. The case $k_x' = -k_x$ must be rejected as non-physical, because it corresponds to the case of reflection of a photon, regardless of the value of magnetic field strength and the frequency of the photon.

The quantities Q_j in the amplitude (6.2) have the form

$$Q_1 = (m^2 + gf)[J^{++}J'^{++} + J^{--}J'^{--}], \quad Q_2 = (m^2 + g\tilde{f})[J^{-+}J'^{-+} + J^{+-}J'^{+-}],$$

$$Q_3 = 2\sqrt{n_g n_f}\,hm^2[J^{++}J'^{--} + J^{--}J'^{++} - J^{-+}J'^{+-} - J^{+-}J'^{-+}],$$

$$Q_4 = -2\sqrt{2n_f}\,hmg_z[J^{-+}J'^{++} + J^{++}J'^{-+} + J^{+-}J'^{--} + J^{--}J'^{+-}],$$

$$Q_5 = 2\sqrt{2n_g}\,hmf_z[J^{+-}J'^{++} + J^{++}J'^{+-} + J^{-+}J'^{--} + J^{--}J'^{-+}], \qquad (6.4)$$

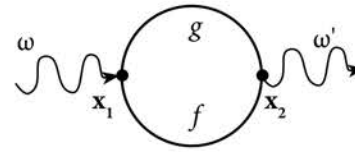

Fig. 6.1. Feynman diagram of the cascade of one-photon e^+e^- pair production and subsequent pair annihilation to a single photon

where $gf = g_0 f_0 - g_z f_z$, $\tilde{gf} = g_0 f_0 + g_z f_z$. The functions J contain the parameters of the initial photon and they are defined as follows

$$J^{++} = J(n_f, n_g) e_z\,,\ J^{--} = J(n_f - 1, n_g - 1) e_z,$$
$$J^{-+} = J(n_f - 1, n_g) H_p\,,\ J^{+-} = J(n_f, n_g - 1) H_m. \tag{6.5}$$

Special functions $J(n_f, n_g)$ are defined by expression (2.37) and polarization functions e_z, H_p, and H_m by expressions (2.43). The functions J' contain the parameters of the last photon and they can be obtained with the expression (6.5) by appropriate substitution and complex conjugation H_p, H_m. In this case, given the presence in the amplitude of the multiplier $\delta^4(k - k')$, we have

$$J'(n_f, n_g) = J(n_f, n_g)\,.$$

Note that the integral in (6.2) diverges logarithmically on the upper bound of the variables g_0, g_z

$$\int dg_0 dg_z \frac{\sum_{j=1}^{5} Q_j}{(g_0^2 - \varepsilon_g^2)(f_0^2 - \varepsilon_f^2)} \xrightarrow{g \to \infty} \int \frac{dg}{g},$$

therefore, it is necessary to carry out the amplitude regularization procedure. We will use Bogolyubov's regularization method [293], according to which such a replacement of the denominator of the Green's function of the intermediate lepton should be performed

$$(g_0^2 - \varepsilon_g^2)^{-1} \to (g_0^2 - \varepsilon_g^2 + im\Gamma)^{-1} - (g_0^2 - \varepsilon_g^2 + m^2 - M^2 + im\Gamma)^{-1}, \tag{6.6}$$

where an additional mass M is introduced, while the magnetic field H should be taken equal to zero. When $M \to \infty$ the expression (6.6) goes to the initial one. In the denominator (6.6) a small imaginary additive $im\Gamma$ according to the Breit-Wigner rule is also introduced for the correct bypass of the poles, while the value Γ makes sense of the width of the intermediate state. A similar substitution is applied to the denominator $(f_0^2 - \varepsilon_f^2)$. Next, the found denominators are converted by Schwinger's proper-time method according to the rule

$$\frac{1}{g_0^2 - \varepsilon_g^2 + im\Gamma} = \frac{1}{i}\int_0^\infty d\tau_1 e^{i\tau_1 (g_0^2 - \varepsilon_g^2 + im\Gamma)},$$
$$\frac{1}{f_0^2 - \varepsilon_f^2 + im\Gamma} = \frac{1}{i}\int_0^\infty d\tau_2 e^{i\tau_2 (f_0^2 - \varepsilon_f^2 + im\Gamma)} \tag{6.7}$$

After the substitutions, the integrals over the variables g_0, g_z in the amplitude (6.2) can be easily calculated using the equality

$$\int_{-\infty}^{\infty} dt e^{\pm i\alpha t^2 + 2i\beta t} = \sqrt{\frac{\pi}{\alpha}} e^{\pm\frac{\pi i}{4} \mp \frac{\beta^2 i}{\alpha}}; \alpha, \beta > 0.$$

Then, according to Bogolyubov's method, the variables are replaced

$$\tau_1, \tau_2 \to \zeta, \lambda: \quad \zeta = \frac{\tau_1}{\tau_1 + \tau_2}, \lambda = \tau_1 + \tau_2.$$

In what follows, we consider the propagation of a photon perpendicular to a magnetic field ($k_z = 0$), which does not affect the generality of the problem.

Elementary integration over λ leads to an amplitude with one integral over ζ. Under $M \to \infty$ and discarding the terms containing the multiplier $\ln(M)$ in the obtained amplitude, the regular part of the amplitude can be reduced to the form

$$A_{if} = \frac{i8\pi^3 e^2 h m^2}{\omega V} \delta^4(k - k') \sum_{n_g=0}^{\infty} \sum_{n_f=0}^{\infty} \int_0^1 d\zeta \times$$

$$\times \left(a - \frac{b}{2} \ln \left| \frac{m^2 \zeta(1-\zeta)}{\omega^2 (\zeta - \zeta_1)(\zeta - \zeta_2)} \right| - \frac{m^2}{\omega^2} \frac{c(\zeta)}{(\zeta - \zeta_1)(\zeta - \zeta_2) - im\Gamma/\omega^2} \right), \qquad (6.8)$$

where

$$a = J^{++} J'^{++} + J^{--} J'^{--} + J^{-+} J'^{-+} + J^{+-} J'^{+-}, \quad b = 2J^{-+} J'^{-+} + 2J^{+-} J'^{+-},$$

$$c(\zeta) = 2a(1 + n_f h) + 4\sqrt{n_f n_g} h J^{++} J'^{--} + 2(n_f - n_g) h a \zeta.$$

The poles ζ_1, ζ_2 have the form

$$\zeta_{1,2} = \frac{1}{2} - \frac{m^2}{\omega^2} h N_- \pm \sqrt{\frac{\omega^2}{m^2} \left(\frac{\omega^2}{m^2} - 4(1 + N_+ h) \right) + 4h^2 N_-^2}, \qquad (6.9)$$

where $N_\pm = n_g \pm n_f$.

The expression for the amplitude (6.8) is obtained in the general relativistic case. What follows, will be analyzed in the LLL approximation. Note that in the LLL approximation near the process threshold $\omega \approx 2m$, both poles $\zeta_{1,2} \approx 1/2$ are within the integration interval.

Resonant conditions. The integrand expression of the amplitude (6.8) generally contains two simple poles, in this case $\zeta_1 \neq \zeta_2$ the width can be neglected. In the case

$$\zeta_1 = \zeta_2, \tag{6.10}$$

two simple poles merge into one second-order pole. The amplitude has a divergence (excluding the width process Γ). This is the resonance of the CPPPA process. The condition (6.10) determines the resonant frequency of the initial photon

$$\omega_{res} = m\sqrt{1+2n_g h} + m\sqrt{1+2n_f h}\,. \tag{6.11}$$

Note that the found expression ω_{res} is accurate. In the previous sections, the resonant frequencies could be found only in the form of a series on the parameter h with accuracy up to the second degree by h. The physical meaning of the resonance condition (6.11) is obvious: in resonance, the frequency of the initial photon is equal to the sum of the energies of the intermediate electron and positron, which are at fixed Landau levels with zero longitudinal momentum

$$\omega_{res} = (\varepsilon^- + \varepsilon^+)\big|_{p^- = p^+ = 0}. \tag{6.12}$$

With a continuous increase of the photon frequency, the resonances will appear in intervals equal to the cyclotron frequency. If the Landau level number of the electron is increased by the fixed value l, and the positron is reduced by the same value, the resonant frequency (6.11) changes slightly. With accuracy up to h^2, this change is equal to

$$\Delta\omega = \omega_{res}(n_g, n_f) - \omega_{res}(n_g + l, n_f - l) = l(n_g + l - n_f)h^2. \tag{6.13}$$

That is, at distances multiple of the cyclotron frequency, a series of resonances are located for which the distance between adjacent peaks is in the order of h^2. In the special case $n_g \neq n_f$, when choosing $l = n_f - n_g$, we can find $\Delta\omega = 0$, in other words, in the same resonant conditions are two different resonances and the amplitude of the process must contain both terms corresponding to them. This result is understandable for reasons of symmetry.

6.3. Probability of the CPPPA process in the resonant and non-resonant conditions

Resonant amplitude and probability of the CPPPA process. Let us take the frequency of the initial photon near the resonance in the form

$$\omega = \omega_{res} + \delta, \quad \delta << \Gamma. \tag{6.14}$$

When the resonant conditions (6.10) are satisfied, the last term in parentheses is the main one in the expression for the amplitude (6.8). After integration over ζ with the subsequent expanding into a power series in small parameter δ and keeping terms linear in h, the amplitude has the form

$$A_{if} = -i\frac{16\pi^4 e^2 h m^5}{V\omega^3\sqrt{\Gamma m}}\delta^4(k-k')c(\zeta_{res})(1+i\frac{2^5\delta}{\Gamma}). \tag{6.15}$$

The expression in parentheses can be rewritten as the denominator of Breit-Wigner

$$(1+i\frac{2^5\delta}{\Gamma}) = \frac{i\Gamma}{2^5}\cdot\frac{1}{\omega-\omega_{res}-i\Gamma/2^5}$$

the probability amplitude of the CPPPA process in the LLL approximation can finally be reduced to the form

$$A_{if} = \frac{\pi^4 e^2 h m^5\sqrt{\Gamma/m}}{2V\omega^3(\omega-\omega_{res}+\frac{i\Gamma}{2^5})}\delta^4(k-k')\times$$

$$\times J^2\left[e_z e'_z(2+h(N_+-2n_g n_f))+hN_+H_m H_m^{'*}\right], \tag{6.16}$$

where $J^2 = e^{-\eta}\eta^{N_+}/(n_g!n_f!)$.

Recalling the probability of one-photon pair production (2.156), we can see that it is expressed through the imaginary part of the amplitude (6.16), thus

$$W_{OPP} = -\sqrt{\frac{4\Gamma}{\delta\omega}}\,\mathrm{Im}\,A_{if}(0), \tag{6.17}$$

where δω is the detuning of the frequency of the initial photon from the threshold of the one-photon pair creation. We note that it is at the threshold of the OPP process that the frequency of the initial photon satisfies the resonant conditions (6.12). $A_{if}(0)$ is the amplitude of the CPPPA process without changing the parameters of the initial photon (with zero changes), in particular, this means

$$e'_z = e_z,\ \delta^4(k-k') = VT/(2\pi)^4.$$

The expression (6.17) is a mathematical notation of the optical theorem. Thus, the optical theorem is valid in resonant conditions.

After integration, the square of the modulus of amplitude (6.16) multiplied by the number of theц final states $Vd^3k/(2\pi)^3$ determines the total prob-

ability of the CPPPA process in resonant conditions, which (ignoring the small correction of the order of h) can lead to the Breit-Wigner formula

$$W_{res} = \frac{\Gamma\delta\omega}{2^{12}} \cdot \frac{W_{OPP}W_{AP}}{[(\omega - \omega_{res}) + \frac{\Gamma^2}{2^{10}}]}, \tag{6.18}$$

where W_{AP} is the probability of one-photon e^+e^- pair annihilation, which differs from W_{OPP} only by replacing the initial photon with the final one and the presence of the Dirac-delta function $\delta(\omega - \omega')$ instead of the multiplier $T/2\pi$. The obtained expression is factorized, which means the decay of the CPPPA process in the resonant conditions into two independent successive processes of the first order: the OPP process and the subsequent one-photon e^+e^- pair annihilation.

In the resonance, expression (6.18) has a simple form

$$W_{res} = \frac{\delta\omega}{4\Gamma} \cdot W_{OPP}W_{AP}. \tag{6.19}$$

We also write an explicit form of the resonant probability

$$W_{res} = \frac{\pi h^2 e^4}{2^5\Gamma} J^4 m^3 T\delta(\omega - \omega') \times$$

$$\times\Big[(1+\xi_3)(1+\xi'_3)(1+(N_+ - 2n_g n_f)h) + N_+ h(\xi_1\xi'_1 + \xi_2\xi'_2)\Big]. \tag{6.20}$$

In Fig. 6.2. the dependence of the probability of the CPPPA process (in relative units) on the value of the magnetic field at different values of the polarization of the initial photon is presented ($n_g = 2$, $n_f = 1$). As follows from Fig. 6.2, the probability of the CPPPA process increases exponentially with increasing magnetic field strength, with the greatest probability of the cascade occurring for abnormally linear polarization of photons ($\xi_3 = 1$).

If the initial photon is set to be normally linearly polarized ($\xi_3 = -1$), then the expression of probability (6.20) with accuracy up to the first degree by the parameter h gives zero, i.e. the process is suppressed. This is a repetition of the situation like in the OPP process (see chapter 2). Taking into account the higher degree of the parameter h gives a nonzero probability value in the case under consideration

$$W_{res}^{\xi_3=-1} = \frac{\pi h^4 e^4}{2^6\Gamma} J^4 m^3 T\delta(\omega - \omega')N_+^2(1 - \xi'_3). \tag{6.21}$$

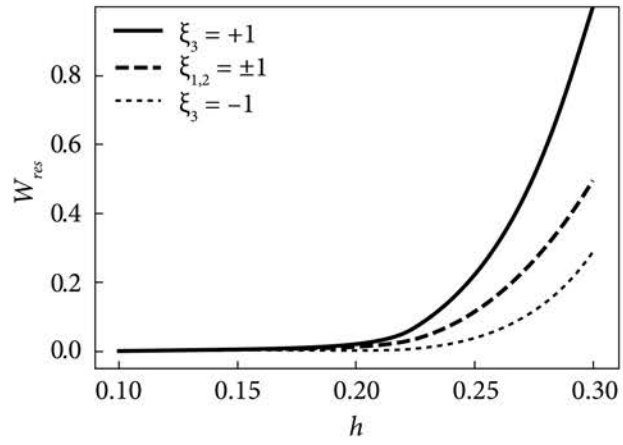

Fig. 6.2. Dependence of probability of the CPPPA process on the magnetic field strength

In the second chapter, it was shown that the probability of one-photon e^+e^- pair production contains a divergence

$$W_{\text{OPP}} \sim \sqrt{\frac{1}{\delta\omega}}$$

in cases when the pair is created with zero longitudinal momentum at fixed Landau levels, i.e. in the resonant conditions. However, since the Landau levels have the finite width Γ, the frequency of the initial photon can only be specified to the nearest width Γ. In other words, in resonance, the detuning of the frequency is approximately equal to the width $\delta\omega \approx \Gamma$.

It should be emphasized that the parameters $\delta\omega$, Γ in the problem of the resonant CPPPA process are phenomenological and the exact proof of the relation between them is beyond the frame of considered approaches. Let us take the detuning of the photon frequency in the form

$$\delta\omega = 4\Gamma. \tag{6.22}$$

This can be argued by the presence of two particles in the intermediate state at fixed Landau levels, remembering that each level is twice degenerate due to spin. Then the probability of the CPPPA process in the resonance (6.19), as well as the optical theorem (6.17) take the form

$$W_{res} = W_{OPP} W_{AP}, \qquad W_{OPP} = -\operatorname{Im} A_{if}(0). \tag{6.23}$$

Note that the probability of the CPPPA process according to expression (6.23) is proportional to the square of the distance traveled by the beam $W_{res} \sim L^2$, which was first noted in [13] for the process of e^+e^- pair production by an electron (analysis of this process will be performed in the next chapter).

Non-resonant CPPPA process. In the range between the resonances, the frequency of the initial photon can be represented as

$$\omega = \omega_{res} + \delta\omega, \ \ \delta\omega = \kappa h m, \tag{6.24}$$

i.e. it consists of the resonant frequency (6.11) and the additional term $\delta\omega$ and which is part of the cyclotron frequency, in this case $0 < \kappa < 1$. In this case and the LLL approximation, the probability amplitude (6.8) can be reduced to the form

$$A_{if} = \frac{-i\pi^4 e^2 h m^2}{V\omega\sqrt{\kappa h}} \delta^4(k - k') J^2 (s_1 e_z e'_z + s_2 H_m H_m^{'*}), \tag{6.25}$$

where $s_1 = 1 + \frac{24i}{\pi}\sqrt{\kappa h} - h(\frac{13}{8}\kappa + \frac{5}{4}N_+ + n_g n_f), \ \ s_2 = \frac{N_+ h}{2}$.

For the amplitude (6.25), the optical theorem holds $W_{OPP} = -\mathrm{Im}\, A_{if}(0)$.

The probability of the CPPPA process in non-resonant conditions corresponding to the amplitude (6.25) has the form

$$W_{nonres} = \frac{\pi e^4 h}{2^{11}\kappa} J^4 m^2 T \delta(\omega - \omega')(1 + \xi_3)(1 + \xi'_3), \tag{6.26}$$

where $s_1 = 1$, $s_2 = 0$.

It should be noted that the found probability (6.26) with accuracy up to a constant factor coincides with the resonant probability (6.20), where small components of the order of the parameter h are discarded. The ratio of the non-resonant probability to the resonant one is equal to

$$\frac{W_{nonres}}{W_{res}} = \frac{\Gamma}{2^6 \kappa h m}. \tag{6.27}$$

For the case $h = 0.1$, $\kappa = 0.5$, this ratio is equal to $W_{nonres}/W_{res} = 3 \cdot 10^{-5}$.

6.4. Polarization effects

Change of photon polarization in the CPPPA process. Let us consider how the polarization of the initial photon changes after the production and annihilation of a pair in a magnetic field. Note that in the expressions for the probabilities of the CPPPA process in resonant (6.20) and non-resonant conditions (6.26) in the largest terms (terms with the least degree of the parameter h), there is the same dependence on the Stokes parameters of the initial and final photons. Thus, the resonance does not change the photon polarization.

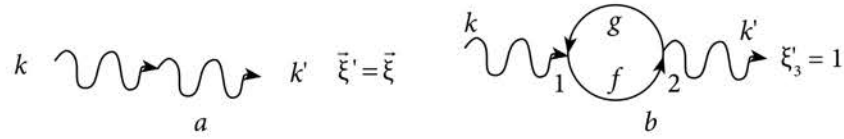

Fig. 6.3. Feynman diagrams of normal *a* — and anomalous *b* — rays for the process of vacuum birefringence in a magnetic field

Let us analyze the photon polarization in the resonant conditions. The polarization degree of the final photon, defined as (2.4), using expressions (6.20) and in this case $\xi_3 \neq -1$ we can be obtained

$$P = \xi'_3 + N_+ h \frac{\xi_1 \xi'_1 + \xi_2 \xi'_2}{1 + \xi_3}, \tag{6.28}$$

whence the expressions for the Stokes parameters of the final photon have the following form

$$\xi'_3 = 1, \quad \xi'_1 = N_+ h \frac{\xi_1}{1 + \xi_3}, \quad \xi'_2 = N_+ h \frac{\xi_2}{1 + \xi_3}. \tag{6.29}$$

Thus, the polarization of the final photon (in the linear approximation by h) is abnormally linear $\xi'_3 = 1$ and it is practically independent of the polarization of the initial photon, and the radiation of the final photon is completely polarized $P = 1$.

In the case when the initial photon is normally linearly polarized $\xi_3 = -1$, the process is suppressed (the probability contains an additional second-order factor of the parameter h). As follows from expression (6.21), the final photon is also normally polarized $\xi'_3 = -1$, i.e. the normal linear polarization of the photon does not change in the CPPPA process.

Note that if a photon is polarized as its polarization mode ($\xi_3 = -1$ is the normal mode, $\xi_3 = 1$ is anomalous mode), its polarization does not change when propagated in a magnetic field, which is a known result [171].

Vacuum birefringence (VB). As follows from an analysis of the above, the CPPPA process in a magnetic field is essentially an «anomalous beam» in the process of birefringence when the beam propagates through an active medium. The active medium is an area of a strong magnetic field. «Normal beam» should be considered the process of photon propagation without production and annihilation of e^+e^- pair, which is described by the diagonal elements of the scattering matrix. The VB process in a magnetic field is described by Feynman diagrams shown in Fig. 6.3. As noted above, the anomalous beam (Fig. 6.3, *b*) almost always has anomalous linear polarization $\xi'_3 = 1$. The normal beam has a polarization that coincides with the polarization of the initial photon $\vec{\xi}' = \vec{\xi}$, because this beam corresponds to the diagonal elements of the scattering matrix *S*.

The amplitude of the VB process corresponding to the Feynman diagrams in Fig. 6.3 consists of two terms

$$A_{if} = A_{if}^{(0)} + A_{if}^{(2)}, \tag{6.30}$$

where $A_{if}^{(2)}$ is the amplitude of the CPPPA process in the general case has the form (6.8), $A_{if}^{(0)}$ is diagonal elements of the scattering matrix for one photon with fixed 4-momentum and polarization, which have the form

$$A_{if}^{(0)} = \frac{(2\pi)^4}{VT}\delta^4(k-k')(\vec{e}\vec{e}'), \tag{6.31}$$

here $(\vec{e}\vec{e}')$ is the convolution of two polarization vectors of the initial and final photons. Let us write the expression for the square of the modulus of this convolution

$$|\vec{e}\vec{e}'|^2 = \frac{1}{2}(1+\vec{\xi}\vec{\xi}'). \tag{6.32}$$

From expression (6.32) follow the obvious properties: 1) the polarization of the final photon is equal to the polarization of the initial one, 2) for the vectors $\vec{e}$ and $\vec{e}'$ such equality is fulfilled

$$\frac{1}{2}\sum_{polar}|\vec{e}\vec{e}'|^2 = 1, \tag{6.33}$$

where $1/2\sum_{polar}$ means averaging over initial and summation over final polarizations. The probability corresponding to the amplitude (6.31) has the form

$$W^{(0)} = \frac{\pi}{T}(1+\vec{\xi}\vec{\xi}')\ (\omega-\omega') \tag{6.34}$$

and it is equal to

$$W^{(0)} = 1, \quad \omega' = \omega,\ \vec{\xi}' = \vec{\xi}. \tag{6.35}$$

The probability of the VB process in a magnetic field corresponding to the amplitude (6.30) in the LLL approximation in resonant conditions (6.12) can be reduced to the form

$$W = \frac{2\pi}{T}\delta(\omega-\omega')M_{\xi\xi'} \tag{6.36}$$

where $M_{\xi\xi'} = \frac{1}{2}(1+\frac{B^2}{2}(1+\xi_3))\left[1+\vec{b}\vec{\xi}'\right]$, $B = \frac{e^2he^{-2/h}}{4\sqrt{\Gamma/m}}mT$. $\vec{b}$ determine the polarization of the final photon and they have the form

$$b_1 = \frac{\xi_1 - B\xi_2}{1+\frac{B^2}{2}(1+\xi_3)},\ b_2 = \frac{\xi_2 + B\xi_1}{1+\frac{B^2}{2}(1+\xi_3)},\ b_3 = \frac{2\xi_3 + B^2(1+\xi_3)}{2+B^2(1+\xi_3)}. \tag{6.37}$$

It should be noted that if we choose for the initial photon $\xi_3 = \pm 1$, $\xi_1 = \xi_2 = 0$ (i.e. the photon is initially abnormally or normally linearly polarized), then from expression (6.37) it follows that $b_3 = \pm 1$, $b_1 = b_2 = 0$. The polarization does not change, which means the well-known above-mentioned result that normal and anomalous linear polarizations are eigenmodes of polarization.

The square of the degree of polarization of the finite photon is equal to

$$P'^2 = 1 - \frac{(1+B^2)(1-P^2)}{(1+B^2(1+\xi_3)/2)^2}, \tag{6.38}$$

where $P^2 = \xi_1^2 + \xi_2^2 + \xi_3^2$ is the square of the degree of polarization of the initial photon. If the initial photon is completely polarized $P = 1$, then the final photon is also completely polarized regardless of the magnetic field strength h and the propagation length of the photon in the magnetic field $L = cT$.

As can be seen from (6.37) the polarization of the finite photon is significantly influenced by L and h, but only due to one parameter B. Let us consider a few limiting cases.

Let $B << 1$ (weak magnetic field and small area size), then the Stokes parameters of the final photon $\vec{b}$ differ slightly from the Stokes parameters of the initial photon $\vec{\xi}$. The change of polarization can be characterized by a change in these parameters $\Delta\vec{\xi} = \vec{b} - \vec{\xi}$, which is equal to

$$b_1 - \xi_1 = -B\xi_2, \quad b_2 - \xi_2 = B\xi_1, \quad b_3 - \xi_3 = 0. \tag{6.39}$$

If $\xi_1 = \pm 1$ (linear polarization at an angle of $\pm 45°$), then

$$b_1 - \xi_1 = 0, \quad b_2 - \xi_2 = \pm B, \quad b_3 - \xi_3 = 0,$$

i.e. in this case, the ellipticity is maximum and proportional to the quantity B. The plane of linear polarization does not change orientation. If $\xi_2 = \pm 1$ (circular polarization), then

$$b_1 - \xi_1 = \mp B, \quad b_2 - \xi_2 = 0, \quad b_3 - \xi_3 = 0,$$

i.e. with accuracy up to the first degree by B, the circular polarization does not change, but the linear polarization at an angle $\mp 45°$ to the magnetic field appears. If $\xi_3 = \pm 1$ (abnormal, normal polarization), then

$$b_1 - \xi_1 = 0, \quad b_2 - \xi_2 = 0, \quad b_3 - \xi_3 = 0,$$

i.e. as mentioned earlier, the polarization does not change. The obtained results are in good agreement with the previously known results of the Cotton-Mouton effect in the framework of classical electrodynamics [294].

Let us consider the case when $B >> 1$ (strong magnetic field and large area). Then $\xi_3 \neq -1$ we have

$$b_1 = -\frac{2\xi_2}{(1+\xi_3)B}, \quad b_2 = \frac{2\xi_1}{(1+\xi_3)B}, \quad b_3 = 1. \tag{6.40}$$

Thus, in the case of large distances and a strong magnetic field, the final photon has predominantly anomalous linear polarization, which weakly depends on the polarization of the initial photon.

If the initial photon is unpolarized $\vec{\xi} = 0$, then after passing the area with the magnetic field, the photon acquires the following Stokes parameters

$$b_1 = 0, \quad b_2 = 0, \quad b_3 = \frac{B^2}{2+B^2} > 0, \tag{6.41}$$

i.e. the final photon is abnormally linearly polarized with the degree of polarization $P' = b_3$, which can be reduced to the form

$$P' = \frac{e^4 h^2 e^{-4/h}}{32\Gamma} m^3 L^2, \tag{6.42}$$

where the width $\Gamma = 4e^2h^2m/3$. In this case, when the linear size L and magnetic field strength H have values characteristic of laboratory conditions ($L \sim 1\ m$, $H < 10^6\ Gs$), the degree P' is negligible, i.e. initially unpolarized ray after passing through such area remains unpolarized, which is a well-known fact. The characteristic value of magnetic field strength for isolated X-ray pulsars is $H = 10^{13}\ Gs$ or $h = 0.2$. For such field values, the degree of polarization is equal to

$$P' \approx 4 \cdot 10^{-13} (L / R_c)^2,$$

where R_c is the Compton wavelength of an electron. The photon ray becomes completely polarized $P' = 1$ at a distance of $L = 1\ \mu m$. Also, it is easy to see from expression (6.42) that for complete polarization of radiation after passing the area ~10km (characteristic size of neutron stars), the required magnetic field strength is $H = 3 \cdot 10^{11}\ Gs$.

6.5. Conclusions

Theory of the cascade of processes of one-photon and electron-positron pair production with subsequent annihilation to a photon taking into account the polarization of photons in a strong external magnetic field in resonant and non-resonant conditions is constructed. As a result, it was shown:

1. In the LLL approximation, the resonances in the CPPPA process occur if the frequency of the initial photon is equal to the sum of the energies of the intermediate electron and positron, which are at fixed Landau levels with zero longitudinal momenta. At distances multiple of the cyclotron frequency, a series of resonances are located for which the distance between adjacent peaks is in the order of h^2.

2. The optical theorem for the probability amplitude of the CPPPA process (the imaginary part of the amplitude without changing the parameters of the initial photon is equal to the total probability of the OPP process with the opposite sign) both in resonant and non-resonant conditions is performed.

3. The expression for the probability of the CPPPA process near the resonance is reduced to the Breit-Wigner form. In the resonance case, the probability of the CPPPA process is equal to the product of the probabilities of the OPP process and one-photon e^+e^- pair annihilation. The greatest probability of the cascade occurs for abnormally linear polarization of photons ($\xi_3 = 1$). The probability of the non-resonant CPPPA process (between resonances) for the field $h = 0.1$ is five orders of magnitude less than for the resonant process.

4. If the initial photon is not normally linearly polarized $\xi_3 \neq -1$, then in the CPPPA process the polarization of the final photon is abnormally linear $\xi'_3 = 1$ and practically it does not depend on the polarization of the initial photon. In the case when the initial photon is normally linearly polarized $\xi_3 = -1$, the process is suppressed (the probability contains an additional factor h^2) and the final photon is also normally polarized $\xi'_3 = -1$. In both cases, the radiation of the final photons is completely polarized $P = 1$.

5. Photons passing through an area with a magnetic field, both without interaction with the vacuum and through the CPPPA process, form two rays of vacuum birefringence. Normally and abnormally linearly polarized photons do not change the polarization in the VB effect. After the photons pass an area of small size (when the change of the polarization of photons is weak), the VB effect coincides with the known quasiclassical result for birefringence in an anisotropic medium in the presence of a magnetic field. If the initial photons ray is unpolarized, then after passing the photons of the area with a magnetic field due to the VB effect, it becomes partially abnormally linearly polarized $\xi'_3 \neq 0$. The degree of polarization depends exponentially on the value of magnetic field strength. In the resonant conditions and the magnetic field $H = 10^{13}$ *Gs*, the photons are completely polarized after passing through the area of size $L = 1\mu m$.

The main scientific results of the section are published in [295—298].

Chapter 7

ELECTRON POSITRON PAIR PRODUCTION BY AN ELECTRON

7.1. Introduction

In this chapter, we study the process of e^+e^- pair production by an electron (trident process), near the threshold in resonance conditions. We aim to calculate the resonant process rate and analyze how the initial electron spin projection influences the process. As an application, we consider the SLAC experiment on the positron production in a collision of a 46.6 GeV electron beam with a terawatt laser pulse [236]. We use the Nikishov-Ritus theorem about the equivalence of the rate of QED processes with ultrarelativistic particles in arbitrary field configuration, and calculate the number of events in the experiment.

7.2. The trident process rate

The probability amplitude of the trident process. The probability amplitude of the process corresponds to Feynman diagrams shown in Fig. 7.1 and can be written as

$$A_{if} = A_1 - A_2, \tag{7.1}$$

$$A_1 = ie^2 \iint d^4x d^4x' (\bar{\Psi}_1 \gamma^\mu \Psi) D_{\mu\nu} (\bar{\Psi}'_2 \gamma^\nu \Psi'_+), \tag{7.2}$$

$$A_2 = ie^2 \iint d^4x d^4x' (\bar{\Psi}_2 \gamma^\mu \Psi) D_{\mu\nu} (\bar{\Psi}'_1 \gamma^\nu \Psi'_+), \tag{7.3}$$

where A_1, A_2 are the amplitudes corresponding to the first and the second diagrams respectively, $\Psi, \bar{\Psi}_1, \bar{\Psi}_2, \Psi_+$ are the wave functions of the initial and final elections and the final positron. Their explicit expressions are given in Chapter 2. The primed functions depend on the primed 4-vector x'; $D_{\mu\nu}$ is the Green function of the intermediate photon

of the form [191]

$$D_{\mu\nu} = \frac{g_{\mu\nu}}{(2\pi)^4} \int d^4k e^{-ik(x-x')} D(k), \quad D(k) = \frac{2\pi}{k^2}. \tag{7.4}$$

Note that when process kinematics allows the denominator of the Green function to vanish (the intermediate photon is on-shell), $k^2 = 0$, (the intermediate photon is on-shell), the process becomes resonant. To eliminate the resonant divergence we use the common Breit-Wigner prescription and introduce the small imaginary term in the photon frequency,

$$\omega \to \omega - i\Delta/2, \tag{7.5}$$

where Δ is a spread in photon frequency (energy width) connected with finite widths of energy levels of the initial and final particles.

Let the magnetic field be directed along the z-axis. The expressions under the integrals in Eqs. (7.2) and (7.3) depend on time and (y, z) coordinates similarly to the considered processes. The integration over these variables yields δ functions expressing the conservation laws of energy and momentum,

$$\varepsilon_l = \varepsilon_1 + \varepsilon_2 + \varepsilon_+, \quad p = p_1 + p_2 + p_+, \tag{7.6}$$

where ε_l, p are the energy and the longitudinal momentum of the initial electron occupying a Landau level l, ε_1, ε_2, ε_+ are the energies of the final particles and p_1, p_2, p_+ are their longitudinal momenta.

Since the magnetic field does not change after Lorentz transformation to a reference frame moving along the z axis, without loss of generality we set the longitudinal momentum of the initial electron to zero,

$$p = 0, \quad \varepsilon_l = m_l = m\sqrt{1 + 2lh}. \tag{7.7}$$

We consider the TRIDENT process near the threshold when the final particles occupy the ground energy level,

$$l_1 = l_2 = l_+ = 0. \tag{7.8}$$

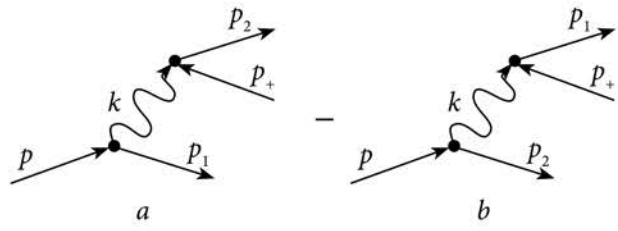

Fig. 7.1. Feynman diagrams of the process of e^+e^- pair production by an electron

After integration in Eq. (7.2) using the special function definition (2.33), the amplitude of the first Feynman diagram (Fig.7.1, *a*) can be transformed to

$$A_1 = \frac{ie^2\pi^2 M_m}{S^2 m_l \sqrt{2\varepsilon_1\varepsilon_2\varepsilon_+}} B_1^\mu \int dk_x D(k) I'^*(l_1,l) I(l_2,l_+) \cdot \delta^3(p - p_1 - p_2 - p_+), \quad (7.9)$$

where the factors B_1^μ are

$$B_1^\mu = \frac{E_m^2 p_1 + E_{1m}^2 p}{E_m E_{1m}} \frac{E_{2m}^2 p_+ + E_{+m}^2 p_2}{E_{2m} E_{+m}} - \frac{E_m^2 E_{1m}^2 + pp_1}{E_m E_{1m}} \frac{E_{2m}^2 E_{+m}^2 + p_2 p_+}{E_{2m} E_{+m}}, \quad (7.10)$$

E_m and M_m are the quantities defined by Eqs. (2.40) and (2.42); S is the normalizing area in the y, z plane; three δ functions express the conservation laws. The arguments of the special functions $I(l_2,l_+)$ and $I'(l_1,l)$ are, respectively,

$$\eta = \frac{\kappa_y^2 + k_y^2}{2hm^2}, \quad \eta' = \frac{\kappa'^2_y + k_y^2}{2hm^2}, \quad (7.11)$$

where

$$\kappa_y = p_{2y} + p_{+y}, \quad \kappa'_y = p_y - p_{+y}. \quad (7.12)$$

Considering the δ functions in Eq. (7.9) we get $\eta = \eta'$, $\kappa_y = \kappa'_y$. Further, due to conditions (7.8), the quantities B_1^μ take the simple form

$$B_1^+ = 4m\sqrt{mm_l}\,\mathrm{sgn}(p_{+z}), \quad B_1^- = 4p_{1z}\sqrt{mm_l}\,\mathrm{sgn}(p_{+z}). \quad (7.13)$$

After the change of variables according to

$$q = \frac{k_x}{m\sqrt{2h}}, \quad s = \frac{p_y - p_{1y}}{m\sqrt{2h}}, \quad u = \frac{p_y - p_{2y}}{m\sqrt{2h}} \quad (7.14)$$

the probability amplitude (7.8) near the process threshold (7.7) finally can be transformed to

$$A_1 = \frac{i2\pi^3 e^2 M_m}{S^2 \sqrt{m_l\varepsilon_1\varepsilon_2\varepsilon_+}\, m\sqrt{l!h}} e^{-a^2} B_1^\mu X_1 \delta^3(p - p_1 - p_2 - p_+), \quad (7.15)$$

Here, the function X_1 is

$$X_1 = \int_{-\infty}^{\infty} dq \frac{(s+iq)^l}{2/h - s^2 - q^2} e^{-q^2 - 2iuq}. \quad (7.16)$$

Amplitude A_2 corresponds to the second Feynman diagram in Fig. 7.1. can be obtained from the expression (7.15) after the change of variables according to

$$e^{-s^2} B_1^{\mu} X_1 \to e^{-u^2} B_2^{\mu} X_2,$$

where B_2^{μ} and X_2 are given by Eqs. (7.13) and (7.15) with index replacements $1 \leftrightarrow 2$ and $s \leftrightarrow u$.

The process kinematics. The kinematics of the trident process is determined by the conservation laws (7.6). The process is possible when $\varepsilon_l \geq 3m$. At first glance, it can be expected that at the process threshold the final particles occupy fixed Landau levels and have zero longitudinal momenta. With the account of (7.6), it results in

$$p_{1z} = p_{2z} = p_{+z} = 0, \quad m_l = m_{l_1} + m_{l_2} + m_{l_+}. \tag{7.17}$$

However, in the general case, these conditions are not fulfilled because the effective masses depend on level numbers, hence they are discrete quantities. Thus, at the process threshold, the final particles can have nonzero longitudinal momenta, in contrast to the SPP process considered in Chapter 2.

Expanding the second equation in (7.17) into a series in small momenta results in an equation of a triaxial ellipsoid in the space of longitudinal momenta of the final particles,

$$\frac{p_{1z}^2}{b_1^2} + \frac{p_{2z}^2}{b_2^2} + \frac{p_{+z}^2}{b_+^2} = 1, \tag{7.18}$$

where $b_1^2 = 2m_{l_1}\delta\varepsilon$, $b_2^2 = 2m_{l_2}\delta\varepsilon$, $b_+^2 = 2m_{l_+}\delta\varepsilon$ and $\delta\varepsilon = m_l - m_{l_1} - m_{l_2} - m_{l_+}$. The possible values of particle momenta correspond to the points λ of an ellipsis defined by the intersection of the ellipsoid (7.18) and a plane defined by the momentum conservation law (7.17) (see Fig. 7.2). Points a and b are the intersections of the ellipsis λ with the plane (p_{+z}, p_{1z}), the points c and d are the intersections of the ellipsis λ with the plane (p_{2z}, p_{+z}).

At the process threshold, the final particles occupy the ground state (see (7.8)) and the following conditions are true,

$$\delta\varepsilon \leq hm, \quad p_{1z} \sim p_{2z} \sim p_{+z} \leq \sqrt{h}m. \tag{7.19}$$

The threshold value of the Landau level number of the initial electron is

$$l_{th} = [4/h] + 1, \tag{7.20}$$

where the square brackets denote the integer part of the number inside.

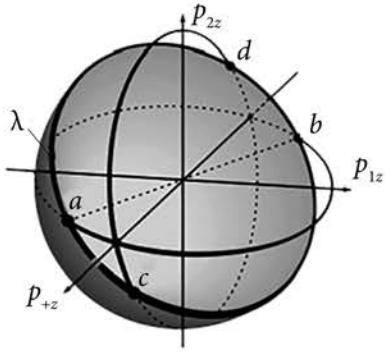

Fig. 7.2. Representation of the threshold momenta of the final particles (ellipsis λ) in the momentum space p_{1z}, p_{2z}, p_{+z}

The trident process rate. The process rate equals the product of the square of the absolute value of the process amplitude and the number of the final states,

$$dN = \frac{S^2 d^2 p_1}{(2\pi)^2} \frac{S^2 d^2 p_2}{(2\pi)^2} \frac{S^2 d^2 p_+}{(2\pi)^2}. \qquad (7.21)$$

The differential rate of the trident process can be transformed to

$$dW^{\mu} = C_0 \left| e^{-s^2} X_1 B_1^{\mu} - e^{-u^2} X_2 B_2^{\mu} \right|^2 \times$$
$$\times \delta^3(p - p_1 - p_2 - p_+) d^2 p_1 d^2 p_2 d^2 p_+, \quad (7.22)$$

where $\mu = \pm 1$ is the spin direction of the initial electron and C_0 is a factor of the form

$$C_0 = \frac{e^4 M_m}{2^7 \pi^3 m^2 \varepsilon_1 \varepsilon_2 \varepsilon_+ m_l^2 l! h}. \qquad (7.23)$$

The integration in $d^2 p_+$ can be carried out using the properties of two Dirac δ functions. After the change of variables $dp_{1y} dp_{2y} = 2m^2 l ds du$, the rate (7.22) takes on the form

$$dW^{\mu} = 2m^2 l C_0 \left[B_1^{\mu 2} Y + B_2^{\mu 2} Y - 2 B_1^{\mu} B_2^{\mu} Y' \right] \delta(m_l - \varepsilon_1 - \varepsilon_2 - \varepsilon_+) dp_1 dp_2, \quad (7.24)$$

where

$$Y = \iint ds du e^{-2s^2} |X_1|^2 = \iint ds du e^{-2u^2} |X_2|^2, \qquad (7.25)$$

$$Y' = \iint ds du e^{-s^2 - u^2} \operatorname{Re}(X_1 X_2^*). \qquad (7.26)$$

Note that the quantity Y' determines the interference term in the process rate.

Consider the case when the final particles occupy the ground level and have nonrelativistic energies, that is

$$p_1, p_2, p_+ << m,$$

Then, near the process threshold the total rate of the trident process can be expressed as

$$W^+ = \frac{e^4 (m_l - m)}{2\pi^3 m_l l!} (Y - Y') \iint \delta(m_l - \varepsilon_1 - \varepsilon_2 - \varepsilon_+) dp_1 dp_2, \qquad (7.27)$$

$$W^- = \frac{e^4 (m_l + m)}{4\pi^3 m^2 m_l l!} (2Y + Y') \iint \delta(m_l - \varepsilon_1 - \varepsilon_2 - \varepsilon_+) dp_1 p_2^2 dp_2, \qquad (7.28)$$

Integrals in Eqs. (7.27) and (7.28) can be calculated using the δ function that depends on the particle's energy. To do so, we transform it according to

$$\delta(f(p_1)) = \frac{\delta(p_1 - g_+)}{\left|\frac{df}{dp_1}\right|_{g_+}} + \frac{\delta(p_1 - g_-)}{\left|\frac{df}{dp_1}\right|_{g_-}}, \tag{7.29}$$

where the function $f(p_1)$ is $f(p_1) = m_l - \varepsilon_1(p_1) - \varepsilon_2 - \varepsilon_+(p_1 + p_2)$ and g_+, g_- are its roots. Near the process threshold, this function and its derivative are

$$f(p_1) = \delta\varepsilon - \frac{p_1^2 + (p_1 + p_2)^2}{2m}, \quad \frac{df}{dp_1} = -\frac{2p_1 + p_2}{m}, \quad \delta\varepsilon = m_l - 3m. \tag{7.30}$$

The roots of the function $f(p_1)$ look like

$$g_\pm = \frac{1}{2}(-p_2 \pm \sqrt{4m\delta\varepsilon - 3p_2^2}). \tag{7.31}$$

It follows from (7.31) that the limit values of the momentum p_2 are

$$-p_{\max} \le p_2 \le p_{\max}, \quad p_{\max} = \sqrt{4m\delta\varepsilon / 3}. \tag{7.32}$$

With these results, the last integration over dp_2 in (7.27) — (7.28) can be easily carried out, and double integrals equal to

$$\iint \delta(m_l - \varepsilon_1 - \varepsilon_2 - \varepsilon_+) dp_1 dp_2 = 2m\pi / \sqrt{3}, \tag{7.33}$$

$$\iint \delta(m_l - \varepsilon_1 - \varepsilon_2 - \varepsilon_+) dp_1 p_2^2 dp_2 = 4\pi m^2 \delta\varepsilon / 3\sqrt{3}. \tag{7.34}$$

Finally, the total rate of the TRIDENT process is

$$W^+ = \frac{e^4 m}{3\sqrt{3}\pi^2 l!}(Y - Y'), \quad W^- = \frac{2e^4 \delta\varepsilon}{9\sqrt{3}\pi^2 l!}(2Y + Y'). \tag{7.35}$$

Note, that the above expressions have been multiplied by the factor of 1/2! to account for particle identity.

Let us now calculate the quantities X_1 and X_2, and consequently Y and Y'. The integral X_1 (7.16) can be easily transformed to

$$X_1 = \sum_{k=0}^{l} C_k^l s^{(l-k)} i^k D_k, \quad C_k^l = \frac{l!}{k!(l-k)!}, \tag{7.36}$$

where C_k^l are the binomial coefficients and D_k are the integrals defined as

$$D_k = \int_{-\infty}^{\infty} \frac{q^k e^{-q^2-2iuq}}{r^2-q^2} dq, \qquad r^2 = \frac{2}{h} - s^2. \tag{7.37}$$

Note that the expression under the integral in (7.37) diverges if the condition $r^2 > 0$ is true. Accordingly, the value of X_1 is small when $r^2 < 0$ and can be neglected. Consequently, we consider the case when the s variable satisfies the condition

$$-\sqrt{2/h} \le s \le \sqrt{2/h}. \tag{7.38}$$

The divergence is eliminated by introducing the width Δ of the intermediate state according to the prescription of Breit and Wigner (7.5),

$$r^2 \to \rho^2 = r^2 + ig, \qquad g = \Delta / mh. \tag{7.39}$$

Let us first calculate the integral D_0 defined by Eq. (7.37) with $k = 0$. It is convenient to use the relation

$$\frac{e^{\rho^2-q^2}}{\rho^2-q^2} = \int_0^1 dt e^{t(\rho^2-q^2)} + \frac{1}{\rho^2-q^2},$$

Inserting this into Eq. (7.37) we obtain

$$D_0 = e^{-\rho^2}(I_1 + I_2), \; I_1 = \int_{-\infty}^{\infty} \frac{e^{-2iuq} dq}{\rho^2-q^2}, \; I_2 = \int_0^1 \sqrt{\frac{\pi}{t}} e^{t\rho^2 - u^2/t} dt. \tag{7.40}$$

Taking into account the prescription (7.39), the first integral I_1 in (7.40) can be written as

$$I_1 = \int_{-\infty}^{\infty} \frac{e^{-2iuq} dq}{\rho^2-q^2} = \frac{-\pi i}{\rho} e^{2i|u|q}. \tag{7.41}$$

To find the integral I_2, take into account the relation

$$\int^t \frac{e^{z-\frac{1}{z}} dz}{\sqrt{z}} = -i\int^t \left(\frac{i}{2\sqrt{z}} + \frac{1}{2z^{3/2}}\right) e^{z-\frac{1}{z}} dz - i\int^t \left(\frac{i}{2\sqrt{z}} - \frac{1}{2z^{3/2}}\right) e^{z-\frac{1}{z}} dz.$$

After a change of variables in the first and the second terms according to

$$y = \sqrt{z}i - \frac{1}{\sqrt{z}}, \; y = \sqrt{z}i + \frac{1}{\sqrt{z}}$$

we get

$$\int_t \frac{e^{z-\frac{1}{z}}dz}{\sqrt{z}} = -i\frac{\sqrt{\pi}}{2}[e^{-2i}erf(\sqrt{t}i-\frac{1}{\sqrt{t}})+e^{2i}erf(\sqrt{t}i+\frac{1}{\sqrt{t}})],$$

where $erf(x)=\frac{2}{\sqrt{\pi}}\int_0^x dye^{-y^2}$ is the error function. The definite integral on an interval [0,1] is

$$\int_0^1 \frac{e^{z-\frac{1}{z}}dz}{\sqrt{z}} = \frac{\sqrt{\pi}}{2}[-2\sin 2+ie^{-2i}erf(1-i)-ie^{2i}erf(1+i)], \tag{7.42}$$

which give us the sought values of the integral I_2,

$$I_2 = \frac{-\pi i}{2\rho}[e^{-2i\rho|u|}erfc(|u|-i\rho)-e^{2i\rho|u|}erfc(|u|+i\rho)], \tag{7.43}$$

Here, $erfc(x)=1-erf(x)$. Finally, by inserting (7.41) and (7.43) in (7.40), the explicit expression of D_0 can be transformed to

$$D_0 = \frac{-i\pi e^{-\rho^2}}{2\rho}[e^{-2i\rho u}erfc(u-i\rho)+e^{2i\rho u}erfc(-u-i\rho)], \tag{7.44}$$

This expression is valid in both cases of $u>0$ and $u<0$.

To find the integral D_k (7.37), we express it as a derivative of D_0 with respect to the parameter u:

$$D_k = \int_{-\infty}^{\infty}\frac{q^k e^{-q^2-2iuq}}{\rho^2-q^2}dq = \frac{1}{(-2i)^k}\frac{\partial^k}{\partial u^k}D_0, \tag{7.45}$$

Finally, with the account of the definition of the Hermite polynomial $H_n(x)$,

$$H_n(x)=(-1)^n e^{x^2}\frac{d^n}{dx^n}e^{-x^2}, \tag{7.46}$$

the expression of D_k can be written in the form

$$D_k = \frac{-i\ e^{-\rho^2}}{2\rho^{1-k}}[e^{-2i\rho u}erfc(u-i\rho)+(-1)^k e^{2i\rho u}erfc(-u-i\rho)]+,$$

$$+\frac{\sqrt{\pi}e^{-u^2}}{i(2i)^k\rho}\sum_{m=1}^{k}C_m^k(2i\rho)^{k-m}[H_{m-1}(u-i\rho)+(-1)^k H_{m-1}(-u-i\rho)]. \tag{7.47}$$

It is clear from Eq. (7.44) that D_0 diverges at the point $\rho = 0$ or $s = \sqrt{2/h}$. At the same time, in this case $k \geq 1$, the expression for D_k (7.47) is finite at the point $\rho = 0$ because it contains factors ρ^{k-1} and ρ^{k-m-1}. It does not diverge in both cases of $m < k$ (apparently), and $m = k$, $\rho = 0$, because of the property of Hermite polynomials,

$$[H_{k-1}(u) + (-1)^k H_{k-1}(-u)] = 0.$$

Consequently, the main contribution in X_1 (7.36) comes from the first term with $k = 0$, i.e.

$$X_1 = s^l D_0. \tag{7.48}$$

Consider now the quantity Y (7.25). The quantity X_1, is an even function of u, hence the integral over u can be written as

$$\int_{-\infty}^{\infty} du\,|e^{-s^2} X_1|^2 = \frac{\pi^2 s^{2l} e^{-4/h}}{2|\rho|^2}(J_1 + J_2), \tag{7.49}$$

$$J_1 = \int_{-\infty}^{\infty} du\,|e^{-2iu\rho} erfc(u - i\rho)|^2, \quad J_2 = \int_{-\infty}^{\infty} du e^{-4iur} erfc(u - ir) \cdot erfc(-u + ir). \tag{7.50}$$

The integral J_1 transforms to

$$J_1 = \frac{1}{\sqrt{\pi}\,\mathrm{Im}(\rho)} \mathrm{Re}(e^{-2ig} j(\rho)), \quad j(\rho) = \int_{-\infty}^{\infty} du e^{-(u+i\rho)^2} erfc(u - i\rho). \tag{7.51}$$

After the change $t = u + i\rho$, the derivative of $j(\rho)$ concerning ρ reduces to the Poisson integral,

$$dj(\rho)/d\rho = 2\sqrt{2} i e^{2\rho^2}. \tag{7.52}$$

With the initial condition $j(\rho) \overset{\rho \to +0}{\to} \sqrt{\pi}$, the solution of the differential equation (7.52) is

$$j(\rho) = \sqrt{\pi} + \sqrt{\pi} erf(i\sqrt{2}\rho). \tag{7.53}$$

Since $\mathrm{Re}(e^{-2ig}) \approx 1$, the quantity J_1 takes the form

$$J_1 = \frac{1}{\mathrm{Im}(\rho)}[1 + \mathrm{Re}(e^{-2ig} erfi(\sqrt{2}\rho))]. \tag{7.54}$$

Similarly, the integral J_2 (7.50) is

$$J_2 = -i \cdot erf(i\sqrt{2}\rho)/r. \tag{7.55}$$

After inserting the obtained expressions (7.54) and (7.55) in (7.49) and (7.25), we can write the sought quantity Y in the form

$$Y = \frac{\pi^2 e^{\frac{-4}{h}}}{2} \int_{-\sqrt{2/h}}^{\sqrt{2/h}} ds \frac{s^{2l}}{|\rho|^2} \left(\frac{1}{\mathrm{Im}\rho} + \frac{\mathrm{Re}(e^{-2ig} erf(i\sqrt{2}\rho))}{\mathrm{Im}\rho} + \frac{erf(i\sqrt{2}\rho)}{ir} \right). \quad (7.56)$$

In the integral over the s variable (7.56), the main contribution comes from small vicinities of the points $s = \pm\sqrt{2/h}$ because of the factor s^{2l}. At these points, the first term in the brackets in (7.56) equals to $\sqrt{2}/\rho$, while the second and the third terms are equal to $\pm\sqrt{8/\pi}$ and can be neglected. The imaginary part of ρ can be written in the form

$$\mathrm{Im}\rho = \sqrt{\sqrt{\rho^4 + g^2} - \rho^2} / \sqrt{2} \quad (7.57)$$

Introducing a new variable $x = s/\sqrt{2/h}$, the quantity Y can be transformed to

$$Y = \frac{\sqrt{2}\pi^2 2^l e^{\frac{-4}{h}}}{g h^l} \int_0^1 dx \cdot x^{2l} \sqrt{\frac{\sqrt{(1-x^2)^2 + \delta^2} + (1-x^2)}{(1-x^2)^2 + \delta^2}}, \quad (7.58)$$

where $\delta = g^2/\sqrt{2/h}$. If δ goes to zero, the integral in x in Eq. (7.58) goes to the value of

$$\frac{\Gamma(1/2)\Gamma(l+1/2)}{\sqrt{2}\Gamma(l+1)}.$$

Finally, the quantity Y takes the form

$$Y = \frac{\pi^2 \sqrt{\pi} 2^l e^{\frac{-4}{h}} \Gamma(l+1/2)}{g h^l l!}. \quad (7.59)$$

The integral Y' (7.26) can be calculated in the same manner. Near the process threshold the condition $2/h >> 1$ is true, and Y' is much less than Y:

$$Y' << Y. \quad (7.60)$$

Finally, near the threshold, the rate of the trident process with the final particles occupying the ground state can be written as

$$W^{+} = \frac{\sqrt{\pi}}{6\sqrt{3}} \cdot \frac{e^4 mh(2/h)^l e^{-4/h} \Gamma(l+\frac{1}{2})}{l!^2\, \Delta / m},$$

$$W^{-} = \frac{2\sqrt{\pi}}{9\sqrt{3}} \cdot \frac{e^4 \delta\varepsilon h(2/h)^l e^{-4/h} \Gamma(l+\frac{1}{2})}{l!^2\, \Delta / m}. \qquad (7.61)$$

The ratio between these rates equals to

$$W^{-} / W^{+} = 4\delta\varepsilon / 3m, \qquad (7.62)$$

Thus, with the account of Eq. (7.19), we conclude that near the process threshold the main channel is a trident with the initial electron in the inverted spin state, ($\mu = +1$). In a particular case when magnetic field strength equals $h = 4/l$ and $\delta\varepsilon = 0$, the trident reaction channel with the initial electron in the ground spin state is forbidden, $W^{-} = 0$.

The obtained Eqs. (7.61) describes the resonant channel of the trident process, when the intermediate photon is on the mass shell. In this case, after averaging over the spin projection of the initial electron, the total process rate decomposes to the product of the rates of the one-vortex processes, namely SR and OPP. It follows from the threshold condition $\varepsilon_l = 3m$ that $hl = 4$ and $l >> 1$ so that the trident rate can be written as

$$W = \frac{\sqrt{\delta\varepsilon / m}}{3\sqrt{6}\,\Delta} \cdot W_{e\to\gamma e} \cdot W_{\gamma\to ee^{+}}, \qquad (7.63)$$

where $W_{e\to\gamma e}$ is the rate of the SR process for the case of radiative transition from a highly excited level $l >> 1$ to the ground level $l' = 0$, and $W_{\gamma\to ee^{+}}$ is the rate of OPP to the ground levels. With the account of Eqs. (2.44), (2.156) and the threshold condition, the rates $W_{e\to\gamma e}$, $W_{\gamma\to ee^{+}}$ are

$$W_{e\to\gamma e} = \sqrt{\pi} e^2 m \frac{(2/h)^l e^{-2/h}}{\Gamma(l+1/2)l}, \quad W_{\gamma\to ee^{+}} = \frac{e^2 mh e^{-2/h}}{2\sqrt{2\delta\varepsilon / m}}. \qquad (7.64)$$

To obtain Eq. (7.63), we used the definition of the gamma function of a half-integer argument and Stirling's formula,

$$\Gamma(l+1/2) = \sqrt{\pi}\,(2l)!/\,4^l l!, \quad l! = \sqrt{2\pi l}\,(l/e)^l.$$

Note that the expression for $W_{\gamma\to ee^+}$ in (7.64) does not account for the electron energy width and diverges if $\delta\varepsilon = \varepsilon_l - 3m$ goes to zero. Account of the corresponding width results in an estimation of the minimum value of $\delta\varepsilon$ of the order of $\Delta \sim e^2h^2m$. On the other hand, to ensure pair production to the ground level we require the condition $\delta\varepsilon < hm$ to be met. Let be $\delta\varepsilon = khm$ with the constant coefficient k and let the magnetic field be $h = h_0 + \varepsilon h$, where h_0 is determined by the threshold condition $kh_0 = \sqrt{1+2lh_0} - 3$. Then, $\delta h = 3kh_0 / l$ which is much less than h_0.

The estimation of the trident rate. As was said before, the quantity Δ entering (7.61) has the meaning of the intermediate state width. The main term in this width is the radiative width, i.e. the full SR rate of the initial electron.

As an example, let the initial parameters be:

$$l = 40,\ h_0 = 0.1 \ \rightarrow\ \delta\varepsilon \approx 0.05m,\ \delta h = 0.00375. \tag{7.65}$$

The width and trident rate estimations are

$$\Delta = 4\cdot 10^{17} c^{-1},\ W^+ = 1.2\cdot 10^4 c^{-1},\ \ W^- = 0. \tag{7.66}$$

According to Eq. (7.64), the corresponding rates of the single-vertex processes are

$$W_{e\to\gamma e} = 2.1\cdot 10^{13} c^{-1},\ \ W_{\gamma\to ee^+} = 7.9\cdot 10^9 c^{-1}. \tag{7.67}$$

Note that in Ref. [13] the resonant e^+e^- pair production by an electron is considered as a two-step cascade of the SR and OPP processes, i.e. the rate was defined as $W = W_{e\to\gamma e}\cdot W_{\gamma\to ee^+}$. The authors use the ultrarelativistic approximation for both the initial electron and the final particles. However, this approximation is not valid near the process threshold when the final particles occupy the ground level. Moreover, Ref. [13] does not take into account the radiative width, and the decay time of the intermediate photon is set to be equal to half the observation time. This results in an overestimation of the process rate near the threshold. In particular, for the parameter values given by (7.56), the estimation is $4.7\cdot 10^7\ s^{-1}$, which is three orders of magnitude greater than the corresponding value (7.66).

Fig. 7.3 shows the dependence of the trident rate on the Landau level number of the initial electron (*a*) and magnetic field strength (*b*) for the parameter values given by (7.56). As can be seen in Fig. 7.3, *a*, the rate W^+ is maximum at the threshold and decreases monotonically with increasing of the level number l. At the same time, the rate W^- reaches its maximum value when the l number exceeds the threshold value by a few levels and then decreases. Note that at sufficiently large values of l the rate W^- exceeds W^+. Fig. shows a moderate decrease of the rate at fixed l while it significantly increases for lower values of the Landau level number of the initial electron.

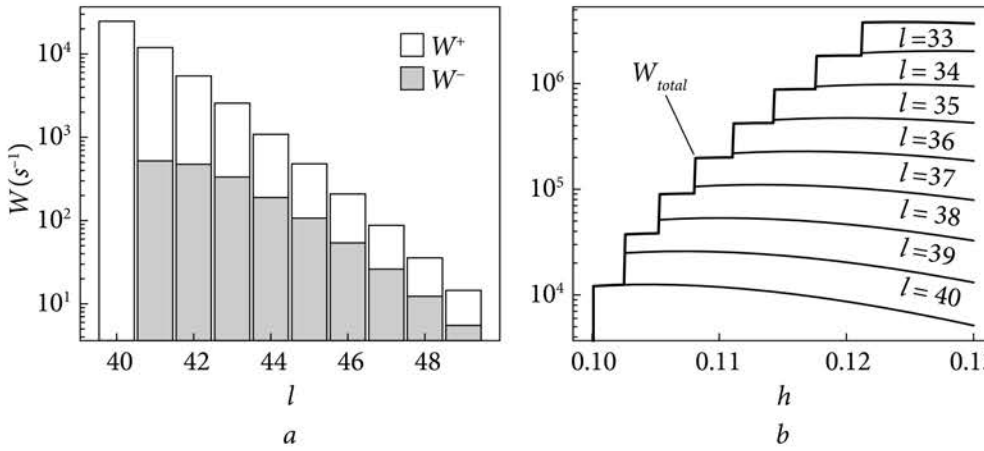

Fig. 7.3. Dependence of the total trident rate on the Landau level number of the initial electron (*a*) and magnetic field strength (*b*) for the parameter values given by (7.56)

Let us now compare the rate of the trident process with the rates of other QED processes in the magnetic field considered in the previous chapters. Table 7.1 shows rates of the SR, OPP, DSR, OPPE, CPPPA, and trident processes in the LLL approximation for magnetic field strength of $h = 0.1$. The first row lists the names of the processes, the second row shows the corresponding Feynman diagrams, the third row lists the initial parameter values and, finally, the last row lists the rate estimation.

To estimate the SR rate we use Eqs. (2.46) — (2.49), with integration over the emission angle, summation over the final polarizations, and averaging over

Table 7.1. **The rates (s^{-1}) of some QED processes in the magnetic field of $h = 0.1$**

SR	OPP	DSR	OPPE	CPPPA	Trident
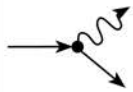	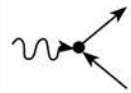	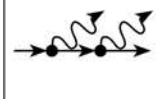	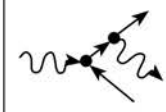	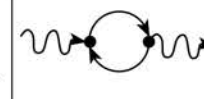	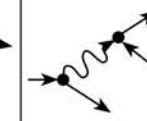
$l = 40$, $l' = 0$	$\omega = 2m$, $l_+ = l_- = 0$	the lowest levels	the lowest levels	the lowest levels	$l = 40$, $\varepsilon_l = 2m$, $l_+ = l_2 = l_1 = 0$
$W^{total}_{e\to\gamma e} \sim 10^{17}$	$W_{\gamma\to e^-e^+} \sim 10^{10}$	$W^{res}_{e\to e\gamma\gamma} \sim W_{e\to e\gamma}$	$W^{nonres}_{\gamma\to\gamma ee^+} \sim 10^6$	$W^{res}_{\gamma\to\gamma} = W_{\gamma\to ee^+} W_{ee^+\to\gamma}$	$W_{e\to eee^+} \sim 10^4$
$W^{\omega>2m}_{e\to\gamma e} \sim 10^{13}$			$W^{res}_{\gamma\to\gamma ee^+} \sim W_{\gamma\to ee^+}$		
$W^{1\to 0}_{e\to\gamma e} \sim 10^{16}$					

the initial electron spin. The initial electron energy is set to $3m$ so that the SR rate equals $W_{e\to\gamma e}^{total} = 2.8\cdot 10^{17}\ s^{-1}$.

Excluding the photon radiation with energy insufficient to produce a pair, it is possible to estimate the rate (7.67) as $W_{e\to\gamma e}^{\omega>2m} = 2.1\cdot 10^{13}\ s^{-1}$. To complete the picture, we also present the estimation of the SR rate for an electron transition from the first excited level to the ground state, $W_{e\to\gamma e}^{1\to 0} = 3\cdot 10^{16}\ s^{-1}$. To estimate the OPP rate we use Eq. (7.64). It was shown in Chapters 3 and 5 that in the resonance conditions, the rates of DSR and OPPE are of the same order of magnitude as the rates of SR and OPP respectively. In other words, adding of another final photon does not change the efficiency of SR and OPP processes at resonance conditions. In resonance conditions, the process of e^+e^- pair production by a photon with subsequent annihilation is purely cascade, and its rate equals the product of the rates of the corresponding first-order processes. Note that the CPPPA process is described by the probability instead of the rate, contrary to the other processes.

7.3. e^+e^- pair production in the SLAC experiment

It is not yet possible to observe the QED processes in an external magnetic field of the strength approaching the critical value. On the other hand, as mentioned in Chapter 1, QED processes have already been observed in experiments with intense laser pulses at SLAC facilities [235—237]. In Ref. [236], the process of e^+e^- pair production by an electron in a pulsed laser field was studied. The schematic layout of the experiment is shown in Fig. 1.6. About 100 positrons have been observed in 21962 collisions of a 46.6 GeV electron beam with green (λ = 527 nm) terawatt laser pulses. The measure of the laser intensity is the work of the field at the wavelength, which equals the classical invariant parameter $\eta = e\sqrt{A^\mu A_\mu}/mc^2$, where A_μ is the electromagnetic 4-potential. In the SLAC experiment conditions, the invariant intensity parameter is η = 0.36.

In Ref. [236], the positron appearance is interpreted as a result of two consequence processes. First, high-energy photons are generated by Compton backscattering in a head-on collision of GeV electrons and a laser pulse. Second, the hard photons create electron-positron pairs in the multiphoton Breit and Wheeler reaction,

$$e^- + n\omega_0 \to e^- + \omega, \tag{7.68}$$

$$\omega + n'\omega_0 \to e^- + e^+, \tag{7.69}$$

where ω_0 denotes a laser photon. Note that in Ref. [236] the two-step process described by (7.68) and (7.69) is distinguished from the less probable «trident» process or PPE process in a laser field,

$$e^- + n''\omega_0 \to e^- + e^- e^+. \tag{7.70}$$

Let us consider in detail how differs descriptions of positron production in both cases, namely two-step production in Compton backscattering and consequent Breit and Wheeler process, and the «trident» production of Bethe-Heitler type. The first case is described by two Feynman diagrams (see Fig. 7.4). The solid lines correspond to wave functions of free electrons (positrons). Note that for the sake of clarity, Fig. 7.4 does not show the exchange diagrams needed for the correct calculation of the process rate.

It should be noted that the description of the generation of a hard photon with energy > $2m_e c^2$ by Compton backscattering according to reaction (7.68) and Feynman diagram 7.4 is not accurate. A more accurate description is the representation of this process by a first-order diagram, namely the photon emission by an electron in an external laser wave. In this case, the Volkov functions are used as wave functions of electrons, which account for the external laser field to all orders of perturbation theory (Fig. 7.5). In Fig. 7.5, the solid lines correspond to the Volkov functions of the electron. As was shown by A.I. Nikishov and V.I. Ritus [202, 203], if the intensity is small and only the absorption of a single photon has a nonzero contribution to the expression of spontaneous photon radiation, then the emission rate coincides with the cross-section of Compton scattering. Thus, reaction (7.68) is entirely contained in the spontaneous emission process shown in Fig. 7.5.

Similarly, the Breit and Wheeler reaction (7.69) should be replaced by single photon e^+e^- pair production in a laser field, Fig. 7.6.

Summarizing the above considerations, the e^+e^- pair production in the SLAC experiment is described by a twostep process: an electron in a laser field emits a hard photon, which propagates in the same laser wave and converts to an e^+e^- pair.

It is worth noting that in this picture the intermediate hard photon ω cannot be observed experimentally. This photon is described by a propagator in the probability amplitude in contrast to the case of a free photon. Therefore the intermediate photon can be either real (i.e., on-shell) or virtual. In particular, the emission and absorption moments are not defined for a virtual photon, hence the situation is possible when e^+e^- pair production happens before the emission of the virtual intermediate photon by the initial electron. Thus, the pair production in the SLAC experiment can be fully described by a Feynman diagram similar to the one shown in Fig. 7.1. This leads us to the second scenario with

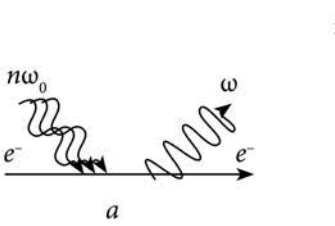

Fig. 7.4. Feynman diagrams: *a* — Compton scattering of *n* laser photons by an electron, *b* — multiphoton Breit-Wheeler process, i.e. pair production of an e^+e^- pair by a hard photon and *n* laser photons

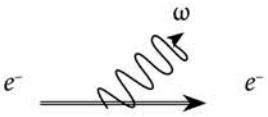

Fig. 7.5. Feynman diagram of photon emission by an electron in a laser wave

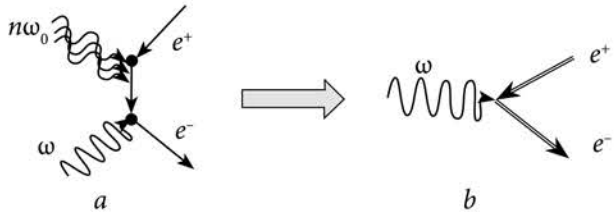

Fig. 7.6. Feynman diagrams: *a* — the Breit-Wheeler process and *b* — the process of single photon e^+e^- pair production in a laser field

the trident process indicated in Ref. [236]. In the resonant conditions, the rate of the trident process decomposes to the product of the rates of the considered one-vertex processes with an additional factor, which can only be obtained within the consistent theoretical treatment.

It is possible to apply the theory of the trident process in a magnetic field (trident process in a magnetic field) to the description of the SLAC experiment [236] by using the Nikishov and Ritus theorem. In Refs. [202, 203], Nikishov and Ritus considered QED processes with relativistic particle energies and proved analytically that the process rates expressed in terms of gauge invariants are the same for any configuration of the external electromagnetic field. In particular, they obtained the rate of spontaneous emission by an electron in a laser field. If the laser field varies slowly, within the limit of vanishing laser frequency, these rates can be applied to the corresponding processes in the crossed electric and magnetic fields when $\vec{E} \perp \vec{H}$ and $|\vec{E}| = |\vec{H}|$. The electromagnetic field enters the total probability of these processes in the form of a single invariant parameter $e^2 (F_{\mu\nu} p^\nu)^2 / m^6$, where $F_{\mu\nu}$ is the electromagnetic field tensor and p^ν is 4-momentum. This allows us to extend the consideration to the case of the arbitrary external electromagnetic field. Note that in the general case the process rates depend on the additional invariants $e^2 (F_{\mu\nu})^2 / m^4$ and $ie^2 \varepsilon_{\mu\nu\rho\sigma} F^{\mu\nu} F^{\rho\sigma}$. In the considered case of crossed fields, $\vec{E} \perp \vec{H}$ and $|\vec{E}| = |\vec{H}|$, the additional parameters are equal to zero. In the general case, they have non-zero values, however, they are

much less than unity for feasible field strength. Moreover, the additional invariants can be safely neglected in comparison with $e^2 (F_{\mu\nu} p^\nu)^2 / m^6$ if particle energy is large. In particular, considering $F^{\mu\nu}$ as a magnetic field, Nikishov and Ritus reproduced the results of Klepikov [8] concerning the radiation intensity and pair production efficiency in a magnetic field. The Nikishov and Ritus theorem have a simple physical meaning: after Lorentz's transformation to the rest frame of an ultrarelativistic particle, any field transforms into almost equal and almost perpendicular electric and magnetic fields.

Let us find the magnetic field H_{eq}, which would be equivalent to a laser field of the strength E_L in the sense described above. If a high-energy electron propagates opposite to an electromagnetic wave of the strength E_L, then in its rest frame it experiences the field of the strength of $E_0 = 2\gamma E_L$, where γ is the gamma factor. On the other hand, if an electron moves perpendicular to a magnetic field H_{eq}, then the electric field strength in the rest frame is $E_{0eq} = \gamma H_{eq}$. Comparing E_0 and E_{0eq} we conclude that the equivalent magnetic field in the laboratory reference frame is

$$H_{eq} = 2E_L. \tag{7.71}$$

Factor 2 emerges in (7.71) because the equivalent magnetic field should «replace» both the electric and magnetic field components of a laser wave.

To account for the time-dependent character of an electromagnetic wave, we need to average the obtained expressions of the PPE rate in a magnetic field (7.61) $W(H)$ over the wave period. This defines the rate of the equivalent PPE process in laser wave [205],

$$W_{eq}(E_L) = \frac{2}{\pi} \int_0^{\pi/2} W(H_{eq} \sin\varphi) d\varphi. \tag{7.72}$$

The above equation allows us to compare the QED process rates in a magnetic field and a field of an intense laser wave.

Note that Eq. (7.61) has been obtained near the process threshold when the condition $\varepsilon_l \approx 3m$ is met. Therefore, we need to pass to a moving «threshold» frame where the electron energy satisfies the same condition $\varepsilon \approx 3m$. Note that this «threshold» reference frame should not be confused with the rest frame, where $\varepsilon = m$. After some calculation, we find that in the experimental conditions the equivalent magnetic field in the threshold frame is

$$H_{eq} = 6.1 \cdot 10^{12}\, G, \text{ or } h = 0.14. \tag{7.73}$$

Note that in the SLAC experiment, e^+e^- pair production has been observed near the reaction threshold too [236]. Despite the high energy of the electron

beam of about 46.6 GeV, a large part of this energy is the energy of the rectilinear motion of the center of mass.

Let us estimate the interaction time Δt_L between the electron beam and a laser pulse, and the electron number N_{int} in the interaction region. According to [236], the electron beam size is about $\sim 25 \times 40\ \mu m^2$, the electron number in a bunch is $\sim 7 \cdot 10^9$, the focal area of the laser beam is $\sim 30\ \mu m^2$, and the intersection angle between electron and laser beams is ~17°. As a result, we find

$$\Delta t_L = 50 \text{ fs}, \quad N_{int} = 2.8 \cdot 10^8. \tag{7.74}$$

Note that both radiative width Δ_{rad} and the width associated with finite interaction time $1/\Delta t_T$ contribute to the total width of the intermediate photon Δ entering (7.61),

$$\Delta = \Delta_{rad} + 1/\Delta t_T = \Delta_{rad} + \gamma/\Delta t_L, \tag{7.75}$$

where Δt_T is the time of beam-laser interaction in the threshold reference frame.

The number of created e^+e^- pairs is given by

$$N_{e^+e^-} = k \cdot N_{int}(1 - e^{-W_{eq}\Delta t_T}), \tag{7.76}$$

where $k = 21962$ is the number of collisions between laser pulses and electron bunches [236]. The number of pairs (7.76) is Lorentz invariant and stays the same in the laboratory frame, though it is defined in the threshold reference frame. With the parameter values given above, the numerical estimation of the event number given by Eq. (7.76) is

$$N_{e^+e^-} = 80. \tag{7.77}$$

The obtained value is in reasonable agreement with the experimental result of 106 ± 14 positron events and the numerical estimation given in Ref. [239]. Note that it is indicated in Ref. [236], that the experimental result possibly includes a residual background of $\sim 2 \cdot 10^{-3}$ positrons per laser pulse due to the interaction of backscattered photons with residual gas. If the experimental data is restricted to events with $\eta > 0.216$, this reduces the positron number to 69 ± 9, which is in an even better agreement with theoretical estimation (7.77).

7.4. Conclusions

In this chapter, we considered the process of pair production by an electron (trident process) in a strong magnetic field within the consistent relativistic theory. The following conclusions can be formulated.

1. In the LLL approximation near the process threshold, the final particles are created at fixed Landau levels and their longitudinal momenta are of the order of $p_{1z} \sim p_{2z} \sim p_z \leq \sqrt{hm}$.

2. The main contribution to the PPE rate near the threshold comes from the resonant channel with the on-shell intermediate photon. In this case, the trident rate factorizes to the product of the rates of the SR and OPP processes.

3. The maximum rate has the channel with the spin projection of the initial electron oriented along the field (inverted spin state). If the initial electron is in the ground spin state (i.e. spin is directed opposite to the field), then the process rate is less by the order of magnitude of the small parameter h.

4. The trident rate is in inverse proportion to the energy width of the intermediate photon. In particular, if at the process threshold the field is $h = 0.1$ and the Landau level number of the initial electron is $l = 40$, then the estimation of the trident rate and the corresponding width are $W = 1.2 \cdot 10^4\ \mathrm{s}^{-1}$ and $\Delta = 4 \cdot 10^{17}\ \mathrm{s}^{-1}$ respectively.

5. The Nikishov and Ritus theorem allows us to estimate the number of events in the SLAC experiment on observation of positron production in collisions of relativistic electron beam and laser pulse. The corresponding value of 80 events is in reasonable agreement with the experimental result of 106 ± 14 events.

The main scientific results of this chapter are published in [299—301].

REFERENCES

1. Blewett J.P. Radiation losses in the induction electron accelerator. *Physical Review*. 1946. Vol. 69, No. 3—4. pp. 87—95. https://doi.org/10.1103/physrev.69.87
2. Elder F.R., Gurewitsch A.M., Langmuir R.V., Pollock H.C. Radiation from electrons in a synchrotron. *Physical Review*. 1947. Vol. 71, No. 11. P. 829—830. https://doi.org/10.1103/physrev.71.829.5
3. Sokolov A.A. Synchrotron radiation. Oxford: Pergamon, 1968. 198 p.
4. Sokolov A.A., Ternov I.M. Relativistic electron. Moscow: Nauka, 1974. 392 p. [in Russian].
5. Ternov I.M. Synchrotron radiation and its applications. Chur, Switzerland: Harwood Academic, 1985. 378 p.
6. Ternov I.M. Synchrotron radiation. *Physics-Uspekhi*. 1995. Vol. 38, No. 4. pp. 409—434. https://doi.org/10.1070/pu1995v-038n04abeh000082
7. Demeur M. Study of the interaction between the eigenfield of a particle and a homogeneous and constant electromagnetic field. *Royal Academy of Belgium. Bulletin of the Sci. Class*. 1953. Vol. 28. P. 1643. [in French].
8. Klepikov N.P. Emission of photons and electron-positron pairs in a magnetic field. *Soviet Physics JETP*. 1954. Vol. 26, No. 1. pp. 19—34.
9. Sokolov A.A. Quantum mechanics. New York: Holt, Rinehart and Winston, 1966. 537 p.
10. Mitrofanov I.G., Pozanenko A.S. Generation of radiation in quantum transitions of electrons in a strong magnetic field. *Soviet Physics JETP*. 1987. Vol. 66, No. 6. pp.1112—1118.
11. Ray R., Sakita B. The electromagnetic interactions of electrons in the lowest Landau level. *Annals of Physics*. 1994. Vol. 230, No. 1. pp. 131—144. https://doi.org/10.1006/aphy.1994.1020
12. Latal H.G. Cyclotron radiation in strong magnetic fields. *The Astrophysical J.* 1986. Vol. 309. pp. 372—382. https://doi.org/10.1086/164609

13. Erber T. High-Energy electromagnetic conversion processes in intense magnetic fields. *Reviews of Modern Physics*. 1966. Vol. 38, No. 4. pp. 626—659. https://doi.org/10.1103/revmodphys.38.626
14. Herold H., Ruder H., Wunner H. Cyclotron emission in strongly magnetized plasmas. *Astronomy and Astrophysics*. 1982. No. 115. pp. 90—96.
15. Pavlov G.G., Bezchastnov V.G., Meszaros P., Alexander S.G. Radiative widths and splitting of cyclotron lines in superstrong magnetic fields. *The Astrophysical J.* 1991. Vol. 380. pp. 541—549. https://doi.org/10.1086/170611
16. Harding A.K., Preece R. Quantized synchrotron radiation in strong magnetic fields. *The Astrophysical J.* 1987. Vol. 319. pp. 939—950. https://doi.org/10.1086/165510
17. Daugherty J.K., Ventura J. Absorption of radiation by electrons in intense magnetic fields. *Physical Review D*. 1978. Vol. 18, No. 4. pp. 1053—1067. https://doi.org/10.1103/physrevd.18.1053
18. Tolhoek H.A. Electron polarization, theory and experiment. *Reviews of Modern Physics*. 1956. Vol. 28, No. 3. pp. 277—298. https://doi.org/10.1103/revmodphys.28.277
19. Sokolov A.A., Ternov I.M. On polarization effects in the radiation of an accelerated electron. *Soviet Physics JETP*. 1957. Vol. 4, No. 3. pp. 396—400.
20. Korolev F.A., Markov V.S., Akimov E.M., Kulikov O.F. Experimental study of the angular distribution and polarization of optical radiation of electrons in a synchrotron. *Doklady Akademii nauk SSSR*. 1956. Vol. 110, No. 4. pp. 542—544. [in Russian].
21. Orlov Iu.F., Kheifets S.A. Depolarization of electrons due to radiation in a magnetic field. *Soviet Physics JETP*. 1959. Vol. 8, No. 2. P. 354.
22. Ternov I.M., Bagrov V.G., Rzaev R.A. Radiation from fast electrons with oriented spin in a magnetic field. *Soviet Physics JETP*. 1964. Vol. 19, No. 1. pp. 255—259.
23. Baring M.G., Gonthier P.L., Harding A.K. Spin-dependent cyclotron decay rates in strong magnetic fields. *The Astrophysical J.* 2005. No. 630. pp. 430—440. https://doi.org/10.1086/431895
24. Bagrov V.G., Zhukovsky V.Ch., Ternov I.M., Khalilov V.R. Spin effects in processes involving high-energy particles in a magnetic field. *Izvestiya Vysshikh Uchebnykh Zavedenii. Fizika*. 1984. No. 7. pp. 12—16. [in Russian].
25. Baier V.N., Katkov V.M. Radiative polarization of electrons in a magnetic field. *Soviet Physics JETP*. 1967. Vol. 25, No. 5. pp. 944—947.
26. Schwinger J., Tsai W. Radiative polarization of electrons. *Physical Review D*. 1974. Vol. 9, No. 6. pp. 1843—1845. https://doi.org/10.1103/physrevd.9.1843
27. Daugherty J.K., Lerche I. Theory of pair production in strong electric and magnetic fields and its applicability to pulsars. *Physical Review D*. 1976. Vol. 14, No. 2. pp. 340—355. https://doi.org/10.1103/physrevd.14.340
28. Daugherty J.K., Harding A.K. Pair production in superstrong magnetic fields. *The Astrophysical J.* 1983. Vol. 273. pp. 761—773. https://doi.org/10.1086/161411
29. Mikheev N.V., Chistyakov N.V. Photon damping caused by electron-positron pair production in a strong magnetic field. *J. of Experimental and Theoretical Physics*. 2001. Vol. 73, No. 12. pp. 642—646. https://doi.org/10.1134/1.1397746
30. Semionova L., Leahy D. Remarks concerning pair creation in strong magnetic fields. *Astronomy & Astrophysics*. 2001. Vol. 373, No. 1. pp. 272—280. https://doi.org/10.1051/0004-6361:20010491

31. Di Piazza A., Calucci G. Pair production in a strong time-depending magnetic field: The effect of a strong gravitational field. *Astroparticle Physics*. 2006. Vol. 24, No. 6. pp. 520—537. https://doi.org/10.1016/j.astropartphys.2005.10.004
32. Luo Y., Ji P. Pair production induced by quantum electrodynamic vacuum polarization in pulsars. *Monthly Notices of the Royal Astronomical Society*. 2011. Vol. 420, No. 2. pp. 1673—1683. https://doi.org/10.1111/j.1365-2966.2011.20158
33. Schwinger J. On gauge invariance and vacuum polarization. *Physical Review*. 1951. Vol. 82, No. 5. pp. 664—679. https://doi.org/10.1103/physrev.82.664
34. Tsai W., Yildiz A. Motion of an electron in a homogeneous magnetic field–modified propagation function and synchrotron radiation. *Physical Review D*. 1973. Vol. 8, No. 10. pp. 3446—3460. https://doi.org/10.1103/physrevd.8.3446
35. Tsai W. Magnetic bremsstrahlung and modified propagation function. Spin-0 charged particles in a homogeneous magnetic field. *Physical Review D*. 1973. Vol. 8, No. 10. pp. 3460—3469. https://doi.org/10.1103/physrevd.8.3460
36. Tsai W. Vacuum polarization in homogeneous magnetic fields. *Physical Review D*. 1974. Vol. 10, No. 8. pp. 2699—2702. https://doi.org/10.1103/physrevd.10.2699
37. Tsai W., Erber T. Photon pair creation in intense magnetic fields. *Physical Review D*. 1974. Vol. 10, No. 2. pp. 492—499. https://doi.org/10.1103/physrevd.10.492
38. Tsai W. Modified electron propagation function in strong magnetic fields. *Physical Review D*. 1974. Vol. 10, No. 4. pp. 1342—1345. https://doi.org/10.1103/physrevd.10.1342
39. Baier V N., Katkov V.M. Processes involved in the motion of high energy particles in a magnetic field. *Soviet Physics JETP*. 1968. Vol. 26, No. 4. pp. 854—860.
40. Baier V.N., Katkov V.M. Quasiclassical theory of bremsstrahlung by relativistic particles. *Soviet Physics JETP*. 1969. Vol. 28, No. 4. pp. 807—813.
41. Baier V.N., Katkov V.M., Strakhovenko V.M. Operator approach to quantum electrodynamics in an external field: The mass operator. *Soviet Physics JETP*. 1975. Vol. 40, No. 2. pp. 225—232.
42. Baier V.N., Katkov V.M., Strakhovenko V.M. Operator approach to quantum electrodynamics in an external field. Electron loops. *Soviet Physics JETP*. 1975. Vol. 41, No. 2. pp. 198—204.
43. Ritus V.I. Eigenfunction method and mass operator in the quantum electrodynamics of a constant field. *Soviet Physics JETP*. 1978. Vol. 48, No. 5. pp. 788—799.
44. Ritus V.I. Quantum effects of the interaction of elementary particles with an intense electromagnetic field. *Trudy FIAN*. 1979. Vol. 111. pp. 5—151. [in Russian].
45. Baier V.N., Katkov V.M., Strakhovenko V.M. Higher-order effects in an external field: pair creation by a particle. *Physics of Atomic Nuclei*. 1971. Vol. 14, No. 5. pp. 1020—1026. [in Russian].
46. Baier V.N., Katkov V.M. Pair creation by a photon in a strong magnetic field. *Physical Review D*. 2007. Vol. 75, No. 7. P. 073009. https://doi.org/10.1103/physrevd.75.073009
47. Baier V.N., Katkov V.M., Fadin V.S. Radiation of relativistic electrons. Moscow: Atomizdat. 1973. 376 p. [in Russian].
48. Parle A. Quantum electrodynamics in strong magnetic fields. IV. Electron self-energy. *Australian J. of Physics*. 1987. Vol. 40, No. 1. pp. 1—21. https://doi.org/10.1071/ph870001

49. Geprägs R., Riffert H., Herold H. et al. Electron self-energy in a homogeneous magnetic field. *Physical Review D*. 1994. Vol. 49, No. 10. pp. 5582—5589. https://doi.org/10.1103/physrevd.49.5582
50. Ternov I.M., Khalilov V.R., Rodionov V.N. Interaction of charged particles with a strong electromagnetic field. Moscow: Moscow University Press. 1982. 304 p. [in Russian].
51. Giacconi R., Gursky H., Kellogg E. et al. Discovery of periodic X-ray pulsations in centaurus X-3 from UHURU. *The Astrophysical J.* 1971. Vol. 167. pp. L67—L73. https://doi.org/10.1086/180762
52. Hewish A., Bell J., Pilkington D. H. et al. Observation of a rapidly pulsating radio source. *Nature*. 1968. Vol. 217, No. 5130. pp. 709—713. https://doi.org/10.1038/217709a0
53. Bird A. J., Bazzano A., Bassani L. et al. The fourth ibis/isgri soft gamma-ray survey catalog. *The Astrophysical J. Supplement Series*. 2009. Vol. 186, No. 1. pp. 1—9. https://doi.org/10.1088/0067-0049/186/1/1
54. Abdo A.A., Ackermann M., Ajello M. et al. The first Fermi large area telescope catalog of gamma-ray pulsars. *The Astrophysical J. Supplement Series*. 2010. Vol. 187, No. 2. pp. 460—494. https://doi.org/10.1088/0067-0049/187/2/460
55. Gnedin Yu.N., Syunyaev R.A. Scattering of radiation by thermal electrons in a magnetic field. *Soviet Physics JETP*. 1974. Vol. 38, No. 1. pp. 51—57.
56. Trümper J., Pietsch W., Reppin C. et al. Evidence for strong cyclotron line emission in the hard X-ray spectrum of Hercules X-1. *The Astrophysical J.* 1978. Vol. 219. pp. L105—L110. https://doi.org/10.1086/182617
57. Gnedin Yu.N., Pavlov G.G., Tsygan A.I. Photoeffect in strong magnetic fields and x-ray emission from neutron stars. *Soviet Physics JETP*. 1974. Vol. 39, No. 2. pp. 201—206.
58. Gnedin Yu.N., Sunyaev R.A. The beaming of radiation from an accreting magnetic neutron star and the X-ray pulsars. *Astronomy and Astrophysics*. 1973. Vol. 25. pp. 233—239.
59. Gnedin Yu.N., Sunyaev R.A. Polarization of optical and X-radiation from compact thermal sources with magnetic field. *Astronomy and Astrophysics*. 1974. Vol. 36. pp. 379—394.
60. Sunyaev R.A., Totarchuk L.G. Comptonization of X-rays in plasma clouds. Typical radiation spectra. *Astronomyand Astrophysics*. 1979. Vol. 86. pp. 121—138.
61. Bussard R.W. Implications of cyclotron features in the X-ray spectrum of Hercules X-1. *The Astrophysical J.* 1980. Vol. 237. pp. 970—987. https://doi.org/10.1086/157943
62. Meszaros P., Nagel W. X-ray pulsar models. I — Angle-dependent cyclotron line formation and comptonization. *The Astrophysical J.* 1985. Vol. 298. pp. 147—160. https://doi.org/10.1086/163594
63. Coburn W., Heindl W.A., Gruber D.E. et al. Discovery of a cyclotron resonant scattering feature in therossi x-ray timing explorerspectrum of 4U 0352+309 (X Persei). *The Astrophysical J.* 2001. Vol. 552, No. 2. pp. 738—747. https://doi.org/10.1086/320565
64. Heindl W.A. RXTE studies of cyclotron lines in accreting pulsars. *Fifth compton symp.*, Portsmouth, New Hampshire (USA). 2000. Vol. 510. pp. 178—182.
65. Heindl W.A., Coburn W., Gruber D.E. et al. Discovery of a cyclotron resonance scattering feature in the x-ray spectrum of XTE J1946+274. *The Astrophysical J.* 2001. Vol. 563, No. 1. pp. L35—L39. https://doi.org/10.1086/339017

66. Ibrahim A.I., Safi-Harb S., Swank J.H. et al. Discovery of cyclotron resonance features in the soft gamma repeater SGR 1806—20. *The Astrophysical J.* 2002. Vol. 574, No. 1. pp. L51—L55. https://doi.org/10.1086/342366
67. Cusumano G., Di Salvo T., Burderi R. et al. Detection of a cyclotron line and its second harmonic in 4U1907+09. *Astronomy and Astrophysics*. 1998. Vol. 338. pp. L79—L82.
68. Dal Fiume D., Orlandini M., Del Sordo S. et al. The broad band spectral properties of binary X-ray pulsars. *Advances in Space Research*. 2000. Vol. 25, No. 3—4. pp. 399—408. https://doi.org/10.1016/s0273-1177(99)00767-x
69. Orlandini M., Dal Fiume M., Del Sordo S. The broad-band spectrum of OAO1657-415 with BeppoSAX: in search of cyclotron lines. *Astronomy and Astrophysics*. 1999. Vol. 349. pp. L9—L12.
70. Santangelo A., Segreto A., Giarrusso S. et al. A BEPPOSAX study of the pulsating transient X0115+63: the first X-ray spectrum with four cyclotron harmonic features. *The Astrophysical J.* 1999. Vol. 523 (1). pp. L85—L88. https://doi.org/10.1086/312249
71. Dal Fiume D., Frontera F., Masetti N. et al. Cyclotron lines in X-ray pulsars as a probe of relativistic plasmas in superstrong magnetic fields. *Fifth compton symp.*, Portsmouth, New Hampshire (USA). 2000. Vol. 510. pp. 183—187. https://doi.org/10.1063/1.1303199
72. Robba N.R., Burderi L., Di Salvo T. et al. The BeppoSAX 0.1-100 keV spectrum of the X-ray pulsar 4U 1538–52. *The Astrophysical J.* 2001. Vol. 562. pp. 950—956. https://doi.org/10.1086/323841
73. La Barbera A., Burderi L., Di Salvo T. The 0.1-100 keV spectrum of LMC X-4 in the high state: evidence for a high-energy cyclotron absorption line. *The Astrophysical J.* 2001. Vol. 553, No. 1. pp. 375—381. https://doi.org/10.1086/320643
74. Wunner G. Comparison of 1γ and 2γ pair annihilation in strong magnetic fields. *Physical Review Letters*. 1979. Vol. 170, No. 2. pp. 79—82. https://doi.org/10.1103/physrevlett.42.79
75. Daugherty J.K., Bussard R.W. Pair annihilation in superstrong magnetic fields. *The Astrophysical J.* 1980. Vol. 238. pp. 296—310. https://doi.org/10.1086/157985
76. Harding A.K. One-photon pair annihilation in magnetized relativistic plasmas. *The Astrophysical J.* 1986. Vol. 300. pp. 167—177. https://doi.org/10.1086/163791
77. Wunner G., Paez G., Herold H., Ruder H. One-quantum annihilation of polarized electron-positron pairs in strong magnetic fields. *Astronomy and Astrophysics*. 1986. Vol. 170. pp. 179—186.
78. Semionova L., Leahy D. Polarization for pair annihilation in strong magnetic fields. *Astronomy and Astrophysics Supplement Series*. 2000. Vol. 144. pp. 307—316. https://doi.org/10.1051/aas:2000102
79. Kaminker A.D., Pavlov G.G., Mamradze P.G. Two-photon annihilation radiation in strong magnetic field: the case of small longitudinal velocities of electrons and positrons. *Astrophysics and Space Sci.* 1987. Vol. 138, No. 1. pp. 1—18. https://doi.org/10.1007/bf00642858
80. Lewicka S., Dryzek J. Two-photon positron–electron annihilation in a strong magnetic field. *Astroparticle Physics*. 2013. Vol. 50—52. pp. 1—10. https://doi.org/10.1016/j.astropartphys.2013.09.001

81. Lewicka S. Electron-positron annihilation in ultra-strong magnetic fields. comparison of one- and two-photon annihilation at middly relativistic regime. *Acta Physica Polonica A*. 2014. Vol. 125, No. 3. pp. 688—690. https://doi.org/10.12693/aphyspola.125.688
82. Kaminker A.D., Gnedin O.Yu., Yakovlev D.G. et al. Neutrino emissivity from e^-e^+ annihilation in a strong magnetic field: hot, nondegenerate plasma. *Physical Review D*. 1992. Vol. 46, No. 10. pp. 4133—4139. https://doi.org/10.1103/physrevd.46.4133
83. Al'ber Y.I., Krotova Z.N., Eidman V.Y. Cascade process in strong magnetic and electric fields under astrophysical conditions. *Astrophysics*. 1975. Vol. 11, No. 2. pp. 189—195. https://doi.org/10.1007/bf01002454
84. Daugherty J.K., Harding A.K. Electromagnetic cascades in pulsars. *The Astrophysical J.* 1982. Vol. 252. pp. 337—347. https://doi.org/10.1086/159561
85. Sturrock P.A., Harding A.K., Daugherty J.K. Cascade model of gamma-ray bursts. *The Astrophysical J.* 1989. Vol. 346. pp. 950—959. https://doi.org/10.1086/168075
86. Baring M.G. Synchrotron pair cascades in strong magnetic fields. *Astronomy and Astrophysics*. 1989. Vol. 225. pp. 260—276.
87. Daugherty J.K., Harding A.K. Gamma-ray pulsars: emission from extended polarcap cascades. *The Astrophysical J.* 1996. Vol. 458. pp. 278—292. https://doi.org/10.1086/176811
88. Akhiezer A.I., Merenkov N.P., Rekalo A.P. On a kinetic theory of electromagnetic showers in strong magnetic fields. *J. of Physics G: Nuclear and Particle Physics*. 1994. Vol. 20, No. 9. pp. 1499—1514. https://doi.org/10.1088/0954-3899/20/9/018
89. Anguelov V., Vankov H. Electromagnetic showers in a strong magnetic field. *J. of Physics G: Nuclear and Particle Physics*. 1999. Vol. 25, No. 8. pp. 1755—1764. https://doi.org/10.1088/0954-3899/25/8/317
90. Fang J., Zhang L. Full electromagnetic cascades in spin-powered pulsars. *The Astrophysical J.* 2006. Vol. 653. pp.573—579. https://doi.org/10.1086/508563
91. Timokhin A.N. Time-dependent pair cascades in magnetospheres of neutron stars — I. Dynamics of the polar cap cascade with no particle supply from the neutron star surface. *Monthly Notices of the Royal Astronomical Society*. 2010. Vol. 408, No. 4. pp. 2092—2114. https://doi.org/10.1111/j.1365-2966.2010.17286
92. Medin Z., Lai D. Pair cascades in the magnetospheres of strongly magnetized neutron stars. *Monthly Notices of the Royal Astronomical Society*. 2010. Vol. 406. pp. 1379—1404. https://doi.org/10.1111/j.1365-2966.2010.16776
93. Sturrock P.A. A model of pulsars. *The Astrophysical J.* 1971. Vol. 164. pp. 529—556. https://doi.org/10.1086/150865
94. Usov V.V. Millisecond pulsars with extremely strong magnetic fields as a cosmological source of γ-ray bursts. *Letters to Nature*. 1992. Vol. 357. pp. 472—474. https://doi.org/10.1038/357472a0
95. Arendt P.N., Eilek J.A. Pair creation in the pulsar magnetosphere. *The Astrophysical J.* 2002. Vol. 581, No. 1. pp. 451—469. https://doi.org/10.1086/344133
96. Asseo E. Pair plasma in pulsar magnetospheres. *Plasma Physics and Controlled Fusion*. 2003. Vol. 45, No. 6. pp. 853—867. https://doi.org/10.1088/0741-3335/45/6/302
97. Istomin Ya.N., Sobyanin D.N. Electron-positron plasma generation in a magnetar magnetosphere. *Astronomy Letters*. 2007. Vol. 33, No. 10. pp. 660—672. https://doi.org/10.1134/s1063773707100040

98. Zhukovsky V.Ch., Vshivtsev A.S., Eminov P.A. Thermodynamic potential and oscillations of the magnetization of a relativistic electron-positron gas in a constant magnetic field. *Physics of Atomic Nuclei*. 1995. Vol. 58, No. 7. pp. 1274—1281. [in Russian].
99. Persson D., Zeitlin V. Note on QED with a magnetic field and chemical potential. *Physical Review D*. 1995. Vol. 51, No. 4. pp. 2026—2029. https://doi.org/10.1103/physrevd.51.2026
100. Harding A.K. Physics in strong magnetic fields near neutron stars. *Science*. 1991. Vol. 251, No. 4997. pp. 1033—1038. https://doi.org/10.1126/science.251.4997.1033
101. Harding A.K. The physics of gamma-ray bursts. *Physical Reports*. 1991. Vol. 206, No. 6. pp. 327—391. https://doi.org/10.1016/0370-1573(91)90055-q
102. Ternov I.M., Dorofeev O.F. Quantum effects in extremely strong magnetic field. *Physics of elementary particles and atomic nucleus*. 1994. Vol. 25, No. 1. pp. 5—93. [in Russian].
103. Harding A.K., Lai D. Physics of strongly magnetized neutron stars. *Reports on Progress in Physics*. 2006. Vol. 69, No. 9. pp. 2631—2708. https://doi.org/10.1088/0034-4885/69/9/r03
104. Dolginov A.Z., Gnedin Yu.N., Silantyev N.A. Propagation and polarization of radiation in the space environment. Moscow: Nauka, 1979. 425 p. [in Russian].
105. Shklovsky I.S. Problems of modern astrophysics. Moscow: Nauka, 1982. 223 p. [in Russian].
106. Oleinik V.P. Resonance effects in the field of an intense laser beam. I. *Soviet Physics JETP*. 1967. Vol. 25, No. 4. pp. 697—708.
107. Oleinik V.P. Resonance effects in the field of an intense laser ray. II. *Soviet Physics JETP*. 1968. Vol. 26, No. 6. pp. 1132—1138.
108. Fedorov M.V. Resonance interaction between electrons and photons. *Soviet Physics JETP*. 1975. Vol. 41, No. 4. pp. 601—605.
109. Baier V.N., Mil'shtein A.I. Radiative effects near cyclotron resonance. *Soviet Physics JETP*. 1978. Vol. 48, No. 2. pp. 196—201.
110. Borisov A.V., Zhukovskii V.Ch., Eminov P.A. Resonant electron-electron bremsstrahlung in the field of an electromagnetic wave. *Soviet Physics JETP*. 1980. Vol. 51, No. 2. pp. 267—270.
111. Roshchupkin S.P. Resonant electron-electron scattering in the field of a light wave: general relativistic case. *Laser Physics*. 1994. Vol. 4. pp. 31—60.
112. Denisenko O.I., Roshchupkin S.P. Resonant scattering of an electron by a positron in the field of a light wave. *Laser Physics*. 1999. Vol. 9. pp. 1108—1112.
113. Landau L.D., Lifshitz E.M. Quantum mechanics: non-relativistic theory. Oxford: Butterworth-Heinemann, 1991. 677 p.
114. Kachelriess M., Berg D., Wunner G. Is Compton scattering in magnetic fields really infrared divergent? *Physical Review D*. 1995. Vol. 51, No. 2. pp. 824—828. https://doi.org/10.1103/physrevd.51.824
115. Graziani C., Harding A.K., Sina R. Elimination of resonant divergences from QED in superstrong magnetic fields. *Physical Review D*. 1995. Vol. 51, No. 12. pp. 7097—7110. https://doi.org/10.1103/physrevd.51.7097
116. Kachelriess M. Unstable states in QED of strong magnetic fields. *Physical Review D*. 1996. Vol. 53, No. 2. pp. 974—979. https://doi.org/10.1103/physrevd.53.974

117. Milton K.A., Tsai W., DeRaad L.L., Dass N.D. Compton scattering in external magnetic fields. II. Spin-1/2 charged particles. *Physical Review D*. 1974. Vol. 10, No. 4. pp.1299—1309. https://doi.org/10.1103/physrevd.10.1299
118. Herold H. Compton and Thomson scattering in strong magnetic fields. *Physical Review D*. 1979. Vol. 19, No. 10. pp. 2868—2875. https://doi.org/10.1103/physrevd.19.2868
119. Daugherty J.K., Harding A.K. Compton scattering in strong magnetic fields. *The Astrophysical J.* 1986. Vol. 309. P. 362. https://doi.org/10.1086/164608
120. Bussard R.W., Alexander S.B., Meszaros P. One- and two-photon Compton scattering in strong magnetic fields. *Physical Review D*. 1986. Vol. 34, No. 2. pp. 440—451. https://doi.org/10.1103/physrevd.34.440
121. Dermer C.D. Compton scattering in strong magnetic fields and the continuum spectra of gamma-ray bursts — Basic theory. *The Astrophysical J.* 1990. Vol. 360. P. 197. https://doi.org/10.1086/169108
122. Harding A.K., Daugherty J.K. Cyclotron resonant scattering and absorption. *The Astrophysical J.* 1991. Vol. 374. P. 687. https://doi.org/10.1086/170153
123. Meisler T.R. Low energy limit of Compton scattering in supersymmetric QED. *Physical Review D*. 1996. Vol. 54, No. 1. pp. 798—807. https://doi.org/10.1103/physrevd.54.798
124. Gonthier P.L., Harding A.K., Baring M.G. et al. Compton scattering in ultrastrong magnetic fields: numerical and analytical behavior in the relativistic regime. *The Astrophysical J.* 2000. Vol. 540, No. 2. pp. 907—922. https://doi.org/10.1086/309357
125. Fomin P.I., Kholodov R.I. Resonance Compton scattering in an external magnetic field. *J. of Experimental and Theoretical Physics*. 2000. Vol. 90. pp. 281—286. https://doi.org/10.1134/1.559101
126. Fomin P.I., Kholodov R.I. Scattering of a photon by a ground-state electron in a strong magnetic field. *Laser Physics*. 2000. Vol. 10, No. 5. pp. 1150—1155.
127. Gonthier P.L., Baring M.G., Eiles M.T. et al. Compton scattering in strong magnetic fields: spin-dependent influences at the cyclotron resonance. *Physical Review D*. 2014. Vol. 90, No. 4. P. 043014. https://doi.org/10.1103/physrevd.90.043014
128. Ternov I.M., Bagrov V.G., Khalilov V.R., Rodionov V.N. Intensity effects in the scattering of electromagnetic waves by electrons moving in an external magnetic field. *Physics of Atomic Nuclei*. 1975. Vol. 22, No. 5. pp. 1040—1046. [in Russian].
129. Ng Y.J., Tsai W. Pair creation by photon-photon scattering in a strong magnetic field. *Physical Review D*. 1977. Vol. 16, No. 2. pp. 286—294. https://doi.org/10.1103/physrevd.16.286
130. Zhukovsky V.Ch., Nikitina N.S. Induced two-photon production of electron-positron pairs in a magnetic field. *Physics of Atomic Nuclei*. 1974. Vol. 19, No. 1. pp. 148—154. [in Russian].
131. Rodionov V.N. Pair production in the scattering of a photon by an intense electromagnetic wave in a uniform magnetic field. *Soviet Physics JETP*. 1980. Vol. 51, No. 1. pp. 52—58.
132. Lobanov A.E., Muratov A.R. Effect of magnetic field on the photoproduction of electron-positron pairs. *Soviet Physics JETP*. 1984. Vol. 60, No. 4. pp. 651—653.
133. Kozlenkov A.A., Mitrofanov I.G. Two-photon production of e^-e^+ pairs in a strong magnetic field. *Soviet Physics JETP*. 1986. Vol. 64, No. 6. pp. 1173—1179.

134. Burns M.L., Harding A.K. Pair production rates in mildly relativistic magnetized plasmas. *The Astrophysical J.* 1984. Vol. 285. pp. 747—757. https://doi.org/10.1086/162552
135. Zhang B., Qiao G.J. Two-photon annihilation in the pair formation cascades in pulsar polar caps. *Astronomy and Astrophysics.* 1998. Vol. 338. pp. 62—68.
136. Zhang B. On the radio quiescence of anomalous x-ray pulsars and soft gamma-ray repeaters. *The Astrophysical J.* 2001. Vol. 562, No. 1. pp. L59—L62. https://doi.org/10.1086/338051
137. Harding A.K., Muslimov A.G., Zhang B. Regimes of pulsar pair formation and particle energetics. *The Astrophysical J.* 2002. Vol. 576, No. 1. pp. 366—375. https://doi.org/10.1086/341633
138. Baring M.G., Harding A.K. Pair production absorption troughs in gamma-ray burst spectra: a potential distance discriminator. *The Astrophysical J.* 1997. Vol. 481, No. 2. pp. L85—L88. https://doi.org/10.1086/310665
139. Dunaev M.A., Mikheev N.V. Production of electron-positron pairs by a photon propagating in a strongly magnetized thermal bath. *J. of Experimental and Theoretical Physics.* 2012. Vol. 114, No. 3. pp. 365—371. https://doi.org/10.1134/s1063776112020033
140. Zhukovskii V.Ch., Nikitina N.S. Induced two-photon synchrotron radiation and Compton scattering in a magnetic field. *Soviet Physics JETP.* 1973. Vol. 37, No. 4. pp. 595—598.
141. Sokolov A.A., Voloshchenko A.M., Zhukovsky V.Ch., Pavlenko Yu.G. Two Photon Synchrotron Radiation. *Izvestiya Vysshikh Uchebnykh Zavedenii. Fizika.* 1976. Vol. 9. pp. 46—52. [in Russian].
142. Semionova L., Leahy D. Two-photon emission process in arbitrarily strong magnetic fields. *Physical Review D.* 1999. Vol. 60, No. 7. P. 073011. https://doi.org/10.1103/physrevd.60.073011
143. Gutbrod H.H., Augustin I., Eickhoff H. et al. FAIR Baseline Technical Report. Volume1 — Executive Summary. Darmstadt: GSI, 2006. 92 p. https://fair-center.eu/for-users/publications
144. Fortov V.E., Sharkov B.Y., Stöcker H. European Facility for Antiproton and Ion Research (FAIR): the new international center for fundamental physics and its research program. *Uspekhi Fizicheskih Nauk.* 2012. Vol. 182, No. 6. pp. 621—644. https://doi.org/10.3367/ufnr.0182.201206c.0621
145. Dirac P.A.M. The quantum theory of the electron. *Proceedings of the Royal Society A.* 1928. Vol. 117. pp. 610—624.
146. Sommerfeld A.Zur Quantentheorie der Spektrallinien. *Annalen der Physik.* 1916. Vol. 356, No. 17. pp. 1—94. https://doi.org/10.1002/andp.19163561702
147. Pomeranchuk I.Ya., Smorodinsky Ya.A. On energy levels in system with Z > 137. *J. of Physics USSR.* 1945. Vol. 9. P. 97.
148. Akhiezer A.I., Berestetskiy A.I. Quantum electrodynamics. Oak Ridge, Tennesee: U. S. Atomic Energy Commission, Technical Inf. Service Extension, 1957. 549 p.
149. Zeldovich Y.B., Popov V.S. Electronic structure of superheavy atoms. *Uspekhi Fizicheskih Nauk.* 1972. Vol. 14, No. 6. pp. 673—694. https://doi.org/10.1070/pu1972v014n06abeh004735

150. Pieper W., Greiner W. Interior electron shells in superheavy nuclei. *Zeitschrift für Physik A Hadrons and nuclei*. 1969. Vol. 218, No. 4. pp. 327—340. https://doi.org/10.1007/bf01670014
151. Soff G., Müller B., Rafelski J. Precise values for critical fields in quantum electrodynamics. *Zeitschrift für Naturforschung A*. 1974. Vol. 29, No. 9. pp. 1267—1275. https://doi.org/10.1515/zna-1974-0905
152. Popov V.S. Spontaneous positron production in collisions between heavy nuclei. *Soviet Physics JETP*. 1974. Vol. 38, No. 1. pp. 18—26.
153. Müller B., Rafelski J., Greiner W. Auto-ionization of positrons in heavy ion collisions. *Zeitschrift für Physik A Hadrons and nuclei*. 1972. Vol. 257, No. 3. pp. 183—211. https://doi.org/10.1007/bf01401203
154. Backe H., Handschug L., Hessberger F. et al. Observation of positron creation in superheavy ion-atom collision systems. *Physical Review Letters*. 1978. Vol. 40, No. 22. pp. 1443—1446. https://doi.org/10.1103/physrevlett.40.1443
155. Backe H., Senger P., Boning W. et al. Estimates of the nuclear time delay in dissipative U + U and U + Cm collisions derived from the shape of positron and γ -ray spectra. *Physical Review Letters*. 1983. Vol. 50, No. 23. pp. 1838—1841. https://doi.org/10.1103/physrevlett.50.1838
156. Schweppe J., Gruppe A., Bethge K. et al. Observation of a peak structure in positron spectra from U+Cm collisions. *Physical Review Letters*. 1983. Vol. 51, No. 25. pp. 2261—2264. https://doi.org/10.1103/physrevlett.51.2261
157. Cowan T., Backe H., Begemann M. et al. Anomalous positron peaks from supercritical collision systems. *Physical Review Letters*. 1985. Vol. 54, No. 16. pp. 1761—1764. https://doi.org/10.1103/physrevlett.54.1761
158. Kozhuharov C., Kienle P., Berdermann E. et al. Positrons from 1.4-GeV uranium-atomcollisions. *Physical Review Letters*. 1979. Vol. 42, No. 6. pp. 376—379. https://doi.org/10.1103/physrevlett.42.376
159. Clemente M., Berdermann E., Kienle P. et al. Narrow positron lines from U-U and U-Th collisions. *Physics Letters B*. 1984. Vol. 137, No. 1—2. pp. 41—46. https://doi.org/10.1016/0370-2693(84)91102-x
160. Tsertos H., Berdermann E., Bosch F. et al. On the scattering-angle dependence of the monochromatic positron emission from U-U and U-Th collisions. *Physics Letters B*. 1985. Vol. 162, No. 4. pp. 273—276. https://doi.org/10.1016/0370-2693(85)90921-9
161. Koenig W., Bosch F., Kienle P. et al. Positron lines from subcritical heavy ion-atom collisions. *Zeitschrift für Physik A Atomic Nuclei*. 1987. Vol. 328. pp. 129—145. https://doi.org/10.1007/bf01290655
162. Koenig W., Berdermann E., Bosch F. et al. On the momentum correlation of (e^+e^-) pairs observed in U+U and U+Pb collisions. *Physics Letters B*. 1989. Vol. 218, No. 1. pp. 12—16. https://doi.org/10.1016/0370-2693(89)90466-8
163. Salabura P., Backe H., Bethge K. et al. Correlated e^+e^- peaks observed in heavy-ion collisions. *Physics Letters B*. 1990. Vol. 245, No. 2. pp. 153—160. https://doi.org/10.1016/0370-2693(90)90126-q
164. Cowan T., Backe H., Bethge K. et al. Observation of correlated narrow-peak structures in positron and electron spectra from superheavy collision systems. *Physical Review Letters*. 1986. Vol. 56, No.5. pp. 444—447. https://doi.org/10.1103/physrevlett.56.444

165. Kienle P. Positrons from heavyion collisions. *Annual Review of Nuclear and Particle Science*. 1986. Vol. 36, No. 1. pp. 605—648. https://doi.org/10.1146/annurev.ns.36.120186.003133
166. Ahmad I., Austin S.M., Back B.B. et al. Search for narrow sum-energy lines in electron-positron pair emission from heavy-ion collisions near the Coulomb barrier. *Physical Review Letters*. 1995. Vol. 75, No. 14. pp. 2658—2661. https://doi.org/10.1103/physrevlett.75.2658
167. Pokotilovsky Yu.N. «Darmstadt effect» and related issues. *Physics of Elementary Particles and Atomic Nuclei*. 1993. Vol. 24, No. 1. pp. 5—80. [in Russian].
168. Fomin P.I., Kholodov R.I. The nature of the narrow peaks in the e^+e^- pair production in heavy-ion collisions. *Reports of the National Academy of Sci. of Ukraine*. 1998. Vol. 12. pp. 91—96. [in Russian].
169. Rumrich K., Greiner W., Soff G. The influence of strong magnetic fields on position production in heavy-ion collisions. *Physics Letters A*. 1987. Vol. 125, No. 8. pp. 394—398. https://doi.org/10.1016/0375-9601(87)90168-x
170. Shabad A.E. Photon dispersion in a strong magnetic field. *Annals of Physics*. 1975. Vol. 90, No. 1. pp. 166—195. https://doi.org/10.1016/0003-4916(75)90144-x
171. Shabad A.E. Polarization of vacuum and quantum relativistic gas in an external field. *Trudy FIAN*. 1988. Vol. 192. pp. 5—152. [in Russian].
172. Shabad A.E. Photon propagation in a supercritical magnetic field. *J. of Experimental and Theoretical Physics*. 2004. Vol. 98. pp. 186—196. https://doi.org/10.1134/1.1675886
173. Shabad A.E., Usov V.V. Real and virtual photons in an external constant electromagnetic field of most general form. *Physical Review D*. 2010. Vol. 81, No. 12. P. 125008. https://doi.org/10.1103/physrevd.81.125008
174. Khalilov V.R., Mamsurov I.V. Polarization operator in the 2+1 dimensional quantum electrodynamics with a nonzero fermion density in a constant uniform magnetic field. *The European Physical J. C*. 2015. Vol. 75, No. 4. P. 167. https://doi.org/10.1140/epjc/s10052-015-3389-6
175. Perez-Rojas H. Polarization operator of electron-positron gas in a constant external magnetic field. *Soviet Physics JETP*. 1979. Vol. 49. pp. 1—8.
176. Skobelev V.V. Propagation of photons in a magnetic field. *Soviet Physics JETP*. 1977. Vol. 46. pp. 684—686.
177. Heisenberg W., Euler H. Folgerungen aus der Diracschen Theorie des Positrons. *Zeitschrift für Physik*. 1936. Vol. 98, No. 11—12. pp. 714—732. https://doi.org/10.1007/bf01343663
178. Euler H., Kockel B. Über die Streuung von Licht an Licht nach der Diracschen Theorie. *Die Naturwissenschaften*. 1935. Vol. 23, No. 15. pp. 246—247. https://doi.org/10.1007/bf01493898
179. Akhieser A., Landau L., Pomeranchook I. Scattering of light by light. *Nature*. 1936. Vol. 138. P. 206. https://doi.org/10.1038/138206a0
180. Klein J.J., Nigam B.P. Birefringence of the vacuum. *Physical Review*. 1964. Vol. 135, 5B. pp. B1279—B1280. https://doi.org/10.1103/physrev.135.b1279
181. Granovskii Ya.I., Dimashko Yu.A. The oscillator representation in Landau's problem of the motion of a particle in a uniform field. *Soviet Physics JETP*. 1975. Vol. 41, No. 6. pp. 996—998.

182. Kruglov S.I. Vacuum birefringence from the effective Lagrangian of the electromagnetic field. *Physical Review D*. 2007. Vol. 75, No. 11. P. 117301. https://doi.org/10.1103/physrevd.75.117301
183. Villalba-Chavez S. The role of photon polarization modes in the magnetization and instability of the vacuum in a supercritical field. *Physics Letters B*. 2010. Vol. 692, No. 5. pp. 317—322. https://doi.org/10.1016/j.physletb.2010.08.002
184. Hattori K., Itakura K. Vacuum birefringence in strong magnetic fields: (I) Photon polarization tensor with all the Landau levels. *Annals of Physics*. 2013. Vol. 330. pp. 23—54. https://doi.org/10.1016/j.aop.2012.11.010
185. Hattori K., Itakura K. Vacuum birefringence in strong magnetic fields: (II) Complex refractive index from the lowest Landau level. *Annals of Physics*. 2013. Vol. 334. pp. 58—82. https://doi.org/10.1016/j.aop.2013.03.016
186. Shakeri S., Kalantari S. Z., Xue S. Polarization of a probe laser beam due to nonlinear QED effects. *Physical Review A*. 2017. Vol. 95, No. 1. P. 012108. https://doi.org/10.1103/physreva.95.012108
187. Mignani R.P., Testa V., Caniulef D.G. et al. Evidence for vacuum birefringence from the first optical-polarimetry measurement of the isolated neutron star RX J1856.5−3754. *Monthly Notices of the Royal Astronomical Society*. 2016. Vol. 465, No. 1. pp. 492—500. https://doi.org/10.1093/mnras/stw2798
188. Grib A.A., Mamaev S.G., Mostepanenko V.M. Vacuum quantum effects in strong fields. Moscow: Energoatomizdat. 1973. 376 p. [in Russian].
189. Gitman D.M., Fradkin E.S., Shvartsman Sh.M. Quantum electrodynamics with unstable vacuum. Moscow: Nauka, 1991. 296 p. [in Russian].
190. Akhiezer A.I., Berestetskiy A.I. Quantum electrodynamics. Moscow: Nauka, 1981. 432 p. [in Russian].
191. Berestetskiy A.I., Lifshits E.M., Pitaevsky L.P. Quantum electrodynamics. Moscow: Nauka, 1989. 728 p. [in Russian].
192. Adler S.L. Photon splitting and photon dispersion in a strong magnetic field. *Annals of Physics*. 1971. Vol. 67, No. 2. pp. 599—647. https://doi.org/10.1016/0003-4916(71)90154-0
193. Skobov V.G. Decay of a photon into two photons in a homogeneous magnetic field. *Soviet Physics JETP*. 1959. Vol. 8, No. 5. P. 919.
194. Sannikov S.S. Fusion of photons in a uniform electromagnetic field. *Soviet Physics JETP*. 1967. Vol. 25, No. 5. P. 867.
195. Mentzel M., Berg D., Wunner G. Photon splitting in strong magnetic fields. *Physical Review D*. 1994. Vol. 50, No. 2. pp. 1125—1139. https://doi.org/10.1103/physrevd.50.1125
196. Weise J.I., Baring M.G., Melrose D.B. Photon splitting in strong magnetic fields: S-matrix calculations. *Physical Review D*. 1998. Vol. 57, No. 9. pp. 5526—5538. https://doi.org/10.1103/physrevd.57.5526
197. Baring M.G., Dubois D.M. Photon splitting and pair conversion in strong magnetic fields. *Computing Anticipatory Systems: CASYS'07–Eighth Int. Conf.*, Liege (Belgium). 2008. Vol. 1051. pp. 53—61. https://doi.org/10.1063/1.3020681
198. Wolkov D.M. Electron in the field of plane unpolarized electromagnetic waves from the point of view of the Dirac equation. *Soviet Physics JETP*. 1937. Vol. 7, No. 11. pp. 1286—1289. [in Russian].

199. Yanovsky V., Chvykov V., Kalinchenko G. et al. Ultra-high intensity- 300-TW laser at 0.1 Hz repetition rate. *Optics Express*. 2008. Vol. 16, No. 3. P. 2109. https://doi.org/10.1364/oe.16.002109
200. Extreme light infrastructure (ELI). URL: http://www5.extreme-light-infrastructure.eu (date of access: 15.10.2018).
201. Exawatt center for extreme light studies (XCELS). URL: https://xcels.ipfran.ru (date of access: 15.10.2018).
202. Nikishov A.I., Ritus V.I. Quantum processes in the field of a plane electromagnetic wave and in a constant field. I. *Soviet Physics JETP*. 1964. Vol. 19, No. 2. pp. 529—541.
203. Nikishov A.I., Ritus V.I. Quantum processes in the field of a plane electromagnetic wave and in a constant field. *Soviet Physics JETP*. 1964. Vol. 19, No. 5. pp. 1191—1199.
204. Ternov I.M., Bagrov V.G., Khalilov V.R. Quantum theory of radiation of a charge moving in a magnetic field and a plane wave. *Izvestiya Vysshikh Uchebnykh Zavedenii. Fizika*. 1968. No. 11. pp. 102—107. [in Russian].
205. Nikishov A.I. Intense external field problems in quantum electrodynamics. *Trudy FIAN*. 1979. Vol. 111. pp. 152—271. [in Russian].
206. Mackenroth F., Di Piazza A. Nonlinear Compton scattering in ultrashort laser pulses. *Physical Review A*. 2011. Vol. 83, No. 3. P. 032106. https://doi.org/10.1103/physreva.83.032106
207. Narozhny N.B., Fedotov A.M. Creation of electron-positron plasma with superstrong laser field. *The European Physical J. Special Topics*. 2014. Vol. 223, No. 6. pp. 1083—1092. https://doi.org/10.1140/epjst/e2014-02159-1
208. Lebed' A.A., Roshchupkin S.P. The influence of a pulsed light field on the electron scattering by a nucleus. *Laser Physics Letters*. 2008. Vol. 5, No. 6. pp. 437—445. https://doi.org/10.1002/lapl.200810013
209. Kuchiev M.Y., Robinson D.J. Electron-positron pair creation by Coulomb and laser fields in the tunneling regime. *Physical Review A*. 2007. Vol. 76, No. 1. P. 112107. https://doi.org/10.1103/physreva.76.012107
210. Di Piazza A., Loetstedt E., Milstein A.I., Keitel C.H. Barrier control in tunneling e^+e^- photoproduction. *Physical Review Letters*. 2009. Vol. 103, No. 17. P. 170403. https://doi.org/10.1103/physrevlett.103.170403
211. Voroshilo A.I., Roshchupkin S.P. Resonant scattering of a photon by an electron in the field of a circularly polarized electromagnetic wave. *Laser Physics Letters*. 2005. Vol. 2, No. 4. pp. 184—189. https://doi.org/10.1002/lapl.200410165
212. Voroshilo A.I., Roshchupkin S.P., Denisenko O.I. Resonance of exchange amplitude of Compton effect in the circularly polarized laser field. *The European Physical J. D*. 2006. Vol. 41, No. 2. pp. 433—440. https://doi.org/10.1140/epjd/e2006-00230-0
213. Voroshilo A.I., Roshchupkin S.P., Nedoreshta V.N. Resonant scattering of photon by electron in the presence of the pulsed laser field. *Laser Physics*. 2011. Vol. 21, No. 9. pp. 1675—1687. https://doi.org/10.1134/s1054660x11180010
214. Nedoreshta V.N., Roshchupkin S.P., Voroshilo A.I. Resonance of the exchange amplitude of a photon by an electron scattering in a pulsed laser field. *Physical Review A*. 2015. Vol. 91, No. 6. P. 062110. https://doi.org/10.1103/physreva.91.062110

215. Lebed' A.A., Roshchupkin S.P. Nonresonant spontaneous bremsstrahlung by a relativistic electron scattered by a nucleus in the field of pulsed light wave. *The European Physical J. D*. 2009. Vol. 53, No. 1. pp. 113—122. https://doi.org/10.1140/epjd/e2009-00050-8
216. Lebed' A.A., Roshchupkin S.P. Nonresonant spontaneous bremsstrahlung by a nonrelativistic electron scattered by a nucleus in the field of pulsed light wave. *Laser Physics Letters*. 2009. Vol. 6, No. 6. pp. 472—481. https://doi.org/10.1002/lapl.200910012
217. Lebed' A.A., Roshchupkin S.P. Resonant spontaneous bremsstrahlung by an electron scattered by a nucleus in the field of a pulsed light wave. *Physical Review A*. 2010. Vol. 81, No. 3. P. 033413. https://doi.org/10.1103/physreva.81.033413
218. Padusenko E.A., Roshchupkin S.P., Voroshilo A.I. Nonresonant scattering of relativistic electron by relativistic muon in the pulsed light field. *Laser Physics Letters*. 2009. Vol. 6, No. 3. pp. 242—251. https://doi.org/10.1002/lapl.200810121
219. Padusenko E.A., Roshchupkin S.P., Voroshilo A.I. Nonresonant scattering of nonrelativistic electron by nonrelativistic muon in the pulsed light field. *Laser Physics Letters*. 2009. Vol. 6, No. 8. pp. 616—623. https://doi.org/10.1002/lapl.200910038
220. Lötstedt E., Jentschura U.D. Nonperturbative treatment of double compton backscattering in intense laser fields. *Physical Review Letters*. 2009. Vol. 103, No. 11. P. 110404. https://doi.org/10.1103/physrevlett.103.110404
221. Lötstedt E., Jentschura U.D. Correlated two-photon emission by transitions of Dirac-Volkov states in intense laser fields: QED predictions. *Physical Review A*. 2009. Vol. 80, No. 5. P. 053419. https://doi.org/10.1103/physreva.80.053419
222. Di Piazza A., Milstein A.I. Quasiclassical approach to high-energy QED processes in strong laser and atomic fields. *Physics Letters B*. 2012. Vol. 717, No. 1. pp. 224—228. https://doi.org/10.1016/j.physletb.2012.09.043
223. Di Piazza A., Mueller C., Hatsagortsyan K.Z., Keitel C.H. Extremely high-intensity laser interactions with fundamental quantum systems. *Reviews of Modern Physics*. 2012. Vol. 84, No. 3. pp. 1177—1228. https://doi.org/10.1103/revmodphys.84.1177
224. Roshchupkin S.P., Voroshilo A.I. Resonant and coherent effects of quantum electrodynamics in the light field. Kiev: Naukova Dumka, 2008. 400 p. [in Russian].
225. Roshchupkin S.P., Lebed' A.A. Effects of quantum electrodynamics in the strong pulsed laser fields. Kiev: Naukova Dumka, 2013. 192 p. [in Russian].
226. Redmond P.J. Solution of the Klein-Gordon and Dirac equation for a particle with a plane electromagnetic wave and a parallel magnetic field. *J. of Mathematical Physics*. 1965. Vol. 6. pp. 1163—1169. https://doi.org/10.1063/1.1704385
227. Oleinik V.P. Green's function and quasi-energy spectrum of an electron in the field of an electromagnetic wave and a uniform magnetic field. *Ukrainian J. of Physics*. 1968. Vol. 13, No.7. pp. 1205—1214. [in Russian].
228. Borgardt O.O., Karpenko D.Ya. An electron in a homogeneous electromagnetic field and in a field of a plane arbitrarily polarized wave. *Ukrainian J. of Physics*. 1974. Vol. 19, No. 2. pp. 228—236. [in Ukrainian].
229. Bagrov V.G., Gitman D.M., Rodionov V.N. et al. Effect of a strong electromagnetic wave on the radiation emitted by weakly excited electrons moving in a magnetic field. *Soviet Physics JETP*. 1976. Vol. 44, No. 2. pp. 228—231.
230. Rodionov V.N. Photon emission by an electron in the field of an intense plane electromagnetic wave, with effects of a constant magnetic field included. *Soviet Physics JETP*. 1981. Vol. 54, No. 6. pp. 1047—1053.

231. Oleinik V. P. Electron-positron pair production by photons in the field of an electromagnetic wave and in a homogeneous magnetic field. *Soviet Physics JETP*. 1972. Vol. 34, No. 1. pp. 14—22.
232. Zhukovskii V.Ch., Herrmann J. Compton scattering and induced Compton scattering in a constant electromagnetic field. *Physics of Atomic Nuclei*. 1971. Vol. 14, No. 1. pp. 150—159. [in Russian].
233. Zhukovskii V.Ch. Bremsstrahlung from an electron passing by a nucleus situated in a constant external field. *Soviet Physics JETP*. 1974. Vol. 39, No. 1. pp. 4—6.
234. Borisov A.V., Zhukovskii V.Ch. Photoproduction of electron-positron pairs on a nucleus in the presence of a constant external field. *Physics of Atomic Nuclei*. 1975. Vol. 21, No. 3. pp. 579—585. [in Russian].
235. Bula C., McDonald K.T., Prebys E.J. et al. Observation of nonlinear effects in compton scattering. *Physical Review Letters*. 1996. Vol. 76, No. 17. pp. 3116—3119. https://doi.org/10.1103/physrevlett.76.3116
236. Burke D.L., Berridge S.C., Bula C. et al. Positron production in multiphoton light-by-light scattering. *Physical Review Letters*. 1997. Vol. 79, No. 9. pp. 1626—1629. https://doi.org/10.1103/physrevlett.79.1626
237. Bamber C., Boege J., Koffas T. et al. Studies of nonlinear QED in collisions of 46.6 GeV electrons with intense laser pulses. *Physical Review D*. 1999. Vol. 60, No. 9. P. 092004. https://doi.org/10.1103/physrevd.60.092004
238. Bula C., McDonald K.T. Williams approximation to trident production in electron-photon collisions. arXiv:hep-ph/0004117
239. Hu H., Müller C., Keitel C.H. Complete QED theory of multiphoton trident pair production in strong laser fields. *Physical Review Letters*. 2010. Vol. 105, No. 8. P. 080401. https://doi.org/10.1103/physrevlett.105.080401
240. Marklund M., Shukla P.K. Nonlinear collective effects in photon-photon and photon-plasma interactions. *Reviews of Modern Physics*. 2006. Vol. 78, No. 2. pp. 591—640. https://doi.org/10.1103/revmodphys.78.591
241. Langer S.H. Collisional excitation of electron Landau levels in strong magnetic fields. *Physical Review D*. 1981. Vol. 23, No. 2. pp. 328—346. https://doi.org/10.1103/physrevd.23.328
242. Crooker S.A., Samarth N. Tuning alloy disorder in diluted magnetic semiconductors in high fields to 89T. *Applied Physics Letters*. 2007. Vol. 90, No. 10. P. 102109. https://doi.org/10.1063/1.2711370
243. Sakharov A.D., Lyudaev R.Z., Sminov E.N. et al. Magnetic cumulation. *Doklady Akademii nauk SSSR*. 1965. Vol. 165, No. 1. pp. 65—68. [in Russian].
244. Selected works of A.D. Sakharov. *Soviet Physics Uspekhi*. 1991. Vol. 161, No. 5. pp. 29—120.
245. Sefcik J., Perry M.D., Lasinski B.F. et al. Gigagauss magnetic field generation from high intensity laser solid interactions. *Proceedings of the int. conf. on megagauss magnetic field generation and related topics*, Tallahassee, Florida, USA. 2004. https://doi.org/10.1142/9789812702517_0029
246. Wagner U., Tatarakis M., Gopal A. et al. Laboratory measurements of 0.7 GG magnetic fields generated during high-intensity laser interactions with dense plasmas. *Physical Review E*. 2004. Vol. 70, No. 2. P. 026401. https://doi.org/10.1103/physreve.70.026401

247. Gopal A. Measurements of ultrastrong fields in laser produced plasmas: PhD Thesis. London University, 2004. 172 p. http://ethos.bl.uk/OrderDetails.do?uin=uk.bl.ethos.415337
248. Law K., Bailly-Grandvaux M., Morace A. et al. Direct measurement of kilo-tesla level magnetic field generated with laser-driven capacitor-coil target by proton deflectometry. *Applied Physics Letters*. 2016. Vol. 108, No. 9. P. 091104. https://doi.org/10.1063/1.4943078
249. Ehret M., Kochetkov Yu, Abe Y. et al. Kilotesla plasmoid formation by a trapped relativistic laser beam. arXiv:1908.11430v1
250. Zhang Zhe, Zhu Baojun, Li Yutong et al. Generation of strong magnetic fields with a laser-driven coil. *High Power Laser Science and Engineering*. 2018. Vol. 6, No. e38. https://doi.org/10.1017/hpl.2018.33
251. Kaluza M., Schlenvoigt H., Mangles S. et al. Measurement of magnetic-field structures in a laser-wakefield accelerator. *Physical Review Letters*. 2010. Vol. 105, No. 11. P. 115002. https://doi.org/10.1103/physrevlett.105.115002
252. Walton B., Dangor A., Mangles S. et al. Measurements of magnetic field generation at ionization fronts from laser wakefield acceleration experiments. *New J. of Physics*. 2013. Vol. 15, No. 2. P. 025034. https://doi.org/10.1088/1367-2630/15/2/025034
253. Wang T., Toncian T., Wei M. et al. Structured targets for detection of Megatesla-level magnetic fields through Faraday rotation of XFEL beams. *Physics of Plasmas*. 2019. Vol. 26, No. 1. P. 013105. https://doi.org/10.1063/1.5066109
254. Baring M.G., Harding A.K. Radio-quiet pulsars with ultrastrong magnetic fields. *The Astrophysical J*. 1998. Vol. 507, No. 1. pp. L55—L58. https://doi.org/10.1086/311679
255. Price D.J., Rosswog S. Producing ultrastrong magnetic fields in neutron star mergers. *Science*. 2006. Vol. 312, No. 5774. pp. 719—722. https://doi.org/10.1126/science.1125201
256. Mereghetti S. The strongest cosmic magnets: soft gamma-ray repeaters and anomalous X-ray pulsars. *The Astronomy and Astrophysics Review*. 2008. Vol. 15, No. 4. pp. 225—287. https://doi.org/10.1007/s00159-008-0011-z
257. Revnivtsev M., Mereghetti S. Magnetic fields of neutron stars in X-ray binaries. *Space Science Reviews*. 2014. Vol. 191, No. 1-4. pp. 293—314. https://doi.org/10.1007/s11214-014-0123-x
258. Kaspi V.M., Beloborodov A.M. Magnetars. Annual Review of Astronomy and Astrophysics. 2017. Vol. 55, No. 1. pp. 261—301. https://doi.org/10.1146/annurev-astro-081915-023329
259. Shabad A.E., Usov V.V. Positronium collapse and the maximum magnetic field in pure QED. *Physical Review Letters*. 2006. Vol. 96, No. 18. P. 180401. https://doi.org/10.1103/physrevlett.96.180401
260. Leung C.N., Wang S.Y. Is there a maximum magnetic field in QED? *Physics Letters B*. 2009. Vol. 674, No. 4-5. pp. 344—347. https://doi.org/10.1016/j.physletb.2009.03.039
261. Newton R.G. Atoms in superstrong magnetic fields. *Physical Review D*. 1971. Vol. 3, No. 2. pp. 626—627. https://doi.org/10.1103/physrevd.3.626
262. Skobelev V.V. Hydrogen-like atom in a superstrong magnetic field: photon emission and relativistic energy level shift. *J. of Experimental and Theoretical Physics*. 2017. Vol. 124, No. 6. pp. 877—885. https://doi.org/10.1134/s1063776117050077

263. Shabad A.E., Usov V.V. γ-Quanta capture by magnetic field and pair creation suppression in pulsars. *Nature*. 1982. Vol. 295, No. 5846. pp. 215—217. https://doi.org/10.1038/295215a0
264. Herold H., Ruder H., Wunner G. Can γ quanta really be captured by pulsar magnetic fields? *Physical Review Letters*. 1985. Vol. 54, No. 13. pp. 1452—1455. https://doi.org/10.1103/physrevlett.54.1452
265. Leinson L.B., Perez A. Relativistic approach to positronium levels in a strong magnetic field. *J. of High Energy Physics*. 2000. Vol. 2000, No. 11. P. 039. https://doi.org/10.1088/1126-6708/2000/11/039
266. Lai D. Matter and radiation in strong magnetic fields of neutron stars. *J. of Physics: Conf. Series*. 2006. Vol. 31. pp. 68—75. https://doi.org/10.1088/1742-6596/31/1/011
267. Lai D. Physics in very strong magnetic fields. *Space Science Reviews*. 2015. Vol. 191, No. 1-4. pp. 13–25. https://doi.org/10.1007/s11214-015-0137-z
268. Ruder H., Herold H., Geyer F., Wunner G. Atoms in strong magnetic fields: quantum mechanical treatment and applications in astrophysics and quantum chaos (astronomy and astrophysics library). Springer-Verlag Telos, 1994. 309 p.
269. Gusynin V.P., Miransky V.A., Shovkovy I.A. Dynamical flavor symmetry breaking by a magnetic field in 2+1 dimensions. *Physical Review D*. 1995. Vol. 52, No. 8. pp. 4718—4735. https://doi.org/10.1103/physrevd.52.4718
270. Gusynin V.P., Miransky V.A., Shovkovy I.A. Dynamical chiral symmetry breaking by a magnetic field in QED. *Physical Review D*. 1995. Vol. 52, No. 8. pp. 4747—4751. https://doi.org/10.1103/physrevd.52.4747
271. Gusynin V.P., Miransky V.A., Shovkovy I.A. Dimensional reduction and catalysis of dynamical symmetry breaking by a magnetic field. *Nuclear Physics B*. 1996. Vol. 462, No. 2-3. pp. 249—290. https://doi.org/10.1016/0550-3213(96)00021-1
272. Gusynin V.P., Miransky V.A., Shovkovy I.A. Dynamical chiral symmetry breaking in QED in a magnetic field: toward exact results. *Physical Review Letters*. 1999. Vol. 83, No. 7. pp. 1291—1294. https://doi.org/10.1103/physrevlett.83.1291
273. Gusynin V.P., Smilga A.V. Electron self-energy in strong magnetic field: summation of double logarithmic terms. *Physics Letters B*. 1999. Vol. 450, No. 1-3. pp. 267—274. https://doi.org/10.1016/s0370-2693(99)00145-8
274. Gusynin V.P., Miransky V.A., Shovkovy I.A. Large N dynamics in QED in a magnetic field. *Physical Review D*. 2003. Vol. 67, No. 10. pp. 107703. https://doi.org/10.1103/physrevd.67.107703
275. Sadooghi N., Jalili A.S. New look at the modified Coulomb potential in a strong magnetic field. *Physical Review D*. 2007. Vol. 76, No. 6. P. 065013. https://doi.org/10.1103/physrevd.76.065013
276. Demchik V., Skalozub V. Spontaneous magnetization of a vacuum in the hot Universe and intergalactic magnetic fields. *Physics of Particles and Nuclei*. 2015. Vol. 46, No. 1. pp. 1—23. https://doi.org/10.1134/s1063779615010037
277. Kostenko A., Thompson C. QED phenomena in an ultrastrong magnetic field. I. electron–photon scattering, pair creation, and annihilation. *The Astrophysical J*. 2018. Vol. 869, No. 1. P. 44. https://doi.org/10.3847/1538-4357/aae0ef
278. Kostenko A., Thompson C. QED phenomena in an ultrastrong magnetic field. II. electron–positron scattering, e ±–ion scattering, and relativistic bremsstrahlung. *The Astrophysical J*. 2019. Vol. 875, No. 1. P. 23. https://doi.org/10.3847/1538-4357/aae82e

279. Thompson C., Kostenko A. Pair plasma in super-qed magnetic fields and the hard x-ray/optical emission of magnetars. *The Astrophysical J.* 2020. Vol. 904, No. 2. P. 184. https://doi.org/10.3847/1538-4357/abbe87
280. Kholodov R.I., Baturin P.V. Polarization effect in synchrotron radiation in ultra-quantum approximation. *Ukrainian J. of Physics*. 2001. Vol. 46, No. 5. pp. 621—626. [in Ukrainian].
281. Fomin P.I., Kholodov R.I. Polarization effects in synchrotron radiation in strong magnetic field. *Problems of Atomic Science and Technology*. 2001. Vol. 6, No. 1. pp. 154—156.
282. Novak O.P., Kholodov R.I. Polarization effects in the photon-induced process of electron-positron pair creation in a magnetic field, studied in the ultra-quantum-mechanical approximation. *Ukrainian J. of Physics*. 2008. Vol. 53, No. 2. pp. 187—195. [in Ukrainian].
283. Novak O.P., Kholodov R.I. Spin-polarization effects in the processes of synchrotron radiation and electron-positron pair production by a photon in a magnetic field. *Physical Review D*. 2009. Vol. 80, No. 2. P. 025025. https://doi.org/10.1103/physrevd.80.025025
284. Fomin P.I., Kholodov R.I. To the theory of resonant quantum-electrodynamic processes in an external magnetic field. *Ukrainian J. of Physics*. 1999. Vol. 44, No. 12. pp. 1526—1529. [in Ukrainian].
285. Voroshilo O.I., Kholodov R.I. The Green function of an electron in constant homogeneous magnetic field and arbitrary flat wave field. *Ukrainian J. of Physics*. 2002. Vol. 47, No. 4. pp. 317—321. [in Ukrainian].
286. Fomin P.I., Kholodov R.I. Resonance double magnetic bremsstrahlung in a strong magnetic field. *J. of Experimental and Theoretical Physics*. 2003. Vol. 96, No. 2. pp. 315—320. https://doi.org/10.1134/1.1560403
287. Diachenko M.M., Novak O.P., Kholodov R.I. Resonant threshold two-photon e^-e^+ pair production onto the lowest landau levels in a strong magnetic field. *Ukrainian J. of Physics*. 2014. Vol. 59, No. 9. pp. 849—855. https://doi.org/10.15407/ujpe59.09.0849
288. Diachenko M.M., Novak O.P., Kholodov R.I. Resonant generation of an electron–positron pair by two photons to excited Landau levels. *J. of Experimental and Theoretical Physics*. 2015. Vol. 121, No. 5. pp. 813—818. https://doi.org/10.1134/s1063776115110126
289. Diachenko M.M., Novak O.P., Kholodov R.I. Pair production in a magnetic and radiation field in a pulsar magnetosphere. *Modern Physics Letters A*. 2015. Vol. 30, No. 25. P. 1550111. https://doi.org/10.1142/s0217732315501114
290. Fomin P.I., Kholodov R.I. Photoproduction of the e^+e^- pair with photon emission kinematics in strong magnetic field. *Problems of Atomic Science and Technology*. 2005. Vol. 6. pp. 43—45.
291. Fomin P.I., Kholodov R.I. Resonant photoproduction of e^+e^- pair with photon emission in strong magnetic field. *Problems of Atomic Science and Technology*. 2007. Vol. 3. pp. 179—183.
292. Fomin P.I., Kholodov R.I. Electron-positron pair photo-production with radiation of a photon in magnetic field at nonresonant regime. *Problems of Atomic Sci. and Tech*. 2012. Vol. 1. pp. 111—114.

293. Bogolyubov N.N, Shirkov N.N. Introduction to the theory of quantized fields. Moscow: Nauka, 1984. 603 p. [in Russian].
294. Beams J.W. Electric and magnetic double refraction. *Reviews of Modern Physics*. 1932. Vol. 4, No. 1. pp. 133—172. https://doi.org/10.1103/revmodphys.4.133
295. Diachenko M.M., Novak O.P., Kholodov R.I. A cascade of e^+e^- pair production by a photon with subsequent annihilation to a single photon in a strong magnetic field. *Laser Physics*. 2016. Vol. 26, No. 6. P. 066001. https://doi.org/10.1088/1054-660x/26/6/066001
296. Diachenko M.M., Novak O.P., Kholodov R.I., Fomina A.P. Electron-positron pair photoproduction in a strong magnetic field through the polarization cascade. *Ukrainian J. of Physics*. 2020. Vol. 65, No. 3. P. 187. https://doi.org/10.15407/ujpe65.3.187
297. Diachenko M.M., Novak O.P., Kholodov R.I. Vacuum birefringence in a supercritical magnetic field. *Ukrainian J. of Physics*. 2019. Vol. 64, No. 3. P. 181. https://doi.org/10.15407/ujpe64.3.181
298. Novak O.P., Diachenko M.M., Padusenko E., Kholodov R. Vacuum birefringence in the fields of a current coil and a guided electromagnetic wave. *Ukrainian J. of Physics*. 2018. Vol. 63, No. 11. P. 979. https://doi.org/10.15407/ujpe63.11.979
299. Novak O.P., Kholodov R.I., Fomin P.I. Electron-positron pair production by an electron in a magnetic field near the process threshold. *J. of Experimental and Theoretical Physics*. 2010. Vol. 110, No. 6. pp. 978—982. https://doi.org/10.1134/s1063776110060075
300. Novak O.P., Kholodov R.I. Threshold electron-positron pair production by a polarized electron in a strong magnetic field. *Problems of Atomic Sci and Tech*. 2012. Vol. 1. pp. 102—104.
301. Novak O.P., Kholodov R.I. Electron-positron pair production by an electron in a magnetic field in the resonant case. *Physical Review D*. 2012. Vol. 86, No. 10. P. 105013. https://doi.org/10.1103/physrevd.86.105013

LIST OF SYMBOLS AND ABBREVIATIONS

QED — Quantum Electrodynamics
QFT — Quantum Field Theory
SR — Syncrotron Radiation, emission of a photon by an electron
OPP — e^+e^- Pair Production by One photon
CS — Compton Scattering, scattering of a photon by an electron
DSR — Double Syncrotron Radiation, emission of two photons by an electron
TPP — e^+e^- Pair Production by Two photons
OPPE — e^+e^- Pair Production by One photon with photon Emission
VB — Vacuum Birefringence
CPPPA — Cascade of processes of e^+e^- Pair Production and subsequent the Pair Annihilation
PPE — Trident process, e^+e^- Pair Production by an Electron
LLL — Lowest Landau Level
FAIR — Facility for Antiproton and Ion Research
SPARC — Stored Particles Atomic Physics Research Collaboration
HESR — High Energy Storage Ring
SLAC — Stanford Linear Accelerator Center

Unit of measurement

The paper uses a relativistic system of units, in which the Planck constant and the speed of light are equal to one. The following units are used:
for energy — eV (electron volts),
for magnetic induction — Gs (Gauss).

CONTENTS

Chapter **3**

RESONANT AND SPIN-POLARIZATION EFFECTS IN THE PROCESS OF PHOTON SCATTERING ON AN ELECTRON

Chapter **4**

e^+e^- PAIR PRODUCTION BY TWO POLARIZED PHOTONS IN RESONANCE CONDITIONS

Chapter **5**

ONE-PHOTON PRODUCTION OF AN ELECTRON-POSITRON PAIR WITH EMISSION OF A PHOTON

Chapter **6**

CASCADE OF e^+e^- PAIR PRODUCTION BY A PHOTON WITH SUBSEQUENT ANNIHILATION TO A SINGLE PHOTON

Chapter **7**

ELECTRON POSITRON PAIR PRODUCTION BY AN ELECTRON

У монографії розглянуто резонансні та поляризаційні ефекти в процесах квантової електродинаміки, що відбуваються у сильному зовнішньому магнітному полі. Розроблено метод аналізу спін-поляризаційних ефектів. Розглянуто факторизацію перерізів процесів у резонансних умовах і представлення цих перерізів у формі Брейта — Вігнера. Показано можливість верифікації зазначених ефектів у сучасних міжнародних проєктах з перевірки квантової електродинаміки у сильних полях.

Для наукових працівників, викладачів, аспірантів і студентів фізичних та фізико-технічних спеціальностей.

Наукове видання

НАЦІОНАЛЬНА АКАДЕМІЯ НАУК УКРАЇНИ
ІНСТИТУТ ПРИКЛАДНОЇ ФІЗИКИ НАН УКРАЇНИ

ХОЛОДОВ РОМАН ІВАНОВИЧ
НОВАК ОЛЕКСАНДР ПЕТРОВИЧ
ДЯЧЕНКО МИХАЙЛО МИХАЙЛОВИЧ

РЕЗОНАНСНІ І ПОЛЯРИЗАЦІЙНІ ЕФЕКТИ В ПРОЦЕСАХ КВАНТОВОЇ ЕЛЕКТРОДИНАМІКИ В СИЛЬНОМУ МАГНІТНОМУ ПОЛІ

Англійською мовою

Редактор-коректор *В.К. Рего*

Художнє оформлення *Є.О. Ільницького*

Технічне редагування і комп'ютерна верстка *О.А. Бурдік*

Підп. до друку 14.12.2022. Формат 70 × 100/16.
Гарн. Minion Pro. Ум. друк. арк. 18,69. Обл.-вид. арк. 19,32.
Тираж 100 прим. Зам. № 6816.

Видавець і виготовлювач Видавничий дім
«Академперіодика» НАН України
01024, Київ, вул. Терещенківська, 4

Свідоцтво про внесення до Державного реєстру суб'єктів
видавничої справи серії ДК № 544 від 27.07.2001 р.

ВИДАВНИЧИЙ ДІМ АКАДЕМ ПЕРІОДИКА